# Ratiometric fluorescent membrane probes sensitive to lipid composition as tools for studies of lipid order, apoptosis and endocytosis

Zeinab Darwich

# UNIVERSITÉ DE STRASBOURG

*ÉCOLE DOCTORALE DES SCIENCES DE LA VIE ET DE LA SANTÉ*

**UMR CNRS 7213**

# THÈSE présentée par :

**Zeinab DARWICH**

soutenue le : **15 novembre 2012**

pour obtenir le grade de : **Docteur de l'université de Strasbourg**

Discipline/ Spécialité : SCIENCES DU VIVANT/ ASPECTS MOLECULAIRES ET CELLULAIRES DE LA BIOLOGIE

## TITRE de la thèse

**SONDES FLUORESCENTES MEMBRANAIRES RATIOMETRIQUES POUR L'ETUDE DES CHANGEMENTS D'ORDRE LIPIDIQUE LORS DE L'APOPTOSE ET DE L'ENDOCYTOSE**

**THÈSE dirigée par :**

| | |
|---|---|
| **Monsieur MELY Yves** | Professeur, Université de Strasbourg |
| **Monsieur KLYMCHENKO Andrey** | Docteur, Université de Strasbourg |

**RAPPORTEURS :**

| | |
|---|---|
| **Madame BRASSELET Sophie** | Docteur, Université d'Aix-Marseille |
| **Monsieur DURROUX Thierry** | Docteur, Université de Montpellier |
| **Madame CHASSEROT-GOLAZ Sylvette** | Docteur, Université de Strasbourg |

**AUTRES MEMBRES DU JURY :**

| | |
|---|---|
| **Monsieur PERRIER-CORNET Jean-Marie** | Professeur, Université de Bourgogne |

# UNIVERSITÉ DE STRASBOURG

*ÉCOLE DOCTORALE DES SCIENCES DE LA VIE ET DE LA SANTÉ*

**UMR CNRS 7213**

# THÈSE présentée par :

**Zeinab DARWICH**

soutenue le : **15 novembre 2012**

pour obtenir le grade de : **Docteur de l'université de Strasbourg**

Discipline/ Spécialité : SCIENCES DU VIVANT/ ASPECTS MOLECULAIRES ET CELLULAIRES DE LA BIOLOGIE

## TITRE de la thèse

**SONDES FLUORESCENTES MEMBRANAIRES RATIOMETRIQUES POUR L'ETUDE DES CHANGEMENTS D'ORDRE LIPIDIQUE LORS DE L'APOPTOSE ET DE L'ENDOCYTOSE**

**THÈSE dirigée par :**

| | |
|---|---|
| **Monsieur MELY Yves** | Professeur, Université de Strasbourg |
| **Monsieur KLYMCHENKO Andrey** | Docteur, Université de Strasbourg |

**RAPPORTEURS :**

| | |
|---|---|
| **Madame BRASSELET Sophie** | Docteur, Université d'Aix-Marseille |
| **Monsieur DURROUX Thierry** | Docteur, Université de Montpellier |
| **Madame CHASSEROT-GOLAZ Sylvette** | Docteur, Université de Strasbourg |

**AUTRES MEMBRES DU JURY :**

| | |
|---|---|
| **Monsieur PERRIER-CORNET Jean-Marie** | Professeur, Université de Bourgogne |

***Acknowledgement***

*I am grateful to Prof. Yves Mely, director of the Laboratoire de Biophotonique et Pharmacologie, for providing me the opportunity of having been hosted in his laboratory.*

*This dissertation would not have been possible without the guidance and the help of the Director of my thesis Prof. Yves Mely. My deepest gratitude to my co-director Dr. Andrey Klymchenko who has been generous with his time and knowledge. His invaluable help of constructive comments and suggestions throughout the experimental and thesis works have contributed to the success of this research.*

*Furthermore, I would like to thank the jury members: Dr. Sophie Brasselet, Dr. Thierry Durroux, Dr. Sylvette Chasserot-Golaz, as well as Prof. Jean-Marie Perrier-Cornet for accepting to evaluate my thesis.*

*I would like to extend my gratitude to Dr. Ludovic Richert, Dr. Pascal Didier and Romain Vauchelles for fluorescence imaging (PIQ platform). Also I would like to thank Dr. Denis DuJardin for his collaboration for biological studies and Ms. Claudine Ebel (IGBMC) for helping me in flow cytometry experiments.*

*My acknowledgement also goes to my ex-colleagues, Dr. Oleksandr Kucherak, Dr. Viktoria Postupalenko, Dr. Kamal kant Sharma and Dr. Namrata Jain also to all members and researchers in our laboratory, for their co-operations.*

*Sincere thanks to all my friends especially Hussein, Israa, Nedal, Ola, Hala, Wissam, Nada, Anji, Sarah and others for their kindness and moral support during my study. Thanks for the friendship and memories.*

*Last but not least, my deepest gratitude goes to my beloved parents and also to my sisters, Dana and Dolly, for their endless love, prayers and encouragement. Special thanks to my brother for his moral support and for sharing with me his own experience in science, also for his wife for her moral support and motivation.*

*To those who indirectly contributed in this research, your kindness means a lot to me. Thank you very much.*

# Table of Contents

# Abbreviations

| | |
|---|---|
| 3HC | 3-Hydroxychromone |
| 3HF | 3-Hydroxyflavone |
| CCP | Clathrin-coated pits |
| CCV | Clathrin-coated vesicles |
| CTxB | Cholera-toxin B subunit |
| Chol | Cholesterol |
| DMF | Dimethylformamide |
| DMSO | Dimethylsulfoxide |
| DOPC | Dioleoylphosphatidylcholine |
| DOPS | Dioleoylphosphatidylserine |
| EE | Early Endosomes |
| ESIPT | Excited-State Intramolecular Proton Transfer |
| FCS | Fluorescence Correlation Spectroscopy |
| FITC | Fluorescein isothiocyanate |
| FRET | Fluorescence Resonance Energy Transfer |
| GM1 | Monosialotetrahexosylganglioside |
| GPI | Glycosylphosphatidylinisotol |
| GUVs | Giant Unilamellar Vesicles |
| LUVs | Large Unilamellar Vesicles |
| Ld | Liquid Disordered phase |
| Lo | Liquid Ordered phase |
| LE | Late Endosomes |
| NR | Nile Red |
| N*/T* | Intensity ratio of the N* and T* bands |
| PC | Phosphatidylcholine |

| | |
|---|---|
| PE | Phosphatidylethanolamine |
| PI | Propidium Iodide |
| PS | Phosphatidylserine |
| QY | Quantum Yield of fluorescence |
| RT | Room Temperature |
| SM | Sphingomyelin |
| SMase | Sphingomyelinase |
| STED | Stimulated Emission Depletion microscopy |
| Tm | Melting (transition) temperature of lipid |
| $\lambda_{abs}$ | Position of absorption maximum |
| $\lambda_{fluo}$ | Position of fluorescence maximum (i.e. emission maximum) |

# General Introduction

The interface between chemistry, physics and biology gains with time a larger place in scientific research. Studies of cell plasma membrane benefits from this globalization in science by mobilizing molecular and instrumental tools for imaging cell membrane structure and function in situ. The fundamental problem is to connect the physico-chemical properties of cellular membranes with its biological functions. To this end, it is essential to utilize the non-invasive in situ techniques, which could monitor these properties at the molecular scale. Fluorescence is probably the most appropriate technique to monitor living processes in situ with high sensitivity and minimum invasive effect. However, to apply successfully this technique to study biological membranes, one has to use fluorescent markers or probes, which could report on changes in its physico-chemical properties by change in their emission characteristics. The field of membrane probes is not sufficiently explored, therefore, new probes are currently being developed and characterized.

In the present work, the attention will be focused on the characterization and applications of new fluorescent probes for imaging lipid composition, membrane structure and their relation with the programmed cell death (apoptosis). These probes are derivatives of 3-hydroxyflavone and Nile red, characterized by sensitivity of their emission to environment properties. Application of the new fluorescent probes together with advanced fluorescence techniques allowed us to better understand the connection between lipid phases, membrane asymmetry and apoptosis. These studies involved characterization of the probes properties in lipid models (large unilamellar vesicles and giant vesicles), and in plasma membranes of living cells using variety of fluorescence techniques, such as fluorescence spectroscopy, microscopy and flow cytometry.

After a bibliographical review in this field, by describing cell plasma membrane organization, lipid rafts then apoptosis, endocytosis and fluorescence concepts, a first part of the dissertation will be devoted to the characterization of 3- hydroxyflavone derivative probes, and their applications for biological issues. A second part will be focused on a similar study of a probe derived from Nile red, NR12S, in order to monitor changes in physico-chemical properties of the membrane related to some physiological phenomena. Finally, a last part will concern a novel application of NR12S as smart marker for following the change in lipid order

in vesicles membranes during the maturation of endosomes, in addition to the appendix part describing another interesting application of NR12S in development of enzymatic probes.

The characterized new probes, due to their ratiometric response and simple utilization, are promising tools for cellular studies and further biomedical applications. In particular these probes are attractive for detection of apoptosis in cancer cells treated with drugs. The fundamental connection between the membrane biophysical properties and apoptosis established in this work is an important insight in the apoptosis research, which will also help to design new improved probes for apoptosis detection.

# *Bibliographical Review*

# Overview of the biological context

Cells, by definition, are the smallest unit of an organism capable of independent life. All life on Earth is divided into 2 categories: Prokaryotes and Eukaryotes. Prokaryotic cells (mainly bacteria) are very simple in structure, having no nucleus and their genetic material swimming freely in the cytoplasm. Eukaryotic cells (animals, plants, protists and fungi) show more complex structure (Fig. 1). Animal eukaryotic cells (most have a size range about 10-50 µm) are made up of various organelles which perform different functions such as the nucleus, mitochondria, endoplasmic reticulum, lysosomes and ribosomes. All these organelles are present in the cell cytoplasm and are protected from the extracellular environment by a hydrophobic film which is called the plasma membrane.

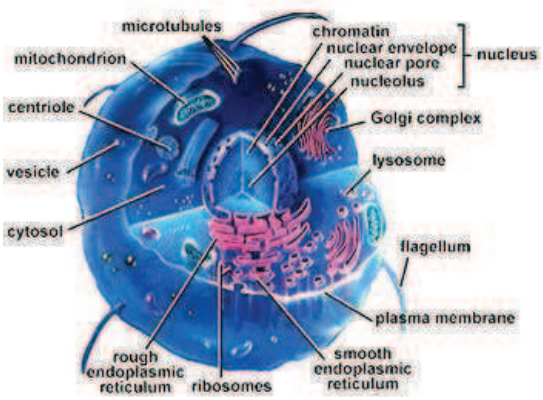


**Figure 1.** Schematic representation of eukaryotic animal cell in 3D *(http://www.beyondbooks.com/lif71/4.asp).*

## 1. Cell plasma membrane

### 1.1. Cell plasma membrane model

Since cell plasma membranes show strong biological interests, many studies were performed to explore their organization. The first experiments were accomplished by Ernest Overton in 1890s. He proposed the hypothesis that cell membrane had some similarities with lipids such as olive oil, so he correctly predicted that cell membranes were composed primarily of *"lipoids"* or lipid molecules. Later on, Langmuir (Langmuir 1917) proposed that membranes are organized of a lipid monolayer or film, with lipids oriented vertically. In the so-called

Langmuir films, hydrocarbon chains are away from water while carboxyl groups are in contact with water.

In 1925, Gorter and Grendel hypothesized a lipid bilayer organization of the plasma membrane with two leaflets (Fig. 2a). They used organic solvent to separate the lipid membrane from the aqueous environment, so they extract lipids from red blood cells (which are devoid of organelles unlike other eukaryotic cells) and found that the area of total lipids extracted was almost double the surface area of cells, suggesting that animal cells are covered by two lipid layers (Gorter and Grendel 1925). In 1935, Daniello and Davson noticed the presence of proteins in membranes (Fig. 2b). They supposed that membrane looks like a sandwich of lipids, coated by globular proteins (Danielli and Davson 1935). Since the resolution of light microscopy is of 200 nm, which is not relevant for the study of the molecular structure of biomembranes with 5-10nm of thickness, in 1950s, using advanced electron microscopy, Robertson extended the Davson-Danielli model to a new model called the unit membrane (with a thickness of 6-8nm) or Davson-Danielli-Robertson (DDR) model, where proteins coated the surface of a lipid bilayer in a ß-sheet configuration (Fig. 2c). He observed two darker outlines with a lighter inner region, he proposed that darker lines were proteins and the inner region was a lipid bilayer (Fig. 2d).

In 1972, the Singer-Nicolson *fluid mosaic model* of cell plasma membrane was proposed, describing a random distribution of components in the membrane by dynamic rearrangement in a fluid state. In this model, the lipid bilayer exists in a fluid state, showing dynamic movement, in which functional proteins float freely (Fig. 2e). The proteins form two classes: peripheral proteins which are loosely attached to the membrane surface, and integral proteins which constitute the main part of membrane proteins. This random appearance of lipid-protein composite gave the membrane a look like a mosaic (Bagatolli, Ipsen et al. 2010). By the Singer-Nicolson model, membranes have been defined as *"a two dimensional oriented solution of integral proteins… in the viscous phospholipid bilayer"* (Singer and Nicolson 1972).

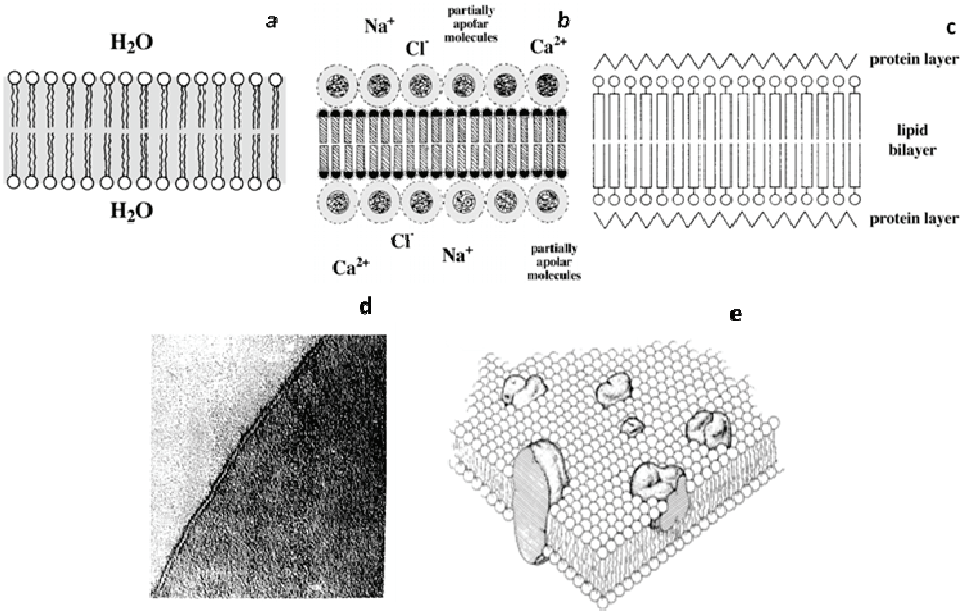


**Figure 2.** Diagram illustrating the chronological order in which membrane models have been proposed. The cell membrane according to (a) Gorter and Grendel (1925), (b) Danielli and Davson (1935), (c) Robertson (1959), (e) Singer and Nicolson (1972). (d) Thin-section electron micrograph of the unit membrane proposed by Robertson. (*Photomicrograph by J.D. Robertson from Dyson, R.D. (1974)*).

In this model, the dynamics of lipids and proteins in membranes have some effect on cellular processes (ligand-receptor recognition, intercellular interactions…). This model represented the most accepted image of biological membranes. However, a number of experimental data further improved this model, for instance, it was shown for adhesion proteins and receptors of growth factors that protein diffusion in membranes is not random, but restricted to some domains. This restriction of diffusion was explained by the connection of the cytoskeleton network to the membrane (Kusumi, Sako et al. 1993). This restriction of lateral diffusion was also demonstrated for some anchor proteins (Simson, Sheets et al. 1995). These data stimulated new discussions about the structure of biological membranes, but were almost ignored till 1997, when functional domains called "lipid rafts" were hypothesized. A number of techniques, including fluorescence resonance energy transfer (FRET) (Varma and Mayor 1998), (Sharma, Varma et al. 2004), scanning confocal microscopy and fluorescence correlation spectroscopy (FCS) (Lenne, Wawrezinieck et al. 2006) evidenced the existence of nanoscale, cholesterol –enriched, dynamic microdomains in the plasma membrane.

## 1.2. Cell plasma membrane composition

Cell plasma membrane plays important roles. It maintains the cellular shape by anchoring the cytoskeleton, and due to its permeability, allows the incoming and the outgoing of materials between the intracellular and extracellular media.

Biological membranes consist of lipids, proteins and sugars. Lipids and proteins are held together mainly by non-covalent interactions, while carbohydrates are attached to the outer side of the membrane by covalent bonds to protein or lipid molecules. Plasma membrane may contain hundreds and even thousands of different lipids species differing in their hydrocarbon chain length, insaturation and structure of headgroup (Mouritsen 2011). These lipids, which are mainly synthesized in the endoplasmic reticulum ER, as essential components of cell membrane are not only important for energy storage but they also play active roles and act as first and second messengers in signal transduction. They may be defined as amphiphilic molecules with a polar head on one side and lipophilic apolar alkyl chains on the opposite side.

Concerning the lipid repertoire, there are three major types of lipids found in biological membranes (Fig. 3): i) glycerophospholipids, which are the most dominant lipids in eukaryotic membranes, having diacylglycerol (glycerol linked to two fatty acid chains) as a backbone carrying a phosphate (phosphatidic acid PA) esterified by a choline in phosphatidylcholine (PC), serine in phosphatidylserine (PS), ethanolamine in phosphatidylethanolamine (PE) and inositol in phosphatidylinositol (PI). PC is the major component (>50%) of biological membranes, with most PC molecules having one unsaturated fatty acyl chain. ii) sphingolipids also participate in plasma membrane structure, with ceramide as hydrophobic part. Sphingomyelin with a saturated fatty acyl chain (SM) and glycosphingolipids are the major sphingolipids present in the membrane of mammalian cells. iii) The third type of lipids is sterols with cholesterol being the most frequent representative in membranes of mammalian cells. Their structure differs from that of phospholipids, as it contains a four-ring steroid structure with a short hydrocarbon chain and a hydroxyl group (van Meer, Voelker et al. 2008).

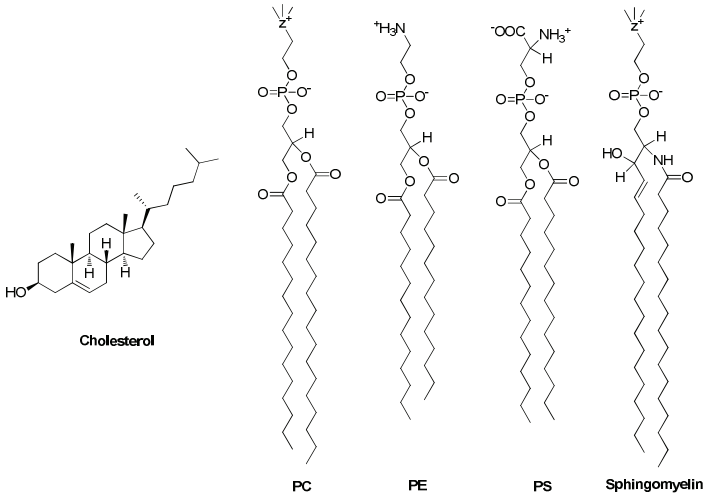


**Figure 3.** Examples of major membrane lipids. For simplicity only saturated lipids are shown.

## 1.3. Lipid bilayer asymmetry and organization

Due to their amphiphilic properties, lipids self-assemble in aqueous media forming different nanostructures. Among them, lipid bilayers are the most important at the biological level. Lipids together with membrane proteins (intrinsic or associated) constitute the skeleton of biological membranes (Bagatolli, Ipsen et al. 2010). The cell plasma membrane bilayer exhibits asymmetric distribution of lipids between the leaflets (Fig. 4), the outer (non-cytosolic) leaflet containing mainly SM and, PC, while PS and PE predominate in the inner (cytosolic) leaflet (Meer 1989), (Feigenson 2007).

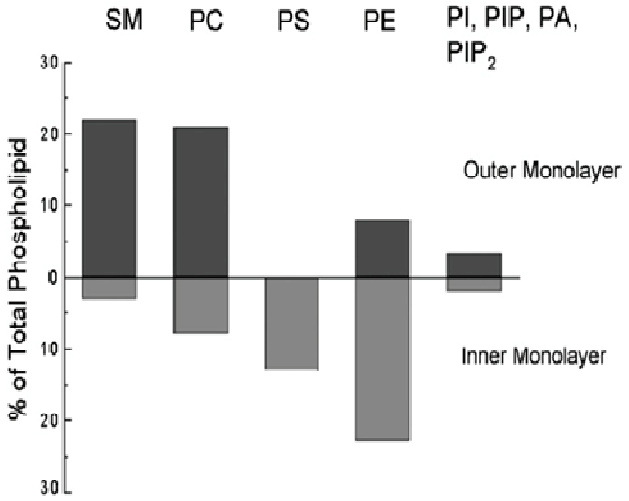


**Figure 4.** Distribution of lipids between the inner and outer leaflets of the cell plasma membrane (Hanshaw and Smith 2005).

This asymmetry is important to be maintained and this is achieved by the activity of ATP-dependent aminophospholipid translocase known as flippase that transports PS and PE from the outer to the inner leaflet (Williamson and Schlegel 1994). The most attractive example of disruption of membrane asymmetry is the exposure of PS to the surface of cells in the early stages of apoptosis.

# 2. Lipid rafts

## 2.1. Raft theory

Cell plasma structure is not static and rigid but is based on a dynamic clustering of several domains. In the last two decades, a new aspect of membrane structure was proposed, supported by the dynamic association of sphingolipids and cholesterol to constitute lipid domains which are called rafts, swimming in the bilayer considered as a "sea" with fluid properties. Rafts are thought to exist in the outer leaflet of the plasma membrane bilayer (Simons and Ikonen 1997). These domains constitute moving platforms allowing the incorporation of some proteins and excluding some others, so that they control protein-protein and protein-lipid interactions and also play a role in the signal transduction of the cell (Ikonen 2001).

## 2.2. Raft domain properties

Cell plasma membranes of polarized epithelial cells (Madin-Darby canine kidney; MDCK cells) triggered the concept of lipid domains, since the delivery to the membrane of newly synthesized lipids is highly regulated.

The apical pole of these cells is enriched in glycosphingolipids and its basolateral pole is enriched in phosphatidylcholine. Mixing up of these two kinds of lipids, which are both localized in the outer leaflet, is avoided by the presence of tight junctions separating the two poles of the cell (Meer 1989), (Simons and Ikonen 1997). Simons and van Meer assumed that the enrichment of glycosphingolipids in the apical pole resulted from a differential sorting of lipids. To explain this, they proposed that these glycosphingolipid clusters are formed already in the exoplasmic leaflet of the Golgi membrane which is known to be the center of delivery of proteins destined to the apical membrane (Simons and Van Meer 1988).

Moreover these lipid domains are able to bind proteins such as glycosylphosphatidylinositol (GPI)-anchored proteins which used these glycolipids as sorting platforms in the apical domains (Brown and Rose 1992). Also caveolae formed by caveolin, which are small invaginations of the membrane allowing the endocytosis of some molecules, are enriched in glycosphingolipids (Caveolin interacts with these domains, precisely with cholesterol). (Parton, Hanzal-Bayer et al. 2006), (Parton and Simons 2007).

Simons and Ikonen proposed in 1997 a model for sphingolipid-cholesterol raft organization.

They predict that sphingolipids associate laterally with each other, while gaps between them are filled with cholesterol. These close-packed associations of lipids constitute domains in the outer leaflet, surrounded by fluid domains containing unsaturated phosphatidylcholine (Simons and Ikonen 1997). In addition, biochemical studies further confirmed that these raft domains rich in cholesterol and sphingolipids exist in the outer leaflet, whereas cholesterol is associated with phospholipids with saturated fatty acyl chain in the inner leaflet (Fridriksson, Shipkova et al. 1999).

## 2.3. Isolation of rafts: detergent-insoluble complexes

Plasma membrane treatment at 4 ºC with the detergent Triton X-100 leads to two fractions: small micelles which are detergent-soluble, enriched in phosphatidylcholine and several proteins, and a non soluble fraction with large particles called detergent resistant membranes (DRM), enriched in cholesterol, sphingomyelin, GPI- anchor proteins and proteins active in cell signaling, which could be separated by gradient centrifugation (Schroeder, London et al. 1994), (Simons and Ikonen 1997), (Patra, Alonso et al. 1999), (London and Brown 2000). Additional indirect proofs of raft existence in plasma membrane were established. For example, depletion of cholesterol or sphingomyelin that perturb the function of several membrane proteins, suggests a raft-dependent functional organization within the cellular membrane (Jacobson and Dietrich 1999). However, it remains unclear how these detergent-resistant membranes (rafts) could be confirmed to be real (Munro 2003), (Shaw 2006), since detergents induce strong artifacts in the structure of membranes. Association of membrane lipids and proteins to detergents may lead to a new arrangement which can be different from the one existing in living organisms (Radeva and Sharom 2004). Moreover, the use of drugs, such as methyl-β-cyclodextrin that deplete cholesterol, a major component of the plasma membrane, could lead to side effects such as lateral protein immobilization (Zidovetzki and

Levitan 2007), (Kenworthy 2008). The only direct way to confirm the existence of rafts in biological membranes is to observe these domains in living cells, by microscopy.

**Table 1**. Biophysical studies of sphingolipid and cholesterol interactions (Simons and Ikonen 1997).

| Technique | Observation |
|---|---|
| Freeze-etch immune-electron microscopy | Clustreing of asialo-GM1 and Forssman glycolipids |
| Fluorescence microscopy | Co-capping of GM-3 and GM-1 gangliosides |
| Differential scanning calorimetry | Higher transition temperature for sphingolipids from the gel to liquid crystalline phase than for glycerolipids |
| Surface pressure-molecular area isotherm studiesof lipid monolayers | Increased packing density of sphingolipids and sphingolipid-cholesterol mixtures as compared to mixtures of glycerolipids |
| Fluorescence spectroscopy of non-perturbing fluorescence lipid probes | Sphingolipids from domains in liquid crystalline bilayers of unsaturated phosphatidylcholine |
| Spin-label electron resonance spectroscopy | Cholesterol associates more readily with sphingomyelin than with glycerolipids |
| Nuclear magnetic resonance spectroscopy | Self-association of cerobrosides |

Single particle tracking studies (Edidin, Zúñiga et al. 1994), (Kusumi, Sako et al. 1993), electron microscopy (Damjanovich, Vereb et al. 1995), and several other techniques suggested the existence of these domains (Table 1). Using confocal laser-scanning microscopy, rafts or aggregates of rafts could be observed; these domains being destroyed by depletion of cholesterol (Vereb, Matkó et al. 2000). The raft size was estimated to be < 50

nm in diameter suggesting that what was observed by fluorescence microscopy is aggregates of rafts (Pralle, Keller et al. 2000).

Also little was known about the stability of these domains till recent studies showing that lipid rafts in cell plasma membrane had a short life-time. The cellular rafts are much smaller than domains observed in artificial systems (Fig. 5). Moreover, they appear extremely dynamic structures that reshape when needed. So it is not possible to detect them because of the limited spatial resolution of conventional fluorescence microscopy with a lateral resolution about 200 nm, and the limited temporal resolution also. Their restructuration was first estimated to tens of seconds (Dietrich, Yang et al. 2002). These nanoscale rafts are thought to merge into larger and much more stable domains that are required in endocytic trafficking and signal transduction (Simons and Toomre 2000), (Hancock 2006), (Pike 2006), (Lingwood and Simons 2010), (Simons and Gerl 2010).

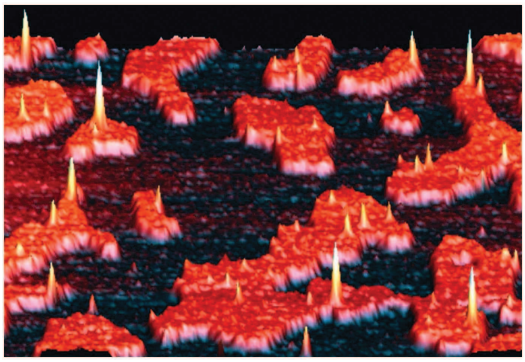

**Figure 5.** Lipid rafts (orange) with associated proteins (lighter peaks), swimming as icebergs on the surface of a sea of unsaturated lipids (dark) in a supported lipid bilayer (Saslowsky, Lawrence et al. 2002).

Recently, a very attractive evidence of rafts in biological membranes was achieved by Stimulated Emission Depletion microscopy STED, which breaks the diffraction limit of visible light, because its detection area can be limited in size, in contrast to classical confocal microscopy (Fig. 6a), by removing the fluorophore excitation from out of the focal point (Fig. 6b).

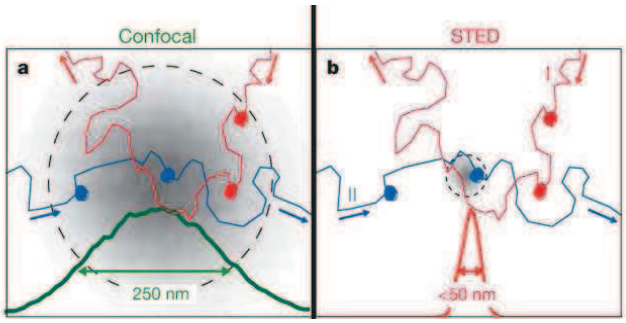


**Figure 6.** Advantage of the STED technique (b) over confocal microscopy (a) (Eggeling, Ringemann et al. 2009).

Combination of STED and fluorescence correlation spectroscopy provided a unique combination of temporal and spatial resolution, demonstrating the existence of small cholesterol enriched domains (~20 nm) surviving for 10-20 ms (Eggeling, Ringemann et al. 2009). Based on these novel details about membrane dynamics, the Singer-Nicholson paradigm should be better defined as a "dynamically structured mosaic model" (Vereb, Szollosi et al. 2003).

## 2.4. Phase transition and phase behavior of lipid mixtures

Cell plasma membrane is constituted by a mixture of lipids, proteins and carbohydrates. These molecules interact with each other by different physical forces such as van der Waals, electrostatic and hydrophobic forces, allowing together with the spontaneous self-assembly of lipids in aqueous media, to maintain the bimolecular sheet (Bagatolli, Ipsen et al. 2010). The Singer-Nicolson model suggested that under physiological conditions, functional cell membranes are mostly in fluid phase rather than in crystalline gel phase.

However, recent studies postulated that several parts of the membrane are not in fluid phase and that lipid bilayers show a number of phase transitions which played important roles (Holl 2008). In the context of lipid-domains, the main transition phase is the one which triggers the membrane from a solid phase with ordered lipid acyl chains to a liquid phase with disordered lipid acyl chains.

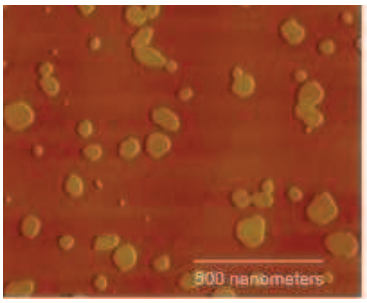


**Figure 7.** Atomic force microscopy image showing phase separation of lipid domains. Gel-phase (light) domains of a few nanometers are restricted on the surface of the fluid phase (dark). (*Lipid rafts observed in cell membranes-Image courtesy of the University of California at Davis) (https://www.llnl.gov/str/May07/Ratto.html)*.

In 1975, Chapman and his group performed a number of experiments in order to determine the phase transition characteristics in biological membranes. They concluded that the modulation of membrane fluidity, by the gel-solid phase transition, had some effects on membrane properties such as membrane permeability, receptor clustering and cell signaling (Chapman 1975). Discovering the phase behavior of lipid mixtures in cell membrane was challenging because bilayer phases cannot be separated physically from each other and analyzed chemically (Fig. 7). To limit the complications related to biomembrane complexity, giant unilamellar vesicles (GUVs) of around 20 μm in diameter, with a defined lipid composition and labeled with fluorescent dyes, were used as simple model systems for domain imaging using fluorescence microscopy (Veatch and Keller 2005).

Biophysical studies on model membranes consisting of three lipid components (Cholesterol, SM and PC), showed the existence of three different phases: gel phase, liquid ordered phase Lo and liquid crystalline or fluid phase Ld (Fig. 8). In the gel-solid phase which is highly ordered, lipids are immobile, and do not allow diffusion of membrane proteins (Maxfield and Tabas 2005). Above their melting point, lipids adopt the fluid phase and form loosely packed structures. Thus, heating the lipid bilayer induces a transition from gel-solid phase with ordered arrangement to a fluid phase with disordered acyl-chain arrangement (Ld). In the presence of cholesterol and lipids with saturated long acyl-chains, a third phase appeared, defined as liquid-ordered phase (Lo) (Lindner and Naim 2009). The coexistence of Lo and Ld in GUVs, is used as model for raft and non-raft domains, respectively (Feigenson and Buboltz 2001). In fact, the gel-phase is not observed in mammalian cells as it requires pure

unsaturated lipids. Thus, there are mainly two relevant fluid phases coexisting in the plasma membrane: the Lo and Ld phases (Simons and Gerl 2010).

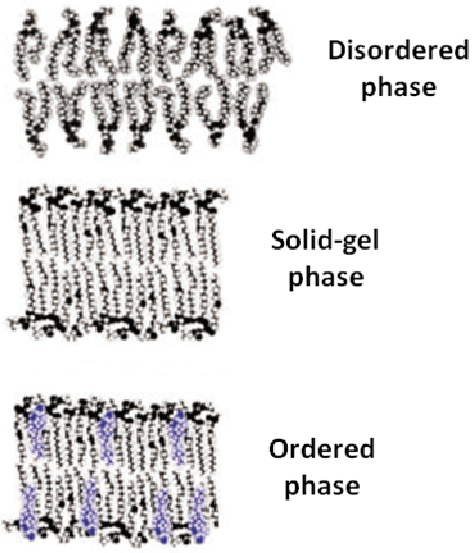


**Figure 8.** Scheme of the different lipid phases (Feigenson 2006).

In vitro, the transition temperature of a lipid bilayer from a gel to fluid phase depends mainly on the length and saturation of the fatty acyl chain. At 37°C, most of glycerophospholipids are in a fluid phase (transition temperature about 0°C), whereas sphingomyelins having long acyl chain (temperature of transition between 40 and 50°C) mainly exist in the gel phase (Schroeder, London et al. 1994). Since the rafts contain sphingolipids and phospholipids with saturated fatty acyl chains (Pike 2003), they exist in a less fluid phase than the surrounding area.

Moreover, another study showed that cholera toxin can induce phase transition in ternary mixtures of PC, SM and cholesterol (Hammond, Heberle et al. 2005). Since cell membranes are not at equilibrium, as a result of the the perturbations caused by the lipid metabolism, lipid transporters, and membrane traffic, the phase separation in plasma membrane is a dynamic phenomenon controlled by the lipid and protein composition (Simons and Gerl 2010).

## 2.5. Enzyme activity: a way to disrupt lipid rafts?

The bacterial enzyme cholesterol oxidase is an enzyme that catalyzes oxidation and isomerization of cholesterol to cholest-4-en-3-one (Lange and Ramos 1983), (Vrielink, Lloyd et al. 1991). It participates in the bacterial metabolic pathway, when bacteria utilize

cholesterol as their carbone source. The enzyme is secreted by Gram-positive soil bacteria. This enzyme is used frequently to detect serum cholesterol levels. The *Streptomyces* enzyme was the most used since it is easy to handle.

The catalytic activity of cholesterol oxidase (from *Streptomyces sp.*) was determined in cholesterol-containing mixed monolayers (Gronberg and Slotte 1990) and lipid bilayers (Ghoshroy, Zhu et al. 1997). Cholesterol oxidase association to the lipid bilayer does not affect the lipid bilayer enough to induce pore formation (Kreit, Lefebvre et al. 1992), (Kreit and Sampson 2009). Therefore, fluorescent membrane probes can be used with no risk of dye leakage, in the presence of this enzyme.

Another important enzyme tool is sphingomyelinase (SMase), which is a hydrolase enzyme involved in sphingolipid metabolism (Fuhrmann, Dobeleit et al. 2002), responsible for hydrolyzing sphingomyelin into phosphatidylcholine and ceramide. The latter is believed to have an important role in signal transduction, notably in cell proliferation, cell differentiation, and apoptotic cell death (Hannun 1996). Different types of SMase exist, mainly divided into neutral and acid SMases. Studies in giant vesicles to evaluate the effect of conversion to ceramide on the assembly of lipid microdomains, speculate that in vivo SM to ceramide conversion can alter the assembly of lipid microdomains in the biological membranes (Taniguchi, Ohba et al. 2006).

Thus, these two enzymes appear as good candidates to induce modifications in lipid raft domains.

## 2.6. Roles of rafts

The lipid organization of membranes can have profound effects on cellular functions such as signal transduction and membrane trafficking. Cholesterol, one of the essential actors in this organization is an important regulator of these functions at the level of rafts (cholesterol-enriched domains). In this section, some possible roles of rafts in cellular functions will be reviewed.

2.6.1. **Biosynthetic traffic to the plasma membrane:** Sphingolipid-cholesterol rafts are thought to play a role in the traffic of proteins to the plasma membrane. In the case of MDCK polarized cells, GPI-anchored proteins and apical transmembrane proteins are redirected preferentially to the apical domains, having GPI anchors

(Lisanti and Rodriguez-Boulan 1990) and membrane-spanning regions (Kundu, Avalos et al. 1996) as apical sorting signals, respectively. Other proteins are delivered to the basolateral part depending on different signals such as tyrosine and dileucine motifs (Matter and Mellman 1994). Even non-polarized cells, fibroblasts show different sorting routes from the trans-Golgi network to the plasma membrane and contain cholesterol-sphingolipid enriched domains (Yoshimori, Keller et al. 1996), (Danielsen and van Deurs 1995).

2.6.2. **Endocytic traffic:** Sphingolipid-cholesterol rafts are involved in transporting proteins by endocytic pathways (Simons and Ikonen 1997). Moreover, caveolar endocytosis and transcytosis can be inhibited by agents that bind cholesterol (*e.g.* filipin) (Rothberg, Ying et al. 1990), (Schnitzer, Oh et al. 1994). Also, several toxins (Shiga toxin, cholera toxin) and viruses (polyoma virus Simian virus 40 SV40), bind glycosphingolipids and are then internalized by a glycosphingolipid-mediated process.

2.6.3. **Secretion regulation:** In different secretory cells, the biogenesis of secretory granules takes place in the trans-Golgi network and then, these cargos are delivered to the cell surface (Tooze 1998). Many studies evidenced that this secretion is raft-dependent, since depletion of cholesterol (Wang, Silver et al. 2000) or inhibition of glycosphingolipid synthesis (Schmidt, Schrader et al. 2001) reduced formation of secretion vesicles in many cell types.

2.6.4. **Membrane signaling:** Many proteins cluster in lipid domains before they become activated. So, one the main functions of rafts could reside in their ability to concentrate receptors, which can interact with ligands on one side, and effectors on the opposite side of the cell membrane (Simons and Ikonen 1997). Also many protein activities depend on cholesterol and sphingolipids that can modulate the binding affinity to their ligand (Klein, Gimpl et al. 1995).

2.6.5. **Virus budding:** Some viruses such as HIV (Waheed and Freed 2009) and influenza (Scheiffele, Rietveld et al. 1999), which acquire a membrane envelope when they bud off from the host cell plasma membrane are suggested to involve lipid rafts. In the case of HIV, the Gag protein binds to the plasma membrane, inducing the formation of rafts platforms. Multimerization of Gag drives the

assembly of the rest of the viral particle, followed by the budding process and then, the release of the viral particle from the plasma membrane (Simons and Gerl 2010). Moreover, if labeled cholera toxin known to bind GM1 confined in raft domains, is used to mark the HIV-expressing cells and the virus, some patches are observed which are different from clusters of non-raft transferrin receptors (Waheed and Freed 2009). All these data suggest that the assembly of the virus envelope is raft-dependent.

### 2.7. Lipid rafts and diseases

Since lipid rafts are thought to be essential for biological functions, it is not surprising that their possible involvement in several pathologies has been reported (Maxfield and Tabas 2005). For instance, lipid rafts may play a role in Alzheimer's disease, as amyloid-ß peptide aggregates and form plaques at the level of rafts (Cordy, Hooper et al. 2006). Possible involvement of rafts in prostate cancer (Freeman, Cinar et al. 2005), hypertension (Callera, Montezano et al. 2007), Parkinson's disease (Fortin, Troyer et al. 2004), autoimmune (Jury, Kabouridis et al. 2004), (Krishnan, Nambiar et al. 2004), and infectious pathologies (Luo, Wang et al. 2008) has also been reported, though further work is awaited to further clarify the role of rafts in these pathologies. Thus, lipid domains may constitute a potential target for pharmacological assays (Michel and Bakovic 2007).

## 3. Apoptosis

### 3.1. Overview

The apoptosis term originates from the Greek, meaning "to fall away from". This phenomenon is highly investigated in biology since 1990s, constituting 2% of all life science publications every year. Apoptosis is the process of programmed cell death that occurs in multicellular organisms. Daily, a large number of cells undergo apoptosis and the whole process of apoptosis in a given cell is believed to take about one hour in vivo (Curtin and Cotter 2003). Apoptosis is constituted by a combination of morphological and biochemical events, distinct from necrosis which is considered as the passive, premature traumatic cell death caused by external factors such as infection, toxins and physical or chemical trauma. Apoptosis is highly beneficial to the organism, in sharp contrast to necrosis where the release of the intracellular contents results in inflammation. During necrosis, early changes in the

mitochondrial shape and function are observed as well as major damages of the cell plasma membrane.

The triggering factors for apoptosis differ from one cell type to another. In some cases, the triggering signal is an external stimulus, such as growth factors or hormones. During neutrophil turnover, the autonomous timing of death is controlled by this physiological phenomenon. Moreover, during the formation of organs, many cells are produced in excess, and thus undergo programmed cell death, in order to contribute to the sculpture of functional organs and tissues. As an example, apoptosis takes place between fingers and toes during the development of human embryo, resulting in the separation of the latter (Fig. 9). So apoptosis acts as a kind of a quality-control in the organism (Meier, Finch et al. 2000).

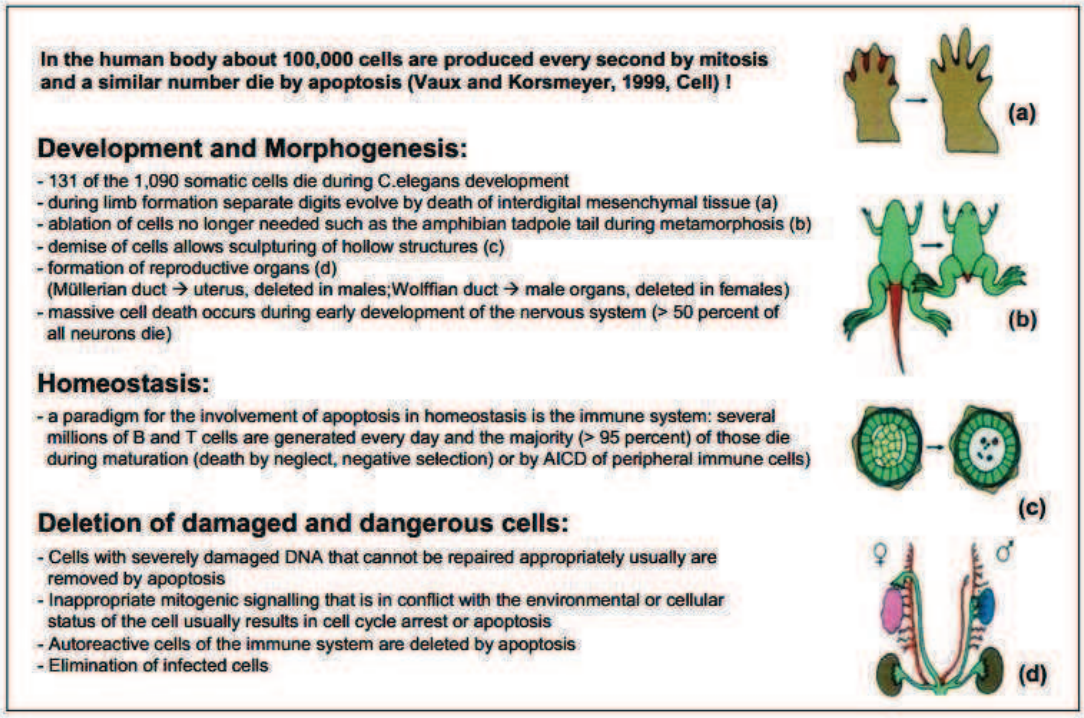


**Figure 9.** Examples of physiological apoptosis (*Introduction to Apoptosis, Aporeview).*

Apoptosis is also essential for organism homeostasis to keep always a correct balance between the increase of cell number related to cell proliferation and the need to destroy old and defective cells, in order to maintain the functional and structural integrity of tissues and organs (Erickson 1997).

The regulation of apoptosis is very tight, since its defect leads to many diseases including cancer, heart failure, neurodegenerative and auto-immune diseases (Reed 2000).

## 3.2. Morphological features of apoptosis

Apoptosis is a morphological phenomenon, the changes in cell undergoing apoptosis involve cell shrinkage, membrane blebbing with fragmentation of the cell into small compact-enclosed structures called apoptotic bodies which are cleared by phagocytosis without any inflammatory effects, and nuclear modifications such as chromatin condensation and nuclear fragmentation. All these changes happened on a background of persistent integrity of the plasma membrane, clearly different from necrosis where membrane fragmentation occurs from the beginning (Fig. 10). These morphological events are the consequence of biochemical events involving fragmentation of DNA related to an endonuclease activation in response to apoptotic stimuli (Wyllie 1980). In contrast during necrosis, the intracellular content is released in an uncontrolled way into the cell environment which results in damages of surrounding cells and a strong inflammatory response in the corresponding tissue (Leist and Jaattela 2001).

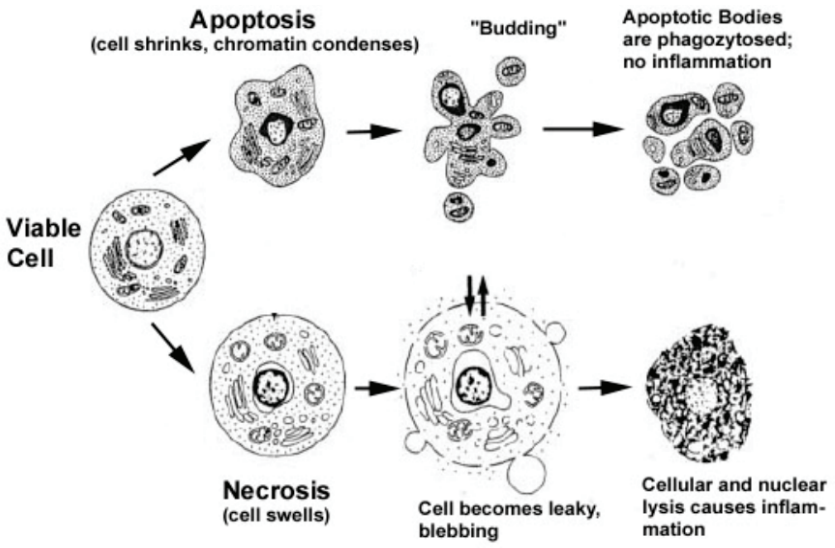


**Figure 10.** Hallmarks of apoptotic and necrotic cell death process modified from (Van Cruchten and Van Den Broeck 2002).

## 3.3. Molecular mechanisms of apoptosis

All changes occurring during apoptosis are caused by the activation of a family of intracellular proteases which cleave their substrates at aspartic acid residues, called caspases for Cystein Aspartyl-specific Proteases (Alnemri, Livingston et al. 1996). Initially, these proteins exist as inactivated zymogens (proenzyme or inactive enzyme precursor) that can be activated by various stimuli (Fig. 11), resulting in the cleavage of the zymogen in two subunits. The active enzyme is a heterotetramer with two large and two small subunits (Thornberry and Lazebnik 1998). Caspases cleave their substrates at Asp residues and are also activated by the same process; suggesting that the process can be viewed as a cascade-like sequence of events (proteolytic cascade effect of caspases) (Reed 2000). Till now, 14 caspases were characterized in humans and mice, which can be divided into two classes: initiator caspases and effector caspases (Salvesen and Dixit 1997).

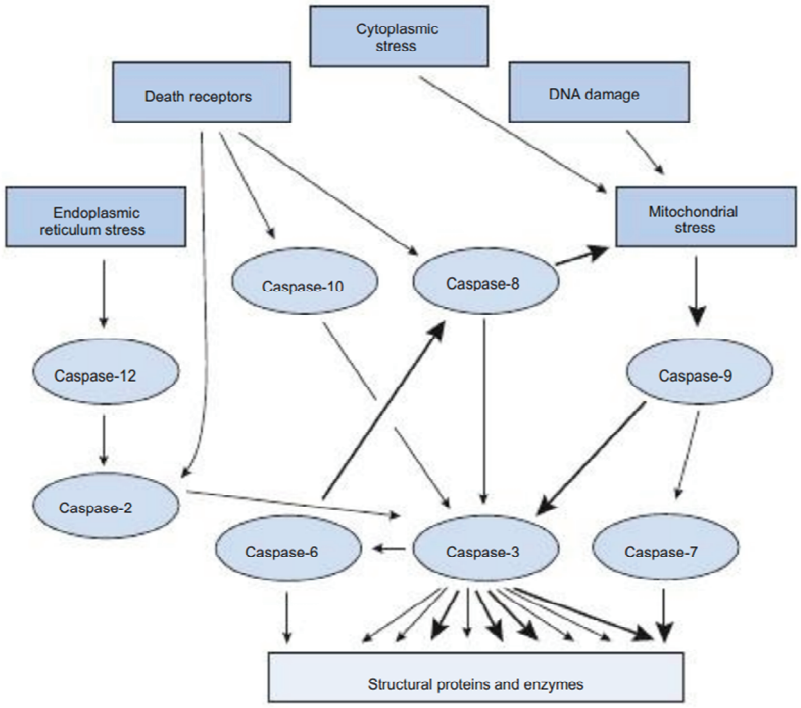


**Figure 11.** Ilustration of caspases as central components of apoptosis in response to different stimuli (Curtin and Cotter 2003).

Initiator caspases (caspase-2, caspase-8, caspase-9, caspase-10 and caspase-12) sense cellular stress signals from different sources. They are able to cleave and activate effector caspases either directly or indirectly. Effector caspases, including caspase-3, caspase-6 and caspase-7,

cleave a variety of downstream target proteins as protein kinases, cytoskeletal proteins, DNA repair proteins and inhibitory subunits of endonucleases (Thornberry and Lazebnik 1998), (Salvesen and Dixit 1997).

Often, the signal of apoptosis comes from the environment, for example, from the tumor necrosis factor (TNF) family receptors (Wallach, Varfolomeev et al. 1999). Other signals required the involvement of mitochondria, resulting in the release of caspase-activating proteins in the cytoplasm. Thus, there are mainly two pathways of apoptosis, death receptor and mitochondrial also known as extrinsic and intrinsic pathways, respectively (Fig. 12).

The TNF family of cytokine receptors (TNFR1, Fas…) contains death domains in their cytosolic regions. Defects in the regulation, structure or function of these death proteins are known to be correlated with many human diseases such as hypoxia of cardiomyocytes which cause elevation in Fas expression resulting in apoptosis induction (Tanaka, Ito et al. 1994).

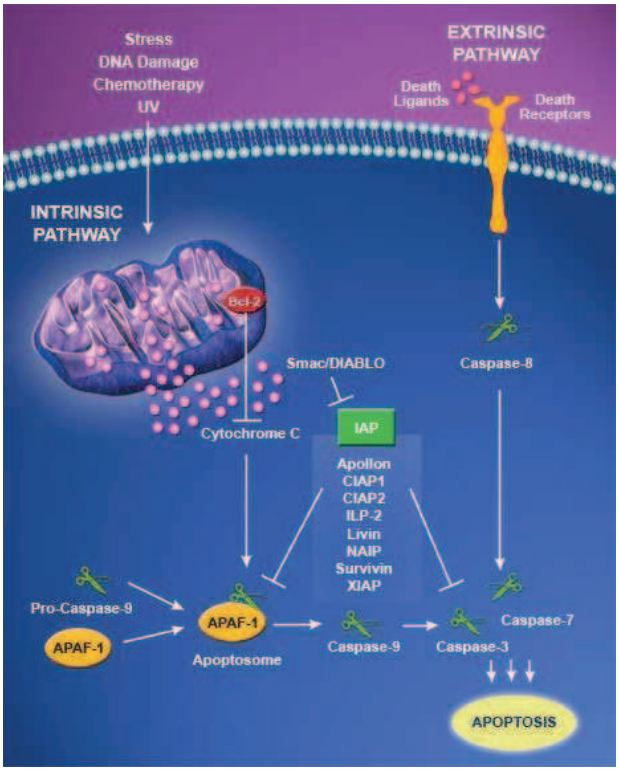


**Figure 12.** Representation of two of the major pathways for caspase activation in mammalian cells, the intrinsic (left) mithochondria-mediated and the extrinsic (right) receptor-mediated, initiated by binding of death ligands to death receptors, (*http://imgenex.com/view_data_page.php?id=168*).

Mithochondria are sensitive to many different stimuli (radiation, stress, DNA damage, chemotherapy, hypoxia, etc), and this mithochondria-dependent pathway is related to the Bcl-2 protein family (Vaux, Cory et al. 1988), which is highly conserved throughout the evolution. Mithochondria dysfunction is correlated with pore formation, which allows the release of various proteins in the cytosol such as cytochrome c involved in the oxidative phophorylation of the mithochondria membrane. This release is associated with the recruitement and activation of a cascade of caspases (Liu, Kim et al. 1996).

There is an additional pathway that involves T-cell mediated cytotoxicity and perforin-granzyme-dependent killing of the cell. The perforin/granzyme pathway can induce apoptosis via either granzyme B or granzyme A. The extrinsic, intrinsic, and granzyme B pathways converge on the same execution pathway (Elmore 2007).

## 3.4. Apoptosis cascade

The apoptosis process is complex and requires the involvement and regulation of many proteins at different levels (Fig. 13).

1. Apoptosis induction is initiated by specific ligand-receptor interactions including binding of TNFα to its receptor TNF-R1 as well as Fas-ligand to Fas-Receptor (Fesus 1993).

2. Ligand-Receptor association contributes to the formation of a death inducing signalling complex (DISC), directly connected to the activation of initiator caspases such as caspase-8 (Hirata, Takahashi et al. 1998), (Kruidering and Evan 2000).

3. Initiator caspases are responsible for the first proteolytic events such as cleavage of cytoskeletal related proteins including vimentin (van Engeland, Nieland et al. 1998) and actin (Kayalar, Ord et al. 1996). These early apoptotic events are suspected to be the major cause of the blebbing of the cell surface (McCarthy, Rubin et al. 1997).

4. Cleavage of flippase and/or activation of scramblase lead to a flip of phosphatidylserine from the inner to the outer leaflet.

5. Since initiator caspases act upstream on the top of the caspase cascade (Cohen 1997), they are able to cleave and activate other caspases called effector caspases.

6. Execution phase of apoptosis is marked by the activation of effector caspases, which are regulated by the bcl-2 family of mitochondrial proteins. Once activated, these effectors cleave a broad range of proteins which are critical for cell survival.

Late or final apoptosis events include down-regulation of transcription, fragmentation and condensation of DNA, alteration of the nuclear and cellular shape resulting finally in the cellular collapse.

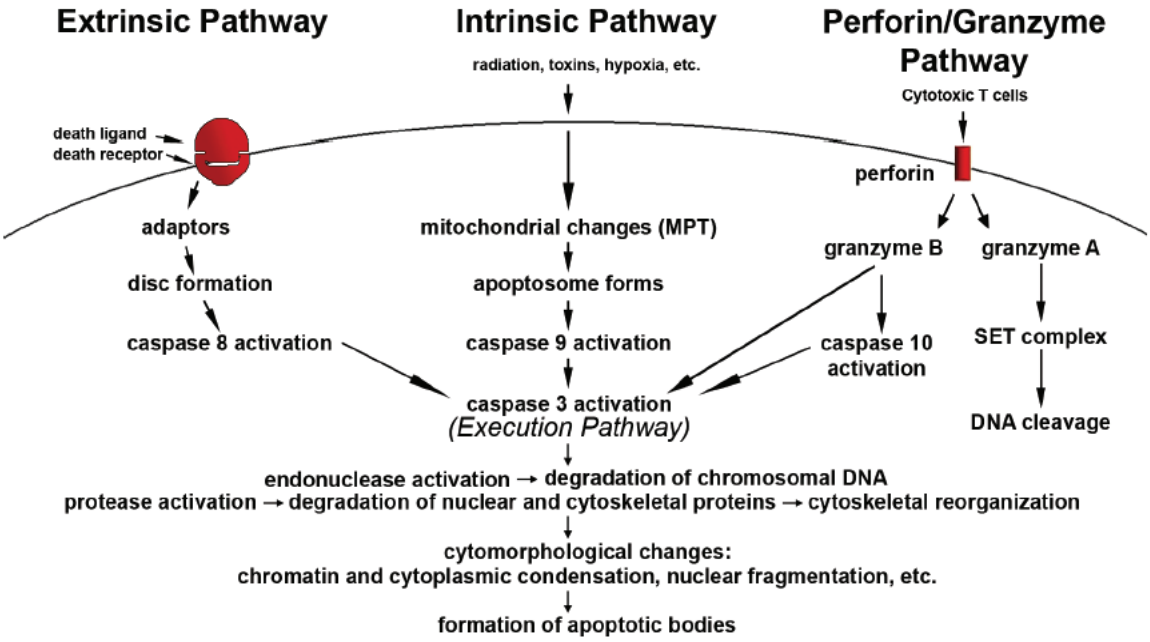


**Figure 13.** Schematic representation of apoptotic events (Elmore 2007).

The failure of cell to undergo apoptosis is thought to be involved in a variety of human diseases and viral infections (Bursch, Oberhammer et al. 1992). In addition, several diseases resulted from accelerated rates of physiological cell death such as AIDS, osteoporosis and neurodegenerative disorders (Ameisen and Capron 1991), (Groux, Monte et al. 1991). So many therapies are aimed at enhancing or inhibiting the capacity of individual cell types to undergo apoptosis.

## 3.5. Apoptosis assays

Since apoptosis is a physiological phenomenon essential for organism homeostasis, its analysis is of key interest for many fundamental and clinically investigations. Therefore, a number of techniques and technologies with the aim to detect its occurrence were developed.

The most used techniques for detection of apoptotic cells can be separated into different groups:

1. The first group of assays can be described as cytomorphological studies using different types of microscopy. Light microscopy allows the visualization of apoptotic cells, using tissue-stained sections. This methodology depends on the nuclear and cytoplasmic condensation that occurs during apoptosis (Elmore 2007). Transmission Electron microscopy can also be applied to detect apoptosis based on the ultrastructural morphological characteristics of apoptotic cells, which present a dense nucleus with nuclear fragmentation, intact cell membranes, disorganized cytoplasmic organelles, large clear vacuoles, and blebs at the cell surface (White and Cinti 2004). In addition, fluorescence microscopy can be also applied using Propidium Iodide and DAPI, which are able to cross the plasma membrane and stain the nucleus of late apoptotic cells only. The main disadvantage of these techniques is their inability to detect early stages of apoptosis.

2. The second group of assays includes DNA degradation analysis. As an example, the DNA laddering technique (Wyllie 1980) results in a characteristic "DNA ladder" with each band separated in size by approximately 180 base pairs. The TUNEL method (Terminal transferase-mediated dUTP nick-end labeling) is used to assay the endonuclease cleavage products by end-labeling the DNA strand breaks by the terminal transferase which is able to add labeled UTP to the 3'-end of the DNA fragments (Kressel and Groscurth 1994). These methods are subject to false positives from necrotic cells and cells in the process of DNA repair and gene transcription. For these reasons, they should be paired with another assay.

3. The third class of apoptosis assays is based on apoptosis associated proteins, such as caspases, their cleaved substrates, as well as regulators and inhibitors of these proteins (Nagata 1997), (Thornberry and Lazebnik 1998), (Chan and Mattson 1999), (Packard, Komoriya et al. 2001). Luminescent and fluorescent assays are used for measuring caspase activity and detecting active caspases using antibodies. Western blot, immunoprecipitation and immunohistochemistry are also used.

4. Mitochondrial assays can also be used as tools to detect apoptosis using mitocondrial dyes to measure the redox potential or the metabolic activity of mitochondria in cells (Zamzami, El Hamel et al. 2000)..

5. Finally, assays based on membrane alterations are also used to monitor apoptosis. These alterations could notably be detected by fluorescently-labeled annexin V (Koopman, Reutelingsperger et al. 1994), using fluorescence microscopy and flow cytometry (Vermes, Haanen et al. 1995). Annexin V binds specifically to apoptotic cells, due to the exposure of PS on their cell surface.

All techniques mentioned above are employed as diagnostic tools for identifying apoptosis, but each assay presents disadvantages that render it acceptable for one application but imperfect for others (Watanabe, Hitomi et al. 2002), (Otsuki, Li et al. 2003). So one assay is not enough and it is important to use more than one independent method before concluding that apoptosis is occurring. The use of different methods is also compulsory to study apoptosis at different stages (early, intermediate or late) of the pathway(s) under investigation.

## 3.6. Membrane changes in apoptotic cells

Generally, viable eukaryotic cells maintain an asymmetric repartition of phospholipids between the inner and outer leaflets of the lipid bilayer (Otsuki, Li et al. 2003). A number of proteins (flippase, floppase and scramblase) work in concert to regulate the membrane lipid asymmetry (Zwaal and Schroit 1997) (Fig. 14). Plasma membrane asymmetry is notably maintained in intact cells by flippases which are membrane proteins capable of translocating specific lipid molecules from the outer leaflet to the inner leaflet (Higgins 1994) together with floppase and scramblase which are nonspecific to the lipid type. Floppase is an ATP-dependent enzyme which slowly transports lipids from the inner to the outer leaflet and scramblase is a $Ca^{2+}$ -dependent enzyme which allows lipids to move randomly between leaflets. During apoptosis, phosphatidylserine which is normally confined to the inner side, flips and becomes abundant in the outer leaflet in a stimulus-independent manner (Fadok, Savill et al. 1992), (Fadok, Voelker et al. 1992), (Fadok, Laszlo et al. 1993).

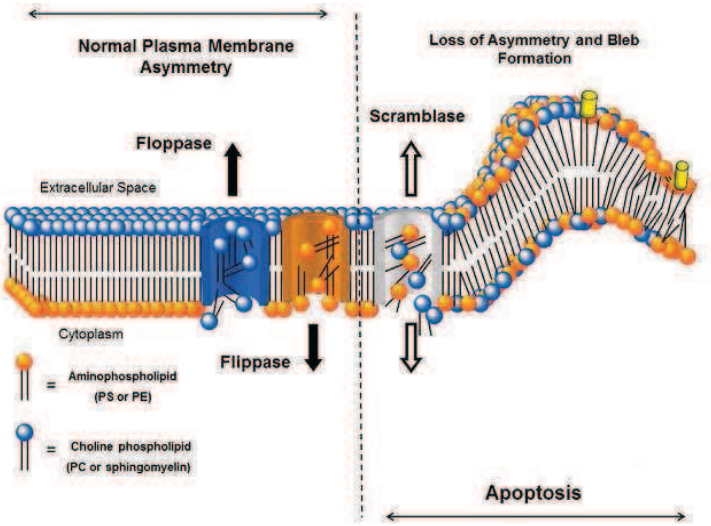


**Figure 14.** Changes in cell membrane organization during apoptosis (Blankenberg and Norfray 2011).

Membrane changes result in the recognition of apoptotic cells by macrophages and uptake of dying cells by phagocytosis (Morris, Hargreaves et al. 1984), (Duvall, Wyllie et al. 1985). Since PS exposure is observed before the manifestation of morphological changes associated to apoptosis processing, this event is considered as a "flag" on the surface of dying cells to be (Newman, Henson et al. 1982), (Zwaal and Schroit 1997). PS exposure has been described as an "eat-me" signal (Ren and Savill 1998). PS being the main anionic phospholipid component of the plasma membrane, its externalization results in the creation of anionic charge on the membrane surface (Cerbon and Calderon 1991) and it seems that PS exposure lasts from the early stages of apoptosis till the final stage, when the cell breaks up into apoptotic bodies.

### 3.6.1. Annexin V and detection of PS

Loss of membrane asymmetry could be used to detect cellular death. The externalization of PS can be detected via Annexin V in tissues, embryos and cultured cells. Annexin V is a phospholipid binding protein that binds with high affinity to PS in the presence of calcium. In intact cells, which do not have PS on the cell surface, Annexin V is not able to bind these cells, but, if a cell is undergoing apoptosis , this binding protein will recognize and attach to the externalized PS molecules (Bossy-Wetzel and Green 2000) (Fig. 15).

Annexin V protein is usually conjugated to a fluorescent molecule such as fluorescein isothiocyanate (FITC), so that apoptotic cells can be visualized using fluorescent microscopy and flow cytometry. The main advantage of this technique is its sensitivity (able

to detect a single apoptotic cell). In vivo or in situ detection of apoptotic cells has become feasible by injecting biotin-labeled Annexin V in the bloodstream of animals to be examined. However, it presents the disadvantage to not discriminate apoptotic from necrotic cells. So a critical control is needed by checking the membrane integrity of the phosphatidylserine-positive cells.

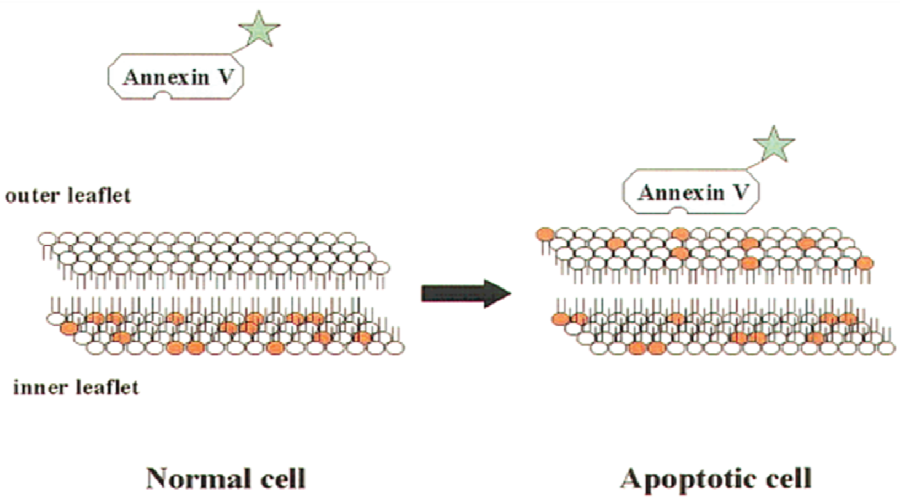


**Figure 15.** Schematic representation of the loss of membrane lipid asymmetry during apoptosis. Labeled Annexin V can bind with high affinity to the exposed PS in the presence of $Ca^{2+}$ (van Engeland, Nieland et al. 1998).

Indeed, during necrotic cell death, the membrane integrity is disrupted. This can be tested by staining cells with membrane impermeable DNA dyes such as propidium iodide and trypan blue. Both molecules are not able to pass through intact plasma membrane, so that it is no possible to stain nuclei unless the plasma membrane integrity is lost. In cells undergoing early stages of apoptosis, but conserving the membrane integrity, exclusion of these dyes is observed (Elmore 2007). So combination of Annexin V with a membrane integrity probe is needed to discriminate apoptosis from necrosis. Viable, early apoptotic and necrotic or late apoptotic cells can thus be distinguished. PI is excluded from viable intact cells which are also FITC-negative (no PS on the surface). Early apoptotic cells are FITC-positive cells/ PI-negative (PS on the surface). Late apoptotic cells are PI-positive/FITC-Annexin V-positive due to the necrotic-like disintegration of the cell membrane.

For the quantification of Annexin V-positive apoptotic cells, flow cytometry can be applied using cell suspensions.

However, this technique presents several limitations, since Annexin V is an expensive protein, and shows several experimental drawbacks.

1. A high concentration of extracellular $Ca^{2+}$ is required for efficient binding of Annexin V to PS, which prevents its use in a medium with low Ca2+ concentration. Moreover, $Ca^{2+}$ ions activate the scramblase protein which also acts on PS flipping to the cell surface, leading to false positives in application of this method (Williamson, Kulick et al. 1992).

2. Annexin V can bind cell membranes that contain by-products of lipid peroxidation, so Annexin V binding cannot be used as an exclusive indicator of cell surface PS exposure and raise the possibility that some false positive attributed to PS exposition may also be due to the presence of lipid peroxidation products (Balasubramanian, Bevers et al. 2001).

3. Detergents in the medium can also change the Annexin V binding specifity *e.g* presence of negative surface charge on medium nonspecifically increases the $Ca^{2+}$ concentration near the cell surface and may also directly enhances the affinity of Annexin V for phospholipids (Meers and Mealy 1993), so it leads to an over-estimation of PS exposure.

4. Cell harvesting techniques such as trypsinization for adherent cells can also produce false positives, since during these steps, membrane changes with PS exposure at the outer plasma membrane occur (van Engeland, Nieland et al. 1998).

5. In addition, this approach presents time limitations since pre-incubation time for efficient Annexin V binding is up to one hour, while other methods are able to monitor phospholipid scrambling with shorter incubation times (Zweifach 2000).

All these disadvantages of Annexin V in sensing the exposure of PS related to apoptosis, confirm the need of alternative methods to detect membrane changes during cell death.

### 3.6.2. Alternative methods of apoptosis detection based on membrane changes

Using monoclonal antibodies against negatively charged lipids was applied as an alternative tool to detect apoptosis (Miyazawa, Inoue et al. 1992). However, this approach shows some limitations because antibodies are expensive and require a complicated protocol. In addition, their binding to membranes inhibits the $Na^+/K^+$-ATPase activity, so they affect the membrane (Stekhoven, Tijmes et al. 1994). For this reason, synthetic peptides derived from a monoclonal antibody, PS4A7, which binds to PS were developed. Sequences of new synthetic peptides keep only the PS-recognizing peptide motif of the antibody, which allows its specific binding to PS exposed at the surface of apoptotic cells (Igarashi, Asai et al. 1995).

Another approach is to monitor the lipid exchange between leaflets using fluorescent labeled lipids (Connor and Schroit 1988), but this is not well tolerated by cells since treatment with exogenous PS induce apoptosis in a dose-dependent manner (Uchida, Emoto et al. 1998).

Other strategies to monitor apoptotic cell membranes include small molecules which are able to sense changes in plasma membrane. These small molecules correspond to fluorescent dyes such as FM1-43 FX, a cationic dye that binds better to membranes with negative charges (apoptotic cells) than intact healthy cells (Zweifach 2000).

Merocyanine dyes also can be included in this section. The Merocyanine dye MC 540 is sensitive to membrane composition and its binding increases when cells become apoptotic (Laakko, King et al. 2002).

Also, small molecules capable to imitate Annexin V were designed. The binding of these molecules ($Zn^{2+}$ coordinated complexes) to PS is supported by the $Zn^{2+}$ affinity to PS. These fluorescent probes allow apoptosis detection in $Ca^{2+}$-free conditions, with fast binding kinetics compared to Annexin V (Hanshaw, Lakshmi et al. 2005), (Hanshaw and Smith 2005).

Additional strategies for detecting apoptosis based on changes in the plasma membrane involve binding to apoptotic cells by cationic labeled liposomes (Bose, Tuunainen et al. 2004). These cationic liposomes were found to homogeneously stain the membranes of apoptotic cells through electrostatic interactions with the anionic phospholipids PS.

Moreover, Heyder et al. designed a FITC-labeled lectin conjugate from *Narcissus pseudonarcissus*. This molecule can detect apoptosis through the cell surface exposure of the modified carbohydrate species that appear during early apoptosis (Heyder, Gaipl et al. 2003).

This most widely used techniques to detect membrane changes during apoptosis show the need of more simple, fast, low-cost and challenging procedures to detect these modifications. Probably, the most attractive tool to monitor membrane changes related to apoptosis is the use of fluorescent dyes.

### 3.6.3. Fluorescent membrane probe: F2N12S detection assay

Fluorescent membrane probes are considered as promising tools to detect changes in the plasma membrane on apoptosis. An interesting example in this respect is the probe F2N12S, developed in our laboratory (Shynkar, Klymchenko et al. 2007).

F2N12S belongs to the family of 3-hydroxyflavone dyes, which exhibit an excited-state intramolecular proton transfer reaction (ESIPT) leading to a dual fluorescence emission, so it shows two emission bands. Ratio of these two bands called N* band and T* band respectively, can be performed, so a two-color ratiometric response can be detected. This probe incorporates selectively into the outer leaflet of plasma membranes and is able to sense the loss of plasma membrane asymmetry related to apoptosis. Details about F2N12S structure, properties and characteristics will be presented later in the Chapter 5.5.

Many techniques such as fluorescence spectroscopy, flow cytometry and fluorescence microscopy were able to report that the ratio of the two emission bands of F2N12S changes significantly in response to apoptosis. Ratiometric response is easy to perform and allows detecting the spatial distribution of apoptotic changes in the plasma membrane.

Moreover, recent studies using F2N12S to stain vesicles and living cells showed that this dye senses the lipid order in cell membranes (Oncul, Klymchenko et al. 2010). After extraction of cholesterol using methyl-ß-cyclodextrin, a loss of liquid ordered Lo phase was observed (change of the ratio N*/T* of the dye in the same direction as vesicles in liquid disordered phase Ld). This effect correlates well with the ratiometric response after apoptosis induction.

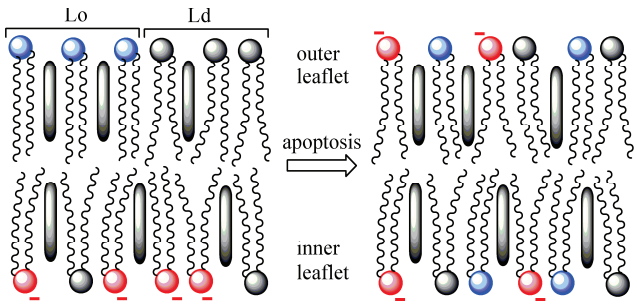


**Figure 16.** Simplified model of the loss of transmembrane asymmetry during apoptosis.

These data suggest that during apoptosis, the loss of lipid asymmetry of the plasma membrane might result also in a loss of the Lo phase in the outer leaflet (Fig. 16) in addition to an increase in the negative charge related to the PS exposure to the surface.

This assay using fluorescent probe constitutes an easy and efficient way for apoptosis detection. The procedure for application of this dye is simple, with 5 minutes staining protocol and no special buffer. Also, there is no damage and false positive results related to cell preparation and harvesting of adherent cells, as in the case of annexin V. But this technique suffers from the relatively low photostability of this dye that limits its use for continuous fluorescence imaging.

## 4. Endocytosis: Transport into the cell from plasma membrane

Animal cells have particular pathways to transport molecules from the external environment to their interior and from internal compartments to the cell surface (Willingham and Pastan 1984). These pathways related to the membrane trafficking include endocytosis and exocytosis (Fig. 17).

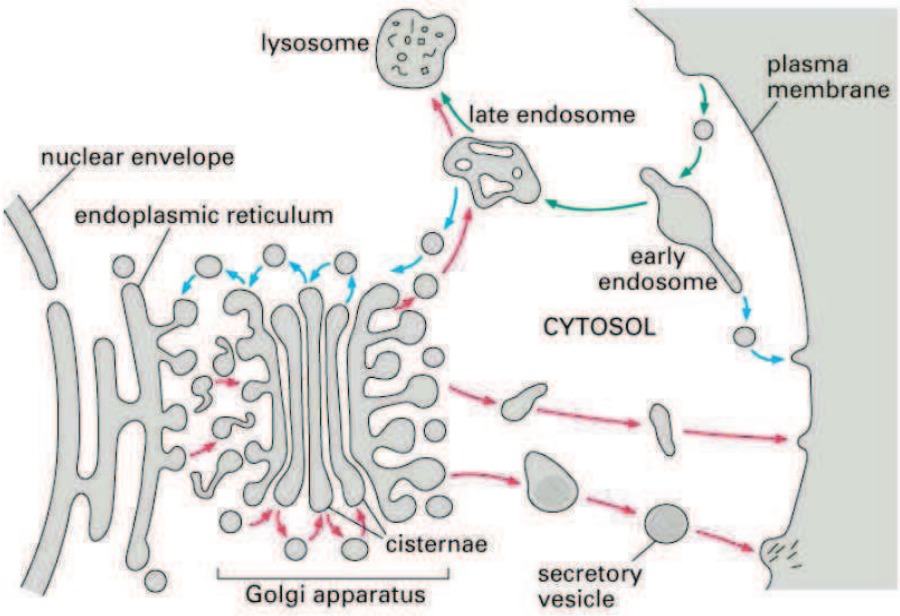


**Figure 17.** Membrane trafficking. In red, the exocytosis pathway. In blue, the endocytosis one (Molecular Biology of the Cell. 4th edition).

The outer leaflet of the cell plasma membrane constitutes the contact surface of the cell with the surrounding environment. In order to conserve this function, the composition of this leaflet should be highly regulated. Endocytosis defined as "*de novo production of internal membranes from the plasma membrane bilayer",* and its morphological opposite, exocytosis defined as *"fusion of entirely internal membranes with the plasma membrane"*, to control the cell homeostasis and the interactions of the cell with its environment (Doherty and McMahon 2008), (Doherty and McMahon 2009).

Endocytosis allows the transport of extracellular or membrane elements to the intracellular environment. It is fundamental for the internalization of nutritive elements, the regulation of the expression of membrane receptors and the equilibrium of the plasma membrane. Also it plays key roles in the regulation of intracellular signaling cascades such as growth factor receptor signaling (Hoeller, Volarevic et al. 2005). Moreover, several pathogens use the endocytic pathway to enter into the host cell (Marsh and Helenius 2006).

Numerous mechanisms are responsible for the endocytic uptake of a large variety of distinctly sized cargoes. The common points of all these pathways are the binding of the cargo to the cell surface, followed by the deformation and curvature of the plasma membrane (Krauss and Haucke 2012), and then the internalized material surrounded by an area of the plasma membrane buds off inside the cell (Ziello, Huang et al. 2010). Two sets of proteins are mainly involved in the intracellular trafficking of endosomes, namely the Rab family of small GTPases (Somsel Rodman and Wandinger-Ness 2000) and some specific protein kinases.

One of the best-characterized mechanisms is clathrin-mediated endocytosis CME, often synonymous to receptor-mediated endocytosis RME, which is considered as an extremely important pathway of endocytosis. However, clathrin-independent endocytosis (Kirkham and Parton 2005) involving caveolae and lipid rafts play also an important role.

Two alternative ways of internalization into the cell, are phagocytosis (cell eating) and pinocytosis (cell drinking) (Silverstein 1977), (Steinman, Mellman et al. 1983). Phagocytosis involves the internalization of large particles (>0.5 µm diameter) such as pathogens, apoptotic bodies, necrotic cells by specialized cells as macrophages and dendritic cells (Chimini and Chavrier 2000). Here, a progressive invagination (cup-shaped membrane) around the cargo is followed by the apparition of large vesicles called phagosomes. During pinocytosis, membrane rufflings surround the extracellular fluid and allow its internalization (Swanson and Watts 1995).

## 4.1. Endocytosis via clathrin-dependent pathway

The clathrin-dependent pathway constitutes the main process for internalization of plasma membrane receptors such as receptors for transferrin, epidermal growth factor (EGF), low-density lipoproteins (LDL), and cytokine receptors (Cavalli, Corti et al. 2001), as well as viruses such as the hepatitis C virus (Mercer, Schelhaas et al. 2010).

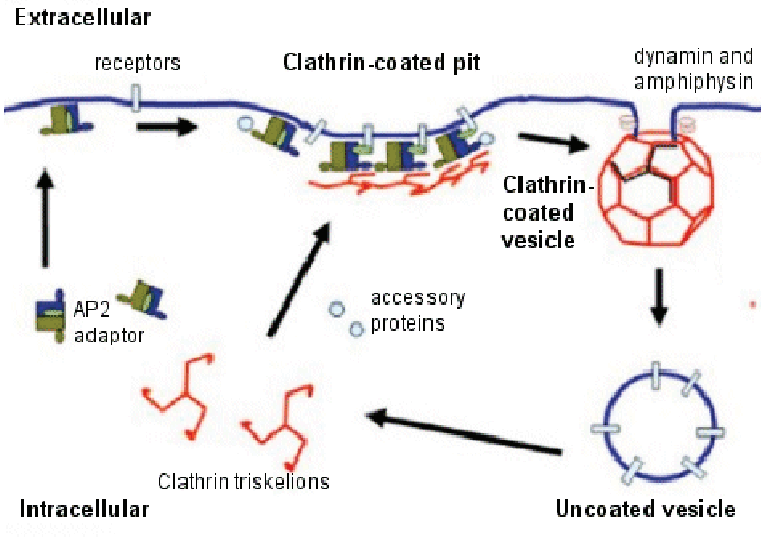


**Figure 18.** Machinery of clathrin-mediated endocytosis. *(http://www.abcam.com/index.html?pageconfig=resource&rid=10236&pid=14).*

First, macromolecules to be internalized bind to trans-membrane receptors on the cell surface. After, the bound receptors concentrate in regions of the cell membrane called clathrin-coated pits (CCP) on the cytosolic side of the plasma membrane (Fig. 18).

Clathrin is the main component of CCP, together with Eps15AP-2 and dynamin. Eps15AP-2 is a multimeric adaptor complex (Schmid 1997), responsible of clathrin nucleation under physiological conditions. Clathrin molecules have the capacity to form triskelion shaped self-assemblies (Kirchhausen 2000), which also self-assemble to form a particular structure called "cage" surrounding CCP.

This protein set induced invaginations of the plasma membrane at the CCP level, called clathrin-coated vesicles (CCV) (Clague 1998), (Marsh and McMahon 1999). Formation of CCV is dependent on the actin cytoskeleton (Yarar, Waterman-Storer et al. 2005), ATP, and GTP- binding proteins among which, dynamin is the most characterized (Damke 1996). Clathrin assembly triggers also the formation of the vesicle neck. Other proteins such as dynamin lead to the detachment of the CCV from the cell membrane (Hinshaw 2000), (Praefcke and McMahon 2004), by acting as constricting rings around the vesicle and allowing its separation from the plasma membrane. Dynamin is a critical regulator of both clathrin-dependent and -independent endocytosis.

Dynamics studies of clathin-mediated endocytosis showed that the rate of internalization via this pathway ranges between 1-5% per minute. Therefore, the lifetime of a CCP fluctuates between 20s and 2 min (Bretscher 1984). The size of CCV is related to the size of the internalized cargo, with a maximum 200 nm of diameter (Ehrlich, Boll et al. 2004). Nevertheless, some even larger cargos are likely internalized via this particular endocytosis pathway such as bacteria (Moreno-Ruiz, Galán-Díez et al. 2009) and latex beads (Aggeler and Werb 1982).

## 4.2. Endocytosis via clathrin-independent pathway

Electron microscopy allows the observation of clathrin coats around spherical buds of the plasma membrane, but also of clathrin-independent budding events, characterized by the absence of clathrin coats. Many molecules are internalized independently from clathrin and are associated with membrane domains (caveolae, lipid rafts…) (Johannes and Lamaze 2002). One of the most studied clathrin-independent carrier (CLIC) pathways is the caveolar-dependent endocytosis involved in transport processes as well in cell signaling (Anderson 1998). Cavoelae were shown to be involved in clathrin-independent endocytosis of SV40 virions, cholera-toxin B subunit and GPI-anchored proteins (Kurzchalia and Parton 1999), (Kirkham and Parton 2005), (Cheng, Singh et al. 2006), (Parton and Simons 2007).

Caveolae appear as small flask-shaped invaginations (50 to 80 nm of diameter) on the surface of many mammalian cell types. They were identified for the first time by electron microscopy in 1953 by Georges Palade. They are defined as lipidic structures localized in the plasma membrane, particularly enriched in cholesterol and glycosphingolipids (Palade 1953).

These caveolae have a protein coat composed mainly of caveolin (Fra, Williamson et al. 1995) which is an integral membrane protein (caveolin-1 is the most ubiquitous). Caveolin is synthesized in the endoplasmic reticulum, and then transported as oligomers to the Golgi apparatus. When the oligomers leave the Golgi apparatus, they associate with glycosphingolipids and lipid rafts enriched with cholesterol (DRM) (Dupree, Parton et al. 1993).

Caveolae fission is dependent on dynamin (Henley, Krueger et al. 1998), and is followed by the formation of caveosomes which can be addressed to endosomes (Parton and Simons 2007).

Many additional endocytic pathways are observed such as RhoA-, CDC42-, ARF6-, and flotillin-mediated endocytosis (Fig. 19), which require the involvement of specific proteins, such as the RhoA proteins, controlling the cytoskeleton dynamics, the cell division cycle 42 (CDC42) protein, the ADP-ribosylation factor 6 (ARF6), and flotillin presenting some analogy with caveolin-1 but not required for caveolae biogenesis, respectively. These pathways are in addition to macropinocytosis and phagocytosis, which were described previously.

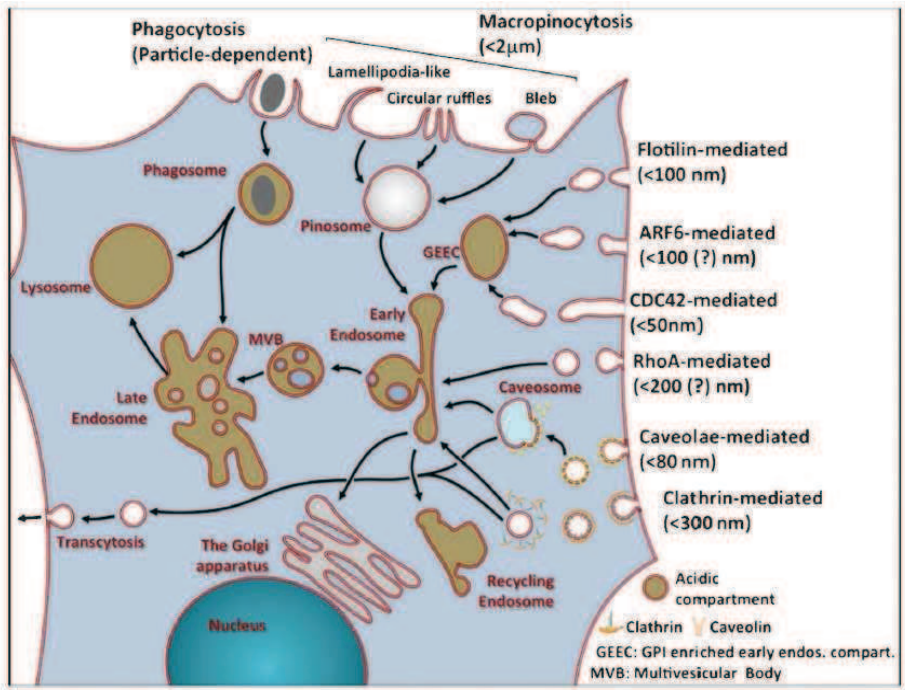


**Figure 19.** Mechanisms of extracellular uptake by endocytosis in a typical eukaryotic cell (Canton and Battaglia 2012).

## 4.3. Intracellular trafficking and endocytic cellular compartments

Once detached from the plasma membrane, primary endocytic vesicles containing cargos are responsible for the delivery of internalized molecules to other cellular compartments. The intracellular pathways followed by CCV are the same as those used for caveolin-dependent endocytosis.

Endosomes constitute a heterogeneous and hierarchical compartmentalization system. First, they were qualified into early and late endosomes, depending on their intracellular localization kinetics. Early endosomes (pH 6-6.5) appeared within one minute just beneath the

plasma membrane. After 10-15 minutes, late endosomes E (pH 5.5) appeared close to the Golgi apparatus (Fig. 20). Later, endocytic organelles were subdivided into four classes, depending on their relative labeling by endocytic markers: EEs, LEs, recycling vesicles, and lysosomes (Kornfeld and Mellman 1989). Early and late endosomes could be distinguished on the basis of their protein compositions and their morphologies. They are associated with different Rab proteins, early endosomes are enriched with Rab5 protein, while late ones contain Rab7 and Rab9 proteins (Mercer, Schelhaas et al. 2010). EE look tubular and are localized in the cell periphery (Tooze and Hollinshead 1991). They can be delivered to the plasma membrane via recycling pathway or progress to LE, which are oriented in the perinuclear region, look more spherical and contain internal vesicles (Multi-vesicular bodies) (Piper and Luzio 2001).

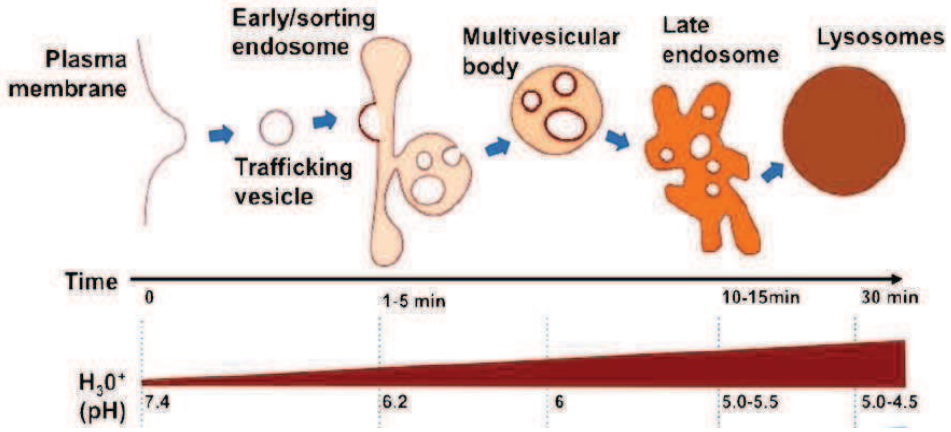


**Figure 20.** Scheme of the different endocytic compartments (Canton and Battaglia 2012).

Several theories were developed to describe the transport of cargos and internalized material between endosomal compartments. The first hypothesis was that a maturation process occurs between early endosomes, late endosomes and lysosomes. Also a vesicular exchange between endosomes and lysosomes was suggested (Vida and Gerhardt 1999). Later, the kiss-and-run theory, with a fusion between endosomes and lysosomes was proposed (Luzio, Pryor et al. 2007), (Luzio, Parkinson et al. 2009).

Several evidences proposed that the different endocytosis pathways are all connected to the same early endosomes, serving as a sorting or distribution station (Gruenberg 2001). In the case of phagocytosis, phagosomes avoid EE and directly fuse with lysosomes (Jutras and Desjardins 2005).

In the case of CME, once separated from the plasma membrane, CCV rapidly lose their coat to facilitate their fusion with EE. An acidic intraluminal pH (pH~6.0-6.8) (Yamashiro and Maxfield 1984) maintained by an ATP-driven proton pump (Forgac 1992) leads to the dissociation of ligand-receptor complexes such as for instance, in the case of the low density lipoprotein LDL (Kornfeld and Mellman 1989).

Free receptors are collected in the EE tubular extensions, and then recycled to the plasma membrane via recycling vesicles (transferrin-receptor) (Hopkins 1983). Some receptors are directed to lysosomes and then degraded (EGF receptor), which is required for nutrient uptake and receptor down-regulation. In contrast, dissociated ligands accumulate in the vesicular portions of the EEs, leading to the formation of multivesicular bodies (MVB). These structures pinch off and migrate on microtubules to the perinuclear region of the cell to fuse with late endosomes and lysosomes (Mellman 1996), (Maxfield and McGraw 2004).

Late endosomes are vesicular structures that accumulate internalized materials after their passage through EEs. They are enriched in lysosomal-associated membrane proteins (lamps), rab7, rab9, and the cation-independent mannose 6-phosphate receptor (MPR) (Geuze, Stoorvogel et al. 1988), (Lombardi, Soldati et al. 1993), (Simons and Zerial 1993), (Feng, Press et al. 1995). LEs contain active lysosomal hydrolases and initiate a degradative process. They are sometimes referred as pre-lysosomes because of this lysosome-like character. In lysosomes, low pH (pH~5.0) and high concentration of lysosomal hydrolases allow the degradation of ligands.

Transferrin receptors follow the recycling pathway (Fig. 21). Transferrin is a soluble protein that carries iron in the blood. When transferrin binds to its receptor in the cell surface, it forms CCP first then CCV, which is then delivered to early endosomes. Low pH of endosomes leads to the release of iron from transferrin. The iron-free transferrin called apotransferrin bound to its receptor is delivered back to the plasma membrane, where it dissociates from the receptor in order to pick up a new ion of iron.

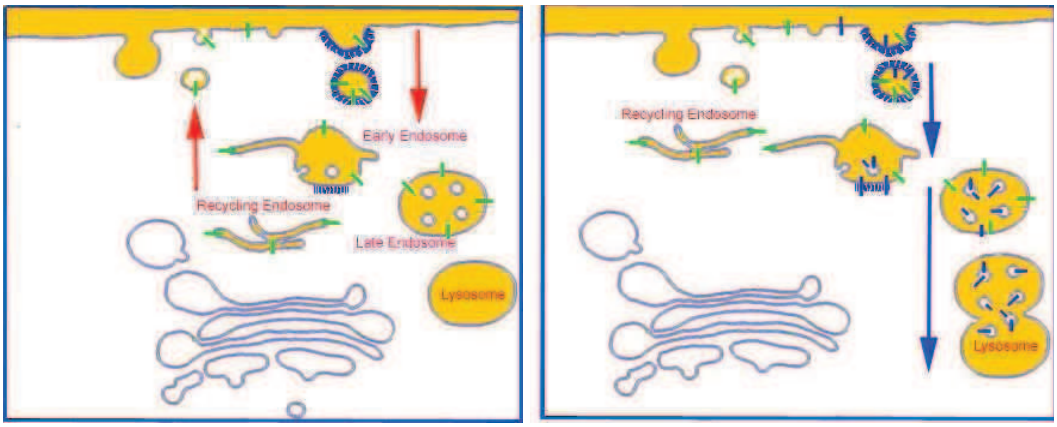


**Figure 21.** Illustration of different pathways of membrane receptors internalization. In the left, transferrin receptors are recycled and delivered back to the cell plasma membrane. In the right, EGF receptors are directed to lysosomes where they are degraded. *(http://colinhopkins.com/new_page_6.htm).*

## 4.4. Endocytosis of bacterial toxins

Many bacterial toxins can traverse the plasma membrane and get inside the host cell. Cholera toxin (CTx) secreted by *Vibrio cholerae* is targeted to the ER via EE and TGN (Ewers and Helenius 2011). The pentameric B-subunits of the bacterial toxin CTx are responsible for binding to the carbohydrate part of GM1, which is a key compoment of membrane microdomains. The binding is then followed by the internalization of the toxin. It was demonstrated that inhibitors of clathrin-dependent pathway have small effect on the CTx internalization, while treatments that inhibit clathrin-independent endocytosis have a stronger effect (Orlandi and Fishman 1998), (Torgersen, Skretting et al. 2001). So cholera toxin is internalized via clathrin-independent endocytosis and the labeled-toxin could be used as a marker for this endocytic mechanism.

## 4.5. Lipid requirement for endocytosis

To describe the role of cholesterol for endocytosis, agents that extract or sequester cholesterol were used. Treatment of cells with MßCD which removes cholesterol from the membrane decreases the number of caveolae on the plasma membrane as well as it affects CME. Moreover, nystatin or filipin which sequester cholesterol showed specific effects on the clathrin-independent pathway (Anderson, Chen et al. 1996).

The sphingolipid requirement for endocytosis was investigated by Cheng (Cheng, Singh et al. 2006). Depletion of cellular SL affects selectively the clathrin-independent endocytosis, without any effect on CME (transferrin and LDL uptake).

## 4.6. Variation of cholesterol content in endosomal vesicles during the endocytic pathway

Cholesterol is distributed in the membranes of the different cellular compartments, but it is the most concentrated in the plasma membrane (Liscum and Munn 1999). Cholesterol is recycled back to the plasma membrane via recycling endosomes which are in consequence enriched with cholesterol (Hornick, Hui et al. 1997), (Hao, Lin et al. 2002). In contrast lysosomes contain much less of this sterol (~6%) (Lange, Ye et al. 1998).

Using immuno-electron microscopy, the distribution of cholesterol could be mapped in the different organelles involved in endocytosis (Mobius, van Donselaar et al. 2003). Early endosomes and recycling endosomes (confirmed by the presence of transferrin receptor), as well as late endosomes (M-6-PR) were found to contain high amounts (~80%) of cholesterol. In contrast, purified lysosomes show very low content of cholesterol (Mobius, van Donselaar et al. 2003), (Swetha, Sriram et al. 2011). This low content may be connected to the action of proteins, such as the Niemann-Pick type C1 (NPC1) protein which transports cholesterol from lysosomes. The mutation of this protein is the main cause of the Niemann-Pick disease, a lysosomal storage disorder, biochemically manifested by an accumulation of cholesterol and sphingolipids due to the failure of cells to esterify exogenously added cholesterol and the accumulation of free (i.e. unesterified) cholesterol in the endo/lysosomal compartment and the Golgi apparatus (Ikonen and Holtta-Vuori 2004).

## 4.7. Physiological importance of endocytosis

Endocytosis is involved in the regulation of nutrient uptake, cell adhesion, cell migration, cell signaling, pathogen entry, receptor down-regulation, growth and differentiation and drug delivery.

For example for receptors like EGFR, clathrin-independent endocytosis directs this receptor to lysosomes for degradation, while the CME targets this receptor by recycling to the plasma membrane for cell signaling (Sigismund, Argenzio et al. 2008).

Since endocytic mechanisms are very important, they can be affected in several human diseases (Aridor and Hannan 2000), (Aridor and Hannan 2002). For instance, mutations of the LDL receptor adaptor protein are detected in autosomal recessive hypercholesterolemia (Hammes, Andreassen et al. 2005). Moreover, caveolin-3 is mutated in myopathies and muscular dystrophies (Brauers, Dreier et al. 2010). Also, neurodegenerative diseases seem to involve endocytosis defects (Nonis, Schmidt et al. 2008), such as Alzheimer's disease and Down's syndrome (Cataldo, Peterhoff et al. 2000).

## 4.8. Assays for endocytosis research

To identify by which pathway a given molecule can be internalized, several methodologies are proposed. The most applied assays for this purpose will be reviewed in this section. These assays are based mainly on inhibition of some pathways by using drugs or by mutations of essential actors of specific mechanisms and through colocalization with known markers.

The first group of assays involves the inhibition of a given endocytic pathway. The clathrin-dependent pathway can be blocked via potassium treatment, hypotonic shock (Bayer, Schober et al. 2001), as well as by drugs such as chlorpromazine, acting on the level of coated pit assembly (Wang, Rothberg et al. 1993) and brefeldin A, an inhibitor of Arf1 (Guanine Nucleotide Binding protein) (Brodsky, Chen et al. 2001). Inhibition of the caveolin-dependent pathway is achieved via sterol-binding drugs such as nystatin and filipin which sequester cholesterol in the cell plasma membrane and methyl-ß-cyclodextrin which depletes cholesterol from the membrane (Neufeld, Cooney et al. 1996), (Rothberg, Heuser et al. 1992), (Orlandi and Fishman 1998). Other types of endocytosis can be also inhibited for monitoring a particular endocytic pathway. For instance, macropinocytosis can be blocked either by Cytochalasin D (Maniak 2001) acting on the actin system, or by amiloride (West, Bretscher et al. 1989) acting as an inhibitor of Na+/H+ exchange.

The second group of assays uses negative mutants of proteins involved in a given pathway, like dynamin (clathrin- and caveolin-mediated endocytosis), EpS15 (clathrin-mediated endocytosis) (Benmerah, Bayrou et al. 1999), and GTPases.

The third group is based on the application of endosomal markers specific for each endocytic compartment. This includes antibodies against early endosomal antigen 1 (EEA1), Mannose-6-phosphate receptor (marker of LE), Rab4 and Rab5. Fluorescent probes and labeled proteins

can also be used to monitor ligand-receptor binding and endocytosis, such as fluorescent LDL, transferrin conjugates, and membrane markers of endocytosis (such as FM dyes).

Nevertheless, the dissection of the endocytic pathways remains challenging, due to the lack of specificity of markers or inhibitors. Moreover, as the result of technical limitations such as spatial and temporal resolution in imaging, and the cross-talk between the different pathways, we never observe internalization through a specific pathway. There is always some contribution of other pathways. Finally, to monitor the complete progression of endocytosis, many distinct markers are needed (Transferrin for EE, Lysotracker for lysosomes, ER tracker for ER…), and there is an obvious need to develop fluorescent reporters which are able to follow this progression, for example through changes in their spectral properties.

# 5. Fluorescence

## 5.1. Principles of fluorescence

Fluorescence constitutes the dominant methodology used in microscopy, biotechnology, flow cytometry, medical diagnostics… Fluorescence techniques are notably important for cellular and molecular imaging to follow and detect molecules inside cells.

Fluorescence is a sub-ensemble of the main photophysical phenomenon called luminescence, which corresponds to the emission of light from the electronically excited state of a given substance after the absorption of infrared, visible or ultraviolet light. Luminescence includes fluorescence and phosphorescence, depending on the nature of the excited state. Fluorescence occurs if the emission takes place from the singlet excited state that has been populated after light absorption. When the emission occurs from the triplet excited state, the phenomenon is described as phosphorescence, where the transition to the ground state is in principle forbidden, resulting in a slow emission rate (~$10^3$ to $10^0$ $s^{-1}$).

These processes of light emission can be illustrated by the Jablonski diagram (Fig. 22).

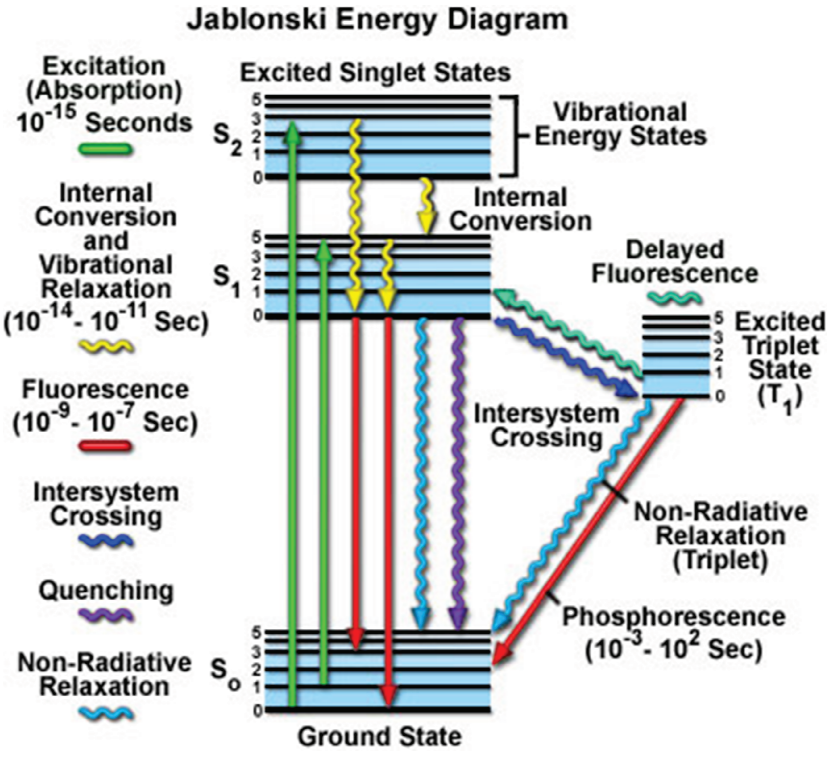


**Figure 22.** Jablonski energy diagram *(http://www.olympusmicro.com/primer/java/jablonski/jabintro/index.html).*

Atoms and molecules absorb light at a particular wavelength and then, can subsequently emit light of longer wavelength after a brief interval, termed the fluorescence lifetime (emission rates of fluorescence are ~ $10^8$ $s^{-1}$, so the lifetime is in the nanosecond range). Phosphorescence had much longer excited state lifetimes (milliseconds to seconds).

For any molecule, different electronic states exist (illustrated as $S_0$, $S_1$, $S_2$ and $T_1$ in Figure 22). Each electronic state is divided into a number of vibrational and rotational energy levels associated with the atomic nuclei and bonding orbitals. The ground state $S_0$ for most organic molecules is an electronic singlet in which all electrons are spin-paired (have opposite spins).

Fluorescence includes three main events: i) excitation by incoming photons (absorption) of a fluorophore existing in its ground state with two electrons of opposite spins ($S_0$), ii) once excited, the fluorophore is transferred to an excited vibrational state of the first electronic excited state called singlet excited state ($S_1$) where one of the two electrons is promoted to a molecular orbital of higher energy, iii) fluorescence emission which is characterized by a photon emission, and the return of the fluorophore to its ground state $S_0$. The difference in energy or wavelength between the absorbed and emitted light is described as the Stokes shift.

The excited molecule can return to its ground state either with fluorescence emission or with phosphorescence which take places after intersystem crossing. Intersystem crossing can be described as the transition between excited states of different spins (from the first singlet excited state $S_1$ to the first triplet state $T_1$ where one of the electrons changed its spin), so finally two electrons with parallel spins are obtained.

Moreover, this excited molecule is exposed to intramolecular charge transfer, conformational change and interactions with other molecules, which can result in a de-excitation phenomenon related to electron transfer, proton transfer or energy transfer.

Briefly, common photophysical processes could be divided into radiative and nonradiative processes. Radiative processes include singlet- singlet absorption (So ---- S1), singlet- singlet emission, called fluorescence (S1 ---- So), singlet- triplet absorption (So ---- T1) and triplet-singlet emission phosphorescence (T1 ----- So). Nonradiative processes include transitions between states of the same spin, called internal conversion (Sn ---- S1+ heat), transitions between states of the same spin, called external (by collision, to other molecules especially solvent) and internal conversion (S1---- So+ heat) and transitions between triplet states and the ground states also called intersystem crossing (T1---- So + heat).

Molecules which are able to show electronic transitions resulting in fluorescence are known as fluorescent dyes or fluorophores. They are classified into intrinsic and extrinsic dyes. Intrinsic fluorophores, such as aromatic amino acids and plant pigments, are those that occur naturally. Extrinsic fluorophores are synthetic dyes or modified biochemicals that are added to a specimen to produce fluorescence with specific spectral properties. Fluorescence occurs typically with polyaromatic molecules such as quinine, fluorescein and Rhodamine B.

Most fluorophores can repeat the excitation and emission cycle many hundreds to thousands of times before they are photobleached, resulting in the loss of fluorescence. Many other nonradiative processes compete with fluorescence emission such as quenching, and fluorescence resonance energy transfer (FRET) together with internal conversion and intersystem crossing.

Scanning through the absorption spectrum of a fluorophore while recording the emission intensity at a single wavelength (usually the wavelength of maximum emission intensity) will generate the excitation spectrum. Likewise, exciting the fluorophore at a single wavelength

(again, preferably the wavelength of maximum absorption) while scanning through the emission wavelengths will reveal the emission spectral profile.

Quantum yield is a fundamental parameter to describe a fluorophore. It corresponds to the ratio of the number of photons emitted to the number of photons absorbed. Quantum yields typically range between a value of zero and one. In general, a high quantum yield is desirable in most imaging applications.

### 5.1.1. Excited-state reactions

Excited-state photoreaction is a molecular phenomenon occurring in the excited state after light excitation. The photoreaction changes the structure of the excited-state fluorophore. One of the most important excited-state reactions is photoinduced intramolecular charge transfer (ICT), which changes dramatically the electronic distribution within the molecule, generating large excited-state dipoles. Another interesting example is the excited-state intramolecular proton transfer (ESIPT) reaction, which results in the transfer of a proton between different groups of the same molecule at the excited state. Some other excited-state reactions exist, such as excited state intermolecular proton transfer, photoinduced electron transfer, etc… but they are less important in the present study.

### 5.1.2. Solvatochromism

The solvent can strongly affect the fluorescence of a particular fluorophore. In the excited state, some fluorophores present a larger dipole moment than in their ground state. After excitation, the solvent dipoles reorient around the excited fluorophore dipole, leading to a decrease in the energy of the excited state resulting in a relaxation process called solvent relaxation (Fig. 23).

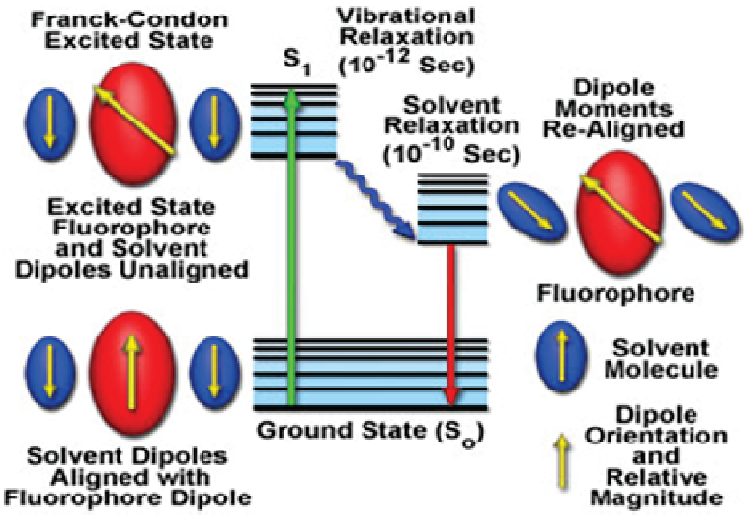


**Figure 23.** Solvent relaxation illustration *(http://www.olympusmicro.com/primer/java/jablonski/solventeffects/index.html).*

This effect of the solvent becomes stronger with the increase in the solvent polarity, leading to a shift of the emission to lower energies (longer wavelengths). This resulting shift is called fluorescence solvatochromism. Only fluorophores possessing high change in the dipole moment on electronic excitation show this solvatochromism and they are called solvatochromic dyes. Typical examples are Prodan, Nile Red, NBD, etc. Other fluorophores, such as fluorescein, rhodamine and cyanine dyes are much less solvatochromic and are not considered as environment-sensitive.

## 5.2. Synthetic fluorescent dyes

Fluorescent dyes are very interesting tools used in biological research. The choice of the appropriate dye depends on the application. We can distinguish: i) natural fluorophores such as aminoacids: tryptophan, plant pigments, and green fluorescent protein GFP (Shaner, Patterson et al. 2007), and ii) synthetic fluorophores classified into environment-sensitive and environment-insensitive dyes.

### 5.2.1. Classical synthetic dyes

Dyes such as fluorescein, rhodamine, cyanine, coumarin and alexa (Fig. 24) are commonly used for biological researches and notably for cellular applications.

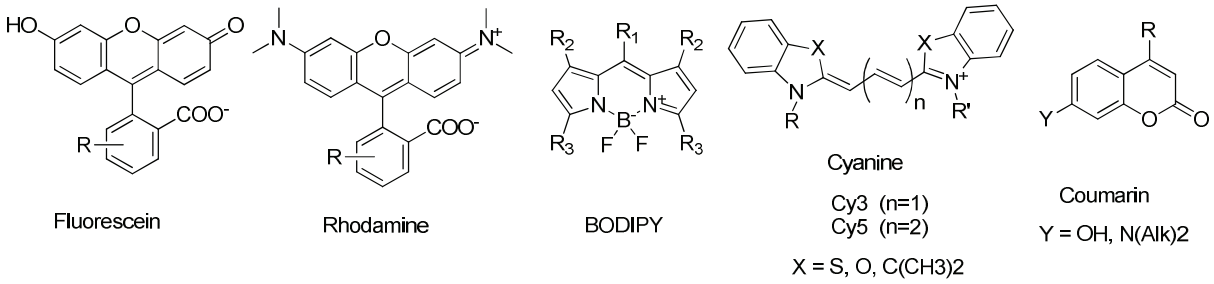


**Figure 24.** Most common synthetic fluorescent dyes.

Some are known for a long time, such as fluorescein which was synthesized for the first time in 1871. Although this dye is still widely used, its photostability is limited and its fluorescent quantum yield depends on pH. Another popular dye is rhodamine which is an amino-containing analog of fluorescein, which is more photostable than fluorescein and shows no pH dependent fluorescence. Other well-established dyes are cyanine dyes (Mishra, Behera et al. 2000), characterized by an exceptional brightness due to their large absorption coefficient, but show low fluorescence lifetime, which limits their use in time-resolved fluorescence applications. Coumarin family of dyes is interesting for biological applications because of its small size and its water solubility, but suffers from its absorption in the UV-region and low photostabilty. More recent examples are BODIPY,Alexa and Atto dyes, which show high quantum yields and photostability, while they are very poorly sensitive to the environment properties (polarity, pH).

### 5.2.2. Environment-sensitive dyes

#### 5.2.2.1. Environment sensitive dyes with one emission band

Environment-sensitive dyes are defined as molecules whose fluorescence properties (fluorescence intensity or maximum of emission) respond to changes in the properties of their molecular environment. These changes of fluorescence properties are due to excited-state reactions (charge and proton transfer etc) and non-covalent interactions of the fluorophore with the surrounding (van der-waals, dipole-dipole, H-bonding, etc).

Solvatochromic dyes are of particular importance for the present study. They present a shift of their maximum of emission depending on the polarity and hydration of the environment. Prodan dye (Fig. 25), (2-propionyl-6-dimethylaminonaphthalne), constitutes the most typical example of this class (Weber and Farris 1979). After excitation of the fluorophore, the dipole moment increases due to an intramolecular charge transfer resulting in a red-shift of its

emission spectrum in response to an increase in solvent polarity (Parasassi, Di Stefano et al. 1994), (Lakowicz 2006). Because of its solvatochromism and high quantum yield, Prodan is useful for protein and membrane studies (Moreno, Cortijo et al. 1999), (Kaur and Horowitz 2004), (Bagatolli 2006), but its absorption in the UV-region around 360 nm constitutes a major drawback. In 2006, Lu and their colleagues developed 2-propionyl-6-dimethylaminoanthracene, Anthradan (Fig. 25), which absorbs in the red range, avoiding overlap with cell autofluorescence and making this dye more convenient for biological applications (Lu, Lord et al. 2006).

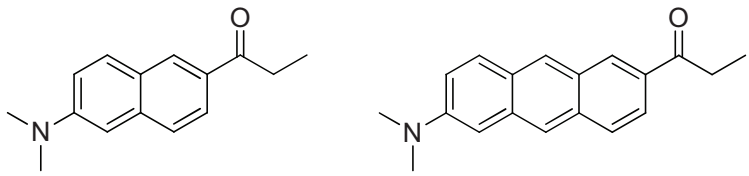


**Prodan** **Anthradan**

**Figure 25.** Prodan and its analogue Anthradan.

Other solvatochromic dyes such as 1,8-ANS and 2,6-TNS, are used for protein and membrane studies (Lakowicz 2006). These environment-sensitive dyes are poorly fluorescent in water, so that their incorporation into proteins and lipid membranes leads to an increase of the fluorescence intensity (Slavik 1982) (Fig. 26).

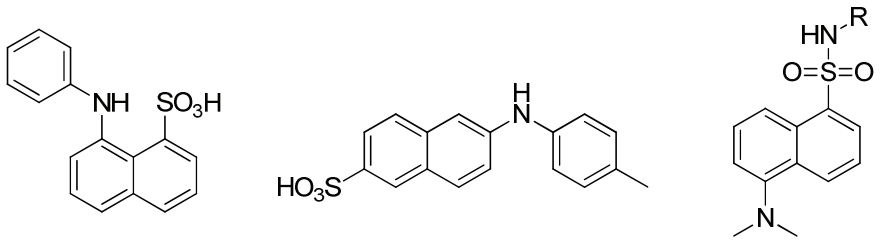


**1,8-ANS** **2,6-TNS** **Dansyl**

**Figure 26.** Commonly used naphthalene sulfonic acid derivatives.

Dansyl derivatives are also used for many applications, showing high sensitivity to the solvent polarity (Goncalves 2009). However, these dyes presented some limitations concerning cellular and biological applications related to their low extinction coefficient and their absorption in the UV region.

Most environment-sensitive probes absorb in the UV-region (prodan, fluoroprobe, dapoxyl etc), while only few show absorption and emission in the red region, such as NBD (Chattopadhyay 1990) and Nile Red (Diaz, Melis et al. 2008). The latter dyes have absorption around 460-480 nm and 530-560 nm, respectively, with a convenient extinction coefficient and quantum yield but they (especially NBD) show limited solvatochromism. (Fig. 27).

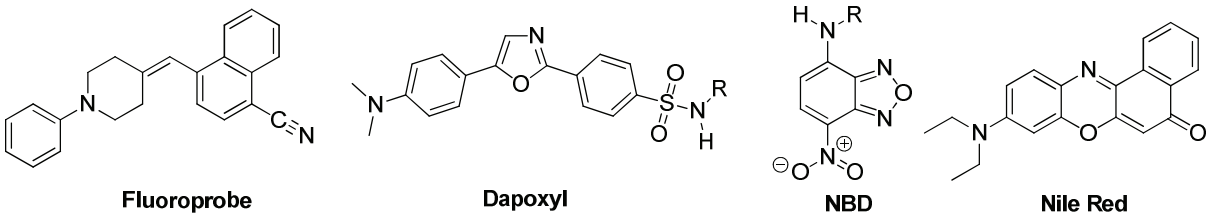


**Figure 27.** Advanced fluorescent solvatochromic dyes.

This overview of environment-sensitive dyes shows that most solvatochromic dyes are limited in terms of convenient absorption and emission for cellular applications. On the other hand, dyes with a red-shifted absorption and emission are less solvatochromic. Thus, dyes with both strong sensibility and improved fluorescent properties are still missing.

#### 5.2.2.2. Environment-sensitive dyes with two emission bands (ESIPT-dyes)

Excited-state intramolecular proton transfer reactions (ESIPT) are involved in many biological processes such as protein-ligand binding (Zhong, Douhal et al. 2000) and biological macromolecule interactions (Miskovsky 2002).

ESIPT reaction was described for the first time for salicylic acid ester (Fig. 28). The large Stokes shift in the emission spectrum of this compound evidenced the proton transfer after photo-excitation from the donor hydroxyl-group to the proton-acceptor carbonyl group. The proton transfer generates the tautomer form (T*) from the normal form of the excited molecule (N*). ESIPT results in a decrease of the energy of the excited state, giving a red-shifted emission band (Formosinho 1993). ESIPT can be tracked by ultrafast techniques (ultra-fast laser spectroscopy) on a femtosecond time scale (Marks, Zhang et al. 1997).

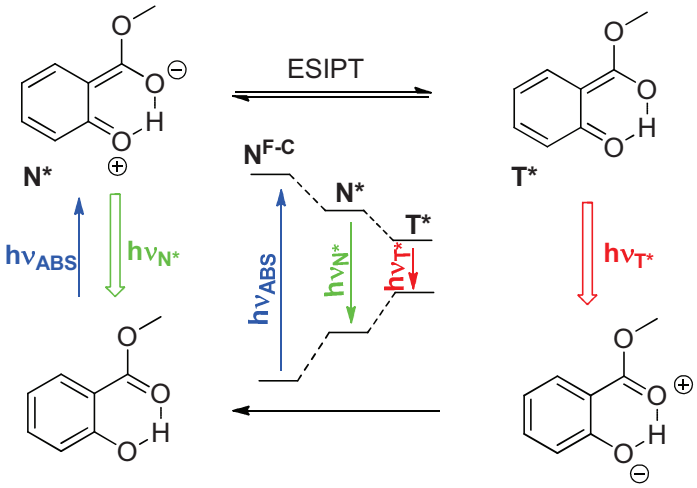


**Figure 28.** Example of ESIPT in methyl salicylate.

In the present study, 3-hydroxychromones (3HC) were of particular interest. These fluorophores form an intramolecular H-bond through a 5-membered cycle, which is pathway for the ESIPT reaction. This H-bond is weaker than in 6-membered cycle, so that it can be easily perturbed by H-bonding interactions, which leads to the dual emission of both N* and T* forms in polar protic solvents.

## 5.3. 3-Hydroxychromone dyes

3-hydroxychromone (3-HC) dyes constitute an attractive tool due to their photochemical properties (Klymchenko, Furukawa et al. 2007).

Chromones or chromen-4-ones exist in the vegetal kingdom, so they are natural dyes. Most chromones contain phenyl substituents in the position 2 of the heterocycle and are called flavones. Flavones with a hydroxyl group in position 3 of the heterocycle are called 3-hydroxyflavones (3-HF) (Fig. 29).

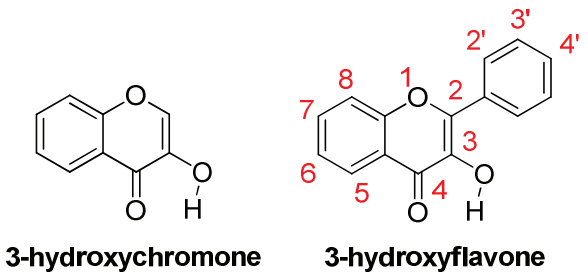


**Figure 29.** Chemical structure of 3-hydroxychromone and 3-hydroxyflavone.

3-HF dyes attracted big attention because of their dual fluorescence emission (Woolfe and Thistlethwaite 1981) due to an ESIPT reaction (Sengupta and Kasha 1979) (Fig. 30). As mentioned before, the proton transfer in these dyes is facilitated by a H-bond through a 5-membered cycle which can be much easier disrupted by intermolecular H-bonding interactions than a 6-membered cycle(McMorrow and Kasha 1984), leading to the appearance of two emission bands, the short-wavelength band, originating from the normal excited state (N*), and the long-wavelength band, corresponding to the photo-tautomer form (T*) (Fig. 31).

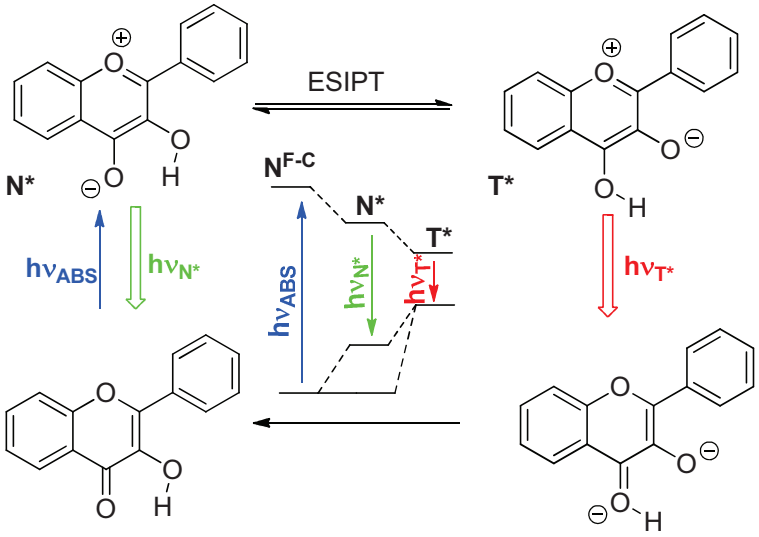


**Figure 30.** ESIPT reaction of 3-hydroxychromone (Sengupta and Kasha 1979).

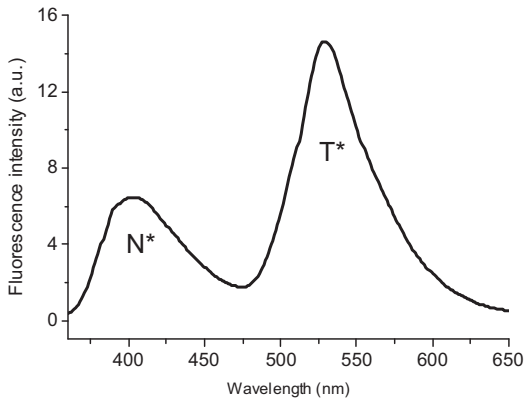


**Figure 31.** Fluorescence spectrum of 3-hydroxyflavone in methanol.

The response of these dyes to changes in the environment can be evaluated by the ratio of intensities of the two emission bands, in contrast to other dyes (with one emission band), whose responses are evaluated by changes of the fluorescence intensity. This ratio of two bands (N*/T*) is more precise and independent of artifacts related to the dye concentration and instrumental settings. Due to these advantages, a variety of fluorescent probes based on 3-HC dyes have been developed and applied for probing polarity, hydration and electric fields in solvents, lipid vesicles, cellular membranes and proteins (Cheng, Pu et al. 2005), (Chou, Pu et al. 2005), (Pivovarenko, Vadzyuk et al. 2006), (Demchenko, Mely et al. 2009).

The parent non-substituted dye 3HF exhibits a dual emission in protic polar solvents, while only the T* band is observed in aprotic solvents (Fig. 32). The development of dialkylamino derivatives of 3-HF (Chou, Martinez et al. 1993), (Ormson, Brown et al. 1994) was particularly important, since due to the 4'-dialkylamino group, the N* excited form shows a high dipole moment, while the T* excited state exhibits a lower one. Therefore, the N* state exhibits higher solvatochromism than the T* state (Fig. 32). In addition to the red shift of the N* band, an increase in solvent polarity increases the N* band relative intensity. Thus, the ratio of intensities $I_{N*}/I_{T*}$ gives a good indication of the solvent polarity.

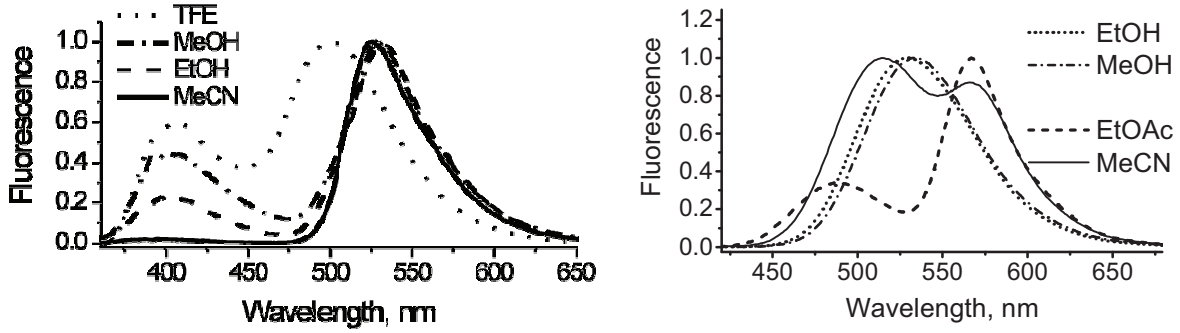


**Figure 32.** Fluorescence of 3HF (left) and its dimethylamino derivative (right) in protic and aprotic solvents.

In addition to their sensitivity to polarity, 3-HF probes are sensitive to electric fields such as those related to membrane potentials (Klymchenko, Duportail et al. 2003), (Shynkar, Klymchenko et al. 2005). Depending on their location in the membrane the 3HF probes can be used to sense a given membrane potential. Derivatives being located in the middle of the upper bilayer leaflet are sensitive to the dipole potential. Changes in the dipole potential

induces a change in the N*/T* ratio accompanied by a shift of the maximum of emission of two bands (Klymchenko, Mely et al. 2004).

3-HF probes, such as F2N12S, being located close to the lipid head groups in the upper leaflet as a result of their coupling with a long alkyl chain and zwitterionic group is able to sense the surface potential (Shynkar, Klymchenko et al. 2007). F2N12S is also able to differently label lipid phases in giant unilamellar vesicles. It binds both Lo and Ld phases, showing a good contrast in N*/T* ratio, with a low ratio in the case of the Lo phase and a higher ratio for the Ld phase (Klymchenko, Oncul et al. 2009). When used with cell membranes, F2N12S is also sensitive to liquid order phase, and shows an increase of the N*/T* ratio after cholesterol depletion and apoptosis (Shynkar, Klymchenko et al. 2007), (Oncul, Klymchenko et al. 2010).

3-HF probes are thus good tools for monitoring the physico-chemical properties of model membranes or cell plasma membranes. The N*/T* ratio is a powerful indicator of polarity, hydration and lipid order in membranes, independently from the dye concentration and the instrument. Despite all these advantages, application of these probes shows limitations related to their blue-shifted excitation which is not convenient for cellular applications. Due to this, a new probe based on Nile Red was developed (Kucherak, Oncul et al. 2010). The new developed dye, NR12S, presents high fluorescence quantum yield, quite good photostability and suitable excitation wavelength for application with common lasers and avoiding the artifact related to auto-fluorescence.

## 5.4. Nile Red dye

### 5.4.1. Solvent effects on the fluorescence spectra of Nile Red

Nile red is a solvatochromic dye that is poorly fluorescent in water, but in non-aqueous solvents it shows strong fluorescence, with fluorescence maxima and intensity as indicators of the dye environment-properties (Fig. 33).

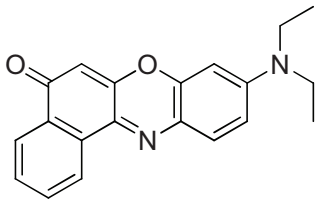


**Figure 33.** Nile Red structure.

Nile Red dye exhibits interesting spectroscopic properties such as long wavelength absorption and emission as well as a large Stokes shift which highlight potential applications for intracellular imaging (Jose and Burgess 2006). On increase in solvent polarity, the emission maximum of Nile Red shifts to the red from 530 up to 640 nm and its fluorescence quantum yield decreases.

### 5.4.2. Nile Red fluorescence in the presence of proteins and lipids

Nile Red has been used to probe the hydrophobic surface of proteins (Sackett, Knutson et al. 1990), to stain lipid membranes and to examine membrane organization, fluctuation and heterogeneity (Gao, Mei et al. 2006). In cells, Nile Red is commonly used to stain intracellular lipid droplets (Greenspan and Fowler 1985), (Klinkner, Bugelski et al. 1997). Nile Red was shown to be a good tool to study the structure and dynamics of model membranes (vesicles and planar supported bilayers). Measuring Nile Red lifetime, heterogeneity in supported membranes due to microdomains of cholesterol and sphingomyelin was hypothesized (Ira and Krishnamoorthy 1998). Nile Red fluoresces also in the presence of serum lipoproteins (low and high density lipoproteins) and some other proteins (Greenspan and Fowler 1985).

In lipids, the excitation and emission spectra of this dye were changing in different lipid preparations. In the presence of phophatidylcholine, Nile Red absorbs at 549 nm and emits at 628 nm. When trioleoylglycerol was added to phosphatidylcholine, the emission maximum shifts to the blue (576 nm), due to the more apolar nature of trioleoylglycerol.

In conclusion, Nile Red shows spectral properties similar to prodan in terms of quenched fluorescence in aqueous media and shifts of its fluorescence spectrum in response to changes of solvent polarity. Nile red exhibits an intense fluorescence in the presence of phospholipid vesicles accompanied by a shift of its emission spectrum depending on the lipid composition. Due to all these characteristics, Nile Red constitutes a powerful fluorescent molecule for

cellular applications, but selective staining of plasma cell membrane is not possible, since this dye enters easily in the cell and stains mainly lipid droplets. Therefore, a new Nile Red derivative should be developed in order to fill this gap and allow structural and dynamic studies of cell plasma membranes. In order to study membrane properties, a new probe derived from Nile Red was developed. This new Nile Red derivative called NR12S has a particular structure with a zwitterionic group and long alkyl chain allowing its specific binding to the outer leaflet of the membrane. The detailed description of NR12S and its characterization in model systems and cell plasma membrane will be given in the section 5.5 and in the results part.

## 5.5. Fluorescent membrane probes

The biological functions of cell membranes are connected to their physicochemical properties such as membrane electrostatics, phase state and hydration. Therefore studying these properties in situ is an interesting task in membrane biophysics (Demchenko, Mely et al. 2009). Fluorescent probes are very useful tools for biomembrane research because of their capacity to monitor membrane organization and dynamics (Mukherjee and Maxfield 2004). A wide variety of fluorescent membrane probes has been developed, providing powerful tools for membrane studies using fluorescence microscopy and/or fluorescence spectroscopy.

In this part, fluorescent membrane probes will be reviewed with a particular focus on fluorescent probes developed in our laboratory.

There are already many fluorescent membrane probes, and hundreds of them are commercially available. Among this great diversity of membrane probes, the common characteristic is their high affinity to membranes. Some of these dyes present charged group (Patman, TMA-DPH), others are without charge (Prodan, Nile Red), and many of them have a lipid-like structure (fluorophore attached to acyl chain or to a polar head group). These dyes can be classified as environment-sensitive (NBD, 3-hydroyflavones) or environment-insensitive. Many parameters can be targeted with the use of fluorescent probes: polarity (Reichardt 1994), hydration (Ho, Slater et al. 1995), (Jurkiewicz, Sýkora et al. 2005), electrostatic potentials (surface, dipole and transmembrane potentials) (Kraayenhof, Sterk et al. 1993), (Gross, Bedlack et al. 1994), (Fluhler, Burnham et al. 1985) and lipid order (Krasnowska, Gratton et al. 1998), (Parasassi, De Stasio et al. 1990).

The first group of probes includes those used for the determination of membrane fluidity. They include diphenylhexatriene (DPH) (Lentz 1993), and its cationic derivative, TMA-DPH which are commonly used for this purpose using fluorescence anisotropy. While DPH has no precise location in the membrane bilayer, its derivative is localized at the membrane-water interface due to its trimethylammonium anchor group (Kuhry, Fonteneau et al. 1983), (Kuhry, Duportail et al. 1985).

The second group of membrane fluorescent probes contains dyes which are sensitive to electric fields and particularly to transmembrane potential. Transmembrane potential plays a fundamental role in cell bioenergetics and membrane transport, and can be classically measured by insertion of microelectrodes into cells. The new dyes constitute an alternative to microelectrodes. The most commonly used dyes are ANEP-dyes, among them di-4-ANEPPDHQ is the most interesting since it shows very low cell internalization and good signal/noise ratio (Obaid, Loew et al. 2004). These dyes are mainly used for systems presenting large changes in transmembrane potential like nervous cells, while they exhibit low sensitivity in other systems having small changes in transmembrane potential.

The third group encompasses environment-sensitive probes and more particularly solvatochromic probes, where the most typical examples are PRODAN (Catalan, Perez et al. 1991), (Sýkora, Kapusta et al. 2002), LAURDAN (Parasassi, Di Stefano et al. 1994), Nile red (Krishna 1999) and NBD derivatives (Alakoskela and Kinnunen 2001). As mentioned before, these dyes respond to environment changes by shifts of their fluorescence emission and/or excitation spectra.

Interestingly, fluorescence probing is one of the most convenient methods for visualizing and quantifying lipid domains on cell membranes. For this purpose a number of dyes were already described and applied. Some of these probes showed only a high and almost exclusive selectivity for domains of a particular phase, so they are able to distribute into Lo phase only or Ld phase. The most attractive example of this type of probes is the fluorescently labeled protein Cholera toxin-B. This bacterial toxin shows high selectivity to Lo phase domains related to its specific interaction with the ganglioside GM1 associated with this latter phase in biomembranes (Lommerse, Spaink et al. 2004), (Lagerholm, Weinreb et al. 2004), (Owen, Neil et al. 2007). Other probes based on saturated lipids labeled with fluorescent molecules (NBD, Cy5 and GFP-labeledglycosylphosphatidylinositol) at their head groups, or fluorescent

dyes conjugated with long alkyl chains (LcTMA-DPH, dil-C20) prefer to distribute on the Lo phase domains of membranes, but the partition is directly dependent on the exact lipid composition of these domains. In contrast, other probes are excluded from the Lo phase because of their structure (lipid-like), so they are not able to stain Lo phase domains in model or cell membranes (van Meer and Simons 1988).

DPH-based probes (TMA-DPH) by reflecting the hydration levels in membranes which correlates with the phase state are also used to monitor lipid phases. Thus, when a high level of hydration is detected, it suggests the presence of a phase with low lipid order (Ho, Slater et al. 1995).

The environment-sensitive molecular probe PRODAN is able to distribute in both Lo and Ld phases of membranes, and its fluorescence emission properties (color, intensity…) and/or lifetime are directly dependent on the local membrane properties that in turn are related to the phase state of the membrane. It shows a large red shift of its fluorescence emission on transition from gel phase to liquid crystalline phase (~50 nm) in lipid bilayers (Krasnowska, Gratton et al. 1998), suggesting a significant increase in the hydration of the probe micro-environment (Parasassi, De Stasio et al. 1991). Moreover, addition of cholesterol induces strong changes in the emission color of this dye (Massey 1998), (Bondar and Rowe 1999). LAURDAN, the hydrophobic analog of PRODAN is also sensitive to phase transition and cholesterol composition in the same manner as PRODAN (Parasassi, De Stasio et al. 1990), (Parasassi, Di Stefano et al. 1994) but distributes better into lipid membranes due to its higher hydrophobicity.

The styrylpiridinium dye, di-ANEPPQ also shows a similar sensitivity to the lipid phase, and exhibits a blue-shifted emission in the Lo phase with respect to the fluid phase (Jin, Millard et al. 2006). All these probes able to bind both phases allow color imaging of the lipid domains (Bagatolli 2006).

Fluorescent membrane probes are also applied to detect apoptosis. During apoptosis, in addition to PS exposure to the cell surface and loss of transbilayer asymmetry, many changes occur on the level of cell plasma membrane properties (lipid order and hydration). The fluorescent probe most used for this aim is Merocyanine 540 (MC540), which binds to the outer membrane of cells and fluoresces in the highly disordered membranes of apoptotic cells.

This dye is applicable for apoptosis detection by flow cytometry (Laakko, King et al. 2002), (Bailey, Nguyen et al. 2009).

Recently, a new 3HC derivative probe was reported as an alternative tool for these applications, in addition to another environment-sensitive probe NR12S derivative from Nile Red probe. Both dyes are able to sense lipid order and detect apoptosis using fluorescence spectroscopy and microscopy, and flow cytometry.

A lot of work was done recently in our laboratory with the aim to develop new fluorescent membrane probes with superior fluorescent properties and high sensitivity to biophysical properties of biomembranes. 3-Hydroxychromones dyes were good candidates for new dye development, due to their high sensitivity to hydration, polarity, lipid order, etc. The work on ratiometric dyes based on 3-hydroxyflavone was started about one decade ago. Fluorescent probes were developed to sense the charge of micelles, the surface charge of phospholipid membranes (Duportail, Klymchenko et al. 2001) and the hydration in biomembranes (Duportail, Klymchenko et al. 2002). Next, 3-hydroxyflavones derivatives capable of giving simultaneous information about hydration and polarity in lipid bilayers were introduced (Klymchenko, Mely et al. 2004), (Shynkar, Klymchenko et al. 2004). Later on, these two-color fluorescent probes were adapted for cell imaging. To reach this aim, selective staining of cell plasma membrane was optimized by adding a zwitterionic group and long hydrocarbon chain which allow a specific positioning of the probe in one membrane leaflet. These dyes were also adapted for multi-color imaging microscopy, using a single wavelength excitation but collecting the light with two distinct detectors (Shynkar, Klymchenko et al. 2005).

One of the most interesting 3-hydroxyflavone derivatives was F2N12S that enables detecting apoptosis by flow cytometry, fluorescence spectroscopy and microscopy (Shynkar, Klymchenko et al. 2007) (Fig. 34). Apoptosis was shown to correlate with the loss of lipid asymmetry and lipid order at the cell plasma membranes (Oncul, Klymchenko et al. 2010).

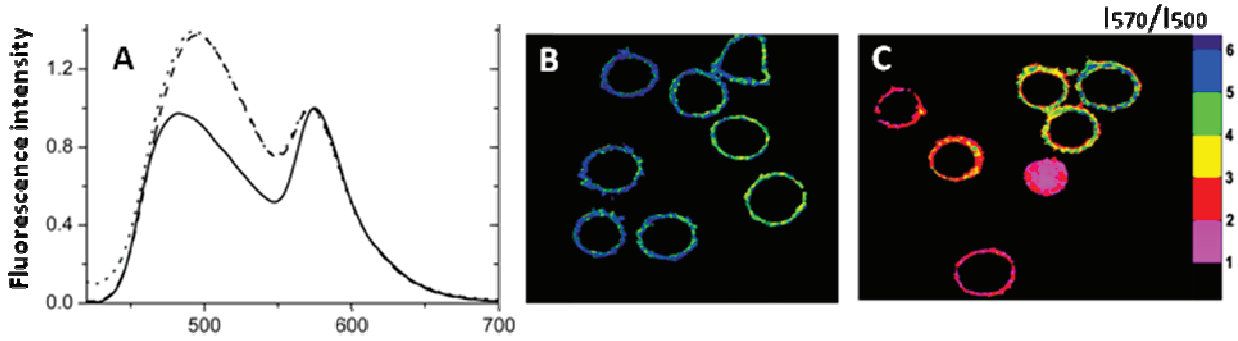


**Figure 34.** Apoptosis detection using probe F2N12S. (*A*) Fluorescence spectra of F2N12S in normal (solid curve) and apoptotic cells (dashed curve). Ratiometric images of (*B*) normal and (*C*) apoptotic cells stained with F2N12S (Shynkar, Klymchenko et al. 2007).

Importantly, flow cytometry assays demonstrated that F2N12S could be a potential alternative to fluorescently-labeled AnnexinV, since it allows simpler and faster staining of the cells. Moreover, ratiometric confocal imaging allows easy discrimination between live and apoptotic cells, by displaying images with a color code that corresponds to the ratios of intensities of the two bands, T*/N* (Fig. 34).

F2N12S was also successfully used to differentiate liquid ordered and disordered phases in large unilamellar vesicles (Fig. 35A) (M'Baye, Mély et al. 2008) and giant vesicles through differences in the ratio of intensities of the two emission bands, N*/T* (Fig. 35B, C and D) (Demchenko, Mely et al. 2009), (Klymchenko, Oncul et al. 2009).

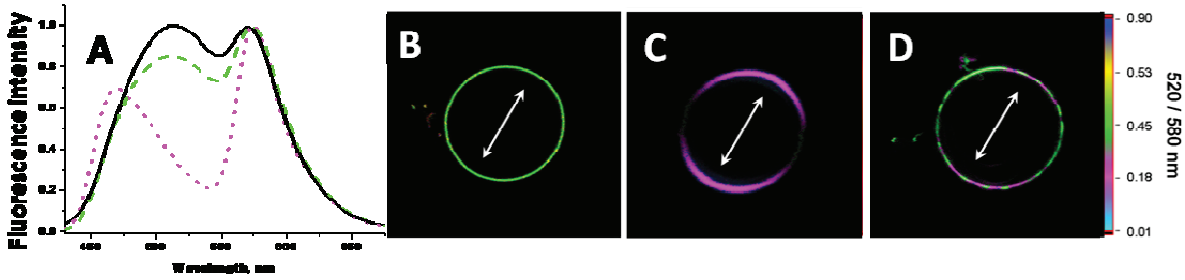


**Figure 35.** Probing raft domains using F2N12S. (*A*) Fluorescence spectra of F2N12S in lipid vesicles composed of DOPC (*black solid curve*), DOPC+cholesterol (*green dashed curve*), and SM +cholesterol (*magenta dotted curve*). Fluorescence ratiometric images of GUVs composed of (*B*) DOPC, (*C*) SM +cholesterol, and (*D*) DOPC/SM/Cholesterol. Two-photon excitation (830 nm) was used (Klymchenko, Oncul et al. 2009).

Recently, F2N12S was shown to be sensitive to the cholesterol content in plasma membranes. Remarkably both cholesterol depletion and apoptosis induce similar spectroscopic effects on the probe, suggesting that both processes may lead to the loss of the lipid order in the outer leaflet of the cell plasma membrane (Oncul, Klymchenko et al. 2010).

In parallel, a new fluorescent membranes probe, NR12S, was developed with more convenient properties for cellular applications. NR12S is a Nile Red derivative that absorbs and emits in the red region. This dye with a zwitterionic group and a long alkyl chain binds specifically the cell plasma membrane. NR12S was shown to stay at the outer leaflet for a long time even at 37°C, with a very slow flip-flop to the inner leaflet. This property of NR12S is of strong interest since it allows to study the properties of one leaflet only (Kucherak, Oncul et al. 2010). In the present work, NR12S will be described as a tool to sense changes in lipid composition and to detect apoptosis.

Another biological process of interest related to the cell plasma membrane is is endocytosis. Many endocytosis pathways were described. All of them are connected to cell plasma membranes, at least in their initial steps. The most popular fluorescent membrane probes for endocytosis studies are FM-dyes. The membrane selective FM4-64 and FM1-43 dyes belong to a class of amphiphilic styryl dyes (Betz, Mao et al. 1996). These dyes fluoresce significantly only when they are in a hydrophobic environment, e.g. a lipid-rich membrane. FM-dyes are unable to cross membranes because of their amphiphilic nature, which anchor them in the outer leaflet of the bilayer. These dyes are thought to enter cells by endocytic vesicles invaginated from the plasma membrane (Bolte, Talbot et al. 2004). Since FM-dyes are membrane selective and stain many organelle membranes, the FM-dyes can be used to monitor organelle organization and dynamics (Hickey, Jacobson et al. 2002). Therefore, we get the idea to use our environment-sensitive probe NR12S (Kucherak, Oncul et al. 2010), to follow the formation of endosomes and endocytic compartments, benefiting from their ability to sense the lipid order through a color change, dependent on the lipid composition. The uptake of this dye was studied, using confocal fluorescence microscopy, by applying numerous pathway-specific markers and inhibitors for the different endocytic pathways and ratiometric imaging to visualize the change of its color after internalization.

Despite strong progresses in the development of new fluorescent molecules for visualizing biological membranes, conception and biological characterization of new probes with more

convenient properties are still needed for cellular applications. In this context, the present work is aimed to characterize new fluorescent membrane probes developed in our laboratory, focusing mainly on the direct visualization of lipid order and apoptosis in model membranes and cell plasma membranes.

# *Materials and Methods*

# Materials:

- **Cell lines:** For cellular studies, we used U87MG human glioblastoma cell line (ATCC) and HeLa cells.

  U87MG human glioblastoma cells were cultured in Eagle's minimal essential medium (EMEM from LONZA) with 10 % heat-inactivated Fetal bovine serum and 0.6 mg/mL glutamine (Biowhittaker) at 37°C in a humidified 5 % $CO_2$ atmosphere.

  HeLa cells were cultured in Dulbecco's modified Eagle medium (D-MEM, high glucose, Gibco-invitrogen) supplemented with 10% (v/v) fetal bovine serum (FBS, Lonza), 1% antibiotic solution (penicillin-streptomycin, Gibco-invitrogen) in a humidified incubator with 5% $CO_2$ /95% air atmosphere at 37°C.

  Cell concentration of 5-10×$10^4$ cells/mL was maintained by removal of a portion of the culture and replacement with fresh medium 2 times per week.

- **Probes:** 3-HF probes (F2N12S, F46NS, F66NS and F86NS) and NR12S were dissolved in DMSO and conserved at -20 °C.

- **Lipids:** Dioleoylphosphatidylcholine (DOPC), 1,2-Dioleoyl-*sn*-Glycero-3-phospho-L-serine (DOPS) and cholesterol were purchased from Sigma-Aldrich. Bovine brain sphingomyelin (SM) was from Avanti Polar Lipids (Alabaster, USA). All lipids were used without further purification.

  **DOPC, DOPS:** The two synthetic lipids, 1,2-Dioleoyl-*sn*-Glycero-3-phosphocholine (DOPC) and 1,2-Dioleoyl-*sn*-Glycero-3-phospho-L-serine (DOPS) (Fig. 1), neutral and anionic, respectively, were used for lipid vesicles preparation.

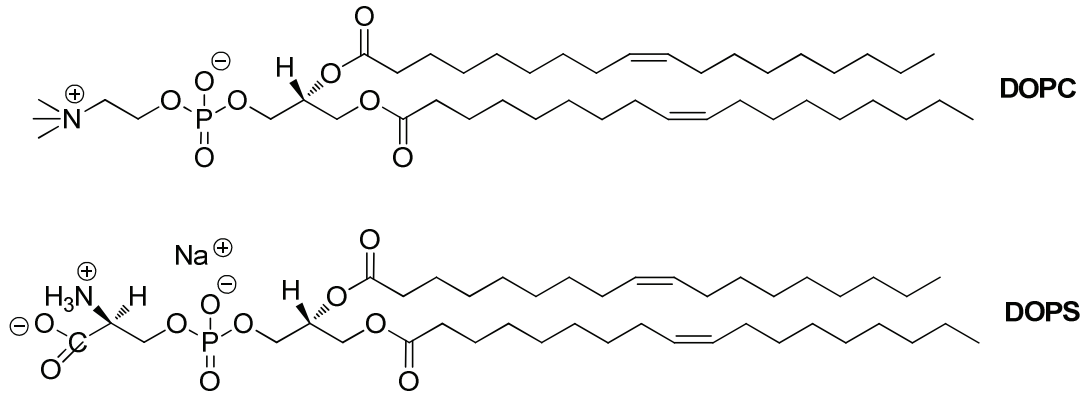


**Figure 1.** Chemical structure of DOPC and DOPS.

**Cholesterol:** is one of the main components of the cell plasma membrane (Fig. 2). This natural lipid is responsible for many important functions in living organisms.

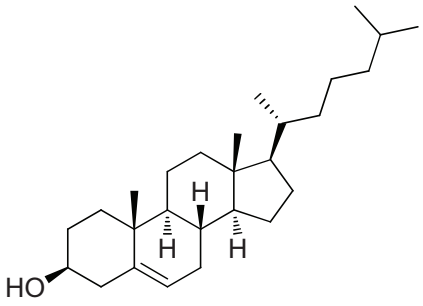


**Figure 2.** Chemical structure of cholesterol

**Sphingomyeline:** is the major sphingolipid present in the membrane of mammalian cells (Fig. 3).

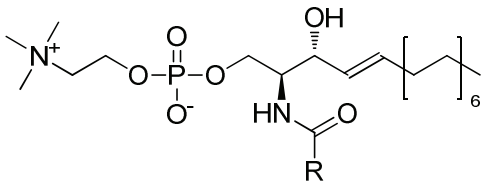


**Figure 3.** Chemical structure of sphingomyeline

- **Sucrose:** A solution of 300 mM sucrose was prepared in mQ water (Sigma-Aldrich).
- **Glucose:** A solution of 300 mM glucose was prepared in mQ water (Sigma-Aldrich).
- **Annexin V**: Annexin V is a $Ca^{2+}$-dependent and phospholipid-binding protein, which binds preferentially to phosphatidylserine (PS) with a high affinity in presence of $Ca^{2+}$.

This feature of Annexin V, labeled with some fluorophore (fluorescein in our case) is used for early detection of apoptosis by flow cytometry. Annexin V was purchased from BD Biosciences.

- **Sodium Dithionite**: A stock solution of 1 M of sodium hydrosulfite (Sigma-Aldrich), 1 M Tris was prepared in mQ water (Alfa Aesar). A solution of 10 mM was used in cuvette for fluorescence spectroscopy measurements, or 20 mM in iBiDi dishe for fluorescence microscopy.

- **Methyl-ß-cyclodextrin**: A 40 mM stock solution of Methyl-ß-cyclodextrin (Sigma-Aldrich) was prepared in phosphate buffer saline. For cholesterol extraction, a solution of 5 mM for 2 h at 37 °C was added to cells.

- **Cholesterol oxidase from *Streptomyces sp.*:** This enzyme (from Sigma-Aldrich) is responsible of the cholesterol oxidation into cholest-5-en-3-one. 2 U/mL of cholesterol oxidase at 37 °C were used.

- **Sphingomyelinase from *Bacillus cereus*:** This enzyme (from Sigma-Aldrich) is responsible of sphingomyelin cleavage into ceramide. For SM hydrolysis, cells were incubated at 37 °C for 2 h with 0.2 U/mL of SMase.

- **Apoptosis agents:**

  **Actinomycin D:** is an antibiotic (from Sigma-Aldrich) which inhibits DNA replication and RNA transcription. A stock solution of 0.25 mg/mL was prepared in DMSO and conserved at -20 °C. For apoptosis induction, 0.5 µg/mL of Actinomycin D was used 18 hours before measurements.

  **Staurosporine:** is a protein kinase inhibitor (from Sigma-Aldrich). A stock solution of 0.2 mM was preapared in DMSO and conserved at -20 °C. For apoptosis induction, 0.1 µM of staurosporine was used 18 hours before measurements.

  **Camptothecin:** inhibits the DNA topoisomerase I (from Sigma-Aldrich). A stock solution of 1 mg/mL was prepared in DMSO and conserved at -20 °C. For apoptosis induction, 5 µg/mL of camptothecin was used 18 hours before measurements.

- **Transferrin:** It is a protein which binds to its receptor on the plasma membrane, then it is internalized via clathrin-dependent endocytosis. Alexa Fluor 488-transferrin (Invitrogen) was used as marker of this particular endocytosis pathway. A solution of 20 µg/mL was used at different incubation time.

- **Chloropromazine:** Chloropromazine (from Sigma-Aldrich) is used as inhibitor of clathrin-dependent endocytosis. A solution of 10 µg/mL was used to inhibit the internalization.

- **Lysotracker:** The LysoTracker® probes are fluorescent acidotropic probes for labeling and tracking acidic organelles in live cells. These probes have several important features, including high selectivity for acidic organelles and effective labeling of live cells at nanomolar concentrations. The LysoTracker® Green DND-26 (Invitrogen) was used at 50 nM**.**

- **ER-tracker:** ER-Tracker™ dyes are cell-permeant, live-cell stains that are highly selective for the endoplasmic reticulum (ER). ER- Tracker Green (BODIPY FL glibenclamide) (Invitrogen) was used at 0.75 µM.

- **FM4-64**: The lipophilic probe, FM™ 4-64 exhibits low fluorescence in water but fluoresces intensely upon binding the outer leaflet of the plasma membrane providing discrete plasma membrane staining. The binding is rapid and reversible. It is also an excellent reagent for identifying actively firing neurons and for investigating the mechanisms of activity-dependent vesicle cycling. FM4-64 (Invitrogen) was used at 1 µM.

- **Two-photon and confocal microscope:** These microscopes are a part of the PIQ (Plateau d'Imagerie Quantitative) imaging facilities in the Faculty of Pharmacy, UMR7213.

# Methods:

### 1. Preparation of lipid vesicles

**1.1. Large Unilamellar Vesicles (LUVs) preparation:** Properties of liposomes can vary depending on their composition (cationic, anionic, neutral lipid species). However, the same preparation method can be used for all lipid vesicles regardless of their composition. The

general steps of the procedure involve: i) preparation of the lipid films, ii) hydration with agitation and iii) sizing to a homogeneous vesicles. LUVs were obtained by the classical extrusion method (Hope et al., 1985) using a Lipex Biomembranes extruder (Vancouver, Canada).

When preparing liposomes with single or mixed lipid compositions, the lipids must first be dissolved in an organic solvent to ensure their homogeneous distribution. Usually this process is carried out using chloroform or chloroform/methanol mixture. The solvent is then removed by rotary evaporation yielding a thin lipid film on the wall of a round bottom flask (Fig. 4). The lipid film is thoroughly dried to remove the residual organic solvent by continuing evaporation with gentle heating (about 35°C) during 30 minutes.

Hydration of the dry lipid film is accomplished simply by adding corresponding buffer to the flask, and the obtained solution is left at the temperature about Tm of corresponding lipid (RT for unsaturated lipids and 55°C for lipids with saturated alkyl chains). Typically, lipid solutions are prepared with the final concentration of 0.2 mM, although higher concentrations may be used. After hydration the solution is vortexed during 2 minutes affording a suspension of multilamellar vesicles with a heterogeneous size distribution.

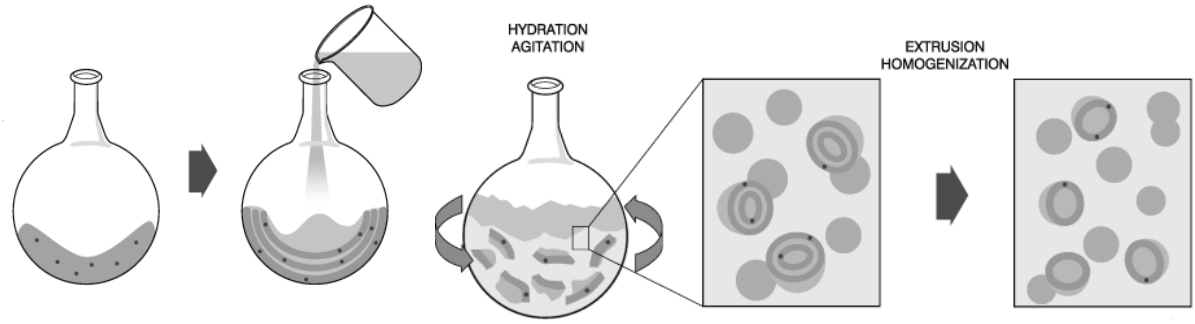


**Figure 4.** Protocol of LUVs preparation by extrusion.

Once a suspension has been produced, the particles are downsized by extrusion. Lipid extrusion is a technique in which a lipid suspension is forced through a polycarbonate filter with a defined pore size to yield particles having a diameter near the pore size. An extruder (Lipex Biomembranes Inc) with polycarbonate filters of calibrated pores (Nucleopore) is used. Prior to extrusion through the final pore size, the lipid suspension is first downsized by passing through a large pore size (0.2 μm) filter seven times. Then the suspension is passed through the filter with the final pore size (0.1 μm) ten times. This final extrusion through

filters with 0.1 µm pores yields large unilamellar vesicles (LUV) with a mean diameter of 110-120 nm. This method ensures a homogeneous size distribution of the final suspension. All preparation steps including hydration, vortexing and the extrusion should be done at a temperature that is higher than the temperature of the gel-liquid crystal transition (Tm) of the lipid. For example, heating at 55°C is needed in the case of lipids like DPPC or sphingomyelin, which bear saturated alkyl chains.

LUVs were labelled by adding aliquots (generally 2µL) of probe stock solution (in DMSO) to 1 mL of vesicle suspension in buffer. Since all the probes were new molecules, the fluorescence experiments were performed at different incubation times (3, 5, 7 and 30 min) and the optimal conditions were found for each dye. A 20 mM phosphate buffer with pH 7.4 was used in all experiments. Concentrations of the probes and lipids were 1 µM and 200 µM respectively unless indicated.

**1.2. Giant Unilamellar Vesicles (GUVs) preparation:** Electroformation is a major method to prepare GUVs. The key principle of this method is to let the dried lipid films to swell and detach after in aqueous solution under applied electric potential, forming the giant vesicles (Fig. 5).

GUVs were generated in a home-built liquid cell (University of Odense, Denmark). Lipids are dissolved in chloroform at 1 mM total concentration. 3 µl of this solution is spread using a 10-µl glass syringe on each platinum wire of the chamber. After deposition, the cell/chamber should be shaken slowly to allow the good dispersion of lipids on the electrodes. Then the organic solvent is evaporated under vacuum in the desiccator for 30 min at room temperature.

The hydration step of dried films is accomplished by adding 500 µL of 300 mM of warm sucrose solution to each well. The chamber, thermostated at 65°C (for lipid mixtures involving high-Tm lipids like sphingomyelin), is sealed with Parafilm to prevent water evaporation (Make sure there is no leakage of the chamber). Then the chamber is connected to a pulse generator and an alternating voltage (10 Hz, 2 V) is applied for ca. 2 hours. During the incubation period, the lipid film will swell and strip away from the Platinum wires to form GUVs. After that vesicles can be collected by gentle aspiration and can be conserved at room temperature in the dark.

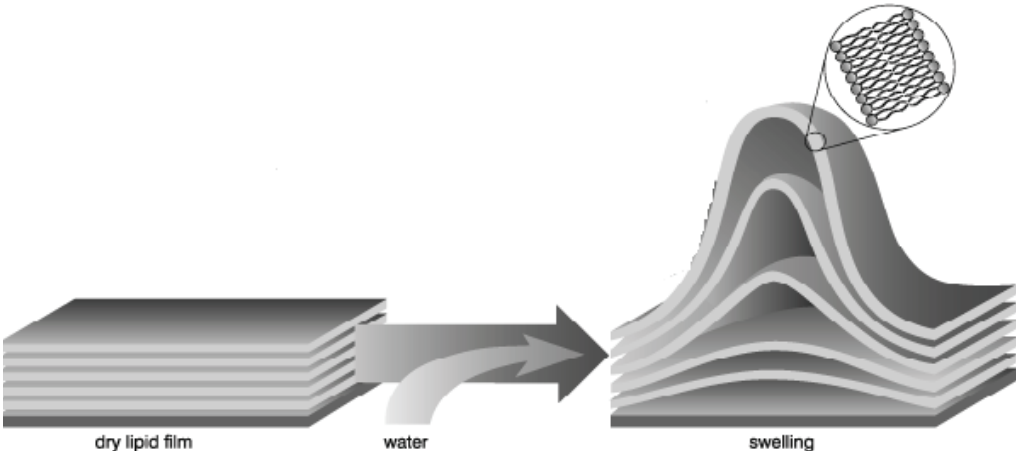


**Figure 5.** Principle of GUVs formation by swelling.

Then 50 ml aliquot of the obtained stock solution of GUVs in sucrose (cooled down to RT) was added to 200 ml of 300 mM glucose solution to give the final suspension of GUVs used in microscopy experiments. The staining of GUVs was performed by addition of an aliquot of the probe stock solution in DMSO to obtain a 0.1µM final probe concentration (final DMSO volume <0.25%).

### 2. Cell preparation and treatements

Cholesterol depletion was performed using methyl-β-cyclodextrin (MβCD). Briefly, stock solution of MβCD in Dulbecco's Phosphate Buffered Saline (DPBS) was prepared at a suitable concentration, filtered by Millipore filter (0.2 µm) and added to the cells to a final concentration of 5 mM. The treated cells were kept in the incubator at 37 °C for 2 h.

For cholesterol oxidation, a stock solution of cholesterol oxidase was prepared in 50 mM potassium phosphate buffer, pH 7.0. The treated cells were kept at 37 °C for 2 h with 2 U/mL of cholesterol oxidase. For SM hydrolysis, cells were incubated at 37 °C for 2 h with 0.2 U/mL of SMase.

For apoptosis studies, 3 different agents were tested. To prepare apoptotic cells, cells were treated with actinomycin D (0.5 µg/ml), camptothecin (5 µg/ml), or staurosporine (0,1 µM) for 18h in the incubator at 37 °C prior the experiments.

### 2.1. Samples for fluorescence spectroscopy

For fluorescence spectroscopy experiments the cells were grown for 3 days in order to obtain sufficient number of cells. Old culture medium was first removed from the culture dish and cells were washed two times with DPBS. Trypsine 10x (LONZA) solution was diluted 10 times with DPBS and added with the cells in the 37 °C incubator for 4 minutes. The solution of trypsinated cells was then diluted by HBSS (Hank's Balanced Salt Solution), transferred to Falcon tubes and centrifuged at 1500 rpm for 5 minutes 2 times. To stain the cell suspension with the probe, an appropriate aliquot of its stock solution in DMSO was added to 0.5 ml of HBSS buffer and after vortexing, the solution was immediately added to 0.5 ml of the cell suspension to obtain a final probe concentration of 0.01 µM for NR12S or 0.1 µM for 3-HF probes (< 0.25% DMSO) and a cell concentration of $1\times10^6$ cells/ml. It should be noted that only freshly prepared solutions of the probe in HBSS should be used (< 3 min) for cell staining, because of the slow aggregation of the probe in water. Before measurements, the cell suspension with probe was incubated for 7 min at room temperature in the dark. Finally, blank sample (without probe) and stained samples (with probe) were measured.

### 2.2. Samples for fluorescence microscopy

For microscopy studies, cells were seeded onto a chambered coverglass (IBiDi) at a density of $5\times10^4$ cells/IBiDi. After that the culture medium was removed from culture dishes and attached cells were washed twice by gentle rinsing with Opti-MEM. Further, a freshly prepared solution of probe in Opti-MEM was added to the cells. Final concentration of the probe was 0.5 µM or 0.05 µM for cell staining and imaging for 3-HF and NR12S, respectively (<0.25% DMSO volume). After incubation for 7 min at room temperature in the darkness the sample was ready for image acquisition.

## 3. Physical measurements

### 3.1. Fluorescence spectroscopy

- **Absorption spectroscopy:** Absorption spectra were recorded on a Cary 4000 spectrophotometer (Varian). The absorbance is characterized by (Valeur 2002):

$$OD= \log(I_0/I)$$

where $I_0$ and I are the incident and transmitted light intensities, respectively.

All spectra were corrected using a baseline. For that, the baseline of the instrument is first recorded with both cuvettes filled with the solvent. Then, the dye is added into the solvent of the sample cuvette and the true absorption spectrum is recorded.

- **Fluorescence spectroscopy:** Fluorescence measurements were performed on a FluoroMax 3.0 (Jobin Yvon, Horiba) spectrofluorometer equipped with a thermostatic cuvette holder. The FluoroMax 3.0 is a photon counting device with a linear response in the range of measurements (< 3 Mcps). The source of light is a xenon lamp. The signals are measured with a photomultiplier. The correction of the excitation beam is performed with a calibrated photodiode.

  Fluorescence emission spectra were systematically recorded at 20°C using the following excitation wavelengths: 400nm for all 3-HF probes, and 520nm for all Nile Red probes. All the spectra were corrected from the fluorescence of the corresponding blank (suspension of cells or lipid vesicles without the probe).

### 3.2. Fluorescence microscopy

- **Confocal microscopy:** Laser scanning confocal microscopy represents one of the most significant advances in optical microscopy used for biological applications. Confocal microscopy technique is based on the illumination of the sample by a laser beam where the fluorescence which does not originate from the focal plane of the lens used is removed using a diaphragm (pinhole) placed in front of the detector (Fig. 6). In this way, only the photons originating from the focal plane cross the diaphragm and participate in the formation of the image. Thus, it is possible to obtain a sharp and thin optical section of the focal plane.

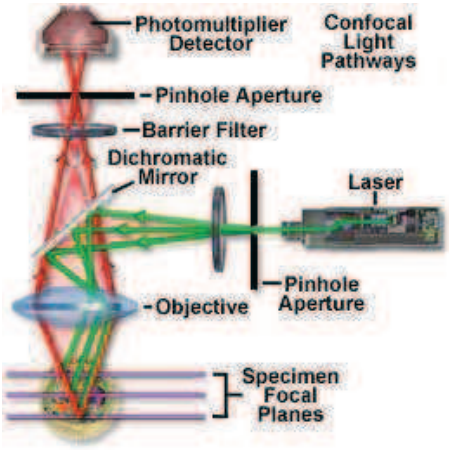


**Figure 6.** Schematic illustration of the Confocal Microscope

Confocal microscopy measurements were performed on a confocal laser scanning microscope Leica SPE II (Fig. 7). This system is equipped with lasers which generate four excitation wavelengths 405, 488, 561 and 635 nm. The focalization and the collection of the signal are obtained through a HXC PL APO 63x/1.40 OIL CS objective. To excite NR12S probe 488 nm excitation was used. The laser power was adjusted in order to excite efficiently the fluorophore avoiding the saturation of images and the photobleaching of the fluorophore.

**Figure 7.** Confocal laser scanning microscope Leica SPE II (PIQ- Laboratoire de Biophotonique et Pharmacologie)

- **Two-photon microscopy:**

**Principle:** The two-photon excited microscopy is based on the absorption of two photons which have approximately half the energy and double the wavelength of the photon

required for a single photon excitation quantum event to occur. The longer excitation wavelengths used with two-photon imaging dramatically increase tissue penetration depth and allow for long-term imaging without affecting the tissue viability and producing minimum of photobleaching.

**Microscope description:** Fluorescence microscopy experiments were performed by using a home-built two-photon laser scanning setup based on an Olympus IX70 inverted microscope with an Olympus 60x1.2NA water immersion objective (Clamme et al., 2003; Azoulay et al., 2003).

Two-photon excitation was provided by a titanium-sapphire laser (Tsunami, Spectra Physics), and photons were detected with Avalanche Photodiodes (APD SPCM-AQR-14-FC, Perkin-Elmer) connected to a counter/timer PCI board (PCI6602, National Instrument). Imaging was carried out using two fast galvo mirrors in the descanned fluorescence collection mode.

**Images acquisition:** Typical acquisition time was 20 ms with an excitation power around 40 mW ($\lambda$= 830 nm) at the laser output level. The signal was split to the green and red channels using a dichroic mirror For 3-HF probes, recorded images correspond to the green and red channels, which were obtained using a 550 DCXR dichroic mirror and two band-pass filters (Brightline HC 520/20 and HQ 585/40) in front of the two APDs. For NR12S, recorded images correspond to the green and red channels, which were obtained using a dichroic mirror (Beamsplitter 585 DCXR), a density filter 630/30 nm and two APDs).

**Ratiometric images generation:** The images were processed with a homemade program under LabView that generates a ratiometric image by dividing the image of the blue (green) channel by that of the red channel. For each pixel a pseudocolor scale was used for coding the ratio while the intensity was defined by the integral intensity recorded for both channels at the corresponding pixel (Klymchenko et al., 2009).

### 3.3. Flow cytometry

**Principle:** Flow cytometry is a powerful technique for the analysis of many parameters (size, scattering, fluorescence detection) of individual cells within heterogeneous populations. This

technique is used for many applications: immunophenotyping, cell counting and some protein expression analysis. It is based on passing a flow of thousands of cells per second through a laser beam, and capturing the light emerging from each cell.

It is composed of several components (Fig. 8): a) the fluidic system, allowing the presentation of samples to the laser beam, b) the lasers which are the light source, c) the optics which gather the light, d) the detectors that receive the light and finally d) electronics which will convert the signals from detectors to digital data.

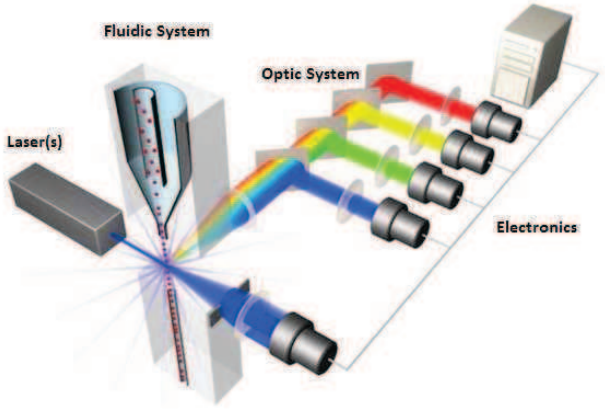




**Figure 8.** The basic components of a flow cytometer.

In the case of fluorescence detection, the fluorescent light coming from labeled cells pass through the laser, following a path directed through a series of filters in such way that particular wavelengths range is delivered to an appropriate detector.

**Flow cytometry for apoptosis detection:** Cells treated with apoptosis agent were stained using different probes. We used the BD LSR II flow cytometer with a violet laser (405 nm excitation laser line) with 2 emission filters: green channel (Alexa Fluor 430) and red channel (Qdot 585) for 3-HF probes or with the blue laser (488 nm excitation laser line) with 2 emission filters: yellow channel (PE: Phycoerythrin) and Red channel (PE-Texas Red) for Nile Red probes.

FITC-labeled AnnexinV was used as a control of staining of apoptotic cells. Data were collected with BD FACSDiva™ software and analysed with FlowJo (Flow Cytometer analysis software). For flow cytometry studies, cells were prepared with the same protocol as

for fluorescence spectroscopy analysis, with 0.1 μM (3-HF probes) or 0.01 μM (NR12S) final probe concentration. 50000 events were counted per sample.

# *Results and Discussions*

# *Chapter 1:*

# *Probes based on 3-hydroxyflavone (3-HF) fluorophore*

Fluorescent membrane probes constitute important tools to study membrane properties and monitor membranes in physiological and pathological conditions. Previously, our laboratory developed a number of membrane probes, based on environment-sensitive dyes of the 3-hydroxyflavone (3HF) family. These probes showed sensitivity to a variety of membrane properties, such as hydration, polarity, lipid order and electrostatics.

Previously, a 3-hydroxyflavone derivative, F2N12S, was developed featuring a structure with a zwitterionic group and long alkyl chain. This probe binds selectively the plasma membrane and can sense apoptosis via flow cytometry and fluorescence spectroscopy and microscopy. F2N12S is also a useful tool to visualize lipid domains in giant unilamellar vesicles, based on the ratio of its two emission bands. In living cells, in addition to apoptosis, F2N12S can detect changes in the lipid order induced by cholesterol depletion. As a first step of my research, I optimized the experimental conditions of utilization of F2N12S, which was the subject of a review article (see below).

In the second part, new improved analogues of F2N12S synthesized by a former PhD student, Oleksander Kucherak, were characterized. The chemical structure of the new probes allows their precise vertical position in lipid membranes, which could improve their sensitivity to the membrane properties. New 3HF probes were tested by fluorescence spectroscopy in cell suspensions and lipid vesicles. As F2N12S, the new probes showed high sensitivity to cholesterol extraction with methyl-ß-cyclodextrin and apoptosis with different agents. Importantly, one of these probes was found to be brighter than F2N12S in cells, while the other appears more sensitive to cholesterol depletion and apoptosis. Moreover, we evidenced that the response of the probes is independent of the cell type and the agent inducing apoptosis. Using two-photon fluorescence microscopy, we further showed that the loss of ordered phase and apoptosis can be detected by these new probes as a change in the color of the cell membranes in ratiometric images. Similarly to F2N12S, the new probes can be used as alternative tools of AnnexinV to detect apoptosis using flow cytometry. The main advantages of these dyes are their simple and fast protocols for staining, the small concentrations needed and the absence of phototoxicity.

Two manuscripts on this work are presented below.

# Manuscript 1: Monitoring membrane properties and apoptosis using membrane probes of the 3-hydroxyflavone family

*Zeinab Darwich, Andrey S. Klymchenko, Yves Mély**

Laboratoire de Biophotonique et Pharmacologie, UMR 7213 CNRS, Université de Strasbourg, Faculté de Pharmacie, 67401 Illkirch, France

*CORRESPONDING AUTHOR: yves.mely@unistra.fr; Tel: +33 36854263.

## Summary

Environment-sensitive fluorescent membrane probes are attractive tools for investigating the membrane properties and their changes under perturbing conditions. Membrane probes of the 3-hydroxyflavone family are of particular interest due to their excited-state intramolecular proton transfer (ESIPT) reaction, which confers a dual emission highly sensitive to the polarity and hydration of the environment. In the present work, we will describe the protocols used with these probes in order to monitor the physico-chemical properties of lipid membrane models and cell plasma membranes, and to detect apoptosis.

**Key words:** fluorescent membrane probe, environment-sensitive dye, excited-state intramolecular proton transfer, F2N12S, ratiometric response, cell membrane, lipid order, lipid domains, apoptosis

### 1. Introduction

Fluorescent membrane probes are important tools to investigate the physico-chemical properties of model and cellular lipid membranes. The most common properties addressed by these probes are the membrane fluidity, hydration and electrostatics, such as surface, dipole

and transmembrane potential *(1)*. These properties correlate with other membrane properties, which generally cannot be directly measured by these probes, such as lipid order, interlipid distance, phase transitions and phase separations, etc. Among the existing membrane probes, the 3-hydroxyflavone derivatives are of particular interest *(2-4)* .These probes exhibit the remarkable property to emit two bands, due to an excited state intramolecular proton transfer (ESIPT). This dual emission provides an additional channel of spectroscopic information and through the ratio of the two bands offers a signal that is independent of the probe concentration. Particularly attracting is the probe F2N12S, which due to its apolar chain and zwitterionic group stains specifically the outer leaflet of plasma membranes, without rapid internalization inside the cells. In contrast to fluorescent lipids, this probe binds spontaneously lipid bilayers and thus, does not require any helper agent, such as surfactants or cyclodextrins. Being bound to lipid membranes, the dual fluorescence spectrum of F2N12S is characterized by a short-wavelength band, originating from the emission of the normal N* (H-bonded and H-bond free) emissive species and a long-wavelength band assigned to the emission of the ESIPT tautomer T* *(5, 6)*. The dual emission of F2N12S is highly sensitive to several membrane properties. By deconvoluting the emission spectrum of F2N12S, both the polarity and hydration, two different properties of lipid membranes can be monitored simultaneously *(4, 7)*. The polarity parameter correlates well with the membrane electrostatics, i.e. surface and dipole potentials, while the hydration parameter shows strong variation in response to changes in the membrane phase state *(1)*. This bi-parametric sensitivity of F2N12S allowed its applications for detecting apoptosis and probing lipid domains.

Apoptosis, the programmed cell death, is a fundamental process controlling cell homeostasis. In normal cells, the plasma membrane is asymmetric, so that the outer leaflet presents a large quantity of sphingomyelin (SM), while phosphatidyl serine (PS) and

phosphatidylethanolamine (PE) are mainly concentrated in the inner leaflet *(8).* In apoptotic cells, due to activation of flippases this asymmetry is lost, so that PS is exposed at the outer leaflet. Moreover, PS exposure is associated with a decrease in SM at the outer leaflet *(9)*, which may decrease the fraction of the liquid ordered, Lo phase at this leaflet. Both exposure of PS and loss of Lo phase induce a significant change in the dual emission of F2N12S, providing an increase in the relative intensity of the short-wavelength band *(4).*

Another application of probe F2N12S is to monitor lipid domains. In cell membranes, lipid domains attracted large attention since they are thought to be involved in the regulation of various cell functions such as signal transduction, lipid trafficking and membrane protein activity *(10).* Lipid domains composed of saturated lipids (SM in particular) and cholesterol form a liquid ordered (Lo) phase. These domains are thought to float in the liquid disordered (Ld) phase, formed by unsaturated lipids and cholesterol. As F2N12S probe is sensitive to the phase state, it was applied for imaging lipid domains in giant vesicles, showing a good contrast between Lo and Ld phases in ratiometric images *(3).* In cell membranes of astrocytoma, we further evidenced the presence of a high fraction of Lo phase, which could be substantially decreased by cholesterol extraction *(4).* Remarkably, cholesterol extraction gave the same spectroscopic response as apoptosis, suggesting that both phenomena lead to similar loss in the Lo phase at the outer membrane leaflet. Thus, F2N12S probe appears as a promising tool for monitoring the biophysical properties of model and cell membranes, and for probing lipid domains and apoptosis. In the present work, we review the sensing methodology based on F2N12S for these two applications. In particular, we will present protocols for (a) spectroscopic studies of phase state in model lipid membranes; (b) imaging membrane domains in giant unilamellar vesicles; (c) spectroscopic studies of membrane

modifications due to apoptosis and cholesterol extraction; (d) detection of apoptosis by flow cytometry and (e) imaging apoptosis by fluorescence microscopy.

## 2. Materials

Prepare stock solution of F2N12S in DMSO at 0.1 μM and store it at -20ºC. Dioleoylphosphatidylcholine (DOPC) and cholesterol were purchased from Sigma-Aldrich (Lyon, France). Bovine brain sphingomyelin was from Avanti Polar Lipids (Alabaster, USA).

All lipids were dissolved in chloroform.

### 2.1. Large unilamellar vesicles:

1. Phosphate buffer: 20 mM, pH 7.4
2. Lipids (DOPC, sphingomyelin, cholesterol) in chloroform
3. Lipex Biomembranes extruder (Vancouver, Canada) with two sizes of filters, 0.2 and 0.1 μm respectively.

### 2.2. Giant Unilamellar vesicles:

1. Home-built liquid cell (University of Odense, Denmark) with platinum wires
2. Lipids (DOPC, sphingomyelin, cholesterol): 0.1 mM in chloroform
3. Sucrose solution: 300 mM
4. Glucose solution: 300 mM
5. Thermostat
6. Power supply: 2-V, 10-Hz.

### 2.3. Cell Culture

1. X-vivo 15 serum-free medium (Cambrex, France) for Human lymphoid CEM T cells
2. EMEM (Eagle's minimal essential medium, Lonza): with 10% heat-inactivated fetal bovine serum (PAN Biotech GmbH) , 0.6 mg/mL glutamine (Biowhittaker) for U87MG human glioblastoma cell line
3. DPBS (Dulbecco's Phosphate Buffered saline-Lonza): without $Ca^{2+}$ and $Mg^{2+}$
4. HBSS (Hank's Buffered Salt Solution-Sigma): with $NaHCO_3$, without Phenol Red, calcium chloride and magnesium sulphate.
5. Trypsin: from Lonza.
6. Opti-MEM: Reduced Serum Medium from Invitrogen
7. Actinomycin D (Sigma-Aldrich): dissolved in DMSO, stored at -20°C
8. Methyl-ß-cyclodextrin (Sigma-Aldrich): dissolved in DPBS, stored at +4°C
9. IBiDi Labtek: to prepare cells for microscopic experiments
10. Cell lines: Human lymphoid CEM T cells and U87MG human glioblastoma cell line.

### 2.4. Fluorescence spectroscopy and microscopy

1. Jobin-Yvon Fluoromax 3 spectrofluorometer equipped with a thermostated cuvette holder was used to record fluorescence spectra in vesicles and cells.
2. Quartz cuvettes of 1mL were used to measure fluorescence spectra.

3. For fluorescence microscopy experiments, a home-built two-photon laser scanning set-up based on Olympus IX70 inverted microscope with an Olympus 60x 1.2NA water immersion objective was used. Two-photon excitation was provided by a titanium-sapphire laser (Tsunami, Spectra Physics) and photons were detected with Avalanche Photodiodes (ADP SPCM-AQR-14-FC, Perkin Elmer) connected to a counter/timer PCI board (PCI6602, National Instrument). Imaging was carried out using two fast galvo mirrors in the descanned fluorescence collection mode. Typical acquisition time was 20 ms with an excitation power around 20 mW ($\lambda$=830nm) at the sample level. Images corresponding to the short-wavelength and the long-wavelength emission bands were recorded simultaneously using a dichroic mirror (Beamsplitter 550DCXR) and two band-pass filters (Brightline HC 520/20 and HQ 585/40) in front of the APDs.

### 2.5. Flow Cytometry

1. Annexin V-FITC Kit: from Immunotech
2. Propidium iodide (PI): from Sigma
3. Binding buffer provided with the annexin V-FITC kit: 10 mM Hepes/NaOH, pH 7.4, 140 mM NaCl, 2.5 mM $CaCl_2$
4. F2N12S
5. FACSAria Cell sorter (BD Biosciences, CA) equipped with an argon laser (488 nm) and a diode laser (405 nm) and emission filters DF30, DF42 and DF20 centered at 530, 585 and 610 nm, respectively.
6. FACSDiva Software (Flow Cytometer analysis software from BD Biosciences).

## 3. Methods

Carry out all procedures at room temperature unless otherwise specified.

### 3.1. Spectroscopic studies of phase state in model lipid membranes

#### 3.1.1. Large Unilamellar vesicle preparation and staining

1. Dissolve 5 mM of lipids (DOPC, DOPC/Chol or SM/Chol) in 5 mL chloroform to ensure their homogeneous distribution

2. Evaporate chloroform by rotary evaporation to get a dry thin lipid film on the wall of a round bottom flask with gentle heating (about 35°C) during 30 minutes.

3. Hydrate the lipid film by adding 10 mL phosphate buffer to the flask

4. Leave the obtained solution at RT for unsaturated lipids or 55° C for lipids with saturated alkyl chains.

5. Vortex the solution for 2 minutes to obtain a suspension of multilamellar vesicles with a heterogeneous size distribution.

6. Use the lipid extruder to downsize the vesicles. Lipid suspension is forced through a polycarbonate filter, firstly, by passing through a large pore size (0.2 μm) filter seven times. Then the suspension is passed ten times through a filter with 0.1 μm pore size. Finally, LUVs obtained have a size about 110-120 nm.

7. Label LUVs by adding aliquots (~ 2 μL) of F2N12S probe stock solution to 1 mL of vesicle suspension (200 μM lipid concentration) in phosphate buffer.

8. Incubate LUVs with the probe (1μM) for 3-5 minutes at RT.

#### 3.1.2. Fluorescence spectroscopy measurements

Transfer stained LUVs to 1 mL quartz cuvettes. Record the emission fluorescence spectrum of the LUV solution at 20 °C, using 400 nm excitation wavelength on the spectrofluorometer described in section 2.4. All the spectra should be corrected from the fluorescence of the corresponding blank solution (vesicles without the probe). The ratio of their two bands (N*/T* ratio) is obtained by dividing the emission intensity at the maximum of the N* band by the intensity at the maximum of emission of the T* band. To better analyze and compare the spectra, a normalization to the T* band maximum could be applied.

Fluorescence spectrum of F2N12S in DOPC vesicles is characterized by a high N*/T* ratio close to 1 (Figure 1. Solid curve). When cholesterol is added to DOPC, this ratio decreases to 0.8 (Figure1. Dashed curve). In SM/Chol vesicles, the fluorescence spectrum of F2N12S is characterized by a blue-shifted N* band with a decrease of the N*/T* ratio to 0.7 (Figure1. Dotted curve). This decrease is related to the low polarity and hydration in SM+cholesterol domains corresponding to Lo phase.

### 3.2. Imaging membrane domains in giant unilamellar vesicles

#### 3.2.1. Giant unilamellar vesicle preparation and staining

1. Dissolve lipids (DOPC, SM/Chol or DOPC/SM/Chol) in chloroform to get 1 M final concentration
2. Deposit 3µL of lipid solution on the platinum wires of the chamber with a micro-syringe
3. Evaporate the solvent under vacuum for 20 minutes
4. Fill the chamber with 500 µL solution of 300 mM sucrose
5. Connect the chamber to an alternative power supply 2-V, 10-Hz for *ca* 2h

6. Store obtained solutions of GUVs at RT in the darkness

7. For GUV staining, add the probe aliquot to 200 µL of 300 mM glucose solution

8. Quickly, add 50 µL of obtained solution of GUVs to the solution of dye in glucose and mix gently (See Note 1)

9. Transfer the obtained stained GUV suspension to the LabTek$^{TM}$ 8-well chamber and incubate it for 3-5 minutes to allow GUVs to sediment at the bottom of the chamber

3.2.2. Microscopic measurements

Visualize stained GUVs with a two-photon microscope using 830 nm excitation wavelength. Alternatively, a single photon laser excitation source at 405 nm can be used in a confocal microscope. Record images corresponding to blue and red channels simultaneously, using a 550 DCXR dichroic mirror and two band-pass filters (Brightline HC 520/20 and HQ 585/40) in front of the two APDs. Process these images with a program that generates a ratiometric image by dividing the image of the short-wavelength channel by the long-wavelength channel. In our case, a home-made program under LabView was used to calculate for each pixel the ratio of the integral intensity of the N* band (below 550 nm) to the integral intensity of the T* band (above 550 nm) and code it in a pseudo-color scale. To avoid artifacts, the N*/T* ratio at a given pixel was only calculated when the integral intensity of both bands exceeds a threshold value.

In DOPC GUVs presenting a Ld phase, the fluorescence intensity of F2N12S is homogeneously distributed all over the vesicles, with a blue/red intensity ratio of 0.45 (Figure 2A.). For SM/Chol GUVs presenting a Lo phase, this ratio decreases to 0.2. (Figure2B). In vesicles composed of a ternary mixture of DOPC/SM/Chol, a heterogeneous color distribution

was observed, showing different domains with different blue/red ratios, corresponding to the separated Lo and Ld phases (Figure 2C.)

### 3.3. Spectroscopic studies of cell membrane modifications due to apoptosis or cholesterol extraction

Cell culture: Maintain cell concentration at 5-10 x $10^4$ cells/mL by removing a portion of the culture and replacing it with a fresh EMEM medium 3 times per week.

For cellular spectroscopic measurements, prepare cells in Nunc Flasks Nunclon (80 $cm^2$) two days in advance.

In apoptosis and cholesterol depletion studies, respectively:

1. Add the apoptosis agent, actinomycin D (0.5 µg/mL) in D-MEM medium to cells 18h before the experiment, and incubate at 37 °C in a humified 5% $CO_2$ atmosphere.
2. For cholesterol extraction, incubate cells with 5 mM methyl-ß-cyclodextrin for 2 h at 37°C.

For adherent cells (U87MG astrocytes, in our case), the day of the measurement:

1. Remove old medium
2. Wash cells 2 times with 10 mL DPBS to remove all traces of medium and dead cells
3. Add 3 mL of 1X diluted trypsin to detach cells, then incubate them at 37°C for 4 min
4. Dilute trypsin with 6 mL DPBS to stop its action. Then, resuspend cells and transfer them to a Falcon tube
5. Centrifuge cell suspension at1500 RPM for 5 min at RT

6. Resuspend the pellet with 3 mL HBSS
7. Recentrifuge one more time at 1500 RPM for 5 min at RT to remove all trypsin and media traces
8. Resuspend the pellet with 1-2 mL HBSS
9. Count cells and dilute them to obtain a final concentration of $2x10^6$ cells/mL

For cells in suspension (Human lymphoid CEM T cells in our case), just centrifuge cells at 1500 RPM for 5 min to remove old medium, then apply the same protocol as for adherent cells, centrifuge twice and resuspend to obtain a final concentration of $2\times10^6$ cells/mL.

The protocol of staining with F2N12S is the same for both types of cells and for all treatments (control cells, cholesterol-depleted cells and apoptotic cells).

1. Mix 500 μL of the cell suspension with 500 μL of dye diluted in HBSS (See Note 2) to obtain a final probe concentration of 0.1 μM (See Note 3).
2. Incubate cells with probe for 7 min at 20 ºC in the dark
3. Transfer the cell suspension to a 1 mL quartz cuvette

Record the emission spectrum of intact, apoptotic or cholesterol-depleted cells at 20°C, using 400 nm excitation wavelength on the spectrofluorometer described in section 2.4. All the spectra should be corrected from the fluorescence of the corresponding blank solution (cell suspension without the probe). The ratio of their two bands (N*/T* ratio) is obtained by dividing the intensity at the maximum of emission of the N* band by the intensity at the maximum of emission of the T* band. The emission spectrum of F2N12S in cells could be normalized to the T* band maximum to facilitate the comparison of the spectra. For intact

cells, a low N*/T* ratio was recorded (Figure3, solide curve). After cholesterol depletion, the N*/T* ratio increases (Figure3, dotted curve). This increase of the ratio is also observed with apoptotic cells (Figure3, dashed curve). These data suggest that during apoptosis, a loss of the Lo phase in the outer leaflet occurred in addition to PS exposure to the cell surface.

### 3.4. Detection of apoptosis by flow cytometry

1. Treat cells with actinomycin D (0.5 µg/mL), 18 h before the measurements.
2. For labeling, cells were washed twice with HBSS, and then resuspended in the binding buffer.
3. Label cells with PI (2.5 µg/ mL) by adding stock solution of PI to the cell suspension and mix gently
4. Keep tubes in ice for 15 min in the dark.
5. Add 400 µL of ice-cold 1X binding buffer and mix gently.
6. Label cells with F2N12S (0.2 µM) for 5 min in the dark at room temperature (See Note 5).
7. Sort cells treated with actinomycin D with the FACSAria Cell Sorter equipped with an argon laser (488 nm) and a diode laser (405 nm) and emission filters DF30, DF42 and DF20 centered at 530, 585 and 610 nm, respectively. The argon laser (488 nm) was used for PI selective excitation, where F2N12S does not absorb and the diode laser 405 nm was used for F2N12S selective excitation.
8. Analyze obtained data with FACSDiva Software

F2N12S-PI labeling allows discriminating 3 populations of cells: apoptotic cells (low T*/N* ratio and PI negative), living cells (high T*/N* ratio and PI negative), and dead cells (low T*/ N* ratio and PI positive) (Figure 4).

### 3.5. Imaging membrane modifications in cells by two photon microscopy: Apoptosis and cholesterol extraction

1. Seed cells in a chambered coverglass (IBiDi) at a density of $5\times10^4$ cells/IBiDi
2. Next day, wash gently cells twice with 1 mL HBSS
3. Add freshly diluted F2N12S in 400 µl HBSS to 400 µl of HBSS to a final concentration of 0.3 µM
4. Add this fresh solution to the cells
5. Incubate 7 min at RT in the darkness
6. Wash once gently with HBSS to remove excess of the probe
7. Visualize cells with a two-photon microscope using 830 nm excitation wavelength. Alternatively, a single photon laser excitation source at 405 nm can be used in a confocal microscope. Perform the image recording and processing as in the chapter 3.2.2. (See Notes 6 and 7)

Intact cells stained with F2N12S show a low blue/red ratio around 0.2 (Figure 5A). After cholesterol depletion and apoptosis induction, an increase of this ratio is noticed (Figure 5B and 5C, respectively). These data are consistent with the fluorescence spectroscopy data described above.

In conclusion, the 3-HF probe F2N12S constitutes a good tool for studying model lipid membranes and cell plasma membranes. It is able to bind to both Lo and Ld phases, and to discriminate them by the ratio of its two emission bands. In cellular applications, F2N12S stains selectively the plasma membrane and shows different intensity ratios for intact cells

and treated cells (cholesterol depleted and apoptotic). Thus, F2N12S can be used to sense changes in lipid composition and order and to detect apoptosis.

**4. Notes**

1. During the staining of GUVs with the probe, respect the order of mixing: first add the probe aliquot to the glucose solution, mix gently, then immediately add GUVs, to get a homogenous staining of GUVs.

2. To stain cells for spectroscopic measurements, prepare each time a fresh solution of F2N12S in HBSS. Diluting the dye in the buffer should be very fast since the solubility of F2N12S is limited in water, leading to probe precipitation. Therefore, the probe solution should be used immediately after preparation.

3. During all spectroscopic measurements, avoid using a high concentration of F2N12S. An excess of dye can lead to an unspecific binding, which modifies the spectrum of the probe. In the optimal concentration range, the shape of the fluorescence spectrum of F2N12S should be independent of the probe concentration.

4. In SM/Chol vesicles, the polarization of the excitation light induces some effect on the fluorescence intensity distribution. The fluorescence intensity of F2N12S depends on the orientation of the lipid bilayer relatively to the polarization plane of the excitation light.

5. For flow cytometry studies, vortex cells immediately before measurement to avoid sedimentation of the cells on the bottom of the tube.

6. For two-photon imaging, the number of photons collected in the green and red channels of a given pixel, should be high enough to get a reliable blue/red ratio value.

7. For two-photon imaging, a threshold was applied with the aim to remove all pixels with too low signal, which would provide erratic blue/red values.

8. F2N12S is available as a product from Molecular probes-Invitrogen-Life Sciences, under the name *Violet Ratiometric Membrane Asymmetry Probe/Dead Cell Apoptosis Kit.* http://tools.invitrogen.com/content/sfs/manuals/mp35137.pdf

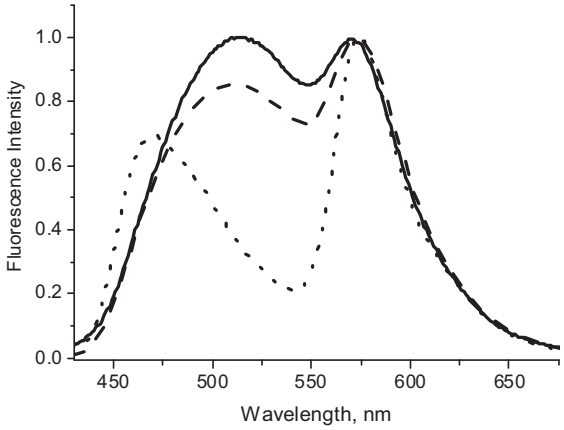


**Figure 1.** Fluorescence spectra of F2N12S in LUVs composed of DOPC (solid curve), DOPC+Chol (dashed curve) and SM+Chol (dotted curve). Data from *(3).*

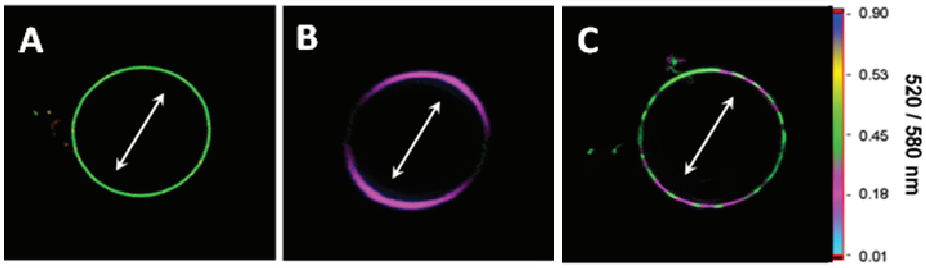


**Figure 2.** Fluorescence ratiometric images (520/580 nm) of GUVs composed of (A) DOPC, (B) SM+Cholesterol, and (C) the ternary mixture (DOPC/SM/cholesterol 1/1/0.7) (See Note 4). Adapted from *(3).* .

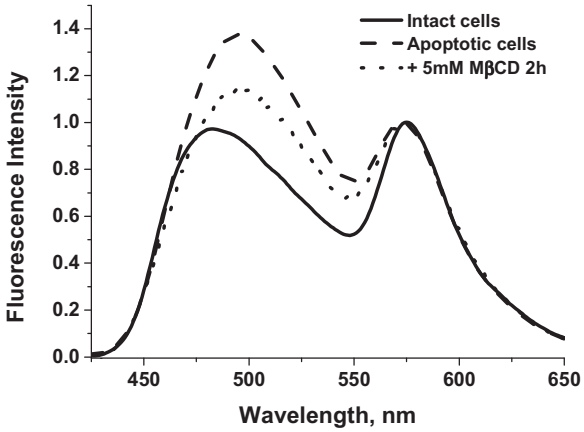


**Figure 3**. Effect of apoptosis (dashed curve) and cholesterol depletion (dotted curve) on the emission spectrum of F2N12S in cell membranes. Excitation wavelength was 400 nm. Final probe concentration was 0.1 μM. Data from *(4)*.

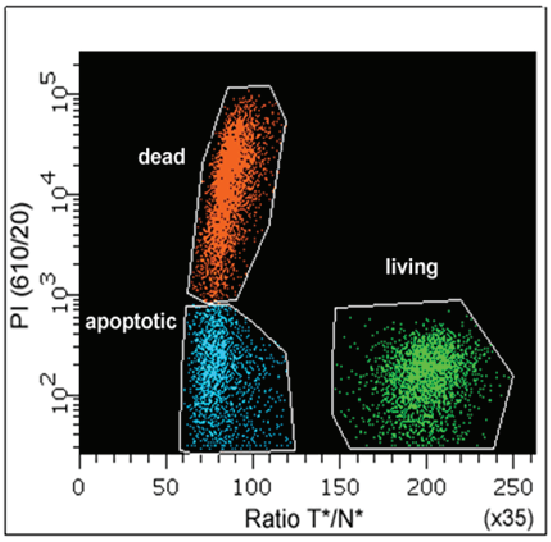


**Figure 4.** Flow cytometry of T lymphoblastoid cells treated by actinomycin D. Cells were stained by PI and F2N12S. F2N12S is selectively excited at 405 nm and its fluorescence was collected simultaneously at 530 and 585 nm. PI was selectively excited at 488 nm, and its fluorescence was detected at 610 nm. The PI fluorescence intensities are plotted versus the T*/N* ratio (585/530 nm) of F2N12S. Three distinct populations of cells were detected, namely living cells in green, apoptotic cells in blue and dead cells in orange. Data from *(2)*.

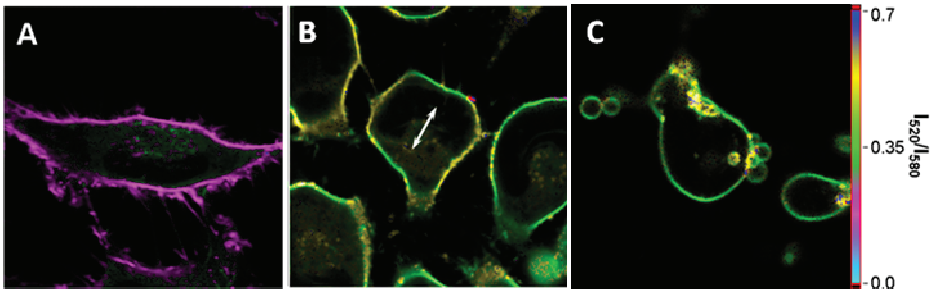


**Figure 5.** Fluorescence ratiometric images (520/580 nm) of U87MG cells stained with F2N12S. (A) Intact, (B) cholesterol depleted, and (C) apoptotic cells. F2N12S concentration was 0.3µM. Data from *(4).*

**Acknowledgements**

This work was supported by ANR grant (fluo-aa-nt) and ANR JCJC (ANR-11-JS07-014-01).

ZD received a fellowship from CNRS and Region Alsace.

**References**

1. Demchenko, A. P., Y. Mely, et al. (2009) Monitoring biophysical properties of lipid membranes by environment-sensitive fluorescent probes. *Biophys J* **96**(9): 3461-3470

2. Shynkar, V. V., A. S. Klymchenko, et al. (2007) Fluorescent biomembrane probe for ratiometric detection of apoptosis. *J Am Chem Soc* **129**(7): 2187-2193
3. Klymchenko, A. S., S. Oncul, et al. (2009) Visualization of lipid domains in giant unilamellar vesicles using an environment-sensitive membrane probe based on 3-hydroxyflavone. *Biochim Biophys Acta* **1788**(2): 495-499.

4. Oncul, S., A. S. Klymchenko, et al. (2010) Liquid ordered phase in cell membranes evidenced by a hydration-sensitive probe: effects of cholesterol depletion and apoptosis. *Biochim Biophys Acta* **1798**(7): 1436-1443.
5. Klymchenko, A. S., G. Duportail et al. (2002) Novel two-band ratiometric fluorescence probes with different location and orientation in phospholipid membranes. *Chem Biol.* **9**(11): 1199-208.

6. Klymchenko, A. S., G. Duportail, et al. (2003) Ultrasensitive two-color fluorescence probes for dipole potential in phospholipid membranes. *Proc Natl Acad Sci U S A* **100**(20): 11219-11224.
7. Klymchenko, A. S., Y. Mely, et al. (2004) Simultaneous probing of hydration and polarity of lipid bilayers with 3-hydroxyflavone fluorescent dyes. *Biochim Biophys Acta* **1665**(1-2): 6-19.
8. Zwaal, R. F. and A. J. Schroit (1997) Pathophysiologic implications of membrane phospholipid asymmetry in blood cells. *Blood* **89**(4): 1121-1132.

9. Tepper, A. D., P. Ruurs, T. Wiedmer, et al. (2000) Sphingomyelin hydrolysis to ceramide during the execution phase of apoptosis results from phospholipid scrambling and alters cell-surface morphology. *J Cell Biol.* **150**(1): 155-64.

10. Brown D. A. and E. London (1998) Structure and origin of ordered lipid domains in biological membranes. *J Membr Biol.* **164**(2): 103-14.

# Manuscript 2: Rational design of membrane probes for apoptosis based on 3-hydroxyflavone

Zeinab Darwich, Oleksandr A. Kucherak, Ludovic Richert, Romain Vauchelles, Yves Mély*, Andrey S. Klymchenko*

Laboratoire de Biophotonique et Pharmacologie, UMR 7213 CNRS, Université de Strasbourg, Faculté de Pharmacie, 74, Route du Rhin, 67401 ILLKIRCH Cedex, France

* Corresponding authors: tel: +33 368 85 42 55; fax: +33 368 85 43 13; e-mail: andrey.klymchenko@unistra.fr; tel: +33 368 85 42 63; fax: +33 368 85 43 13; e-mail: yves.mely@unistra.fr

**Abstract**

Environment-sensitive probes constitute powerful tools for monitoring changes in the physico-chemical properties of cell plasma membranes. Among these probes, 3-hydroxyflavone probes are of high interest due to their dual emission and ratiometric response. Here, three probes derived from the parent F2N12S were designed, characterized and applied to monitor the membrane changes occurring during apoptosis. These three probes were designed to orient the dye vertically in the membrane. They differ by the length of their alkyl chain (from 4 to 8 C), which was included to optimize their affinity to the lipid membranes. The new probes were found to be sensitive to both the lipid phase and surface charge in model and cell plasma membranes. Interestingly, apoptosis induced by different agents lead to similar spectroscopic effects as the combined effect of loss of lipid order and change in surface charge, confirming that apoptosis decreases the lipid order and the surface charge in the upper leaflet of cell membranes. Among these three probes, the one with the longest alkyl chain (8C) did not efficiently stain the membranes. The one with the shortest chain (4C) was found to be the most sensitive to apoptosis, while the one with a 6 C chain was the brightest. In conclusion, these studies report a rational relationship between the probe structures and their sensitivity to lipid order, surface charge and apoptosis.

**Key words:** Cell plasma membrane, fluorescent probes, apoptosis, cholesterol depletion, 3-hydroxyflavone, probe orientation

## Introduction

Apoptosis defined as a programmed cell death is a physiological phenomenon occurring in multicellular organisms (Erickson 1997). It is a combination of morphological and biochemical events (Wyllie 1980), distinct from necrosis, which is considered as the passive, premature traumatic cell death (Leist and Jaattela 2001). During apoptosis, cellular changes involve cell shrinkage, chromatin condensation, nuclear fragmentation and membrane blebbing, resulting in the formation of apoptotic bodies. Despite all these modifications, the plasma membrane integrity is conserved during apoptosis while in the case of necrosis, membrane fragmentation occurs from the beginning. Apoptosis is a complex process described as a cascade of events requiring the involvement and regulation of many proteins at different levels (Thornberry and Lazebnik 1998), (Salvesen and Dixit 1997). In the early steps of apoptosis, cleavage of flippase (ATP-dependent aminophospholipid translocase) and/or activation of scramblase lead to a flip of phosphatidylserine from the inner to the outer leaflet, resulting in a loss of the asymmetry of the cell plasma membrane. In healthy cells, the asymmetric distribution of lipids between the leaflets is mainly maintained by the flippase that transports PS and PE from the outer to the inner leaflet (Williamson and Schlegel 1994). As a result, the inner leaflet is enriched in PS and PE, while the outer leaflet is enriched in SM and PC (Meer 1989) (Feigenson 2007). The exposure of PS to the cell surface during the early stages of apoptosis is a signal for macrophages to clear cells undergoing apoptosis (Zwaal and Schroit 1997).

Many efforts were done to develop new methods for apoptosis detection (Elmore 2007), such as cytomorphological assays using electron and fluorescence microscopy (White and Cinti 2004) (White and Cinti 2004), DNA degradation assays (Wyllie 1980), (Kressel and Groscurth 1994), analysis of apoptosis associated proteins (Nagata 1997), (Thornberry and Lazebnik 1998), (Chan and Mattson 1999), (Packard, Komoriya et al. 2001), mitochondrial assays (Zamzami, El Hamel et al. 2000)and detection of membrane alterations. The most common assay in this last category is based on fluorescently labeled annexin V that recognizes PS exposed at the outer plasma membrane leaflet of apoptotic cells (Vermes, Haanen et al. 1995). Alternatively, organic ligands complexed with Zn ions can also be used to specifically recognize the exposed PS lipids (Truong-Tran, Carter et al. 2001).

In addition to PS exposure to the cell surface, the loss of transbilayer asymmetry may alter several biophysical properties of the cell plasma membrane, such as surface charge, lipid packing, fraction of the liquid ordered phase, hydration, etc. Therefore, development of new fluorescent probes able to detect apoptosis through their sensitivity to changes in these physico-chemical properties is of particular interest. The first fluorescent probe based on this principle was Merocyanine 540 (MC540), which binds selectively to the highly disordered membranes of apoptotic cells. This dye is applicable for apoptosis detection by flow cytometry (Laakko, King et al. 2002), (Bailey, Nguyen et al. 2009). More recent examples are probes F2N12S and NR12S based on 3-hydroxychomone and Nile Red fluorophores, respectively. The former senses apoptosis as a result of its sensitivity to both the increase in the negative surface charge and decrease in the lipid order (fraction of Lo phase) of the plasma membrane occurring on apoptosis (Demchenko, Mely et al. 2009), (Klymchenko, Oncul et al. 2009), (Kucherak, Oncul et al. 2010), while the latter senses apoptosis exclusively due to the decrease in the lipid order (Darwich, Klymchenko et al. 2012). Both dyes are able to detect apoptosis using fluorescence spectroscopy, microscopy, and flow cytometry.

In the present work, we modified the design of F2N12S and report on new improved apoptosis probes. In this new design, a zwitterionic group and long alkyl chains were attached on the opposite sides of the fluorophore moiety, in order to favor the vertical orientation of the fluorophore within the lipid bilayer. This new design improved the sensitivity of their dual emission to changes in the lipid order and/or surface charge of model and cell membranes. Therefore, compared to F2N12S they showed better response to apoptosis or superior fluorescence brightness.

**Materials and methods**

All chemicals and solvents for synthesis were from Sigma-Aldrich.

**Synthesis of new probes.**

**5-(3-Chloro-propoxy)-2-hydroxy-acetophenone (1).** In a round-bottom flask 2,5-dihydroxy-acetophenone (3.05 g, 0.020 mol) was dissolved in 20 mL of DMF. Then 1-bromo-3-chloro-propane (2.36 mL, 0.022 mol) and potassium carbonate (5.54 g, 0.040 mol) were added. Reaction mixture was stirred upon heating at 80 °C for 4 h. Solution became dark. After

cooling it was poured into 200 mL of water, neutralized with 10 % aq. HCl and extracted with $CHCl_3$ (2 times). Combined organic layers were dried with sodium sulfate. Inorganic salt was filtered off, and chloroform was removed by vacuum evaporation. Obtained dark oil was purified by column chromatography (eluent $CH_2Cl_2$) to produce compound **1** as colourless oil. Yield 2.55g (56%). $^1$H NMR (400MHz, $CDCl_3$): δ 11.84 (s, 1H), 7.18 (d, 1H), 7.09 (dd, 1H), 6.90 (d, 1H), 4.08 (t, 2H), 3.74 (t, 2H), 2.59 (s, 3H), 2.21 (m, 2H). LCMS (m/z): MM-ES+APCI, found $[M+1]^+$ 229.1 (calcd for $C_{11}H_{14}ClO_3^+$ 229.1).

**5-(3-Dimethylamino-propoxy)-2-hydroxy-acetophenone (2).** Compound **1** (2.55 g, 0.011 mol) was dissolved in a small amount of acetone. Then, 5 mL of saturated solution of sodium iodide in acetone were added. After 2 min of stirring, a white precipitate of NaCl appeared. Stirring was continued at RT for 1h. Inorganic salt was filtered off, and resulted solution was evaporated under vacuum. Obtained iodo-derivative was treated with 2 M solution of dimethylamine in THF (17.0 mL, 0.033 mol). Reaction mixture was warmed up, and a white residue was formed in 2 min. It was stirred at RT for 2 h. Organic solvent was removed by vacuum evaporation. Residue was treated with aq. sodium carbonate in order to decompose the ammonium salt. Free amine was extracted with chloroform (2 times). Combined organic layers were dried with sodium sulphate. Inorganic salt was filtered off, and chloroform was removed by vacuum evaporation. Obtained dark oil was purified by column chromatography (eluent $CH_2Cl_2$/MeOH = 9/1) to produce compound **2** as white solid. Yield 1.10g (41%). $^1$H NMR (400MHz, $CDCl_3$): δ 11.82 (s, 1H), 7.16 (d, 1H), 7.07 (dd, 1H), 6.87 (d, 1H), 3.96 (t, 2H), 2.58 (s, 3H), 2.48 (t, 2H), 2.26 (s, 6H), 1.94 (m, 2H). LCMS (m/z): ESI, found $[M+1]^+$ 238.1 (calcd for $C_{13}H_{20}NO_3^+$ 238.1).

**General procedure for synthesis of 3-hydroxyflavones.** 2-Hydroxyacetophenone derivative (200 mg, 1.00 eq) was mixed with corresponding aldehyde (1.05 eq) in 2 mL of DMF. To the obtained solution, sodium methoxide (4 eq) was added. The reaction mixture became dark orange. It was stirred at RT overnight and then diluted with 10 mL of ethanol. New portion of sodium methoxide (12 eq) and 30% aqueous $H_2O_2$ (10 eq) were added. The resulting solution was refluxed for 3 min, cooled and poured into 100 mL of water. After neutralization with 10% HCl, the formed precipitate was filtered off. If the precipitate was not formed, the product was extracted with an organic solvent (2 times). Combined organic layers were dried

with sodium sulphate and evaporated under vacuum. Obtained residue was purified by preparative TLC or column chromatography (eluent $CH_2Cl_2$/MeOH = 9/1).

**4'-Dibutylamino-6-(3-dimethylamino-propoxy)-3-hydroxy-flavone (3).** It was synthesized according to the general procedure starting from 4-dibutylamino-benzaldehyde and compound **2** (200 mg, 0.84 mmol). The product was purified by preparative TLC (eluent $CH_2Cl_2$/MeOH = 9/1). Yellow solid, yield 100 mg (25%). $^1$H NMR (300 MHz, $CDCl_3$): δ 8.12 (d, 2H), 7.52 (d, 1H), 7.42 (d, 1H), 7.20 (dd, 1H), 6.71 (d, 2H), 4.08 (t, 2H), 3.32 (t, 4H), 2.44 (t, 2H), 2.24 (s, 6H), 1.96 (m, 2H), 1.60 (m, 4H), 1.36 (m, 4H), 0.96 (t, 6H). LCMS (m/z): MM-ES+APCI, found $[M+1]^+$ 467.3 (calcd for $C_{28}H_{39}N_2O_4^+$ 467.3).

**4'-Dihexylamino-6-(3-dimethylamino-propoxy)-3-hydroxy-flavone (4).** It was synthesized according to the general procedure starting from 4-dihexylamino-benzaldehyde and compound **2** (200 mg, 0.84 mmol). The product was purified by preparative TLC (eluent $CH_2Cl_2$/MeOH = 9/1). Yellow solid, yield 170 mg (38%). $^1$H NMR (400 MHz, $CDCl_3$): δ 8.12 (d, 2H), 7.51 (d, 1H), 7.42 (d, 1H), 7.20 (dd, 1H), 6.70 (d, 2H), 4.09 (t, 2H), 3.31 (t, 4H), 2.57 (t, 2H), 2.33 (s, 6H), 2.03 (m, 2H), 1.60 (m, 4H), 1.40-1.20 (m, 12H), 0.89 (t, 6H). LCMS (m/z): MM-ES+APCI, found $[M+1]^+$ 523.3 (calcd for $C_{32}H_{47}N_2O_4^+$ 523.3).

**4'-Dioctylamino-6-(3-dimethylamino-propoxy)-3-hydroxy-flavone (5).** It was synthesized according to the general procedure starting from 4-dioctylamino-benzaldehyde and compound **2** (200 mg, 0.84 mmol). The product was purified by preparative TLC (eluent $CH_2Cl_2$/MeOH = 9/1). Yellow solid, yield 100 mg (20%). **$^1$H NMR** (300 MHz, $CDCl_3$): δ 8.12 (d, 2H), 7.52 (d, 1H), 7.42 (d, 1H), 7.22 (dd, 1H), 6.71 (d, 2H), 4.11 (t, 2H), 3.32 (t, 4H), 2.50 (t, 2H), 2.28 (s, 6H), 2.00 (m, 2H), 1.61 (m, 4H), 1.40-1.20 (m, 20H), 0.88 (t, 6H). **LCMS** (m/z): ESI, found $[M+1]^+$ 579.4 (calcd for $C_{36}H_{55}N_2O_4^+$ 579.4).

**General procedure for quaternization of amines with 1,3-propanesultone.** Tertiary amine (1 eq) and 1,3-propanesultone (2 eq) were mixed together in dry acetonitrile. The reaction mixture was refluxed overnight at 90° C. After cooling, it was stirred at RT for additional 1 h. Organic solvent was removed by vacuum evaporation. Obtained residue was purified by preparative TLC to give the final product.

**Probe F46NS (**N-[3-(4'-Dibutylamino-3-hydroxy-flavonyl-6-oxy)-propyl]-N,N-dimethyl-N-(3-sulfopropyl)-aminium, inner salt). It was synthesized according to the general procedure

for the amine quaternization starting from 30 mg of previously obtained compound **3**. The product was purified by preparative TLC (eluent $CH_2Cl_2$/MeOH = 85/15). Yellow solid, yield 27 mg (70%). **$^1$H NMR** (300 MHz, $CDCl_3$): δ 8.05 (d, 2H), 7.40 (d, 1H), 7.38 (d, 1H), 7.15 (dd, 1H), 6.66 (d, 2H), 4.10 (t, 2H), 3.67 (m, 2H), 3.53 (m, 2H), 3.30 (m, 4H), 3.14 (s, 6H), 2.91 (m, 2H), 2.38 (m, 2H), 2.24 (m, 2H), 1.56 (m, 4H), 1.33 (m, 4H), 0.93 (t, 6H). **HRMS** (m/z): ESI, found $[M+1]^+$ 589.29 (calcd for $C_{31}H_{45}N_2O_7S^+$ 589.29).

**Probe F66NS (**N-[3-(4'-Dihexylamino-3-hydroxy-flavonyl-6-oxy)-propyl]-N,N-dimethyl-N-(3-sulfopropyl)-aminium, inner salt). It was synthesized according to the general procedure for the amine quaternization starting from 30 mg of previously obtained compound **4**. The product was purified by preparative TLC (eluent $CH_2Cl_2$/MeOH = 85/15). Yellow solid, yield 30 mg (80%). **$^1$H NMR** (300 MHz, $CDCl_3$): δ 7.86 (d, 2H), 7.14 (d, 1H), 7.03 (d, 1H), 6.88 (dd, 1H), 6.49 (d, 2H), 3.90 (t, 2H), 3.65 (m, 2H), 3.55 (m, 2H), 3.30 (m, 4H), 3.15 (s, 6H), 3.05 (m, 2H), 2.33 (m, 2H), 2.20 (m, 2H), 1.50 (m, 4H), 1.40-1.15 (m, 12H), 0.86 (t, 6H). **HRMS** (m/z): ESI, found $[M+1]^+$ 645.35 (calcd for $C_{35}H_{53}N_2O_7S^+$ 645.35).

**Probe F86NS.** N-[3-(4'-Dioctylamino-3-hydroxy-flavonyl-6-oxy)-propyl]-N,N-dimethyl-N-(3-sulfopropyl)-aminium, inner salt. It was synthesized according to the general procedure for the amine quaternization starting from 30 mg of previously obtained compound **5**. The product was purified by preparative TLC (eluent $CH_2Cl_2$/MeOH = 85/15). Yellow solid, yield 24 mg (66%). **$^1$H NMR** (200 MHz, $CDCl_3$): δ 7.87 (d, 2H), 7.17 (d, 1H), 7.05 (d, 1H), 6.88 (dd, 1H), 6.49 (d, 2H), 3.90 (t, 2H), 3.65 (m, 2H), 3.55 (m, 2H), 3.30 (m, 4H), 3.15 (s, 6H), 3.05 (m, 2H), 2.33 (m, 2H), 2.20 (m, 2H), 1.50 (m, 4H), 1.40-1.10 (m, 20H), 0.86 (t, 6H). **HRMS** (m/z): ESI, found $[M+1]^+$ 701.42 (calcd for $C_{39}H_{61}N_2O_7S^+$ 701.42).

**Lipid vesicles.** Large unilamellar vesicles (LUVs) were obtained by the extrusion method. Briefly, a suspension of multilamellar vesicles was extruded by using a Lipex Biomembranes extruder (Vancouver, Canada). The size of the filters was first 0.2 μm (7 passages) and thereafter 0.1 μm (10 passages). This generates monodisperse LUVs with a mean diameter of 0.11 μm, as measured with a Malvern Zetamaster 300 (Malvern, UK). A 20 mM phosphate buffer pH 7.4 was used in these experiments. LUVs were labeled by adding aliquots of probe stock solutions in dimethylsulfoxide to 1 mL solutions of vesicles.

Giant unilamellar vesicles (GUVs) were generated by electroformation in a home-built liquid cell (University of Odense, Denmark). A 0.1 mM solution of lipids in chloroform was

deposited on the platinum wires of the chamber and the solvent was evaporated under vacuum for 30 min. The chamber, thermostated at 55°C, was filled with a 300 mM sucrose solution, and a 2-V, 10-Hz alternating electric current was applied to this capacitor-like configuration for ca. 2 h. Then, 50 mL aliquot of the obtained stock solution of GUVs in sucrose (cooled down at RT) was added to 200 mL of 300 mM glucose solution to give the final suspension of GUVs used in microscopy experiments. The staining of GUVs was performed by addition of an aliquot of the probe stock solution in DMSO to obtain a 0.1 μM final probe concentration (final DMSO volume <0.25%).

**Cell lines, culture conditions and treatment.** U87MG human glioblastoma cell line (ATCC) was cultured in Eagle's minimal essential medium (EMEM from LONZA) with 10% heat-inactivated fetal bovine serum (PAN Biotech GmbH) and 0.6 mg/mL glutamine (Biowhittaker) at 37 °C in a humidified 5% $CO_2$ atmosphere. HeLa cells were cultured in Dulbecco's modified Eagle medium (D-MEM, high glucose, Gibco-invitrogen) supplemented with 10% (v/v) fetal bovine serum (FBS, Lonza), 1% antibiotic solution (penicillin-streptomycin, Gibco-invitrogen) in a humidified incubator with 5% $CO_2$ /95% air atmosphere at 37°C. Cell concentration of 5-10×$10^4$ cells/mL was maintained by removal of a portion of the culture and replacement with fresh medium 3 times per week.

Cholesterol depletion was performed using methyl-β-cyclodextrin (MβCD) (Sigma-Aldrich). Briefly, a stock solution of MβCD in Dulbecco's Phosphate Buffered Saline (DPBS) was prepared at a suitable concentration, filtered by a Millipore filter (0.22 μm) and added to the cells to a final concentration of 5 mM. The treated cells were kept in the incubator at 37 °C for 2 h.

To induce apoptosis, cells were treated with actinomycin D (0.5 μg/ml), camptothecin (5 μg/ml), or staurosporine (0.1 μM) for 18h at 37 °C.

In fluorescence spectroscopy experiments, cells were detached by trypsinization. Old culture medium was first removed from the culture dish and cells were washed two times with DPBS. Trypsin 10x (LONZA) solution was diluted 10 times with DPBS and added to the cells at 37 °C for 3 minutes. The solution of trypsinated cells was then diluted by HBSS (Hank's Balanced Salt Solution), transferred to Falcon tubes and centrifuged at 1500 rpm for 5 min, two times. To stain the cell suspension with a probe, an appropriate aliquot of its stock solution in DMSO was added to 0.5 mL of HBSS buffer and after vortexing, the solution was

immediately added to 0.5 mL of the cell suspension to obtain a final probe concentration of 0.1 μM (< 0.25% DMSO) and a cell concentration of $1\times10^6$ cells/mL. It should be noted that only freshly prepared solutions of the probe in HBSS should be used (< 1 min) for cell staining, because of the slow aggregation of the probe in water. Before measurements, the cell suspension with the probe was incubated for 7 min at room temperature in the dark. For microscopy studies, cells were seeded onto a chambered coverglass (IBiDi) at a density of $5\times10^4$ cells/IBiDi. After 18-24h, cells in iBiDi dishes were washed with Opti-MEM. Staining of these cells was achieved by adding a freshly prepared solution of probe in Opti-MEM to the cells to a final concentration of 0.5 μM (< 0.25% DMSO volume) and incubated for 7 min in the dark at room temperature.

**Fluorescence spectroscopy and microscopy.** Absorption spectra were recorded on a Cary 4 spectrophotometer (Varian) and fluorescence spectra on a FluoroMax 3.0 (Jobin Yvon, Horiba) spectrofluorometer. Fluorescence emission spectra were systematically recorded at 400 nm excitation wavelength at room temperature. All the spectra were corrected from the fluorescence of the corresponding blank (suspension of cells or lipid vesicles without the probe). Fluorescence microscopy experiments were performed by using a home-built two-photon laser scanning set-up based on an Olympus IX70 inverted microscope with an Olympus 60x 1.2NA water immersion objective (Clamme, Azoulay et al. 2003). Two-photon excitation was provided by a titanium-sapphire laser (Tsunami, Spectra Physics) and photons were detected with Avalanche Photodiodes (APD SPCM-AQR-14-FC, Perkin Elmer) connected to a counter/timer PCI board (PCI6602, National Instrument). Imaging was carried out using two fast galvo mirrors in the descanned fluorescence collection mode. Typical acquisition time was 5 s with an excitation power around 30 mW (λ = 830 nm) at the laser output level. Images corresponding to the short- and long-wavelength emission bands were recorded simultaneously using a dichroic mirror (Beamsplitter 550 DCXR), and two band-pass filters (Brightline HC 520/35 and HQ 585/40) in front of the APDs. The images were processed with a home-made program under LabView that generates a ratiometric image by dividing the image of the short-wavelength band by that of the long-wavelength band. For each pixel, a pseudo-color scale is used for coding the ratio, while the intensity is defined by the integral intensity recorded for both channels at the corresponding pixel (Shynkar, Klymchenko et al. 2005).

**Flow Cytometry:** Cells treated with apoptosis agents were stained with the different 3HF probes. For the validation of these dyes in cell cytometry, we used a BD LSR II flow cytometer with a 405 nm excitation laser line with 2 emission filters: green channel (Alexa Fluor 430) and Red channel (Qdot 585). Data were collected with the BD FACSDiva™ software and analyzed with FlowJo (Flow Cytometer analysis software). For flow cytometry studies, cells were prepared with the same protocol as for fluorescence spectroscopy analysis, with 0.1 μM final dye concentration. 50000 events were counted per sample to get enough signal.

## Results and discussion

### Design and Synthesis.

The newly designed generation of flavone probes includes three molecules, displayed in Fig. 1. Their structure combines a zwitterionic group and long alkyl chains attached to opposite sides of the fluorophore moiety. In contrast to F2N12S presenting a rather tilted orientation of its fluorophore with respect to the fatty acid chains, the new molecular design should favor vertical dye orientation in the membrane (Fig. 1). To optimize the probe affinity to the lipid membranes, the length of the alkyl chains in these probes was varied from 4C (F46NS) to 6C (F66NS) and to 8C (F86NS).

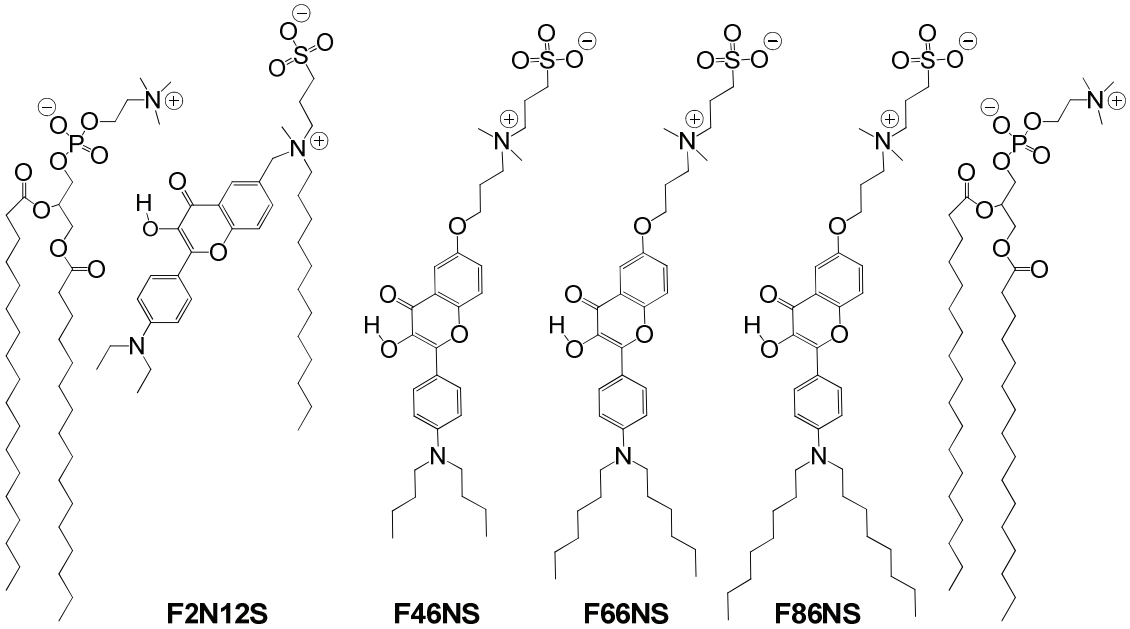

**Figure 1.** Newly synthesized probes with respect to F2N12S and their hypothetic localization with respect to lipids in membranes.

Synthesis of probes was started from 2,4-dihydroxy-acetophenone (or isomeric 2,5-substituted derivative), which was alkylated with 1-bromo-3-chloropropane under basic conditions (Materials and Methods). Obtained product **1** was activated by sodium iodide in acetone (Finkelstein reaction) and was subsequently coupled with dimethyl-amine in THF to produce the acetophenone **2** with a tertiary amino group. In the second part of synthesis, aniline was reacted with an alkyl iodide in the presence of potassium carbonate in DMF, and the formed intermediate was formylated by Vilsmeier reaction to produce the corresponding 4-dialkylamino-benzaldehyde. The obtained 4-dialkylamino-benzaldehydes were condensed with the acetophenone **2**, using excess of sodium methoxide in DMF. The resulting chalcone intermediates were further transformed into 3-hydroxyflavones **3**-**5** by oxidative cyclization (Olgar-Flynn-Oyamada reaction) with hydrogen peroxide and excess of sodium methoxide. The obtained flavones with tertiary amino moiety were reacted with 1,3-propanesultone to yield the desired probes.

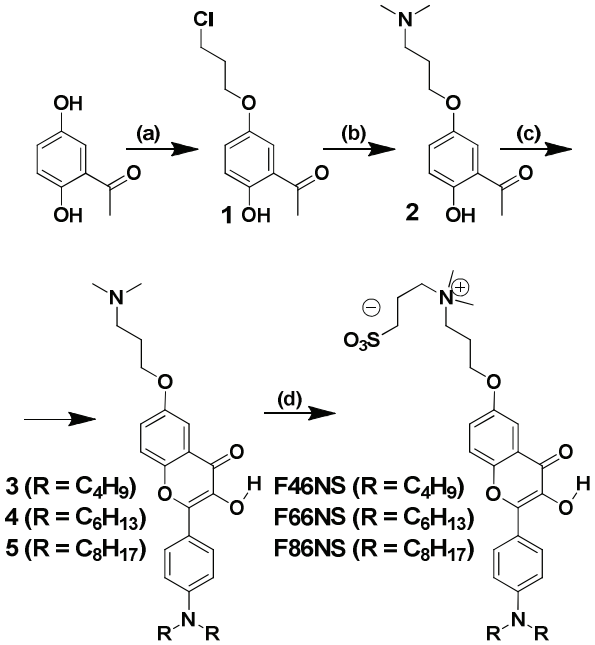


**Scheme 1.** Synthesis of the new probes. (a) DMF, 1-bromo-3-chloro-propane, $K_2CO_3$, 80°C 4h; (b) acetone, NaI, RT 1h, then THF, $HNMe_2$, RT 2h; (c) DMF, 4-dialkylamino-benzaldehyde, MeONa, then EtOH, 30% $H_2O_2$, MeONa, reflux for 3 min; (d) $CH_3CN$, 1,3-propanesultone, 90°C overnight.

Structures of all obtained substances were elucidated by NMR spectroscopy and Mass spectrometry. All the final probes were purified by column chromatography (or preparative TLC) and were pure according to NMR and LCMS data, TLC analysis and their absorption spectra.

**Binding to Lipid Vesicles and sensitivity to lipid order and surface charge.**

All the new probes, similarly to F2N12S are non-fluorescent in water and appear highly fluorescent on binding to large unilamellar vesicles (LUVs) (Fig. 2A). Fluorescence of all four probes bound to lipid membranes is characterized by two emission bands, which according to previous studies of 3-hydroxyflavones (Klymchenko, Duportail et al. 2002), (Klymchenko, Mely et al. 2004) can be assigned to N* and T* forms for the short and long-wavelength bands, respectively.

To explore the binding properties of 3-HF dyes, titration experiments were done, where the concentration of lipid vesicles was varied (probe concentration remained constant). F2N12S, F46NS, F66NS and F86NS (0.5 μM) were titrated with increased amount of DOPC vesicles. For all new probes and the parent F2N12S, when lipid concentration increases, the fluorescence intensity of the probes increases and reaches saturation around 100 μM lipid, corresponding to a dye/lipid ratio of 1:200 (Fig. 2). Thus, the probes, being non-fluorescent in water turn on their fluorescence on binding to lipid vesicles, similarly to their parent analogue F2N12S (Shynkar, Klymchenko et al. 2007). Remarkably, at the conditions of saturation (excess of lipids), the new probes show significantly different fluorescence intensity, which varies in the following order: F66NS> F46NS>F86NS. Thus, the increase of the length of alkyl chains from butyl to hexyl improves the brightness, while further increase to octyl drastically decreases it. This suggests that hexyl chains are probably optimal for probe binding and insertion into the bilayer, while the more apolar octyl chains lead probably to aggregation, preventing the efficient binding of the probe to lipid membranes. Remarkably, F66NS appears brighter than F2N12S, indicating that an improvement of the fluorescence properties was achieved through the new probe design.

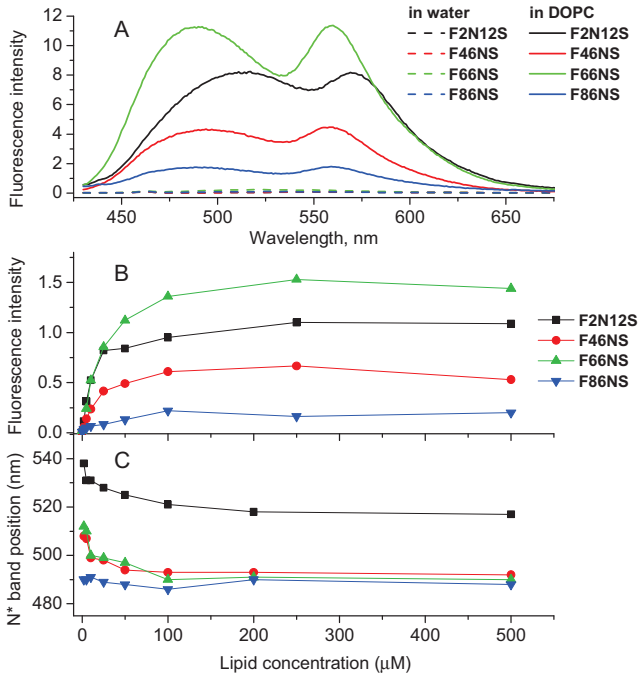


**Figure 2.** Binding of the probes to lipid vesicles. (A) Fluorescence spectra of the studied probes in water and in DOPC vesicles (200 μM) (B) Integral fluorescence intensity of the probes as a function of DOPC lipid concentration in LUVs. (B) Position of the emission maximum of the N* band of the probes. Dye concentration was 0.5 μM. Phosphate buffer 20 mM, pH 7.4 was used. Incubation time at 20 °C was 3 min.

For all four probes, the maximum of emission of the N* band shifts to the blue when increasing the amount of lipids, but stabilizes above 100 μM. Thus, at high probe/lipid ratio, the probe excess may bind to lipid membranes with an inappropriate shallow insertion of the probe, which could explain the red shifted position of the solvatochromic N* band. Similar concentration effects were recently shown for another environment-sensitive membrane probe based on Nile Red (Darwich, Klymchenko et al. 2012). Thus, a stable fluorescence spectrum with these probes can be obtained at probe/lipid ratio ≤ 1/200. Remarkably, all new probes at low probe/lipid ratios present the same position of the N* emission band, which appears ca 20 nm blue-shifted with respect to that of F2N12S. According to previous studies of 3HF probes, this shift suggests a much lower hydration of the fluorophore environment for the new probes. As the probes are expected to be vertically oriented in lipid membranes (Fig. 1), the fluorophore of the new probes should localize deeper in the bilayer compared to that in F2N12S, which may explain the decrease in the fluorophore hydration.

Further, to investigate the effect of lipid order on the probe spectral properties, LUVs of various lipid compositions were stained with F2N12S, F46NS or F66NS. Similarly to F2N12S, the new probes showed a significantly decreased N*/T* ratio in SM-Chol LUVs representing Lo phase as compared to DOPC LUVs, representing Ld phase. The decrease in the N*/T* ratio is accompanied with a blue shift of the emission maximum of the N* band (Fig. 3). These spectroscopic changes are similar to those for F2N12S and indicate that in the Lo phase, presenting a tighter lipid packing, the probes experience an environment of lower polarity and hydration. Noticeably, we also observe a lower N*/T* ratio for the Ld phase in the presence of cholesterol (DOPC-chol) (Table 1), indicating that the decrease in the polarity and hydration caused by cholesterol in the Ld phase also considerably affects the probe spectra. Remarkably, the changes of the N*/T* ratio for F66NS and especially F46NS to Lo-Ld phase changes were larger than for F2N12S, so that the new probes are more sensitive to the lipid order.

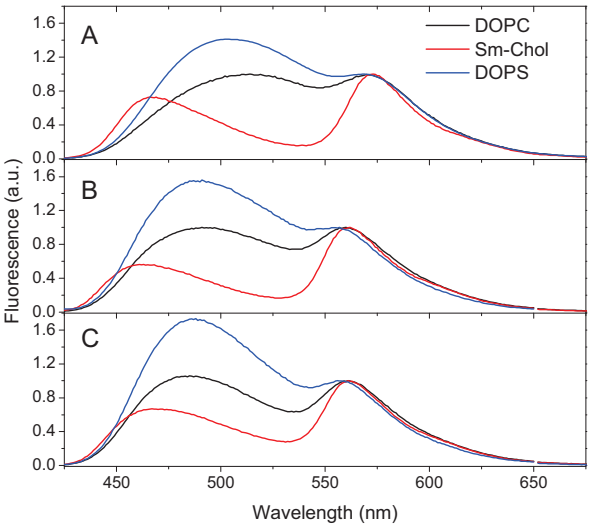


**Figure 3.** Comparison of the emission properties of F2N12S (A), F46NS (B) and F66NS (C) in LUVs of different lipid composition.

**Table 1.** Spectroscopic properties of 3-HF probes in model membranes.

| | F2N12S | | F46NS | | F66NS | |
|---|---|---|---|---|---|---|
| Lipid vesicles | N* max, nm | N*/T* | N* max, nm | N*/T* | N* max, nm | N*/T* |
| DOPC | 513 | 1.00 | 491 | 1.00 | 485 | 1.05 |
| DOPC-Chol 2:1 | 501 | 0.79 | 479 | 0.72 | 476 | 0.78 |
| Sm-Chol 2:1 | 472 | 0.70 | 463 | 0.56 | 471 | 0.66 |
| DOPS | 503 | 1.41 | 487 | 1.55 | 488 | 1.73 |

N* max is maximum of the N* band (nm); N*/T* - the intensity ratio of the two emission bands. Dye concentration was 1 μM, lipid concentration was 200 μM in phosphate buffer 10 mM, pH 7.0. Incubation time was 5 min at 20 °C.

Finally, DOPC and DOPS vesicles with neutral and negative surface, respectively, were compared to further investigate the effect of the surface charge on the probe behavior (Fig. 3). Similarly to F2N12S (Shynkar, Klymchenko et al. 2007), the new probes show a strong increase of their N*/T* ratio in negatively charged membranes. Interestingly, the changes in the N*/T* ratio of both new probes are superior to those observed with F2N12S, indicating that these probes exhibit an increased sensitivity to the surface charge. This increased sensitivity is likely a consequence of the vertical orientation of these probes that allows a stronger interaction between the probe dipole moment and the electric field associated with the surface potential, as compared to the tilted orientation of F2N12S.

In conclusion, studies in LUVs showed that two out of three probes showed strong turn-on fluorescence on binding to lipid membranes and it is comparable or even better (for F66NS) than that for F2N12S. Moreover, these two probes presented superior variation in the fluorescence spectra in response to changes in both the membrane phase (Lo vs. Ld phases) and charge surface.

These promising results prompted us to apply these probes to visualize lipid domains in giant unilamellar vesicles (GUVs). GUVs composed of DOPC, SM/Chol and DOPC/SM/Chol

representing pure Lo phase, pure Ld phase and mixture of both phases, respectively, were studied. The images were recorded simultaneously at 520 and 580 nm, using a linearly polarized infra-red femtosecond laser as a two-photon excitation source. From these images at two different wavelengths, ratiometric images were obtained, where the color of each pixel was associated with $I_{520}/I_{580}$ intensity ratio, while its intensity is associated with the number of counted photons. In DOPC GUVs, the intensity ratio was *ca* 2-fold as high as the ratio in SM/Chol GUVs (Fig. 4), in agreement with spectroscopic data (Fig. 3). Moreover, in Lo/Ld mixtures, F46NS and F66NS were able to bind both phases, showing different $I_{520}/I_{580}$ values. This new generation of probes can thus be applied as well as F2N12S to monitor lipid phases in model membranes, with F66NS showing improved brightness as compared to F2N12S and F46NS. The orientation of light polarization with respect to the bilayer showed strong effect for all three probes in Lo phase. According to previous work on F2N12S, this polarization effect is linked to the vertical orientation of the fluorophore imposed by highly ordered fatty acid chains of lipids (Klymchenko, Oncul et al. 2009). However, in contrast to F2N12S, the new probes show also a strong polarization effect in Ld phase, suggesting that they are also vertically oriented in this phase. As we expected (Fig. 1), the new molecular design, where charged and apolar groups are located at the opposite ends of the probe, allowed a more vertical orientation of its fluorophore, independently of the phase state.

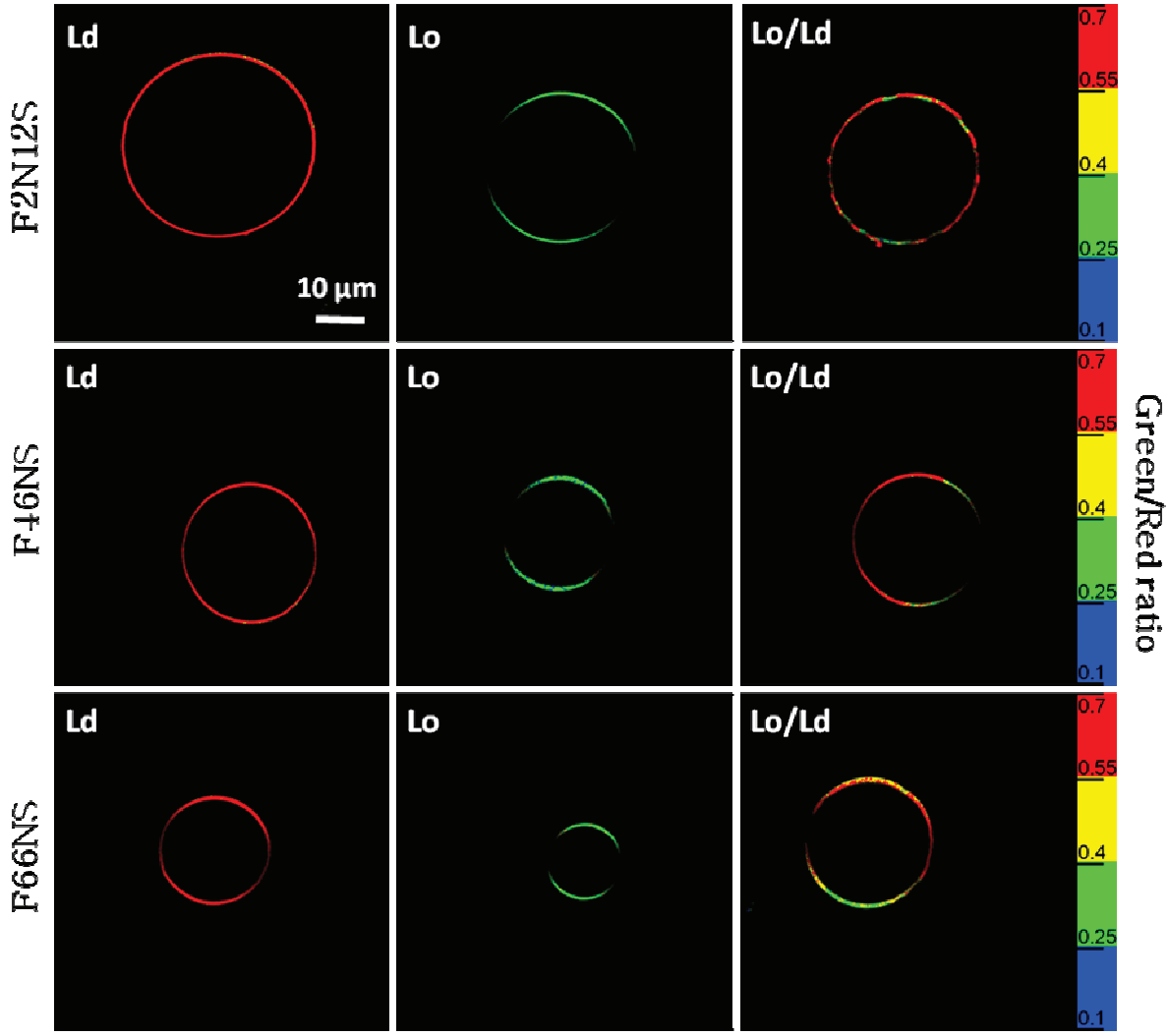


**Figure 4.** Fluorescence ratiometric images of GUVs composed of DOPC, SM/Chol 2/1 and DOPC/SM/Chol 1/1/0.7. The ratio between the green (520/35 nm) and red (585/40 nm) channels is presented. Dye concentration was 0.5 µM. Incubation time was 5 min at 20 °C.

**Cellular studies**

Similarly to F2N12S, the new probes bind readily to live cells (U87MG glioblastoma and HeLa cells), showing dual emission. Remarkably, the integral fluorescence intensity (i.e. probe brightness) was the highest in the case of F66NS (Fig. 5A), in line with the data in LUVs. To further evaluate the affinity of 3-HF probes to cell membranes, the fluorescence intensity of F2N12S, F46NS and F66NS (0.5 µM) was studied for increasing concentrations of HeLa cells (Fig. 5B). All the probes showed an increase in the fluorescence intensity with increasing cell concentrations. The strongest intensity increase is observed for F66NS. This intensity reaches asaturation above $2\times10^5$ cells/mL. For the reference probe F2N12S, this increase is less and

saturation is observed above $6\times10^5$ cells/mL. F46NS exhibits the smallest increase without saturation behavior. These observations indicate that the 3-HF probes exhibit significantly different affinity to cell membranes, which varies in the following order: F66NS> F2N12S>F46NS. The longer alkyl chains of F66NS in comparison to F46NS favor higher affinity to cellular membranes because F66NS is significantly more hydrophobic and thus its distribution between water and apolar membranes is shifted towards the latter. The F66NS affinity is even better than that of F2N12S, likely as a consequence of its vertical orientation that probably requires less space in the the bilayer than the tilted orientation of F2N12S.

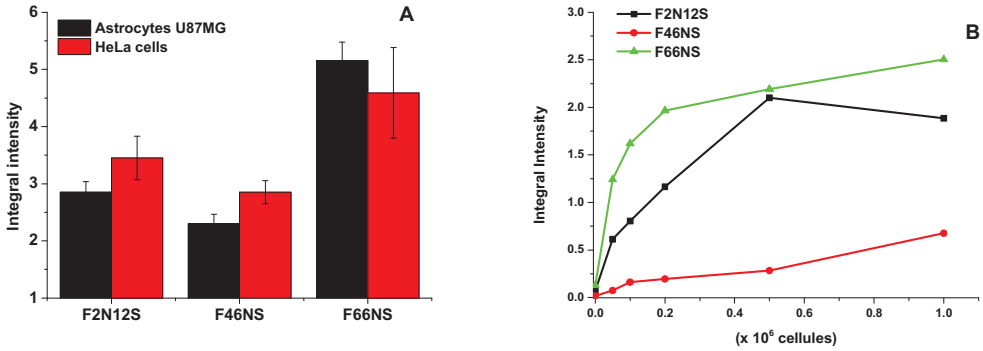


**Figure 5.** Spectroscopic properties of dyes in cells. (A) Emission intensities of 3-HF probes in membranes of intact cells. (B) Binding of the probes to intact cells: Integral fluorescence intensity of the probes as a function of cell concentrations. Dye concentration was 0.1 µM. Incubation time was 7 min at 20°C.

To vary the Lo phase content in cell membranes, their cholesterol was extracted using methyl-ß-cyclodextrin. Cholesterol depletion increases the N*/T* ratio for all three dyes, but the spectroscopic changes are significantly larger in the case of the new probes. It can be estimated from Figure 6B that on cholesterol depletion, the N*/T* ratio increases 1.37-fold for F2N12S, while for F46NS and F66NS, this change is 2- and 1.6-fold, respectively. The increase in the N*/T* ratio indicates the decrease in the fraction of the Lo phase in the outer leaflet of cell membranes, which results from the decrease in the cholesterol content. The higher sensitivity of the new probes to cholesterol depletion is in agreement with the data in LUVs, where the new probes, especially F46NS showed higher response to Lo-Ld phase changes.

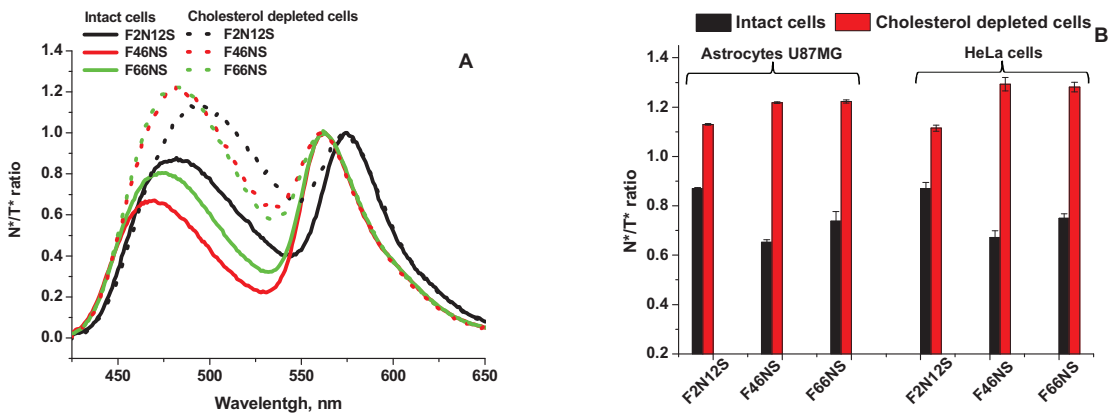


**Figure 6.** Effect of cholesterol extraction on the emission properties of 3-HF probes. (A) Fluorescence spectra of F2N12S (black curves), F46NS (red curves) and F66NS (green curves) in U87MG suspension of intact cells (solid cuves) and cholesterol depleted cells, treated 2h with 5 mM of methyl-ß-cyclodextrin (dashed curves). (B) N*/T* ratio of the probes in U87MG glioblastoma cells and HeLa cells. Dye concentration was 0.1 μM. Incubation time was 7 min at 20°C.

Then, we analyzed the spectroscopic response of our probes to apoptosis induced by actinomycin D. (Fig. 7A) In both U87MG and HeLa cells, apoptosis increases the N*/T* ratio of the probes. Thus, the new probes similarly to F2N12S are sensitive to apoptosis, and the response can be observed in different cell types. (Fig. 7B) It should be noticed that for all three studied dyes, the changes in the ratio were larger in HeLa cells compared to U87MG cells, which could reflect the differences in the resistance of these two cell lines to this antibiotics. Remarkably, the ratiometric response to apoptosis of F46NS is the highest among the three dyes showing 39% changes in Hela cells. F2N12S and F66NS are less sensitive showing 15% and 23% response, respectively. It should be noted that the sensitivity of these probes to apoptosis correlates with the sensitivity to lipid order changes, i.e. F46NS shows the highest sensitivity to lipid order and apoptosis among the three dyes. Moreover, both new probes show improved sensitivity to the surface charge, which may also contribute to better sensitivity of these probes to apoptosis. These observations confirm the fundamental connection between the changes in the membrane properties (lipid order and surface charge) and apoptosis, which was recently evidenced with F2N12S (Shynkar, Klymchenko et al. 2007), (Oncul, Klymchenko et al. 2010), (Kucherak, Oncul et al. 2010) and a Nile Red-based probe (Kucherak, Oncul et al. 2010). Thus, the higher

sensitivity to apoptosis was achieved through improving sensitivity to both the phase state and surface charge in the case of F46NS.

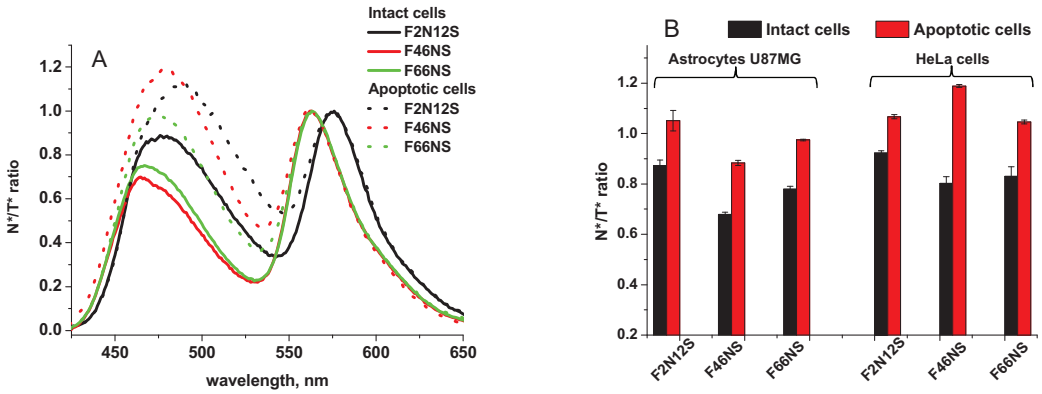


**Figure 7.** Effect of apoptosis on the emission properties of 3-HF probes labeling cells. (A) Fluorescence spectra of F2N12S (black curves), F46NS (red curves) and F66NS (green curves) in suspensions of intact HeLa cells (solid cuves) and apoptotic cells, treated 18h with 0.5 μg/mL actinomycin D (dashed curves). (B) N*/T* ratio of the probes in U87MG glioblastoma cells and HeLa cells in response to apoptosis induced by actinomycin D. Dye concentration was 0.1 μM. Incubation time was 7 min at 20°C.

To check whether the response of these probes is independent on the apoptosis inducing agent, we also tested camptothecin and staurosporine, which induce apoptosis through different mechanisms. Indeed, while actinomycin D inhibits DNA replication and RNA transcription (Sobell 1985), camptothecin inhibits the DNA topoisomerase I (Hsiang, Hertzberg et al. 1985), and staurosporine is a protein kinase inhibitor (Tamaoki, Nomoto et al. 1986). Figure 8 shows that the other two agents produced a similar increase in the N*/T* intensity ratio, though the response was somewhat lower. Importantly for all three agents, F46NS showed the strongest response to apoptosis, confirming its superior sensitivity.

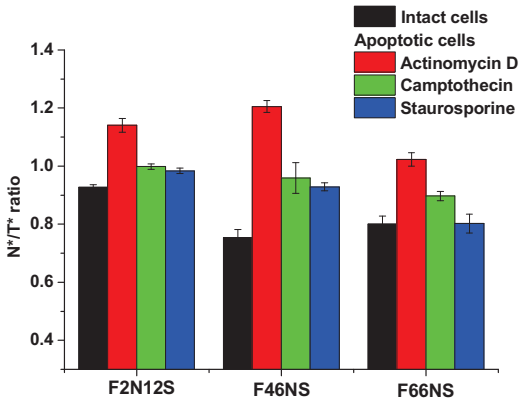


**Figure 8.** Ratiometric response of 3HF probes to apoptosis induced with different agents in HeLa cells (0.5 μg/mL was used for actinomycin D, 5 μg/mL for camptothecin and 0.1 μM for staurosporine for 18h at 37 °C). Dye concentration was 0.1 μM. Incubation time was 7 min at 20°C.

Thus, studies in cell suspensions showed that the new probes bind efficiently to cells, showing comparable or even superior brightness with respect to the parent F2N12S. On the other hand, one of the new probes showed significantly improved sensitivity to apoptosis, which is connected with its superior sensitivity to Lo-Ld phase and surface charge changes in lipid membranes.

The new probes were further tested on attached cells using fluorescence microscopy. The new probes showed perfect membrane staining, similar to the parent probe F2N12S. In line with data in cell suspensions and model lipid vesicles, the brightness of the images depended on the probe in the following order: F66NS>F2N12S>F46NS (Fig. 9). The ratio of two emission bands derived from the images was constant all over the cellular membrane for the three dyes, confirming that it is impossible to observe membrane heterogeneity on the timescale of seconds with the resolution of optical microscopy (Oncul, Klymchenko et al. 2010). Cholesterol depletion by M-ß-CD and apoptosis induced by actinomycin D produced an increase in the green/red ratio, in full line with the spectroscopic data in cell suspensions. However, these imaging experiments could not reveal significant differences in the sensitivity of the studied probes, as all showed more or less similar color change.

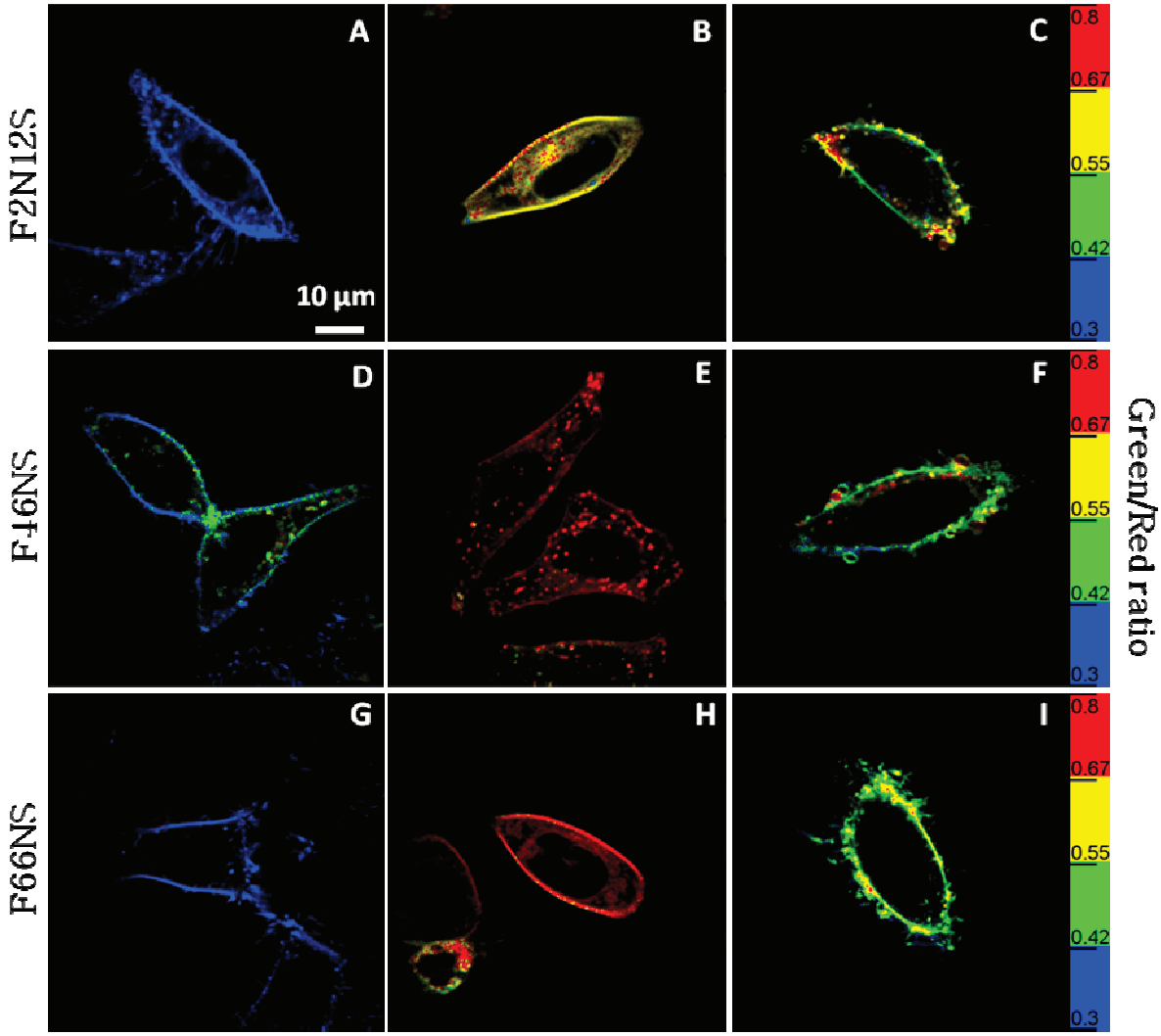


**Figure 9.** Two-photon fluorescence ratiometric images of intact (A, D and G), cholesterol-depleted (B, E and H), and apoptotic (C, F and I) HeLa cells stained with F2N12S, F46NS and F66NS respectively. The ratio between the green (520/35 nm) and red (585/40 nm) channels is presented. Dye concentration was 0.5 µM. Incubation time was 7 min at 20 °C.

Through its two emission bands that allow recording its fluorescence in two channels separately, F2N12S was previously validated as a good tool to detect apoptosis by using flow cytometry. (Shynkar, Klymchenko et al. 2007) Due to its simple and fast protocol, F2N12S appears thus as an interesting alternative to the Annexin V assay, the most used assay to detect apoptosis using flow cytometry. Thus, our next step was to validate whether the new probes could also be used to discriminate apoptotic from intact cells by flow cytometry. To this end, Hela cells were treated with actinomycin D to induce apoptosis and then split into three samples, labeled with F2N12S, F46NS and F66NS, respectively.

As the three 3HF-probes show different N*/T* values for intact and apoptotic cells, flow cytometry data are presented in a bi-parametric form: Red channel versus Green channel. When intact cells are stained with F2N12S, only one population, corresponding to living cells is observed (Fig. 10A). In contrast, cells treated with actinomycin D show two distinct populations, differing by the ratio of the two channels (Fig. 10D). The new population, which exhibits a higher Green/Red ratio can be readily assigned to the combined population of apoptotic and dead cells, in line with our previous data on F2N12S (Shynkar, Klymchenko et al. 2007). Interestingly, the new probes show similar flow cytometry data, where intact cells are mainly represented by one population (Fig. 10B and C), while actinomycin D-treated cells present clearly two populations with distinct green/red ratios (Fig. 10E and F).

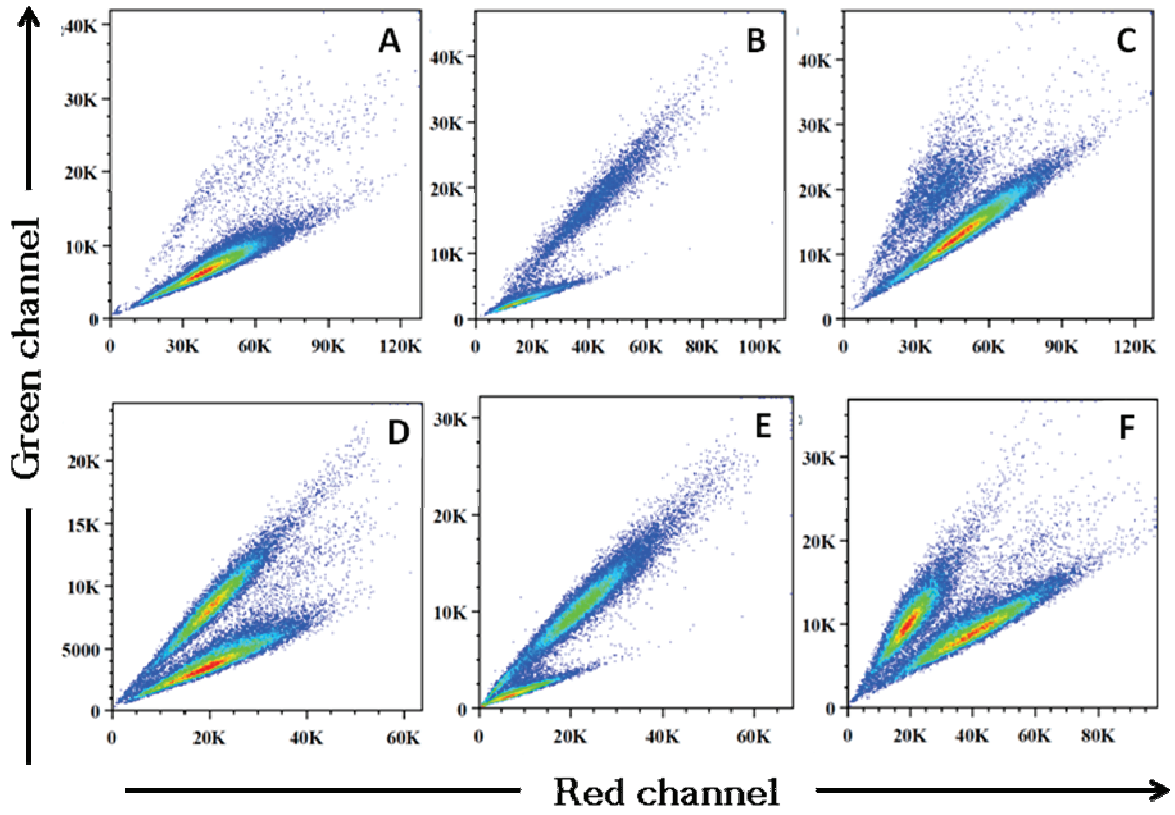


**Figure 10.** Flow cytometry measurements of intact (A-C) and actinomycin D-treated Hela cells (D-F) using F2N12S (A, D), F46NS (B, E) and F66NS (C, F). For each probe (0.1μM), the fluorescence intensity of red channel (x axis) and green channel (y axis) were presented.

The increase in the green/red intensity ratio of F46NS in response to apoptosis is the highest among the two new dyes, showing a 90% of change for F46NS (Fig. 11A). F66NS is less

sensitive showing a similar response as for F2N12S (77% of change for F66NS, and 76% for F2N12S). Remarkably, in intact cells, F66NS presented the highest fluorescence intensity, while for F46NS it was the lowest (Fig. 11B), in line with our spectroscopic data. On the other hand, while F2N12S showed almost no variation in the integral intensity in response to apoptosis, the new probes did change this parameter. Indeed, the fluorescence intensity of F66NS decreased in apoptotic cells, while for F46NS it increased strongly. These variations likely correlate with the affinity of the probes to the cellular membrane. As it was shown in Fig. 5B, probe F66NS presents the highest affinity to plasma membranes of intact cells. Therefore, we could speculate that this probe is bound well to both normal and apoptotic cells. However, the intensity per cell is lower in apoptotic cells probably because of cell shrinkage that is commonly associated with apoptosis (Van Cruchten and Van Den Broeck 2002). In contrast, F46NS, due to its higher polarity and therefore solubility in water, exhibits much weaker partitioning into membranes of normal cells (Fig. 5). It binds much better apoptotic cells, which due to lower lipid order compared to intact cells, can more easily accommodate organic dyes, as it was previously shown for merocyanin 540 (Laakko, King et al. 2002; Bailey, Nguyen et al. 2009). F2N12S probably shows an intermediate behavior between F46NS and F66NS. It should be noted, that higher affinity of F46NS to apoptotic cells compared to normal ones can additionally contribute to higher sensitivity of this probe to apoptosis observed in cell suspensions. As the cell suspensions treated with the apoptosis agent are composed of the mixture of normal and apoptotic cells, F46NS probe may bind preferably to the apoptotic cells and show stronger response compared to its close analogue F66NS. Moreover, the observed >4-fold increase in the fluorescence intensity of F46NS could be considered as an additional independent signal for apoptosis detection, so that this probe can be used for apoptosis detection in flow cytometry using both ratiometric and intensiometric approaches. Thus, flow cytometry studies showed important advantages of F46NS probe compared to the other two in terms of probe sensitivity to apoptosis.

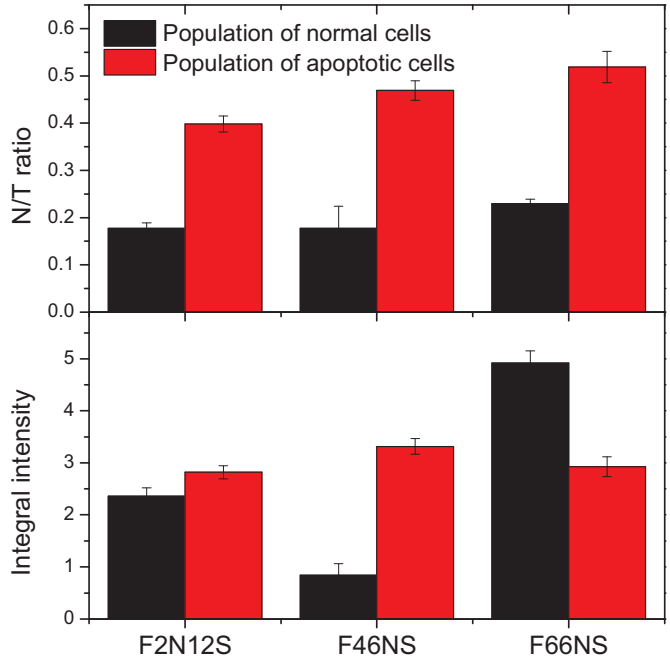


**Figure 11.** Fluorescence intensity ratio (Green/Red) (A) and integral fluorescence intensity per cell (B) of 3HF probes in two populations of actinomycin D – treated HeLa cells corresponding to normal and apoptotic cells.

**Conclusions.** In the present work, a new generation of membrane probes of the 3-hydroxyflavone family was synthesized presenting an amphiphilic structure that favors the vertical orientation of their fluorophore in the lipid bilayers. Variation of alkyl chain lengths in the 4'-dialkylamino group of the probes from 4 to 8 carbon atoms showed that the medium chain (6 carbon atoms) length is optimal for membrane staining, while the longest-chain analogue cannot efficiently stain the membranes. The new probes exhibited improved properties as compared to the parent probe F2N12S, in terms of fluorescence brightness and/or sensitivity to membrane phase, surface charge and apoptosis. Remarkably, the probe bearing shortest alkyl chains, presented the highest sensitivity to the phase changes as well as to apoptosis. This probe showed both the highest ratiometric response to apoptosis together with a strong increase in its fluorescence intensity in apoptotic cells. Thus, the rational design of the membrane probes allows obtaining new membrane probes with superior properties. These probes constitute powerful tools for studying lipid membrane organization and to detect apoptosis using fluorescence spectroscopy, fluorescence microscopy and flow cytometry techniques.

**Acknowledgments**

This work was supported by ANR JCJC (ANR-11-JS07-014-01). Financial support of ZD from CNRS and Region Alsace is acknowledged. We thank C. Ebel from flow cytometry service (IGBMC) for help with flow cytometry experiments.

**References**

Bailey, R. W., T. Nguyen, et al. (2009). "Sequence of Physical Changes to the Cell Membrane During Glucocorticoid-Induced Apoptosis in S49 Lymphoma Cells." Biophys J **96**(7): 2709-2718.

Chan, S. L. and M. P. Mattson (1999). "Caspase and calpain substrates: roles in synaptic plasticity and cell death." J Neurosci Res **58**(1): 167-190.

Clamme, J. P., J. Azoulay, et al. (2003). "Monitoring of the Formation and Dissociation of Polyethylenimine/DNA Complexes by Two Photon Fluorescence Correlation Spectroscopy." Biophysical Journal **84**(3): 1960-1968.

Darwich, Z., A. S. Klymchenko, et al. (2012). "Detection of apoptosis through the lipid order of the outer plasma membrane leaflet." Biochim Biophys Acta.

Demchenko, A. P., Y. Mely, et al. (2009). "Monitoring biophysical properties of lipid membranes by environment-sensitive fluorescent probes." Biophys J **96**(9): 3461-3470.

Elmore, S. (2007). "Apoptosis: a review of programmed cell death." Toxicol Pathol **35**(4): 495-516.

Erickson, G. F. (1997). "Defining apoptosis: players and systems." J Soc Gynecol Investig **4**(5): 219-228.

Feigenson, G. W. (2007). "Phase boundaries and biological membranes." Annu Rev Biophys Biomol Struct **36**: 63-77.

Hsiang, Y. H., R. Hertzberg, et al. (1985). "Camptothecin induces protein-linked DNA breaks via mammalian DNA topoisomerase I." Journal of Biological Chemistry **260**(27): 14873-14878.

Klymchenko, A. S., G. Duportail, et al. (2002). "Novel Two-Band Ratiometric Fluorescence Probes with Different Location and Orientation in Phospholipid Membranes." Chemistry & Biology **9**(11): 1199-1208.

Klymchenko, A. S., Y. Mely, et al. (2004). "Simultaneous probing of hydration and polarity of lipid bilayers with 3-hydroxyflavone fluorescent dyes." Biochim Biophys Acta **1665**(1-2): 6-19.

Klymchenko, A. S., S. Oncul, et al. (2009). "Visualization of lipid domains in giant unilamellar vesicles using an environment-sensitive membrane probe based on 3-hydroxyflavone." Biochim Biophys Acta **1788**(2): 495-499.

Kressel, M. and P. Groscurth (1994). "Distinction of apoptotic and necrotic cell death by in situ labelling of fragmented DNA." Cell Tissue Res **278**(3): 549-556.

Kucherak, O. A., S. Oncul, et al. (2010). "Switchable Nile Red-Based Probe for Cholesterol and Lipid Order at the Outer Leaflet of Biomembranes." J Am Chem Soc **132**(13): 4907-4916.

Laakko, T., L. King, et al. (2002). "Versatility of merocyanine 540 for the flow cytometric detection of apoptosis in human and murine cells." J Immunol Methods **261**(1–2): 129-139.

Leist, M. and M. Jaattela (2001). "Four deaths and a funeral: from caspases to alternative mechanisms." Nat Rev Mol Cell Biol **2**(8): 589-598.

Meer, G. V. (1989). "Lipid Traffic in Animal Cells." Annu Rev Cell Biol **5**(1): 247-275.

Nagata, S. (1997). "Apoptosis by death factor." Cell **88**(3): 355-365.

Oncul, S., A. S. Klymchenko, et al. (2010). "Liquid ordered phase in cell membranes evidenced by a hydration-sensitive probe: effects of cholesterol depletion and apoptosis." Biochim Biophys Acta **1798**(7): 1436-1443.

Packard, B. Z., A. Komoriya, et al. (2001). "Caspase 8 activity in membrane blebs after anti-Fas ligation." J Immunol **167**(9): 5061-5066.

Salvesen, G. S. and V. M. Dixit (1997). "Caspases: intracellular signaling by proteolysis." Cell **91**(4): 443-446.

Shynkar, V. V., A. S. Klymchenko, et al. (2005). "Two-color fluorescent probes for imaging the dipole potential of cell plasma membranes." Biochim Biophys Acta **1712**(2): 128-136.

Shynkar, V. V., A. S. Klymchenko, et al. (2007). "Fluorescent biomembrane probe for ratiometric detection of apoptosis." J Am Chem Soc **129**(7): 2187-2193.

Sobell, H. M. (1985). "Actinomycin and DNA transcription." Proceedings of the National Academy of Sciences **82**(16): 5328-5331.

Tamaoki, T., H. Nomoto, et al. (1986). "Staurosporine, a potent inhibitor of phospholipid/Ca++dependent protein kinase." Biochemical and biophysical research communications **135**(2): 397-402.

Thornberry, N. A. and Y. Lazebnik (1998). "Caspases: enemies within." Science **281**(5381): 1312-1316.

Truong-Tran, A. Q., J. Carter, et al. (2001). "The role of zinc in caspase activation and apoptotic cell death." BioMetals **14**(3): 315-330.

Vermes, I., C. Haanen, et al. (1995). "A novel assay for apoptosis. Flow cytometric detection of phosphatidylserine expression on early apoptotic cells using fluorescein labelled Annexin V." J Immunol Methods **184**(1): 39-51.

White, M. K. and C. Cinti (2004). "A morphologic approach to detect apoptosis based on electron microscopy." Methods Mol Biol **285**: 105-111.

Williamson, P. and R. A. Schlegel (1994). "Back and forth." Mol Membr Biol **11**(4): 199-216.

Wyllie, A. H. (1980). "Glucocorticoid-induced thymocyte apoptosis is associated with endogenous endonuclease activation." Nature **284**(5756): 555-556.

Zamzami, N., C. El Hamel, et al. (2000). "Bid acts on the permeability transition pore complex to induce apoptosis." Oncogene **19**(54): 6342-6350.

Zwaal, R. F. and A. J. Schroit (1997). "Pathophysiologic implications of membrane phospholipid asymmetry in blood cells." Blood **89**(4): 1121-1132.

# *Chapter 2:*

# *Probes based on Nile Red fluorophore*

In the first chapter, 3-HF probes were described. These environment-sensitive dyes were shown to be useful for sensing lipid order and apoptosis using different fluorescent techniques. Though these dyes show a number of advantages, they present limitations in their fluorescence emission. Indeed, they absorb and emit in the blue region which implies a strong overlap with cell auto fluorescence in cellular applications. To avoid this, new fluorescent probes derived from Nile Red were synthesized. The Nile Red derivative probe NR12S shows convenient fluorescence absorption and emission for biological applications. This new probe binds selectively to the cell plasma membrane and exhibits only one emission band, which can shift depending on the solvent polarity. Using dithionite to switch off the external fluorescence of NR12S, we were able to follow the flip-flop of NR12S in large unilamellar vesicles. These studies demonstrate that NR12S stains selectively the outer leaflet of the lipid bilayer, and shows a very slow flip-flop to the inner leaflet. In LUVs, NR12S binds both to the Lo and Ld phases. The emission spectrum of NR12S is different in these two phases, the emission maximum being shifted to the blue in the Lo phase and to the red in the Ld phase. To better analyze and compare the probe response, we split the spectra in two at 585 nm and we evaluate the ratio of the integrated intensity of the green region to the red region (Ratio G/R).

The two phases can be imaged separately with high contrast using fluorescence microscopy in GUVs.

Furthermore, NR12S can also be used to sense changes in lipid order after cholesterol depletion, cholesterol oxidation and sphingomyelinase treatment in cell membranes. These treatments induce a shift of the emission maximum of the probe to the red, indicating a loss of lipid order in cell membranes. Moreover, NR12S can also be used to sense apoptosis induced by different agents in different cell lines. The G/R ratio of NR12S decreases after apoptosis

induction, similar to the effect of cholesterol depletion, indicating a transition from Lo phase to Ld disordered phase. This sensibility of NR12S to apoptosis was further monitored by two-photon fluorescence microscopy. Apoptotic cells differ from intact cells, by their lower G/R ratio, in addition to changes in their morphologies. Finally, this sensitivity of NR12S to apoptosis could also be used in flow cytometry to distinguish intact from apoptotic cells.

In conclusion, our studies on NR12S indicate that this probe is a powerful tool for monitoring changes in lipid composition in cell plasma membrane and for detecting apoptosis. The protocols of NR12S application are simple and fast which constitutes a distinctive advantage of this probe over other methodologies.

Two articles published on this subject are presented below.

# *Publication 1*

# *Switchable Nile Red-based probe for cholesterol and lipid order at the outer leaflet of biomembranes*

J|A|C|S
ARTICLES

Published on Web 03/12/2010

# Switchable Nile Red-Based Probe for Cholesterol and Lipid Order at the Outer Leaflet of Biomembranes

Oleksandr A. Kucherak, Sule Oncul,† Zeinab Darwich, Dmytro A. Yushchenko, Youri Arntz, Pascal Didier, Yves Mély, and Andrey S. Klymchenko*

*Laboratoire de Biophotonique et Pharmacologie, UMR 7213 CNRS, Université de Strasbourg, Faculté de Pharmacie, 74, Route du Rhin, 67401 Illkirch Cedex, France*

Received January 14, 2010; E-mail: andrey.klymchenko@unistra.fr

***Abstract:*** Cholesterol and sphingomyelin form together a highly ordered membrane phase, which is believed to play important biological functions in plasma membranes of mammalian cells. Since sphingomyelin is present mainly at the outer leaflet of cell membranes, monitoring its lipid order requires molecular probes capable to bind specifically at this leaflet and exhibit negligibly slow flip-flop. In the present work, such a probe was developed by modifying the solvatochromic fluorescent dye Nile Red with an amphiphilic anchor group. To evaluate the flip-flop of the obtained probe (NR12S), we developed a methodology of reversible redox switching of its fluorescence at one leaflet using sodium dithionite. This method shows that NR12S, in contrast to parent Nile Red, binds exclusively the outer membrane leaflet of model lipid vesicles and living cells with negligible flip-flop in the time scale of hours. Moreover, the emission maximum of NR12S in model vesicles exhibits a significant blue shift in liquid ordered phase (sphingomyelin-cholesterol) as compared to liquid disordered phase (unsaturated phospholipids). As a consequence, these two phases could be clearly distinguished in NR12S-stained giant vesicles by fluorescence microscopy imaging of intensity ratio between the blue and red parts of the probe emission spectrum. Being added to living cells, NR12S binds predominantly, if not exclusively, their plasma membranes and shows an emission spectrum intermediate between those in liquid ordered and disordered phases of model membranes. Importantly, the emission color of NR12S correlates well with the cholesterol content in cell membranes, which allows monitoring the cholesterol depletion process with methyl-$\beta$-cyclodextrin by fluorescence spectroscopy and microscopy. The attractive photophysical and switching properties of NR12S, together with its selective outer leaflet staining and sensitivity to cholesterol and lipid order, make it a new powerful tool for studying model and cell membranes.

## Introduction

The structure and function of cell plasma membranes is largely controlled by their lipid composition and particularly by cholesterol, which represents up to 40% of the lipids in plasma membranes.[1] Cholesterol interacts strongly with phospholipids in membranes and, notably, with sphingomyelin (SM), another major lipid component of cell membranes.[2−4] Cholesterol and SM form a highly packed state, called liquid ordered (Lo) phase, in lipid bilayers. This phase is clearly separated in model membranes from the loosely packed liquid disordered (Ld) phase formed by unsaturated lipids and cholesterol.[5] The presence of Lo domains (or rafts) in cell plasma membranes was hypothesized from the discovery of detergent-insoluble membrane fractions enriched with SM, saturated phospholipids, and cholesterol.[6] This hypothesis stimulated intensive research and debates,[1−7] since their evidence was mainly provided from indirect techniques,[8] while their direct visualization remains a challenge. Estimation of the fraction of Lo phase in cell

† Present address: Acibadem University, School of Medicine, Department of Biophysics, Fevzi Cakmak Cd. Divan Sk. No. 1, 34848 Maltepe, Istanbul, Turkey.

(1) (a) Yeagle, P. L. *Biochim. Biophys. Acta* **1985**, *822*, 267–287. (b) Simons, K.; Ikonen, E. *Nature* **1997**, *387*, 569–572. (c) Simons, K.; Ikonen, E. *Science* **2000**, *290*, 1721–1726. (d) Brown, D. A.; London, E. *J. Membr. Biol.* **1998**, *164*, 103–114. (e) Brown, D. A.; London, E. *J. Biol. Chem.* **2000**, *275*, 17221–17224. (f) Ohvo-Rekila, H.; Ramstedt, B.; Leppimaki, P.; Peter Slotte, J. *Prog. Lipid Res.* **2002**, *41*, 66–97. (g) Maxfield, F. R.; Tabas, I. *Nature* **2005**, *438*, 612–621.

(2) (a) Lange, Y.; Ye, J.; Rigney, M.; Steck, T. *J. Biol. Chem.* **2000**, *275*, 17468–17475. (b) Lange, Y.; Swaisgood, M. H.; Ramos, B. V.; Steck, T. L. *J. Biol. Chem.* **1989**, *264*, 3786–3793.

(3) (a) Radhakrishnan, A.; McConnell, H. M. *J. Am. Chem. Soc.* **1999**, *121*, 486–487. (b) McConnell, H. M.; Radhakrishnan, A. *Biochim. Biophys. Acta* **2003**, *1610*, 159–173.

(4) Sankaram, M. B.; Thompson, T. E. *Biochemistry* **1990**, *29*, 10670–10675.

(5) (a) Dietrich, C.; Bagatolli, L. A.; Volovyk, Z. N.; Thompson, N. L.; Levi, M.; Jacobson, K.; Gratton, E. *Biophys. J.* **2001**, *80*, 1417–1428. (b) Veatch, S. L.; Keller, S. L. *Phys. Rev. Lett.* **2002**, *89*, 268101. (c) Veatch, S. L.; Keller, S. L. *Biophys. J.* **2003**, *85*, 3074–3083. (d) Baumgart, T.; Hess, S. T.; Webb, W. W. *Nature* **2003**, *425*, 821–824. (e) Ahmed, S. N.; Brown, D. A.; London, E. *Biochemistry* **1997**, *36*, 10944–10953. (f) De Almeida, R. F. M.; Fedorov, A.; Prieto, M. *Biophys. J.* **2003**, *85*, 2406–2416.

(6) (a) Brown, D. A.; Rose, J. K. *Cell* **1992**, *68*, 533–544. (b) Schroeder, R.; London, E.; Brown, D. *Proc. Natl. Acad. Sci. U.S.A.* **1994**, *91*, 12130–12134. (c) London, E.; Brown, D. A. *Biochim. Biophys. Acta* **2000**, *1508*, 182–195.

(7) (a) Simons, K.; Toomre, D. *Nat. Rev. Mol. Cell Biol.* **2000**, *1*, 31–39. (b) Brown, D. A.; London, E. *Annu. Rev. Cell Dev. Biol.* **1998**, *14*, 111–136. (c) Field, K. A.; Holowka, D.; Baird, B. *J. Biol. Chem.* **1997**, *272*, 4276–4280. (d) Hanzal-Bayer, M. F.; Hancock, J. F. *FEBS Lett.* **2007**, *581*, 2098–2104. (e) Tian, T.; Harding, A.; Inder, K.; Plowman, S.; Parton, R. G.; Hancock, J. F. *Nat. Cell Biol.* **2007**, *9*, 875–877.

membranes ranges from 10% to 80%, depending on the method used for its quantification. The difficulties to characterize Lo phase in cell membranes are first connected with their complex lipid composition, the presence of membrane proteins and cytoskeleton.[9] The second complication raises from the asymmetric distribution of lipids between the two leaflets. Indeed, while the outer leaflet contains a large amount of SM (up to 40%), its fraction in the inner leaflet is marginal.[10] Therefore, correct evaluation of Lo phase requires high specificity to this phase as well as high selectivity to the outer membrane leaflet.

To characterize the cholesterol content in membranes, the most classical method is to directly measure the lipid composition by isolation of cell plasma membrane fractions.[2] However, it is an invasive method, which does not allow real-time in situ measurements and may lead to artifacts because cholesterol can migrate between different cellular compartments[1] during the membrane isolation. More recent approaches are based on the extraction of radiolabeled cholesterol by cyclodextrin[11] and cholesterol-oxidation by microelectrode,[12] which allow real-time kinetics measurements of cholesterol in cells. However, these methods cannot address the spatial distribution of Lo and Ld phases in lipid membranes.

Fluorescent probes are probably the most attractive tool to study Lo/Ld phase separation and lipid compositions in model and cell membranes. Two classes of probes are mainly used. The first class corresponds to probes that stain selectively the Lo phase in model vesicles. This class includes the fluorescently labeled cholera toxin B-subunit (CT-B),[8a,13] saturated phospholipids labeled with NBD[5a] or Cy5[14] and GFP-labeled glycosylphosphatidylinositol (GPI),[15] as well as fluorescent dyes with long alkyl chains, such as LcTMA-DPH,[16] diI-C20, or polycyclic probes such as Terrylene or Naphtopyrene.[17] Though these probes are useful for imaging the phase separation in model and cell membranes, they cannot provide information about the actual composition of the separated phases. The second class corresponds to environment-sensitive probes, such as Laurdan[18] and its derivatives,[19] di-4-ANEPPDHQ[20] and 3-hydroxyflavone derivatives.[21] These probes distribute in both Ld and Lo phases, and their emission color or intensity depends strongly on the local polarity/hydration or fluidity, which in turn is related to the lipid composition and the actual phase state of the membrane.[18] Thus, these probes provide a unique possibility to study the membrane phases in connection to their lipid composition. However, only a small number of these probes is really applicable to membranes of living cells,[19,20,22] because most of them internalize rapidly inside the cell. Moreover, the flip-flop of these probes is not clearly addressed in literature, since the flip-flop studies are mainly based on indirect measurements,[20,22] so that it is difficult to evaluate precisely the distribution of the probes between the two leaflets. Therefore, it still remains a challenge to develop an environment-sensitive fluorescent probe that stains exclusively the outer leaflet of cell membranes. In the present work, we selected Nile Red[23] (Chart 1) as an environment-sensitive fluorophore for designing this fluorescent probe. Nile Red shows a number of attractive features, such as high fluorescence quantum yield, suitable excitation wavelength for application with common lasers and satisfactory photostability.[24] This dye found a variety of applications to characterize hydrophobic domains of proteins, dendrimers, micelles and model lipid membranes.[25] However, it cannot be used for studying cell plasma membranes, because it internalizes readily inside the cell and binds specifically to lipid droplets,[23] which are the most apolar cell compartments. Recently, we showed that a selective localization of a hydrophobic fluorophore at the plasma membrane can be achieved


(8) (a) Dietrich, C.; Yang, B.; Fujiwara, T.; Kusumi, A.; Jacobson, K. *Biophys. J.* **2002**, *82*, 274–284. (b) Pralle, A.; Keller, P.; Florin, E. L.; Simons, K.; Horber, J. K. *J. Cell. Biol.* **2000**, *148*, 997–1008. (c) Schultz, G. J.; Kada, G.; Pastushenko, V. P.; Schindler, H. *EMBO J.* **2000**, *19*, 892–901. (d) Lenne, P. F.; Wawrezinieck, L.; Conchonaud, F.; Wurtz, O.; Boned, A.; Guo, X. J.; Rigneault, H.; He, H. T.; Marguet, D. *EMBO J.* **2006**, *25*, 3245–3256. (e) Wawrezinieck, L.; Rigneault, H.; Marguet, D.; Lenne, P. F. *Biophys. J.* **2005**, *89*, 4029–4042. (f) Swamy, M. J.; Ciani, L.; Ge, M.; Smith, A. K.; Holowka, D.; Baird, B.; Freed, J. H. *Biophys. J.* **2006**, *90*, 4452–4465.

(9) Kusumi, A.; Sako, Y. *Curr. Opin. Cell Biol.* **1996**, *8*, 566–574.

(10) (a) Van Meer, G. *Annu. Rev. Cell Biol.* **1989**, *5*, 247–275. (b) Zwaal, R. F.; Schroit, A. J. *Blood* **1997**, *89*, 1121–1132.

(11) (a) Haynes, M. P.; Phillips, M. C.; Rothblat, G. H. *Biochemistry* **2000**, *39*, 4508–4517. (b) Lange, Y.; Ye, J.; Steck, T. L. *Proc. Natl. Acad. Sci. U.S.A.* **2004**, *101*, 11664–11667.

(12) Jiang, D.; Devadoss, A.; Palencsár, M. S.; Fang, D.; White, N. M.; Kelley, T. J.; Smith, J. D.; Burgess, J. D. *J. Am. Chem. Soc.* **2007**, *129*, 11352–11353.

(13) (a) Janes, P. W.; Ley, S. C.; Magee, A. I. *J. Cell. Biol.* **1999**, *147*, 447–461. (b) Kenworthy, A. K.; Petranova, N.; Edidin, M. *Mol. Biol. Cell* **2000**, *11*, 1645–1655.

(14) Schultz, G. J.; Kada, G.; Pastushenko, V. P.; Schindler, H. *EMBO J.* **2000**, *19*, 892–901.

(15) (a) Sharma, P.; Varma, R.; Sarasij, R. C.; Ira; Gousset, K.; Krishnamoorthy, G.; Rao, M.; Mayor, S. *Cell* **2004**, *116*, 577–589. (b) Vrljic, M.; Nishimura, S. Y.; Brasselet, S.; Moerner, W. E.; McConnell, H. M. *Biophys. J.* **2002**, *83*, 2681–2692. (c) Kenworthy, A. K.; Nichols, B. J.; Remmert, C. L.; Hendrix, G. M.; Kumar, M.; Zimmerberg, J.; Lippincott-Schwartz, J. *J. Cell. Biol.* **2004**, *165*, 735–46.

(16) (a) Haluska, C. K.; Schröder, A. P.; Didier, P.; Heissler, D.; Duportail, G.; Mély, Y.; Marques, C. M. *Biophys. J.* **2008**, *95*, 5737–5747. (b) Xu, X.; Bittman, R.; Duportail, G.; Heissler, D.; Vilchéze, C.; London, E. *J. Biol. Chem.* **2001**, *276*, 33540–33546.

(17) (a) Korlach, J.; Schwille, P.; Webb, W. W.; Feigenson, G. W. *Proc. Natl. Acad. Sci. U.S.A.* **1999**, *96*, 8461–8466. (b) Baumgart, T.; Hunt, G.; Farkas, E. R.; Webb, W. W.; Feigenson, G. W. *Biochim. Biophys. Acta* **2007**, *1768*, 2182–2194.

(18) (a) Bagatolli, L. A. *Biochim. Biophys. Acta* **2006**, *1758*, 1541–1556. (b) Parasassi, T.; Gratton, E.; Yu, W. M.; Wilson, P.; Levi, M. *Biophys. J.* **1997**, *72*, 2413–2429. (c) Gaus, K.; Gratton, E.; Kable, E. P. W.; Jones, A. S.; Gelissen, I.; Kritharides, L.; Jessup, W. *Proc. Natl. Acad. Sci. U.S.A.* **2003**, *100*, 15554–15559.

(19) (a) Kim, H. M.; Choo, H.-J.; Jung, S.-Y.; Ko, Y.-G.; Park, W.-H.; Jeon, S.-J.; Kim, C. H.; Joo, T.; Cho, B. R. *ChemBioChem* **2007**, *8*, 553–559. (b) Kim, H. M.; Jeong, B. H.; Hyon, J.-Y.; An, M. J.; Seo, M. S.; Hong, J. H.; Lee, K. J.; Kim, C. H.; Joo, T.; Hong, S.-C.; Cho, B. R. *J. Am. Chem. Soc.* **2008**, *130*, 4246–4247.

(20) (a) Jin, L.; Millard, A. C.; Wuskell, J. P.; Clark, H. A.; Loew, L. M. *Biophys. J.* **2005**, *89*, L4–L6. (b) Jin, L.; Millard, A. C.; Wuskell, J. P.; Dong, X.; Wu, D.; Clark, H. A.; Loew, L. M. *Biophys. J.* **2006**, *90*, 2563–2575.

(21) (a) Klymchenko, A. S.; Oncul, S.; Didier, P.; Schaub, E.; Bagatolli, L.; Duportail, G.; Mély, Y. *Biochim. Biophys. Acta* **2009**, *1788*, 495–499. (b) M'Baye, G.; Mély, Y.; Duportail, G.; Klymchenko, A. S. *Biophys. J.* **2008**, *95*, 1217–25. (c) Klymchenko, A. S.; Mély, Y.; Demchenko, A. P.; Duportail, G. *Biochim. Biophys. Acta* **2004**, *1665*, 6–19.

(22) Shynkar, V. V.; Klymchenko, A. S.; Kunzelmann, C.; Duportail, G.; Muller, C. D.; Demchenko, A. P.; Freyssinet, J.-M.; Mély, Y. *J. Am. Chem. Soc.* **2007**, *129*, 2187–2193.

(23) (a) Greenspan, P.; Mayer, E. P.; Fowler, S. D. *J. Cell. Biol.* **1985**, *100*, 965–973. (b) Diaz, G.; Melis, M.; Batetta, B.; Angius, F.; Falchi, A. *Micron* **2008**, *39*, 819–824.

(24) Greenspan, P.; Fowler, S. D. *J. Lipid Res.* **1985**, *26*, 781–789.

(25) (a) Lampe, J. N.; Fernandez, C.; Nath, A.; Atkins, W. M. *Biochemistry* **2008**, *47*, 509–516. (b) Gillies, E. R.; Jonsson, T. B.; Freíchet, Jean M. J. *J. Am. Chem. Soc.* **2004**, *126*, 11936–11943. (c) Maiti, N. C.; Krishna, M. M. G.; Britto, P. J.; Periasamy, N. *J. Phys. Chem. B* **1997**, *101*, 11051–11060. (d) Freeman, D. M.; Kroe, R. R.; Ruffles, R.; Robson, J.; Coleman, J. R.; Grygon, C. A. *Biophys. J.* **2001**, *80*, 2375. (e) Gao, F.; Mei, E.; Lim, M.; Hochstrasser, R. M. *J. Am. Chem. Soc.* **2006**, *128*, 4814–4822. (f) Nath, A.; Koo, P. K.; Rhoades, E.; Atkins, W. M. *J. Am. Chem. Soc.* **2008**, *130*, 15746–15747. (g) Chen, G.; Guan, Z. *J. Am. Chem. Soc.* **2004**, *126*, 2662–2663. (h) Mukherjee, S.; Raghuraman, H.; Chattopadhyay, A. *Biochim. Biophys. Acta* **2007**, *1768*, 59–66.

***Chart 1.*** Probes Nile Red and NR12S and Their Hypothetic Localization with Respect to Lipids (Blue) in Membranes; Anchor Part of the NR12S Probe Is in Red

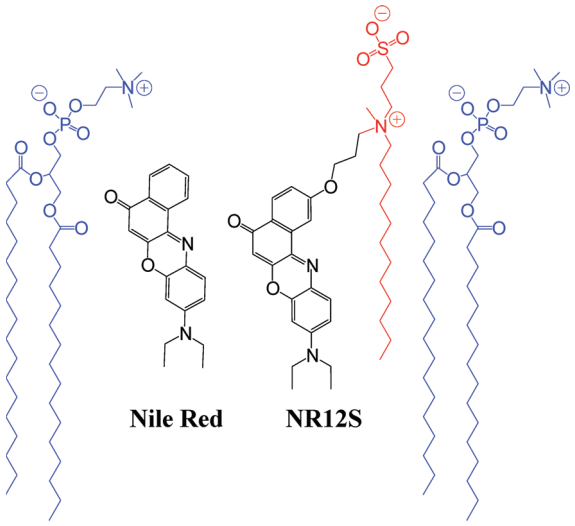


by conjugating it with a zwitterionic group and a long hydrophobic chain.[22] Though the obtained probe was hypothesized to bind to the outer biomembrane leaflet without further fast flip-flop, we could not provide a direct evidence for this.

In the present work, using the same design, we developed a new Nile Red based probe for cell plasma membranes. Moreover, using a unique switching property of Nile Red fluorophore that was not reported before, we showed that, unlike the parent Nile Red, the novel probe stains exclusively the outer leaflet of lipid vesicles and cells. Furthermore, the probe was found to exhibit strongly different emission in Lo and Ld phases, and in living cells, its emission color varies with the cholesterol content. Thus, this probe constitutes a new tool for quantification of cholesterol-rich Lo phase in cell plasma membranes.

## Materials and Methods

All chemicals and solvents for synthesis were from Sigma-Aldrich. Synthesis of NR12S is described in Supporting Information.

**Lipid Vesicles.** Dioleoylphosphatidylcholine (DOPC), dioleoylphosphatidylserine (DOPS), and cholesterol were purchased from Sigma-Aldrich. Bovine brain sphingomyelin (SM) was from Avanti Polar Lipids (Alabaster, AL). Large unilamellar vesicles (LUVs) were obtained by the extrusion method as previously described.[26] Briefly, a suspension of multilamellar vesicles was extruded by using a Lipex Biomembranes extruder (Vancouver, Canada). The size of the filters was first 0.2 $\mu$m (7 passages) and thereafter 0.1 $\mu$m (10 passages). This generates monodisperse LUVs with a mean diameter of 0.11 $\mu$m as measured with a Malvern Zetamaster 300 (Malvern, U.K.). LUVs were labeled by adding aliquots (generally 2 $\mu$L) of probe stock solutions in dimethyl sulfoxide to 1-mL solutions of vesicles. Since the probe binding kinetics is very rapid, the fluorescence experiments were performed a few minutes after addition of the aliquot. A 20 mM phosphate buffer, pH 7.4, was used in these experiments. Concentrations of the probes and lipids were generally 1 and 200 $\mu$M, respectively.

Giant unilamellar vesicles (GUVs) were generated by electroformation in a home-built liquid cell (University of Odense, Denmark), using previously described procedures.[27] A 0.1 mM solution of lipids in chloroform was deposited on the platinum wires of the chamber, and the solvent was evaporated under vacuum for 30 min. The chamber, thermostatted at 55 °C, was filled with a 300 mM sucrose solution, and a 2-V, 10-Hz alternating electric current was applied to this capacitor-like configuration for ca. 2 h. Then, a 50 $\mu$L aliquot of the obtained stock solution of GUVs in sucrose (cooled down to room temperature) was added to 200 $\mu$L of 300 mM glucose solution to give the final suspension of GUVs used in microscopy experiments. The staining of GUVs was performed by addition of an aliquot of the probe stock solution in DMSO to obtain a 0.1 $\mu$M final probe concentration (final DMSO volume <0.25%).

**Reversible Bleaching of Nile Red and NR12S with Sodium Dithionite and Flip-Flop Studies.** A 1 M stock solution of sodium dithionite in 1 M Tris was used for the experiments. To 1 mL of 5 $\mu$M solution of Nile Red or NR12S in a 1:1 (v/v) ethanol/water mixture in a quartz cuvette was added an aliquot of the stock solution of dithionite to a final concentration 2 mM. Then, approximately 25 mL of air was applied to this solution through a syringe for approximately 20 s. The procedure of dithionite and air treatment was repeated several times. During all steps of this cyclic treatment, the absorbance at 590 nm (Nile Red) was measured as a function of time. For the flip-flop studies, DOPC LUVs were labeled with probes Nile Red and NR12S by two different methods. In method 1, the probe was mixed with lipids in chloroform, and the vesicles were prepared from this mixture as described above. This method ensured symmetric distribution of the probe between both leaflets. In method 2, the probe was added to 0.5 mL of buffer and then mixed with 0.5 mL of suspension of nonlabeled vesicles and incubated at room temperature for 5 min, which allowed initial staining of the outer membrane leaflet. The final probe concentration for both methods was 1 $\mu$M. To study the flip-flop kinetics, the fraction (%) of NR12S probe flipped from the outer to the inner leaflet in LUVs was evaluated as a function of time at 20 and 37 °C. The suspension of LUVs was stained with a probe by method 2. After a given incubation time (at 20 or 37 °C), the fluorescence intensities at 610 nm before ($I_0$) and 3 min after addition of 10 mM sodium dithionite ($I_{DT}$) were measured. The fraction of flipped probe for a given incubation time was expressed as $I_{DT}/I_0 \times 100\%$.

**Cell Lines, Culture Conditions, and Treatment.** The U87MG human glioblastoma cell line (ATCC) was cultured in Eagle's minimal essential medium (EMEM from LONZA) with 10% heat-inactivated fetal bovine serum (PAN Biotech GmbH) and 0.6 mg/mL glutamine (Biowhittaker) at 37 °C in a humidified 5% $CO_2$ atmosphere. Cell concentration of $5-10 \times 10^4$ cells/mL was maintained by removal of a portion of the culture and replacement with fresh medium 3 times per week. Cholesterol depletion and enrichment of cell membranes was performed using methyl-$\beta$-cyclodextrin (M$\beta$CD) and M$\beta$CD−cholesterol complex (Sigma-Aldrich), respectively, according to described procedures.[28] Briefly, stock solutions of M$\beta$CD and M$\beta$CD−cholesterol complex in Dulbecco's phosphate-buffered saline (DPBS) were prepared at a suitable concentration, filtered by Millipore filter (0.2 $\mu$m), and added to the cells to a final concentration of 5 mM. The treated cells were kept in the incubator at 37 °C for 30 min or 2 h.

In fluorescence spectroscopy experiments, cells were detached by trypsinization. EMEM medium was first removed from the culture dish, and cells were washed two times with DPBS. Trypsin 10x (LONZA) solution was diluted 10 times by DPBS and incubated with the cells at 37 °C for 4 min. The solution of trypsinized cells was then diluted by DPBS, transferred to Falcon tubes and centrifuged at 1500 rpm for 5 min. The washing procedure was repeated one more time with HBSS solution. To stain the cell suspension with the NR12S probe, an appropriate aliquot of its stock

(26) Hope, M. J.; Bally, M. B.; Webb, G.; Cullis, P. R. *Biochim. Biophys. Acta* **1985**, *812*, 55–65.

(27) (a) Angelova, M. I.; Dimitrov, D. S. *Faraday Discuss.* **1986**, *81*, 303–311. (b) Fidorra, M.; Duelund, L.; Leidy, C.; Simonsen, A. C.; Bagatolli, L. A. *Biophys. J.* **2006**, *90*, 4437–4451. (c) Kahya, N.; Scherfeld, D.; Bacia, K.; Poolman, B.; Schwille, P. *J. Biol. Chem.* **2003**, *278*, 28109–28115.

(28) Zidovetzki, R.; Levitan, I. *Biochim. Biophys. Acta* **2007**, *1768*, 1311–1324.

solution in DMSO was added to 0.5 mL of HBSS buffer, and after vortexing the solution was immediately added to 0.5 mL of the cell suspension to obtain a final probe concentration of 0.1 $\mu$M (<0.25% DMSO) and a cell concentration of $5 \times 10^5-10^6$ cells/mL. It should be noted that only freshly prepared solutions of the probe in HBSS should be used (<1 min) for cell staining, because of the slow aggregation of the probe in water. Before measurements, the cell suspension with probe was incubated for 7 min at room temperature in the dark. For the microscopy studies, attached cells were washed two times by gentle rinsing with HBSS. A freshly prepared solution of NR12S or Nile Red in HBSS was then added to the cells to a final concentration of 0.3 $\mu$M (<0.25% DMSO volume) and incubated for 7 min in the dark at room temperature.

**Fluorescence Spectroscopy and Microscopy.** Absorption spectra were recorded on a Cary 4 spectrophotometer (Varian) and fluorescence spectra on a FluoroMax 3.0 (Jobin Yvon, Horiba) spectrofluorometer. Fluorescence emission spectra were systematically recorded at 520 nm excitation wavelength at room temperature, unless indicated. All the spectra were corrected from the fluorescence of the corresponding blank (suspension of cells or lipid vesicles without the probe). Fluorescence quantum yields (QY) were measured using solution of Nile Red in methanol as a reference (QY = 38%).[29] Fluorescence microscopy experiments were performed by using a home-built two-photon laser scanning setup based on an Olympus IX70 inverted microscope with an Olympus 60x 1.2NA water immersion objective.[30] Two-photon excitation was provided by a titanium-sapphire laser (Tsunami, Spectra Physics), and photons were detected with Avalanche Photodiodes (APD SPCM-AQR-14-FC, Perkin-Elmer) connected to a counter/timer PCI board (PCI6602, National Instrument). Imaging was carried out using two fast galvo mirrors in the descanned fluorescence collection mode. Typical acquisition time was 5 s with an excitation power around 2.5 mW ($\lambda$ = 830 nm) at the sample level. Images corresponding to the blue and red channels were recorded simultaneously using a dichroic mirror (Beamsplitter 585 DCXR) and two APDs. The images were processed with a homemade program under LabView that generates a ratiometric image by dividing the image of the blue channel by that of the red channel. For each pixel, a pseudocolor scale is used for coding the ratio, while the intensity is defined by the integral intensity recorded for both channels at the corresponding pixel.[21a]

## Results and Discussion

**Design and Synthesis.** The design of the new probe NR12S (Chart 1) is based on the conjugation of the Nile Red fluorophore with an anchor group, which was recently proposed for localizing 3-hydroxychromone dyes at the outer leaflet of the cell plasma membrane.[22] This anchor group is composed of a long alkyl chain and a zwitterionic group, allowing strong interactions with the lipid membranes and thus their specific staining.

To functionalize Nile Red, we prepared 2-hydroxy-substituted Nile Red from 5-(diethylamino)-2-nitrosophenol and naphthalene-1,6-diol according to an available procedure.[31] The obtained 2-hydroxy-Nile Red was alkylated with 1-bromo-3-chloropropane. The product was further reacted with dodecylmethylamine, and the obtained tertiary amine was then quaternized by 1,3-propane sultone affording the final probe NR12S (see Supporting Information).

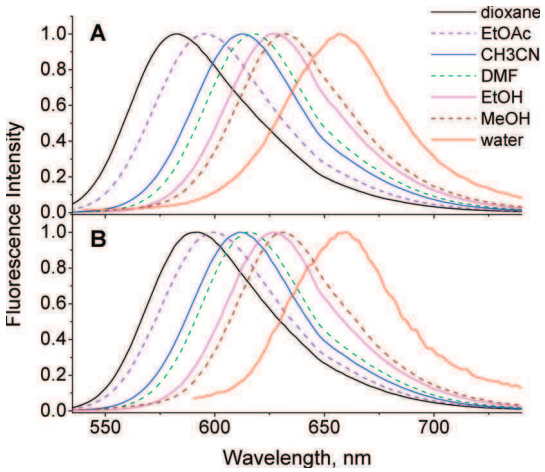


***Figure 1.*** Normalized fluorescence spectra of Nile Red (A) and NR12S (B) in different solvents.

***Table 1.*** Spectroscopic Properties of Studied Dyes in Organic Solvents[a]

| | | dye | | | | | |
|---|---|---|---|---|---|---|---|
| | | Nile Red | | | NR12S | | |
| solvent | $E_T(30)$ | $\lambda_{abs}$, nm | $\lambda_{fluor}$, nm | QY, % | $\lambda_{abs}$, nm | $\lambda_{fluo}$, nm | QY, % |
| dioxane | 36.0 | 520 | 583 | 91 | 526 | 592 | 74 |
| EtOAc | 38.1 | 525 | 595 | 87 | 527 | 599 | 84 |
| THF | 37.4 | 530 | 595 | 90 | 530 | 597 | 81 |
| $CH_2Cl_2$ | 40.7 | 541 | 601 | 88 | 542 | 602 | 80 |
| DMF | 43.2 | 544 | 618 | 63 | 544 | 615 | 69 |
| DMSO | 45.1 | 554 | 629 | 46 | 554 | 627 | 55 |
| $CH_3CN$ | 45.6 | 536 | 612 | 82 | 536 | 612 | 81 |
| EtOH | 51.9 | 550 | 626 | 52 | 550 | 626 | 52 |
| MeOH | 55.4 | 553 | 632 | 38[b] | 555 | 631 | 40 |
| buffer | 63.1 | 591 | 657 | 5.0 | 521 | 657 | 0.2 |

[a] $\lambda_{abs}$ and $\lambda_{fluor}$, are absorption and emission maxima, respectively. Buffer refers to a 20 mM phosphate buffer (pH 7.4). [b] The QY value is from ref 29.

**Characterization in Solvents.** The spectroscopic properties of NR12S were studied in comparison to the parent Nile Red in different organic solvents. The absorption and fluorescence spectra of the two dyes were highly similar (Figure 1), especially in solvents of medium polarity. Moreover, both dyes show a similar strong red shift of their emission on increase in solvent polarity. However, differences in the emission spectra were observed in less polar solvents (dioxane and ethyl acetate), which could be connected with the effect of the proximal polar charged group.[32]

Similarly to the parent Nile Red, NR12S shows high fluorescence QY in most organic solvents (Table 1). Remarkably, in aqueous buffer NR12S is almost nonfluorescent (QY = 0.2%), whereas Nile Red is significantly fluorescent (QY = 5.0%). This could be explained by the detergent-like structure of NR12S, so that in water it may form oligomers or micelles, where its fluorophore is probably self-quenched. The existence of NR12S oligomers in water is also supported by the strongly blue-shifted absorption maximum in water as compared to that in organic solvents (Table 1). A similar quenching in water was observed for 3-hydroxyflavone derivatives bearing an amphiphilic group analogous to NR12S.[22,32b]

(29) Deda, M. L.; Ghedini, M.; Aiello, I.; Pugliese, T.; Barigelletti, F.; Accorsi, G. *J. Organomet. Chem.* **2005**, *690*, 857–861.
(30) (a) Clamme, J.-P.; Azoulay, J.; Mély, Y. *Biophys. J.* **2003**, *84*, 1960–1968. (b) Azoulay, J.; Clamme, J.-P.; Darlix, J.-L.; Roques, B. P.; Meĺy, Y. *J. Mol. Biol.* **2003**, *326*, 691–700.
(31) (a) Martin-Brown, S. A.; Fu, Y.; Saroja, G.; Collinson, M. M.; Higgins, D. A. *Anal. Chem.* **2005**, *77*, 486–494. (b) Briggs, M. S. J.; Bruce, I.; Miller, J. N.; Moody, C. J.; Simmonds, A. C.; Swann, E. *J. Chem. Soc. Perkin Trans. 1* **1997**, 1051–1058.
(32) (a) Klymchenko, A. S.; Demchenko, A. P. *J. Am. Chem. Soc.* **2002**, *124*, 12372–12379. (b) Klymchenko, A. S.; Duportail, G.; Ozturk, T.; Pivovarenko, V. G.; Mély, Y.; Demchenko, A. P. *Chem. Biol.* **2002**, *9*, 1199–1208.

***Table 2.*** Spectroscopic Properties of Nile Red and NR12S in Lipid Vesicles[a]

| | | dye | | | | | |
|---|---|---|---|---|---|---|---|
| | | Nile Red | | | NR12S | | |
| composition | phase state | $\lambda_{abs}$, nm | $\lambda_{fluo}$, nm | QY, % | $\lambda_{abs}$, nm | $\lambda_{fluo}$, nm | QY, % |
| DOPC | Ld | 549 | 628 | 42 | 530 | 608 | 48 |
| DOPC/CL | Ld | 550 | 624 | 48 | 527 | 605 | 47 |
| DPPC | L$\beta$ | 550 | 608 | 34 | 527 | 599 | 8 |
| DPPC/CL | Lo | 552 | 595 | 60 | 521 | 556 | 32 |
| DPPC/CL (60) | Ld | | 603 | 72 | | 601 | 57 |
| SM | L$\beta$ | 543 | 617 | 40 | 528 | 596 | 18 |
| SM/CL | Lo | 530 | 586 | 45 | 521 | 572 | 30 |
| SM/CL (60) | Ld | | 612 | 53 | | 593 | 45 |
| DOPS | Ld | 553 | 628 | 41 | 532 | 606 | 50 |

[a] $\lambda_{abs}$ and $\lambda_{fluor}$ are absorption and emission maxima, respectively. All spectra were recorded at 20 °C, except those marked "(60)", which were recorded at 60 °C. In lipid mixtures, the cholesterol/lipid ratio was 1:2, mol/mol. Ld, Lo, and L$\beta$ correspond to liquid disordered, liquid ordered, and solid gel phases.

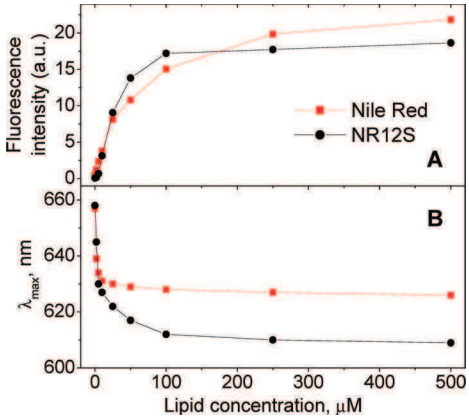


***Figure 2.*** Fluorescence of Nile Red and NR12S probes at different concentrations of DOPC LUVs. Integral intensity (A) and position of the maximum (B) vs DOPC concentration (phosphate buffer 20 mM, pH 7.4). Probe concentration was 0.5 $\mu$M.

**Binding to Lipid Vesicles.** Binding of the NR12S probe to DOPC lipid vesicles results in an about 200-fold increase of its fluorescence intensity, as can be seen from the quantum yields in aqueous buffer and in lipid vesicles (Tables 1 and 2). With the parent Nile Red, this increase is much less pronounced (only ca. 8-fold) due to its relatively high quantum yield in aqueous buffer. Therefore, NR12S dye is advantageous as a membrane probe, since unlike Nile Red its background fluorescence from the buffer can be neglected. The high fluorescence quantum yield of NR12S in lipid vesicles indicates that the probe oligomerization in water is likely reversible, so that an efficient membrane staining is achieved without additional solubilization techniques (with detergents or cyclodextrins). Moreover, titrations (Figure 2A) show that on increase in the lipid concentration, the fluorescence intensity of NR12S grows steeply and saturates at a probe/lipid ratio of 1:200, while for Nile Red this increase is less steep and saturation is reached only at a probe/lipid ratio 1:1000. These results suggest that NR12S binds more strongly to lipid membranes than Nile Red as a result of its amphiphilic anchor group. In addition, the position of the emission maximum of NR12S in DOPC LUVs at low probe/lipid ratio ($\leq$1:200) is significantly blue-shifted (17 nm) with respect to Nile Red (Figure 2B), indicating a deeper embedding of the fluorophore in the bilayer. However, at high probe/lipid ratios ($\geq$1:10), the emission maximum of NR12S becomes nearly the same as that of Nile Red, suggesting that the excess of NR12S probe binds nonspecifically to DOPC lipid bilayers and exhibits a shallower fluorophore insertion, similar to that of Nile Red.

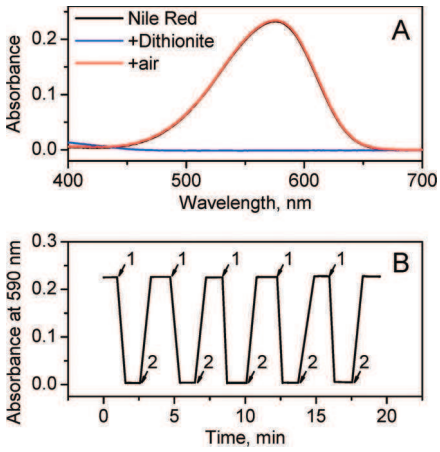


***Figure 3.*** On/off redox switching of Nile Red by dithionite/air treatment. (A) Absorption spectra of Nile Red in ethanol/water mixture (1:1, v/v) before treatment, after addition of 2 mM dithionite, and after further bubbling of air for 20 s. Extended spectral data are presented in Supporting Information. (B) Absorbance at 590 nm of Nile Red solution (ethanol/water) on repetitive treatment with 2 mM dithionite (1) and air bubbling (2). Inclined lines in (B) are used only for convenient presentation (connecting the experimental data points) and do not represent the transition kinetics between the low and high values of absorbance.

**Flip-Flop Studies Using Nile Red Reversible Bleaching with Dithionite.** One important issue in application of biomembrane probes is to evaluate their ability to stain selectively the outer membrane leaflet without fast flip-flop redistributing the dye between both leaflets. This problem was previously addressed for lipids modified with the NBD[33] fluorophore or spin-labels[34] using reducing agents, sodium dithionite and ascorbate, respectively, which inactivate the labels selectively in the outer leaflet of lipid vesicles. Though Nile Red is a chemically stable dye, it contains a quinoid fragment, which is a potential target for reduction. Moreover, the Nile Red analogues Nile Blue and resorufin can be reversibly reduced by different agents,[35] including dithionite. We checked the ability of Nile Red to be reduced by sodium dithionite in water/ethanol (1:1, v/v) solution. Addition of 2 mM dithionite leads to a complete disappearance of the absorption band of Nile Red (Figure 3A). Remarkably, after bubbling of air through this sample, the absorption band is fully recovered. This indicates that bleaching of Nile Red by dithionite is a fully reversible reduction process, so that this fluorophore can be switched off and on in a well-controlled manner. Furthermore, our data show that the reduction−oxidation cycle can be repeated many times without noticeable loss of the fluorophore (Figure 3B). The same results were obtained with the NR12S dye (see Supporting Information).

(33) McIntyret, J. C.; Sleight, R. G. *Biochemistry* **1991**, *30*, 11819–11827.
(34) (a) Seigneuret, M.; Devaux, P. F. *Proc. Natl. Acad. Sci. U.S.A.* **1984**, *81*, 3751–3755. (b) Kornberg, R. D.; McConnell, H. M. *Biochemistry* **1971**, *10*, 1111–1120.
(35) (a) Lemmon, T. L.; Westall, J. C.; Ingle, J. D., Jr. *Anal. Chem.* **1996**, *68*, 947–953. (b) Gorodetsky, A. A.; Ebrahim, A.; Barton, J. K. *J. Am. Chem. Soc.* **2008**, *130*, 2924–2925. (c) Cincotta, L.; Foley, J. W.; Cincotta, A. H. *Cancer Res.* **1993**, *53*, 2571–2580. (d) Erb, R. E.; Ehlers, M. H. *J. Dairy Sci.* **1950**, *33*, 853–864. (e) Zhou, M.; Diwu, Z.; Panchuk-Voloshina, N.; Haugland, R. P. *Anal. Biochem.* **1997**, *253*, 162–168. (f) Talbot, J. D.; Barrett, J. N.; Barrett, E. F.; David, G. *J. Neurochem.* **2008**, *105*, 807–819.

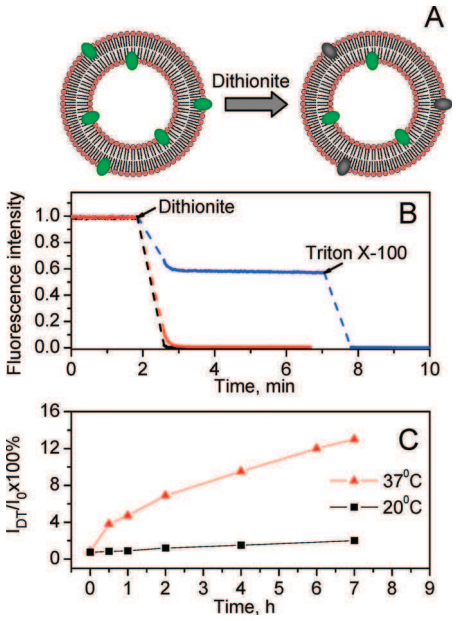


***Figure 4.*** Flip-flop studies of probes Nile Red and NR12S in DOPC LUVs using the dithionite bleaching method. (A) Schematic presentation of the selective bleaching of the probes at the outer leaflet of LUV by dithionite. (B) Evolution of the probe fluorescence intensity after addition of 10 mM dithionite and 1% (vol) of Triton X-100. Dyes were added to lipids either before LUV preparation to achieve staining of both leaflets (Nile Red = black line, NR12S = blue line) or after LUV preparation to stain the outer leaflet (NR12S = red line). (C) Fraction (%) of NR12S probe flipped from the outer to the inner leaflet in LUVs as a function of time at 20 and 37 °C. The suspension of LUVs was stained with the probe by method 2. After a given incubation time (at 20 or 37 °C), the fluorescence intensities at 600 nm before ($I_0$) and 3 min after addition of 10 mM sodium dithionite ($I_{DT}$) were measured. The fraction of flipped probe for a given incubation time was expressed as $I_{DT}/I_0 \times 100\%$. The probes concentration for both methods was 1 $\mu$M.

Since sodium dithionite is unable to penetrate the lipid bilayers, it can bleach the Nile Red fluorophore exclusively on the external leaflet (Figure 4A) and thus allows evaluation of the probe flip-flop, as it was done previously with NBD-labeled lipids.[33] For this purpose, we stained the lipid membranes in two different ways. In method 1, the probe was mixed with lipids first and then the vesicles were prepared, which ensured its symmetric distribution between both leaflets. In method 2, the probe was added to the vesicles from the external bulk solution to target the outer membrane leaflet. When the parent Nile Red probe was distributed in both leaflets (method 1), the addition of 10 mM dithionite resulted in complete bleaching (Figure 4B). An identical result was observed when the dye was added to vesicles from the bulk water (method 2, data not shown). Thus, Nile Red undergoes probably a very fast flip-flop, so that addition of dithionite can rapidly bleach the dye located initially on both leaflets. In contrast, when dithionite was added to vesicles stained with NR12S symmetrically on both leaflets (method 1), the fluorescence intensity drops rapidly until approximately 50% of the initial value (Figure 4B) and then remains relatively stable. Further addition of Triton X-100, which disrupts the lipid vesicles, leads to complete disappearance of fluorescence. This result is fully in line with that previously reported for NBD-lipids,[33] indicating that selective bleaching of NR12S fluorophore at the outer leaflet was achieved (Figure 4A), while the other 50% of the probe at the inner leaflet remained intact. The stabilization of the fluorescence intensity at ca. 50% of its initial value suggests that NR12S does not flip

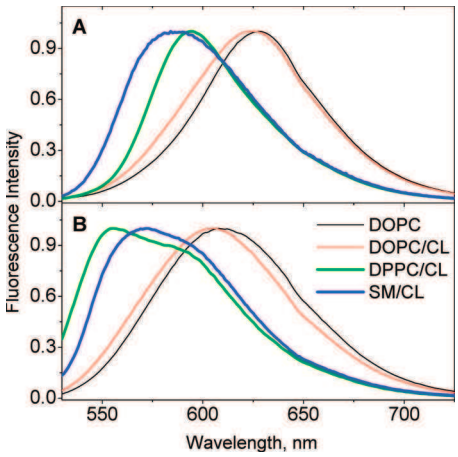


***Figure 5.*** Normalized fluorescence spectra of Nile Red (A) and NR12S (B) in LUVs of different lipid compositions. Probe and lipid concentrations were 1 and 200 $\mu$M, respectively.

to the outer leaflet within the experimental time. Importantly, when the staining was performed by addition of the probe to blank vesicles (method 2), the treatment with sodium dithionite resulted in rapid and complete bleaching (Figure 4B). The absence of residual fluorescence in this case clearly shows that NR12S stains exclusively the outer leaflet of vesicles and remains there at least within the incubation time (7 min, rt). We also incubated vesicles with the NR12S probe initially bound to the outer leaflet for longer time periods at 20 and 37 °C. Remarkably, at room temperature the residual fluorescence after dithionite treatment was still negligible even after 2 h of incubation and became significant (2%) only after 7 h of incubation (Figure 4C). Thus, at room temperature, the flip-flop process for NR12S is extremely slow. At 37 °C, the flip-flop was faster, though after 4 h only 9% of the probe migrated to the inner leaflet (Figure 4C).

Thus, according to our data, Nile Red redistributes between the two leaflets on the time scale of seconds or faster, whereas NR12S shows only marginal flip-flop for hours at room temperature. This dramatically decreased flip-flop dynamics of NR12S is evidently due to the anchor group containing a zwitterion and a long alkyl chain, which interact strongly with lipids, preventing the probe flip-flop. This is one of the first reports where a spontaneous binding of a nonlipidic membrane fluorescent probe to the outer leaflet is demonstrated by a chemical method. Previously, outer leaflet staining was suggested for styrylpyrydinium and 3-hydroxyflavone dyes from their sensitivity to the transmembrane electric potential and lipid asymmetry, or detection of second harmonic generation signal in cell membranes.[20,22] It should be also noted that, similarly to our data in water/ethanol mixtures, the bleached NR12S probe in lipid vesicles can be further switched "on" by air bubbling. However, the fluorescence recovery in this case takes more time (data not shown).

**Sensitivity to Lipid Composition in Model Membranes.** Nile Red, being an environment-sensitive probe, shows a dependence of its spectrum on the lipid composition and the phase state in lipid bilayers (Figure 5). Since spectroscopic differences between the Lo and Ld phases are an important requirement for the development of probes for lipid domains,[18–21] the new probe NR12S was compared to Nile Red in these two phases. Similar to Nile Red, the new probe shows a significantly blue-shifted emission maximum in Lo phase vesicles composed of sphingomyelin and cholesterol (SM/CL) or DPPC and cholesterol

(DPPC/CL), compared to Ld phase vesicles composed of DOPC or DOPC/CL (Figure 5). These results are in line with other environment-sensitive probes such as Prodan, Laurdan,[18] di-4-ANEPPDHQ,[20] and 3-hydroxyflavone derivatives[21] showing a less polar and less hydrated environment in the Lo phase. Importantly, in DPPC and SM vesicles presenting gel phase (L$\beta$), the probes show intermediate positions of their emission maxima (Table 2). Thus, for both probes the emission maximum shifts to the blue in the following sequence of membrane phases: Ld → L$\beta$ → Lo, in line with recent data[20,21b] suggesting that the environment of these probes is the most dehydrated in the Lo phase.

An outstanding feature of the present dyes is that within the Ld phase, the position of their emission maximum is poorly sensitive to the presence of cholesterol (DOPC/CL vs DOPC, Figure 5, Table 2) Therefore, these dyes can clearly distinguish between cholesterol-rich Ld (DOPC/CL) and Lo (SM/CL or DPPC/CL) phases. In contrast, Prodan, Laurdan, 3-hydroxyflavone-based and di-4-ANEPPDHQ probes show a significant dependence of their spectra on the cholesterol content in the Ld phase,[18,20,36] so that the spectral differences between cholesterol-rich Ld and Lo phases are less pronounced for these probes. Moreover, unlike 3-hydroxyflavone-based probes, Nile Red and NR12S are insensitive to the surface charge (DOPS vs DOPC) (Table 2). Thus, in contrast to the other mentioned probes, Nile Red and NR12S show a characteristic blue-shifted emission only in cholesterol-rich Lo phase.

The fluorescence quantum yield of the probes also depends on the phase state of the lipid membranes, especially in the case of probe NR12S. Indeed, the highest quantum yields are observed with the Ld phase, and the lowest ones are associated with the L$\beta$ phase. Because of its highly dense packing, the L$\beta$ phase is likely characterized by a relatively low number of binding sites for the probe, leading to a less efficient probe binding (so that a significant fraction of the probe is in bulk solution), which decreases the apparent fluorescence quantum yield of the probe. In contrast, the loosely packed Ld phase presents a much larger number of binding sites, thus explaining a more efficient probe binding accompanied by a higher fluorescence intensity. The Lo phase presents an intermediate case. The weaker dependence of the fluorescence quantum yield of Nile Red on the phase state is probably due to its smaller size and less specific binding to lipid bilayers as compared to NR12S, which ensures a sufficient number of binding sites independently of the membrane phase. Noticeably, in contrast to data in organic solvents, the emission of NR12S in all studied lipid vesicles is systematically blue-shifted with respect to Nile Red (Tables 1 and 2). This indicates that the fluorophore of NR12S is more deeply embedded in the bilayer than Nile Red, in line with our conclusions on a more specific binding of NR12S to lipid membranes.

To further characterize the sensitivity of the dyes to the Lo phase, the effect of temperature was investigated. In SM/CL vesicles at 60 °C, both NR12S and Nile Red show significantly red-shifted spectra compared to those at 20 °C (Table 2), confirming the strong sensitivity of the probes to the Lo → Ld transition. This transition also increases the fluorescence quantum yield of the NR12S probe, likely due to the increase in the number of the probe binding sites.

Thus, the experiments in model membranes show that the new probe similarly to the parent Nile Red is highly sensitive to the phase state of lipid bilayers and distinguishes Lo from Ld phases by the color of its emission.

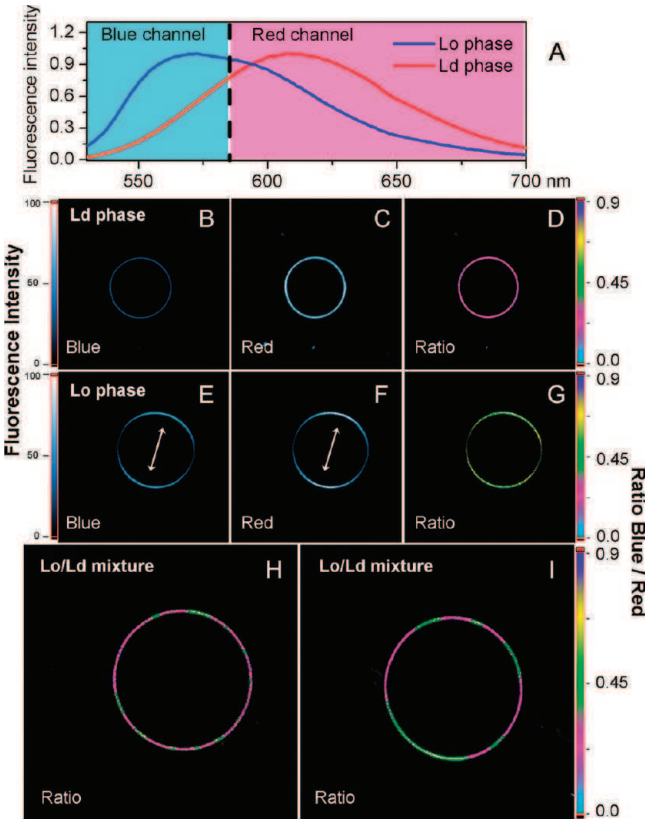


***Figure 6.*** Fluorescence microscopy imaging of Lo and Ld phases in GUVs using NR12S. (A) Normalized fluorescence spectra of NR12S in Ld (DOPC) and Lo (SM/Chol) phases of LUVs. The cyan and magenta regions separated at 585 nm represent the detection range for the blue and red channels of the microscope. GUVs were composed of DOPC (Ld phase: B, C, D), SM/Chol, 2/1 (Lo phase: E, F, G), and DOPC/SM/Chol, 1/1/0.7 (mixed Lo/Ld phases: H,I). Intensity images at the blue (<585 nm, B and E) and the red (>585 nm, C and F) channels. In the ratiometric images (D, G, H, and I), the color of each pixel represents the value of the intensity ratio $I_{blue}/I_{red}$, while the pixel intensity corresponds to the total intensity at both channels. Two-photon excitation wavelength was at 830 nm. Arrows indicate the orientation of the light polarization. Sizes of the images were 70 $\mu$m × 70 $\mu$m. Probe concentration was 1 $\mu$M.

**Imaging Cholesterol-Rich Phases in Giant Vesicles.** Because of their relatively large size (5−100 $\mu$m), giant vesicles (GUVs) are an excellent biomembrane model for fluorescence microscopy studies.[27] We thus performed two-photon fluorescence imaging of GUVs using NR12S, in order to evaluate its capability to visualize Ld and Lo phases. We first measured the two-photon absorption cross-section of Nile Red and NR12S at 830 nm using Rhodamine B as a standard as described previously (see Supporting Information).[37] The observed values 32 and 30 GM ($10^{-50}$ cm$^4$ × s × photon$^{-1}$) for Nile Red and NR12S, respectively, are sufficiently large for their application in two-photon microscopy.[37] Since the position of the emission maximum of NR12S changes in response to the phase state, ratiometric imaging[18,20] can be performed by splitting its emission into blue and red regions (Figure 6A). For the Ld phase (DOPC), the area under the NR12S emission spectrum in the blue region (<585 nm) is much smaller as compared to the red

(36) Massey, J. B. *Biochim. Biophys. Acta* **1998**, *1415*, 193–204.

(37) (a) Xu, C.; Webb, W. W. *J. Opt. Soc. Am. B* **1996**, *13*, 481–491. (b) Albota, M. A.; Xu, C.; Webb, W. W. *Appl. Opt.* **1998**, *37*, 7352–7356.

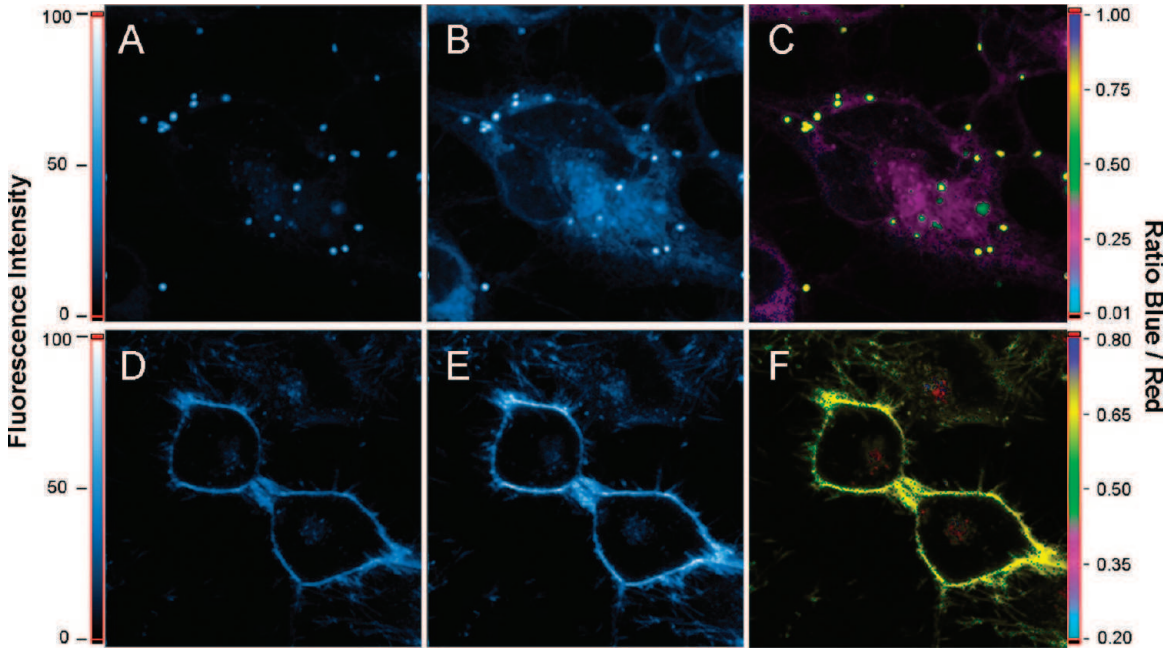


***Figure 7.*** Fluorescence intensity (A, B, D, E) and ratiometric (C, F) images of cells stained with Nile Red (A−C) and NR12S (D−F). Intensity images at the short-wavelength "blue" (<585 nm, A and D) and the long-wavelength "red" (>585 nm, B and E) channels are presented. In the ratiometric images, the color of the pixel represents the value of the intensity ratio of the blue channel to that of the red channel, while the pixel intensity corresponds to the total number of photons collected at both channels. Two-photon excitation wavelength was at 830 nm. Sizes of the images were 70 $\mu$m × 70 $\mu$m. Probe concentration was 0.3 $\mu$M.

region (>585 nm), so that the estimated ratio of the integral intensities $I_{blue}/I_{red}$ is ca. 0.23. In contrast, for Lo phase (SM/Chol), these areas are similar, and the corresponding $I_{blue}/I_{red}$ value is ca. 0.88. This 4-fold difference in the ratio should be easily detectable by a fluorescence microscope having blue (<585 nm) and red (>585 nm) detection channels. In line with these expectations, the fluorescence images of the equatorial section of GUVs composed of DOPC (Ld phase) show that the intensity at the blue channel is much lower than at the red channel (Figure 6B and C), while for SM/Chol GUVs (Lo phase) these intensities are comparable (Figure 6E and F). In the ratiometric images, the GUV membranes in Ld phase appear predominantly in pink pseudocolor corresponding to a ratio around 0.20−0.25 (Figure 6D), which matches perfectly the predicted ratio from the fluorescence spectra. For Lo phase, GUV membranes appear in green-yellow pseudocolor corresponding to a ratio around 0.62−0.67 (Figure 6G), which also matches well the expected ratio.

Importantly, the ratiometric images of GUVs composed of DOPC/SM/Chol (1/1/0.7 molar ratios) present clear separated domains with two different pseudocolors (Figure 6H and I). These pseudocolors correspond well to those observed in pure Ld and Lo phases, which allows unambiguous assignment of the pink domains (low $I_{blue}/I_{red}$ ratio) to Ld phase and the green domains (high $I_{blue}/I_{red}$ ratio) to Lo phase. Importantly, the high fluorescence intensity from both Lo and Ld phases in the ternary mixture suggests that NR12S partitions evenly between them, though it is difficult to estimate the exact partition ratio. Since most fluorescent dyes preferentially bind Ld phase in ternary mixtures,[17] the even distribution of NR12S between Lo and Ld phases is an important advantage for their simultaneous visualization. Only few environment-sensitive dyes show this ability: Prodan derivatives, styrylpyrydinium dyes and, to lesser extent, 3-hydroxyflavone derivatives.[18–21]

Noticeably, while the fluorescence intensity of NR12S is homogeneously distributed all over the DOPC GUV membrane (Figure 6B and C), it depends on the orientation of the bilayer plane with respect to the polarization plane of the excitation light in SM/Chol GUVs (Figure 6E and F). In line with already reported data for other environment-sensitive and rod-shaped probes,[18,19,21a] the fluorescence intensity of NR12S in Lo phase is the highest when the light polarization is parallel to the probe fluorophore exhibiting preferentially vertical orientation due to the constrained lipid packing. In contrast, the loosely packed Ld phase of DOPC membrane imposes no preferential orientation for the fluorophore, so that efficient probe excitation can always be achieved.

**Cellular Studies.** Two-photon fluorescence imaging of living cells stained with the probes shows that Nile Red exhibits mainly intracellular fluorescence (Figure 7A−C), which according to the literature corresponds to a staining of lipid droplets.[23] Remarkably, the fluorescence ratio (blue/red channels) from the intracellular droplets is much larger than from other parts of the cell, in line with their highly apolar nature. In contrast, the new probe NR12S stains exclusively the cell plasma membrane, as it can be seen from the typical membrane staining profile and the rather uniform fluorescence intensity ratio within the image (Figure 7D−F). Thus, the conjugation of the Nile Red fluorophore with the detergent-like anchor group allows localizing the fluorophore on the cell membrane. Moreover, addition of 10 mM dithionite results in >90% bleaching of NR12S bound to the cells (see Supporting Information), showing a specific binding to the outer leaflet of the plasma membrane with almost no internalization into the cell.

The new probe showing high binding specificity together with high sensitivity to the membrane phase appears thus as an attractive tool for studying the lipid phases at the outer leaflet of living cells. The fluorescence maximum of NR12S in intact

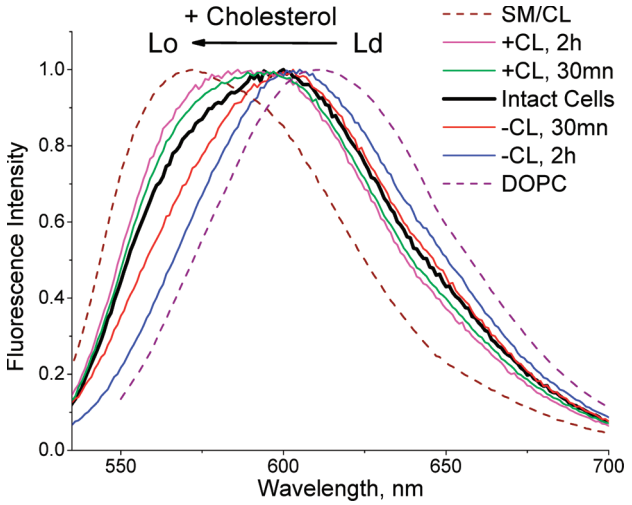


***Figure 8.*** Normalized fluorescence spectra of 0.1 $\mu$M NR12S in cells at different levels of cholesterol depletion/enrichment and in model membranes presenting Lo (SM/CL) and Ld (DOPC) phases.

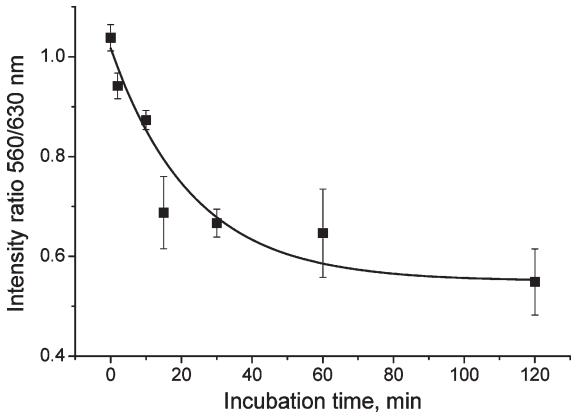


***Figure 9.*** Monitoring the kinetics of cholesterol extraction from astrocytoma cells using NR12S probe. Ratio of the emission intensities at 560 and 630 nm of NR12S in cells treated with 5 mM M$\beta$CD for different times. The curve represents a single exponential fit to the experimental data. Each data point is the average of three measurements.

cells is intermediate to those with the Lo and Ld phases of model membranes (Figure 8), in line with the high content in plasma membranes of unsaturated lipids, sphingomyelin and cholesterol favoring both phases.[1,10] Other reports also suggested a significant fraction of Lo phase in the cell plasma membranes.[38] Importantly, the emission maximum of NR12S is stable for 30 min, confirming that flip-flop and internalization of the probe are relatively slow. Since cholesterol is a key component of the Lo phase, we modified its content in cell membranes, using methyl-$\beta$-cyclodextrin (M$\beta$CD).[11,28] On cholesterol depletion, the NR12S probe shows a red shift (Figure 8), so that the obtained spectrum is close to that with the Ld phase vesicles (DOPC, Figure 8). As NR12S is rather insensitive to cholesterol variation within Ld phase (see above), it likely reports on the disappearance of the Lo phase after cholesterol depletion. It should be noted that the present data do not provide a proof for the presence of separated Lo phase domains in cell membranes. Indeed, cell membranes can present a special phase, having features of both Lo and Ld phases, which can be converted into Ld phase after cholesterol depletion. Importantly, the red shift value depends on the incubation time of the cells with M$\beta$CD, suggesting an application of NR12S for a quantitative description of cholesterol depletion.

In order to monitor the kinetics of cholesterol depletion, we took the intensity ratio at the blue and red sides of the NR12S spectra, namely, 560 and 630 nm, where the variations of the relative intensities are maximal (Figure 8). Incubation with 5 mM M$\beta$CD results in a relatively rapid decrease in the intensity ratio 560/630 nm within the first 15 min, followed by slower changes at longer incubation times (Figure 9). Fitting the data to a single exponential decay provided a cholesterol depletion time constant of 23 $\pm$ 6 min, in excellent agreement with the half-time of 21 $\pm$ 6 min obtained previously from extraction of $^3$H-labeled cholesterol with 2-hydroxypropyl-$\beta$-cyclodextrin.[11a] Other reports on model[39] and cellular membranes[11b,28] also suggest a similar time scale of cholesterol depletion, though the rate of the process depends strongly on the initial cholesterol content. The correspondence of our data with the literature shows that our method using NR12S can quantify cholesterol in cell membranes and describe its depletion kinetics.

In contrast to its depletion, cholesterol enrichment in living cells using M$\beta$CD−cholesterol complex shifts the NR12S emission to the blue, so that the obtained spectrum becomes closer to that of model vesicles presenting a homogeneous Lo phase (SM/CL, Figure 8). The spectroscopic effect increases with the time of incubation with the M$\beta$CD−cholesterol complex. Thus, the new probe can monitor in a rather broad range the cholesterol content and the fraction of cholesterol-rich Lo phase in cell membranes.

To visualize cells at different concentrations of cholesterol, we performed fluorescence ratiometric imaging before and after treatment with M$\beta$CD. After cholesterol depletion, there is a clear change in the pseudocolor of the cells, indicating a decrease in the intensity ratio recorded at the blue (<585 nm) and the red (>585 nm) parts of the probe emission spectrum (Figure 10). This decrease is in agreement with the red shift of the fluorescence spectra in cell suspensions (Figure 8). It can be also noticed that after cholesterol depletion, the cells differ one from another by their blue/red intensity ratio (Figure 10C), suggesting that the efficiency of cholesterol extraction varies from cell to cell. Moreover, after cholesterol extraction the cell membranes appear smoother, so that the numerous extensions of cell membranes are no more observed (Figure 10). These changes in morphology can be attributed to the disruption of the native cytoskeleton, which is highly cholesterol-dependent.[40] It can also be noted that neither intact cells nor cells treated with M$\beta$CD show membrane heterogeneity, which one would expect from separated Lo/Ld phase domains in the microscopic scale. Thus, though our data suggests the presence of

(38) (a) Hao, M.; Mukherjee, S.; Maxfield, F. R. *Proc. Natl. Acad. Sci. U.S.A.* **2001**, *98*, 13072–13077. (b) Gidwani, A.; Holowka, D.; Baird, D. *Biochemistry* **2001**, *40*, 12422–12429. (c) Swamy, M. J.; Ciani, L.; Ge, M.; Smith, A. K.; Holowka, D.; Baird, B.; Freed, J. H. *Biophys. J.* **2006**, *90*, 4452–4465. (d) Oncul, S.; Klymchenko, A. S.; Kucherak, O. A.; DemchenkoA. P.; Martin, S.; Dontenwill, M.; Arntz, Y.; Didier, P.; Duportail, G.; Mély, Y. *Biochim. Biophys. Acta* **2010**, in press, doi: 10.1016/j.bbamem.2010.01.013.

(39) Radhakrishnan, A.; McConnell, H. M. *Biochemistry* **2000**, *39*, 8119–8124.

(40) (a) Martin, S.; Phillips, D. C.; Szekely-Szucs, K.; Elghazi, L.; Desmots, F.; Houghton, J. A. *Cancer Res.* **2005**, *65*, 11447–11458. (b) Ramprasad, O. G.; Srinivas, G.; Rao, K. S.; Joshi, P.; Thiery, J. P.; Dufour, S.; Pande, G. *Cell Motil. Cytoskeleton* **2007**, *64*, 199–216. (c) Patra, S. K. *Biochim. Biophys. Acta* **2008**, *1785*, 182–206.

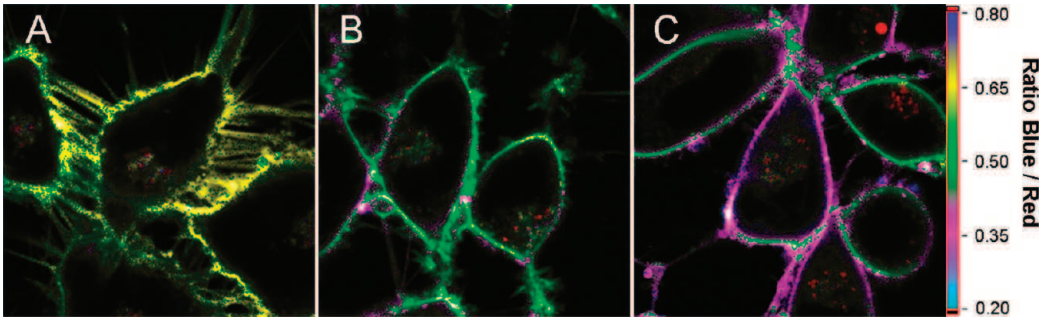


***Figure 10.*** Fluorescence ratiometric images of cells stained with NR12S at different levels of cholesterol depletion. Intact cells (A) and cells after incubation with 5 mM M$\beta$CD for 30 min (B) and 2 h (C). The color of each pixel represents the value of the intensity ratio of the blue to the red channel, while the pixel intensity corresponds to the total number of photons collected at both channels. Two-photon excitation wavelength was at 830 nm. Sizes of the images were 50 $\times$ 50 $\mu$m. Probe concentration was 0.3 $\mu$M.

cholesterol-rich Lo phase in cell membranes, we cannot visualize separated domains with optical microscopy. The hypothetic Lo phase domains, if they exist, are probably too small and dynamic to be detected in our fluorescence images, due to the limited spatial and temporal resolution of the imaging technique.[41]

## Conclusions

A probe based on Nile Red has been synthesized for studying cholesterol and lipid order in biomembranes. Unlike the parent Nile Red, the new probe binds spontaneously to the outer leaflet of model and cell plasma membranes with very slow flip-flop and internalization. Spectroscopy studies of LUVs and fluorescence imaging of GUVs further show that the probe can distinguish by its emission color between liquid ordered and disordered phases. Using cholesterol depletion/enrichment with methyl-$\beta$-cyclodextrin, we showed that the emission color of this probe correlates well with the cholesterol content in cell membranes. The key advantages of the new probe compared to existing membranes probes arise from its Nile Red fluorophore: superior brightness, red-shifted absorption and emission, high photostability and on/off switching capability. These properties make the new probe a powerful tool for monitoring cholesterol and lipid order selectively at the outer leaflet of cell membranes.

**Acknowledgment.** This work was supported by Conectus Alsace and ANR blanc grants.

**Supporting Information Available:** Synthesis of NR12S, additional data on bleaching by dithionite, and two-photon absorption cross section results. This material is available free of charge via the Internet at http://pubs.acs.org.

JA100351W

(41) (a) Lenne, P. F.; Wawrezinieck, L.; Conchonaud, F.; Wurtz, O.; Boned, A.; Guo, X. J.; Rigneault, H.; He, H. T.; Marguet, D. *EMBO J.* **2006**, *25*, 3245–3256. (b) Wawrezinieck, L.; Rigneault, H.; Marguet, D.; Lenne, P. F. *Biophys. J.* **2005**, *89*, 4029–4042. (c) Veatch, S. L.; Cicuta, P.; Sengupta, P.; Honerkamp-Smith, A.; Holowka, D.; Baird, B. *ACS Chem. Biol.* **2008**, *3*, 287–293.

# *Publication 2*

# *Detection of apoptosis through the lipid order of the outer plasma membrane leaflet*

Biochimica et Biophysica Acta 1818 (2012) 3048–3054

Contents lists available at SciVerse ScienceDirect

Biochimica et Biophysica Acta

journal homepage: www.elsevier.com/locate/bbamem

# Detection of apoptosis through the lipid order of the outer plasma membrane leaflet

Zeinab Darwich, Andrey S. Klymchenko *, Oleksandr A. Kucherak, Ludovic Richert, Yves Mély

*Laboratoire de Biophotonique et Pharmacologie, UMR 7213 CNRS, Université de Strasbourg, Faculté de Pharmacie, 74, Route du Rhin, 67401 ILLKIRCH Cedex, France*

ARTICLE INFO

*Article history:*
Received 25 April 2012
Received in revised form 16 July 2012
Accepted 23 July 2012
Available online 27 July 2012

*Keywords:*
Apoptosis
Lipid order
Asymmetry of plasma membrane
Fluorescent probe
Sphingomyelin
Cholesterol

ABSTRACT

Cell plasma membranes of living cells maintain their asymmetry, so that the outer leaflet presents a large quantity of sphingomyelin, which is critical for formation of ordered lipid domains. Here, a recently developed probe based on Nile Red (NR12S) was applied to monitor changes in the lipid order specifically at the outer leaflet of cell membranes. Important key features of NR12S are its ratiometric response exclusively to lipid order (liquid ordered vs. liquid disordered phase) and not to surface charge, the possibility of using it at very low concentrations (10–20 nM) and the very simple staining protocol. Cholesterol extraction, oxidation and sphingomyelin hydrolysis were found to red shift the emission spectrum of NR12S, indicating a decrease in the lipid order at the outer plasma membrane leaflet. Remarkably, apoptosis induced by three different agents (actinomycin D, camptothecin, staurosporine) produced very similar spectroscopic effects, suggesting that apoptosis also significantly decreases the lipid order at this leaflet. The applicability of NR12S to detect apoptosis was further validated by fluorescence microscopy and flow cytometry, using the ratio between the blue and red parts of its emission band. Thus, for the first time, an environment-sensitive probe, sensitive to lipid order, is shown to detect apoptosis, suggesting a new concept in apoptosis sensing.



## 1. Introduction

Cell plasma membranes exhibit remarkable asymmetry of their bilayer leaflet [1,2]. Thus, while the outer leaflet contains large quantities of sphingomyelin (SM) and phosphatidylcholine (PC), the inner leaflet is characterized by significant fractions of phosphatidylserine (PS) and phosphatidylethanolamine (PE). This asymmetry plays an important role for the function of membrane proteins and can participate in key processes such as apoptosis [3]. Indeed, it is well established that apoptosis results in the exposure of PS at the outer leaflet, which is responsible for the recognition of apoptotic cells by the macrophages [4] and used for apoptosis detection [5–8]. However, it remains unclear so far what happens with the other lipids on apoptosis, SM in particular. SM together with cholesterol form domains of the liquid ordered (Lo) phase, so-called rafts, which "float in the sea" of the liquid disordered (Ld) phase formed by unsaturated lipids and cholesterol [9,10]. These Lo phase domains were hypothesized to regulate the activity of proteins in cell plasma membranes [11–14]. A previous work suggested that the executive step of apoptosis is accompanied with the transfer of SM from the outer to the inner leaflet [15]. Moreover, it has been already shown that SM undergoes hydrolysis during apoptosis to give ceramide [16], which produces dramatic effects on the membrane structure and properties [15]. Thus, it can be hypothesized that apoptosis should lead to significant changes in the lipid organization of the outer leaflet. Previous early work using a fluorescent membrane probe merocyanine 540 showed the alternation of the "lipid packing" in apoptotic thymocytes [17]. Later this probe was proposed as a tool for detection of apoptosis in different cell lines [18], indicating that the changes in the "lipid packing" on apoptosis can be a rather general phenomenon. Later works suggested that apoptosis may decrease the "lipid packing" in B lymphocytes [19] and increase the "interlipid spacing" in S49 Lymphoma cells [20]. Nevertheless, these reports are scattered and it remains unclear whether these changes are related to one or both plasma membrane leaflets.

Our recent studies showed that the fluorescent probe F2N12S (Fig. 1), specific to the outer membrane leaflet, is able to detect apoptosis [21]. This is an environment-sensitive probe of 3-hydroxyflavone family undergoing excited state proton transfer (ESIPT) [22,23] and is sensitive to surface charge and hydration of lipid membranes [24,25]. Remarkably, the hydration estimated by this probe and its analogs correlated well with the membrane phase, so that the hydration of Lo phase is lower than that of the Ld phase [26]. This property is similar to that of other environment-sensitive probes, such as Laurdan [10,27] and di-ANNEPS [28,29], allowing differentiation between liquid disordered and ordered phases (i.e. to sense "lipid order") in model vesicles [30] and cellular membranes [25]. However, as F2N12S probe was shown to sense both lipid order and surface charge, the loss of the lipid order as well as the exposure of PS at the outer leaflet could be responsible for the probe response to apoptosis [25]. To address more specifically the lipid order at the outer leaflet, without side effects of the surface charge, we recently developed a probe NR12S (Fig. 1) [31] based on environment-sensitive dye Nile Red [32]. NR12S binds selectively at the outer membrane leaflet and changes its emission color in

* Corresponding author. Tel.: +33 368 85 42 55; fax: +33 368 85 43 13.
*E-mail address:* andrey.klymchenko@unistra.fr (A.S. Klymchenko).

0005-2736/$ – see front matter © 2012 Elsevier B.V. All rights reserved.
http://dx.doi.org/10.1016/j.bbamem.2012.07.017

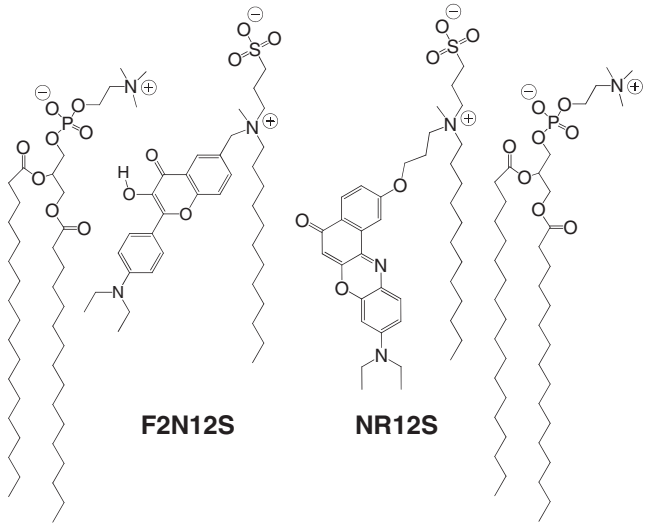


**Fig. 1.** Probes F2N12S and NR12S and their hypothetic localization with respect to lipids in membranes.

liquid ordered phase enriched in SM and cholesterol [31]. It has already been successfully applied to study transmembrane asymmetry in small and giant unilamellar vesicles [33,34]. In contrast to F2N12S, the NR12S probe is insensitive to the surface charge, and thus enables the study of specifically lipid order during apoptosis. In the present work, cellular studies were performed to validate that this probe can sense lipid order changes induced by different means: cholesterol extraction, cholesterol oxidation and sphingomyelin hydrolysis. Remarkably, apoptosis, induced by three different agents, produced very similar spectroscopic effects, providing clear evidence that the high lipid order at the outer leaflet, similar to that of Lo phase in model vesicles, is lost during apoptosis. Finally, flow cytometry data showed that NR12S can be used for quantitative detection of apoptosis in cells, similarly to the commercial assay based on fluorescently labeled annexin V [5,35].

## 2. Materials and methods

Probe NR12S was synthesized as described elsewhere [31]. Dioleoylphosphatidylcholine (DOPC) and cholesterol were purchased from Sigma-Aldrich. Bovine brain sphingomyelin (SM) was from Avanti Polar Lipids (Alabaster, USA).

### 2.1. Lipid vesicles

Large unilamellar vesicles (LUVs) were obtained by the extrusion method as previously described [36]. Briefly, a suspension of multilamellar vesicles was extruded by using a Lipex Biomembrane extruder (Vancouver, Canada). The size of the filters was first 0.2 μm (7 passages) and thereafter 0.1 μm (10 passages). This generates monodisperse LUVs with a mean diameter of 0.11 μm as measured with a Malvern Zetamaster 300 (Malvern, UK). A 20 mM phosphate buffer pH 7.4 was used in these experiments. LUVs were labeled by adding aliquots of probe stock solutions in dimethylsulfoxide to 1 mL solutions of vesicles.

### 2.2. Cell lines, culture conditions and treatment

U87MG human glioblastoma cell line (ATCC) was cultured in Eagle's minimal essential medium (EMEM from LONZA) with 10% heat-inactivated fetal bovine serum (PAN Biotech GmbH) and 0.6 mg/mL glutamine (Biowhittaker) at 37 °C in a humidified 5% $CO_2$ atmosphere. HeLa cells were cultured in Dulbecco's modified Eagle medium (D-MEM, high glucose, Gibco-invitrogen) supplemented with 10% (v/v) fetal bovine serum (FBS, Lonza), 1% antibiotic solution (penicillin–streptomycin, Gibco-invitrogen) in a humidified incubator with 5% $CO_2$ atmosphere at 37 °C. A cell concentration of 5–10 × $10^4$ cells/mL was maintained by removal of a portion of the culture and replacement with fresh medium, three times per week.

Cholesterol depletion, cholesterol oxidation and SMase treatment were performed using methyl-β-cyclodextrin (MβCD), cholesterol oxidase from *Streptomyces* sp., and sphingomyelinase from *Bacillus cereus* (Sigma-Aldrich), respectively. Briefly, stock solution of MβCD in Dulbecco's Phosphate Buffered Saline (DPBS) was prepared at a suitable concentration, filtered by Millipore filter (0.2 μm) and added to the cells to a final concentration of 5 mM. The treated cells were kept at 37 °C for 2 h. For cholesterol oxidation, a stock solution of cholesterol oxidase was prepared in 50 mM potassium phosphate buffer, pH 7.0. The treated cells were kept at 37 °C for 2 h with 2 U/mL of cholesterol oxidase. For SM hydrolysis, cells were incubated at 37 °C for 2 h with 0.2 U/mL of SMase.

For apoptosis studies, three different agents were tested. To induce apoptotis, cells were treated with actinomycin D (0.5 μg/mL), camptothecin (5 μg/mL), or staurosporine (0.1 μM) for 18 h at 37 °C.

In fluorescence spectroscopy experiments, cells were detached by trypsinization. The culture medium was first removed from the culture dish and cells were washed two times with DPBS. Trypsine 10× (LONZA) solution was diluted 10 times with DPBS and added to the cells at 37 °C for 4 min. The solution of trypsinated cells was then diluted by HBSS (Hank's Balanced Salt Solution), transferred to Falcon tubes and centrifuged at 1500 rpm for 5 min, two times. To stain the cell suspension with the NR12S probe, an appropriate aliquot of its stock solution in DMSO was added to 0.5 mL of HBSS buffer and after vortexing, the solution was immediately added to 0.5 mL of the cell suspension to obtain a final probe concentration of 0.01 μM (<0.25% DMSO) and a cell concentration of 1 × $10^6$ cells/mL. It should be noted that only freshly prepared solutions of the probe in HBSS should be used (<3 min) for cell staining, because of the slow aggregation of the probe in water. Before measurements, the cell suspension with probe was incubated for 7 min at room temperature in the dark.

For microscopy studies, cells were seeded onto a chambered cover glass (IBiDi) at a density of 5 × $10^4$ cells/IBiDi. After washing the cells with Opti-MEM, a freshly prepared solution of NR12S in Opti-MEM was added to the cells to a final concentration of 0.05 μM (<0.25% DMSO volume) and incubated for 7 min in the dark at room temperature.

### 2.3. Fluorescence spectroscopy and microscopy

Absorption spectra were recorded on a Cary 4 spectrophotometer (Varian) and fluorescence spectra on a FluoroMax 3.0 (Jobin Yvon, Horiba) spectrofluorometer. Fluorescence emission spectra were systematically recorded at 520 nm excitation wavelength at room temperature. All the spectra were corrected from the fluorescence of the corresponding blank (suspension of cells or lipid vesicles without the probe). Fluorescence microscopy experiments were performed by using a home-built two-photon laser scanning set-up based on an Olympus IX70 inverted microscope with an Olympus 60× 1.2NA water immersion objective [31]. Two-photon excitation was provided by a titanium-sapphire laser (Tsunami, Spectra Physics) and photons were detected with Avalanche Photodiodes (APD SPCM-AQR-14-FC, Perkin Elmer) connected to a counter/timer PCI board (PCI6602, National Instrument). Imaging was carried out using two fast galvo mirrors in the descanned fluorescence collection mode. Typical acquisition time was 5 s with an excitation power around 4 mW (λ = 830 nm) at the sample level. Images corresponding to the green and red channels were recorded simultaneously using a dichroic mirror (Beamsplitter 585 DCXR), a density filter 630/30 nm and two APDs. The images were processed with a home-made program under LabView that generates a ratiometric image by dividing the image of the green channel by that of the red channel. For each pixel, a pseudo-color scale is used for coding the ratio, while the intensity is

defined by the integral intensity recorded for both channels at the corresponding pixel. Both spectroscopy and microscopy measurements were performed at 20 °C.

### 2.4. Flow cytometry

Cells treated with an apoptosis-inducing agent were stained using FITC-labeled annexin V and monitored with a BD LSR II flow cytometer. For the validation of NR12S in cell cytometry, we used the same flow cytometer with a blue laser 488 nm excitation laser line with 2 emission filters: yellow channel (PE) and red channel (PE-Texas Red). Data were collected with the BD FACSDiva™ software and analyzed with FlowJo (Flow Cytometer analysis software). For Flow cytometry studies, cells were prepared with the same protocol as for fluorescence spectroscopy analysis, with 0.01 μM final NR12S concentration. 50,000 events were counted per sample to get enough signal.

## 3. Results

### 3.1. Optimization of the staining protocol

Initially, to find optimal conditions at which NR12S probe binds both Lo and Ld phases and distinguishes them by emission color, we used model vesicles of different lipid compositions. Lipid vesicles composed of DOPC or DOPC/cholesterol (2/1, molar ratio) represented Ld phase [10,37,38], those composed of SM/cholesterol (2/1) — Lo phase [39], while those composed of ternary mixture DOPC/SM/cholesterol (1/1/1) — mixture of Lo and Ld phases [10,37,38].

Being non-fluorescent in water NR12S binds all the types of lipid vesicles at room temperature showing efficient fluorescence [31]. Titrations of LUVs with NR12S show that the fluorescence intensity of NR12S grows with the probe concentration and reaches a plateau around 2 μM (Fig. 2A), which corresponds to a probe/lipid ratio of 1/100 (~1/50 taking into account only the outer membrane leaflet). Partitioning of the probe into the membranes at higher probe/lipid ratio is probably energetically not favorable, as it would disturb the lipid bilayer structure. Moreover, at high probe concentration, self-quenching phenomenon should take please, which is an additional explanation for the observed saturation of the fluorescence intensity. Integral intensity of NR12S is higher in DOPC and DOPC/Chol vesicles compared to SM/Chol, probably because of the higher affinity of the probe for the disordered Ld phase, as compared to the ordered Lo phase. The higher lipid order of Lo phase probably decreases the partitioning of the probe into the membrane, as commonly observed for other membrane probes [40]. Moreover, the position of the emission maximum of NR12S in all types of lipids is red-shifted with the increase in its concentration (Fig. 2B). This red shift indicates that at higher concentrations, the probe molecules experience higher environment polarity and hydration in the lipid membranes. We can speculate that at higher probe/lipid ratios the probe molecules cannot localize at the same depth in the membrane (compared to low probe/lipid ratios), because they would disturb the lipid bilayer, and therefore may incorporate shallower at the membrane surface. Thus, the probe should be used at the lowest concentration possible in order to prevent saturation of the membranes with the probe, corresponding to its less defined shallow localization at the interface. Importantly, in the ternary lipid mixture, the probe shows intermediate fluorescence intensities (Fig. 2A) and position of the emission maximum (Fig. 2B), indicating that it binds both Lo and Ld phases, in line with our previous imaging data in GUVs [31]. However, both the intensity and the position of the maximum are much closer to those of the Ld phase, confirming the higher affinity of the probe for this phase. Interestingly, at higher probe concentrations, the observed emission maximum in ternary mixtures is almost an average of the positions in Ld and Lo phases, confirming that at higher concentrations, NR12S incorporates shallower into the membrane and thus stains almost equally both phases.

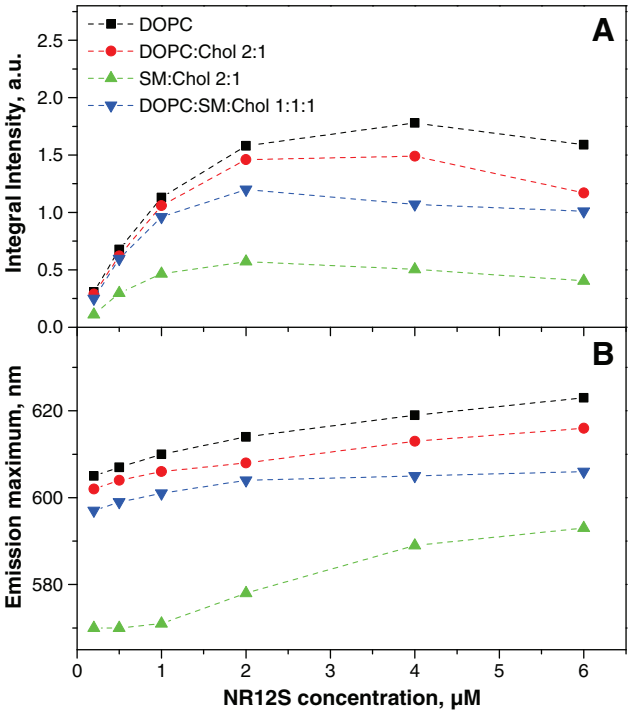


**Fig. 2.** Fluorescence of NR12S in different types of lipid vesicles. Integral fluorescence intensity (A) and position of the emission maximum (B) of NR12S at different concentrations in lipid vesicles of different compositions (200 μM lipid in phosphate buffer 20 mM, pH 7.4).

Similar titration experiments were performed in HeLa cells. Similarly to the model vesicles, the emission maximum shows an intensity saturation profile and a significant red-shift on increase in the dye concentration (Fig. S1). The red-shift is observed at lower probe concentration than in model vesicles, indicating that saturation of the plasma membranes with the probe is faster. The difference between cells and vesicles can be explained by the lower lipid concentration in cell suspensions compared to lipid vesicles. Assuming that the volume of HeLa cells is $2.6\times10^3$ μm$^3$ [41], the average area per lipid at the plasma membrane is 0.7 nm$^2$ (0.62 nm$^2$ for dipalmitoylphosphatidylcholine [42] and 0.72 nm$^2$ for dioleoylphosphatidylcholine [43]), the cells are of spherical shape in the suspension and the lipids occupy 100% of their plasma membrane surface, we can estimate that ~$1.3\times10^9$ lipid molecules are present at the outer membrane leaflet of a single HeLa cell. As the cellular concentration in our experiments is $10^6$ cells/mL, concentration of the lipids at the outer leaflet of HeLa cells in the suspension is ~2.2 μM. This value is slightly overestimated as some part of the plasma membrane surface is taken by the membrane proteins. Nevertheless, this rough estimation explains why at very low NR12S concentrations, 10–20 nM, corresponding to probe/lipid ratio 1/220-1/110, the emission spectrum of NR12S is independent of its concentration (Fig. S1).

It was also found that at relatively high concentrations of NR12S, the probe shows some phototoxicity (Fig. S2). Indeed, at 0.2 μM of NR12S, after 30 s of exposition to light (530 nm) under an epi-fluorescence microscope, HeLa cells showed dramatic changes in their morphology — formation of bubbles within minutes followed by cell detachment from the surface (Fig. S2B). In contrast, at 10–20 nM NR12S showed no detectable phototoxicity (Fig. S2D). Thus, the cellular studies suggest that, the probe should be used at rather low concentrations (10–20 nM) in order to avoid artifacts related to excessive binding and photo-toxicity.

### 3.2. Spectroscopic effects of lipid order and apoptosis

Emission spectra of NR12S were recorded in living cells at the optimized low probe concentration (Fig. 3) and compared to those in lipid vesicles of different phases. Interestingly, the position of the

maximum in both HeLa and U87MG cells was found to be close to that of lipid vesicles in Lo phase and to significantly differ from the emission maximum of the ternary mixtures. Thus, the latter cannot really model the situation in live cells, as was already noticed with the ratiometric probe F2N12S [25].

To get further insight in the probe response to the lipid order of the plasma membrane, the latter was modified by three different methods: (1) cholesterol extraction by methyl-β-cyclodextrin [44], (2) cholesterol oxidation into cholest-5-en-3-one by cholesterol oxidase [45] and (3) sphingomyelin cleavage into ceramide by sphingomyelinase (SMase) [46]. In the first approach the cells were incubated with 5 mM methyl-β-cyclodextrin for 2 h, which according to previous studies extracts 60 and 90% of the plasma membrane cholesterol from CHO [47] and aortic endothelial cells [48], respectively [24]. In the second approach, the cholesterol was oxidized using 2 U/mL of cholesterol oxidase for 2 h. These conditions gave about 70% of cholesterol oxidation according to previous data in CHO cells [49]. In the third approach, the cells were incubated for 2 h with 0.2 U/mL of SMase. Previous studies on Jurkart cells suggested that at these conditions SM content decreases by 70% and did not change significantly for longer incubation times [15]. In our experiments with HeLa cells, all three treatments produced minor changes in the cell morphology (sometimes cell membranes appeared smoother) without their detachment from the surface (data not shown). All three cell treatments shifted the emission spectrum of NR12S to the red, with the strongest shift being observed with methyl-β-cyclodextrin (Fig. 4A). The red shift of NR12S probe indicates increase in the polarity/hydration of the probe environment, which based on the previous studies [31] suggests a decrease in the lipid order (fraction of the Lo phase) after all three treatments. To quantitatively analyze the spectral changes of the probe, the emission spectrum was split at 585 nm in two parts, to calculate the ratio of areas of the green to red regions of the spectra. This approach was found to be quite sensitive, since methyl-β-cyclodextrin was found to decrease this ratio by a factor close to 2 (Fig. 4C).

Next, apoptosis was induced in HeLa cells by three different agents, actinomycin D, camptothecin, staurosporine, acting by different mechanisms. Indeed, actinomycin D inhibits DNA replication and RNA transcription [50], camptothecin inhibits the DNA topoisomerase I [51], while staurosporine is a protein kinase inhibitor [52]. After incubation with these apoptosis agents, we stained cell membranes with NR12S, and emission spectra were measured. For all three agents, the emission maximum of NR12S spectra shifted to the red (Fig. 4B), so that the probe detects apoptosis independently from the type of apoptosis agent and its mechanism of action. Remarkably, the response is similar to that observed for the decrease in the Lo phase in model and cell membranes. Quantitative ratiometric analysis further shows that the probe response is comparable for the three agents and close to that observed with methyl-β-cyclodextrin, cholesterol oxidase and SMase (Fig. 4C). The obtained results suggest that apoptosis likely decreases the Lo phase at the outer leaflet. This conclusion is supported by the previously observed increased hydration [25], increased interlipid spacing [20] and decreased lipid packing [19], evidenced by other membrane probes. These drastic changes in the plasma membrane of the apoptotic cells are likely connected with the loss of

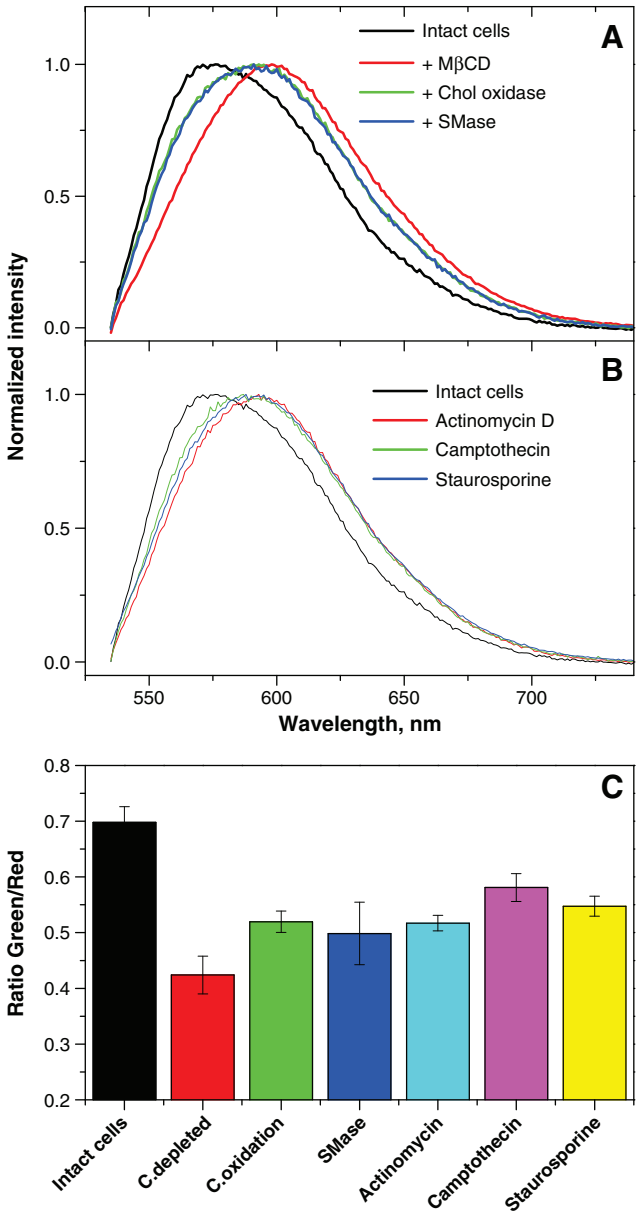


**Fig. 4.** Normalized fluorescence spectra of 0.01 μM NR12S in HeLa cells. (A) Intact cells (black line), cholesterol depleted cells with methyl-β-cyclodextrin 5 mM for 2 h at 37 °C (red line), cholesterol (Chol) oxidase treated cells 2 U/mL for 2 h (green line), and SMase treated cells 0.2 U/mL for 2 h (blue line). (B) Cells treated with different apoptosis agents: intact cells (black line), actinomycin D 0.5 μg/mL (red line), camptothecin 5 μg/mL (green line) and staurosporine 0.1 μM (blue line) treated cells at 37 °C. (C) Ratiometric response of NR12S probe (green/red intensity ratio) to modification of the lipid composition in cell membrane and to apoptosis induction.

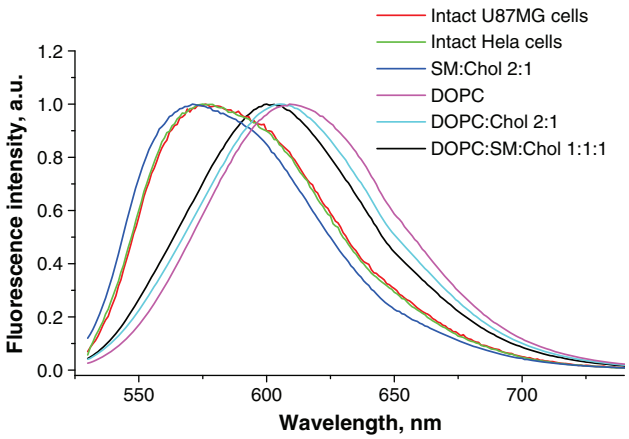


**Fig. 3.** Normalized fluorescence spectra of NR12S in cells and model membranes. NR12S concentration was 0.5 μM in lipid vesicles and 0.01 μM in living cells. 200 μM lipids in phosphate buffer 20 mM, pH 7.4 or $10^6$ cells/ml in HBSS buffer were used.

the transmembrane asymmetry, so that the outer leaflet probed by NR12S becomes less rich in sphingolipids [15,16].

### 3.3. Ratiometric imaging with NR12S

Two-color ratiometric imaging was performed using two-photon microscopy. In line with our previous studies [31], the obtained images show that the probe stains exclusively the cell membrane with a uniform fluorescence intensity ratio (Fig. 5). It can be seen from the ratiometric images of untreated cells (Fig. 5A) that the green/red intensity ratio is high, in corroboration with the spectroscopic data (Fig. 3). In contrast, in cells treated with methyl-β-cyclodextrin (Fig. 5B), we observed a decrease of the ratio, related to the shift of NR12S spectrum to the red (Fig. 4A) [31]. In apoptotic cells treated with actinomycin D (Fig. 5C), the green/red ratio was also decreased, similarly to the effect of cholesterol extraction. Moreover, dramatic changes in the morphology were observed for apoptotic cells, such as formation of bubbles and detachment from the surface. Thus, in line with the spectroscopic observations, the NR12S ratiometric imaging shows that apoptosis leads to drastic changes in the lipid order, which is associated with changes in the cell morphology [15,53].

### 3.4. NR12S versus annexin V-FITC in flow cytometry

Fluorescently labeled annexin V is known as a major tool for discriminating apoptotic from living cells by flow cytometry [5,35]. Thus, our next step was to validate NR12S as an alternative tool in this application. To this end, Hela cells were treated with actinomycin D, camptothecin or staurosporine. For each condition, cells were split into two samples; one labeled with FITC-annexin V and the second one, labeled with NR12S. As annexin V stains only apoptotic cells, non-treated intact cells appear essentially as a single population with low FITC fluorescence intensity (Fig. 6A). In contrast, cells treated with any of the three apoptosis-inducing agents exhibit a second population with high FITC signal (Fig. 6B–D). The combined population of apoptotic and dead cells was 44, 22 and 22% of total cells (Fig S3B), for actinomycin D, camptothecin and staurosporine, respectively.

Flow cytometry data of NR12S-labeled cells are presented in a bi-parametric form: red channel versus green channel (Fig. 6E–H). While mainly one population was observed with intact cells, two distinct populations were observed when apoptosis was induced. The new population, which exhibits a lower green/red ratio can be readily assigned to the combined population of apoptotic and dead cells, similarly to color changes observed from spectroscopy and microscopy data. Remarkably, the new population represented 47, 22 and 21% of total cells for actinomycin D, camptothecin and staurosporine, respectively, in good accordance with the FITC-Annexin V data (Fig. S3B). Thus, the response of NR12S to apoptosis correlates well with the response of fluorescently labeled annexin V assay, so that NR12S could be used as for apoptosis detection by flow cytometry. The advantage of this probe with respect to Annexin V is the much simpler and faster protocol of cell staining. This dye could also be compared to F2N12S, a recently developed ratiometric probe of the 3-hydroxychromone family [21]. The advantage of NR12S is its red-shifted absorption and emission so that it can be used at significantly lower concentrations (10 nM) due to the lower contribution of cell auto-fluorescence at these wavelengths. Compared to merocyanine 540 [17,18], NR12S can be used at >1000 times lower concentrations (10–20 nM NR12S vs 30 μM merocyanine 540 [18]) and its response to apoptosis is ratiometric (i.e. color response) in contrast to the intensiometric response of merocyanine 540.

## 4. Conclusions

A recently developed fluorescent membrane probe NR12S based on Nile Red was applied to monitor changes in the lipid order at the outer leaflet of cell plasma membranes. This probe changes its emission color in response to lipid order (liquid ordered vs. liquid disordered phase) and can be used at concentrations as low as 10 nM. We showed that cholesterol extraction and oxidation as well as sphingomyelin hydrolysis produce a red-shift in the emission spectrum of NR12S, indicating that the probe can sense the decrease in the lipid order at the outer plasma membrane leaflet. Remarkably, apoptosis induced by three different agents (actinomycin D, camptothecin, staurosporine) produced very similar spectroscopic effects, suggesting that apoptosis also significantly decreases the lipid order at this leaflet. The loss of lipid order on apoptosis is probably connected with sphingomyelin hydrolysis and lipid scrambling at its executive step, leading to a flux of sphingomyelin/ceramide from the outer to the inner leaflet [15,16]. The applicability of NR12S to detect apoptosis was validated using also fluorescence microscopy and flow cytometry, where the signal was recorded as a ratio between the blue and red parts of its emission band. Thus, using the recently developed NR12S probe, we show a connection between apoptosis and the decrease in the lipid order at the outer plasma membrane leaflet, which suggests a new concept in apoptosis detection based on environment-sensitive dyes.

## Acknowledgements

This work was supported by ANR JCJC (ANR-11-JS07-014-01). Financial support of ZD from CNRS and Region Alsace is acknowledged. We thank D. Dujardin and R. Vauchelles from PIQ imaging platform for the help with fluorescence imaging.

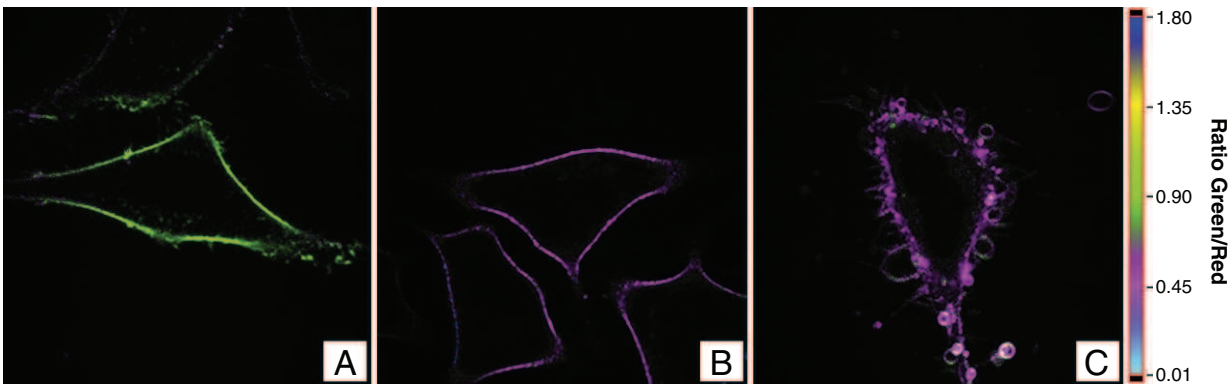


**Fig. 5.** Fluorescence ratiometric images of HeLa cells stained with NR12S. (A) Intact cells (B) cholesterol-depleted cells with 5 mM MβCD for 2 h at 37 °C (C) apoptotic cells treated with 0.5 μg/mL actinomycine D for 18 h at 37 °C. NR12S concentration was 0.05 μM.

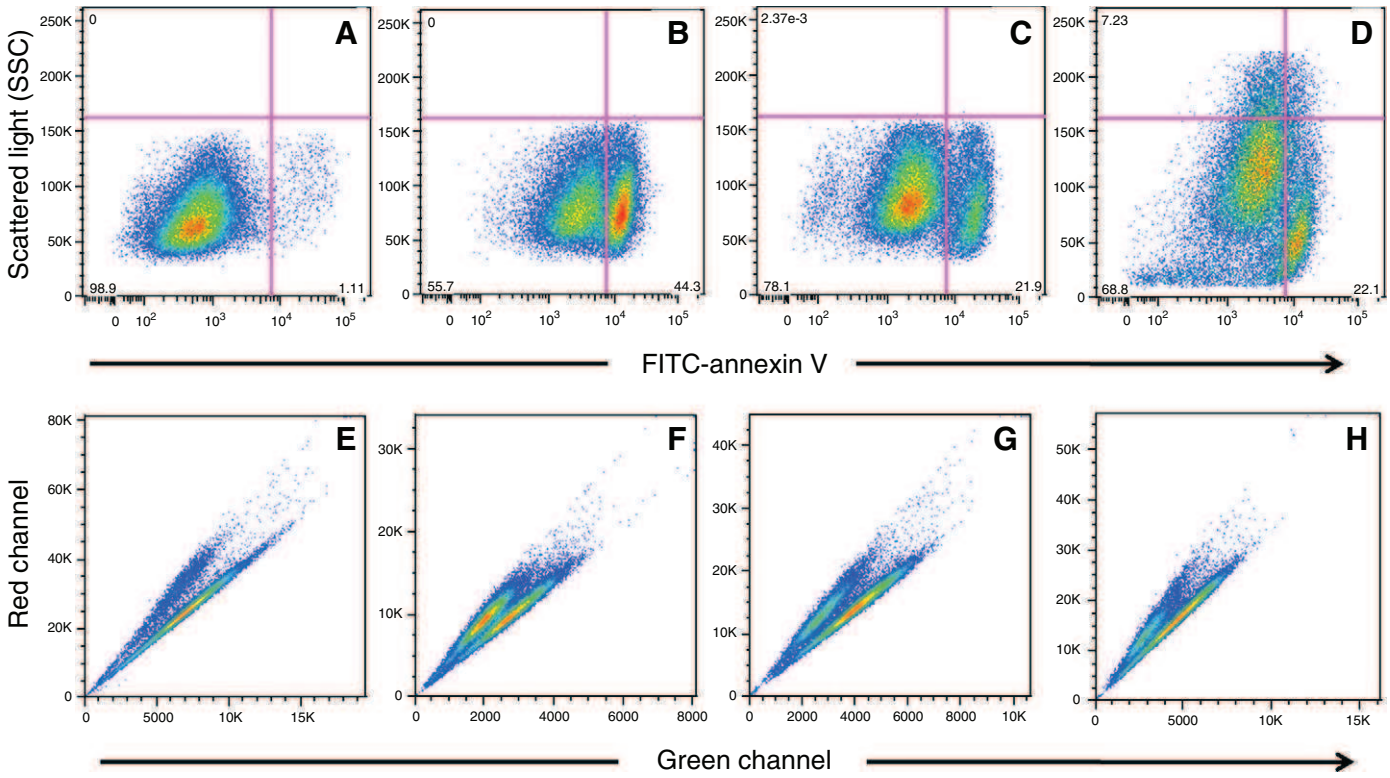


**Fig. 6.** Flow cytometry data for intact and apoptotic HeLa cells using FITC-annexin V (A–D) and NR12S probe (E–H). (A,E) Intact cells (B,F) actinomycin D treated cells (C,G) camptothecin treated cells and (D,H) staurosporine treated cells. Cells treated with apoptosis agents showed two populations: intact cells with low FITC signal, and apoptotic cells with high FITC signal. For NR12S (0.01 μM), the fluorescence intensity of green channel (x axis) and red channel (y axis) was represented. Cells treated with apoptosis agents show two populations differing by the ratio of their intensities in the green and red channels: intact cells with high green/red ratios and apoptotic + dead cells with low green/red ratios.

## Appendix A. Supplementary data

Supplementary data to this article can be found online at doi:10.1016/j.bbamem.2012.07.017.

## References

[1] G. Van Meer, Lipid traffic in animal cells, Ann. Rev. Cell Biol. 5 (1989) 247–275.
[2] R.F.A. Zwaal, A.J. Schroit, Pathophysiologic implications of membrane phospholipid asymmetry in blood cells, Blood 89 (1997) 1121.
[3] B. Fadeel, D. Xue, The ins and outs of phospholipid asymmetry in the plasma membrane: roles in health and disease, Crit. Rev. Biochem. Mol. Biol. 44 (2009) 264–277.
[4] V.A. Fadok, D.R. Voelker, P.A. Campbell, J.J. Cohen, D.L. Bratton, P.M. Henson, Exposure of phosphatidylserine on the surface of apoptotic lymphocytes triggers specific recognition and removal by macrophages, J. Immunol. 148 (1992) 2207–2216.
[5] I. Vermes, C. Haanen, H. Steffens-Nakken, C. Reutelingsperger, A novel assay for apoptosis. Flow cytometric detection of phosphatidylserine expression on early apoptotic cells using fluorescein labelled annexin V, J. Immunol. Methods 184 (1995) 39–51.
[6] R.G. Hanshaw, B.D. Smith, New reagents for phosphatidylserine recognition and detection of apoptosis, Bioorg. Med. Chem. 13 (2005) 5035–5042.
[7] L. Quinti, R. Weissleder, C.H. Tung, A fluorescent nanosensor for apoptotic cells, Nano Lett. 6 (2006) 488–490.
[8] E. Kimura, S. Aoki, E. Kikuta, T. Koike, A macrocyclic zinc(II) fluorophore as a detector of apoptosis, Proc. Natl. Acad. Sci. U. S. A. 100 (2003) 3731–3736.
[9] D.A. Brown, E. London, Structure and function of sphingolipid- and cholesterol-rich membrane rafts, J. Biol. Chem. 275 (2000) 17221.
[10] C. Dietrich, L.A. Bagatolli, Z.N. Volovyk, N.L. Thompson, M. Levi, K. Jacobson, E. Gratton, Lipid rafts reconstituted in model membranes, Biophys. J. 80 (2001) 1417.
[11] K. Simons, E. Ikonen, Functional rafts in cell membranes, Nature 387 (1997) 569.
[12] K. Jacobson, O.G. Mouritsen, R.G.W. Anderson, Lipid rafts: at a crossroad between cell biology and physics, Nat. Cell Biol. 9 (2007) 7–14.
[13] D. Lingwood, K. Simons, Lipid rafts as a membrane-organizing principle, Science 327 (2010) 46–50.
[14] K. Simons, D. Toomre, Lipid rafts and signal transduction, Nat. Rev. Mol. Cell Biol. 1 (2000) 31–39.
[15] A.D. Tepper, P. Ruurs, T. Wiedmer, P.J. Sims, J. Borst, W.J. Van Blitterswijk, Sphingomyelin hydrolysis to ceramide during the execution phase of apoptosis results from phospholipid scrambling and alters cell-surface morphology, J. Cell Biol. 150 (2000) 155–164.
[16] N. Andrieu-Abadie, T. Levade, Sphingomyelin hydrolysis during apoptosis, Biochim. Biophys. Acta 1585 (2002) 126–134.
[17] R.A. Schlegel, M. Stevens, K. Lumley-Sapanski, P. Williamson, Altered lipid packing identifies apoptotic thymocytes, Immunol. Lett. 36 (1993) 283–288.
[18] T. Laakko, L. King, P. Fraker, Versatility of merocyanine 540 for the flow cytometric detection of apoptosis in human and murine cells, J. Immunol. Methods 261 (2002) 129–139.
[19] J.I. Elliott, A. Sardini, J.C. Cooper, D.R. Alexander, S. Davanture, G. Chimini, C.F. Higgins, Phosphatidylserine exposure in B lymphocytes: a role for lipid packing, Blood 108 (2006) 1611–1617.
[20] R.W. Bailey, T. Nguyen, L. Robertson, E. Gibbons, J. Nelson, R.E. Christensen, J.P. Bell, A.M. Judd, J.D. Bell, Sequence of physical changes to the cell membrane during glucocorticoid-induced apoptosis in S49 lymphoma cells, Biophys. J. 96 (2009) 2709–2718.
[21] V.V. Shynkar, A.S. Klymchenko, C. Kunzelmann, G. Duportail, C.D. Muller, A.P. Demchenko, J.M. Freyssinet, Y. Mely, Fluorescent biomembrane probe for ratiometric detection of apoptosis, J. Am. Chem. Soc. 129 (2007) 2187.
[22] P.-T. Chou, M.L. Martinez, J.H. Clements, Reversal of excitation behavior of proton-transfer vs. charge-transfer by dielectric perturbation of electronic manifolds, J. Phys. Chem. 97 (1993) 2618–2622.
[23] A.S. Klymchenko, A.P. Demchenko, Multiparametric probing of intermolecular interactions with fluorescent dye exhibiting excited state intramolecular proton transfer, Phys. Chem. Chem. Phys. 5 (2003) 461–468.
[24] A.P. Demchenko, Y. Mély, G. Duportail, A.S. Klymchenko, Monitoring biophysical properties of lipid membranes by environment-sensitive fluorescent probes, Biophys. J. 96 (2009) 3461–3470.
[25] S. Oncul, A.S. Klymchenko, O.A. Kucherak, A.P. Demchenko, S. Martin, M. Dontenwill, Y. Arntz, P. Didier, G. Duportail, Y. Mely, Liquid ordered phase in cell membranes evidenced by a hydration-sensitive probe: effects of cholesterol depletion and apoptosis, Biochim. Biophys. Acta 1798 (2010) 1436–1443.
[26] G. M'Baye, Y. Mély, G. Duportail, A.S. Klymchenko, Liquid ordered and gel phases of lipid bilayers: fluorescent probes reveal close fluidity but different hydration, Biophys. J. 95 (2008) 1217–1225.
[27] L.A. Bagatolli, To see or not to see: lateral organization of biological membranes and fluorescence microscopy, Biochim. Biophys. Acta 1758 (2006) 1541–1556.

[28] L. Jin, A.C. Millard, J.P. Wuskell, H.A. Clark, L.M. Loew, Cholesterol-enriched lipid domains can be visualized by di-4-ANEPPDHQ with linear and nonlinear optics, Biophys. J. 89 (2005) L4–L6.
[29] D.M. Owen, C. Rentero, A. Magenau, A. Abu-Siniyeh, K. Gaus, Quantitative imaging of membrane lipid order in cells and organisms, Nat. Protoc. 7 (2011) 24–35.
[30] A.S. Klymchenko, S. Oncul, P. Didier, E. Schaub, L. Bagatolli, G. Duportail, Y. Mély, Visualization of lipid domains in giant unilamellar vesicles using an environment-sensitive membrane probe based on 3-hydroxyflavone, Biochim. Biophys. Acta 1788 (2009) 495–499.
[31] O.A. Kucherak, S. Oncul, Z. Darwich, D.A. Yushchenko, Y. Arntz, P. Didier, Y. Mely, A.S. Klymchenko, Switchable nile red-based probe for cholesterol and lipid order at the outer leaflet of biomembranes, J. Am. Chem. Soc. 132 (2010) 4907.
[32] P. Greenspan, E.P. Mayer, S.D. Fowler, Nile red: a selective fluorescent stain for intracellular lipid droplets, J. Cell Biol. 100 (1985) 965–973.
[33] S. Chiantia, A.S. Klymchenko, E. London, A novel leaflet-selective fluorescence labeling technique reveals differences between inner and outer leaflets at high bilayer curvature, Biochim. Biophys. Acta 1818 (2012) 1284–1290.
[34] S. Chiantia, P. Schwille, A.S. Klymchenko, E. London, Asymmetric GUVs prepared by MβCD-mediated lipid exchange: an FCS study, Biophys. J. 100 (2011) L01–L03.
[35] M. Van Engeland, L.J.W. Nieland, F.C.S. Ramaekers, B. Schutte, C.P.M. Reutelingsperger, Annexin V-affinity assay: a review on an apoptosis detection system based on phosphatidylserine exposure, Cytometry 31 (1998) 1–9.
[36] M.J. Hope, M.B. Bally, G. Webb, P.R. Cullis, Production of large unilamellar vesicles by a rapid extrusion procedure. Characterization of size distribution, trapped volume and ability to maintain a membrane potential, Biochim. Biophys. Acta 812 (1985) 55–65.
[37] S.L. Veatch, S.L. Keller, Organization in lipid membranes containing cholesterol, Phys. Rev. Lett. 89 (2002) 268101.
[38] S.L. Veatch, S.L. Keller, Separation of liquid phases in giant vesicles of ternary mixtures of phospholipids and cholesterol, Biophys. J. 85 (2003) 3074–3083.
[39] M.B. Sankaram, T.E. Thompson, Interaction of cholesterol with various glycerophospholipids and sphingomyelin, Biochemistry 29 (1990) 10670–10675.
[40] T. Baumgart, G. Hunt, E.R. Farkas, W.W. Webb, G.W. Feigenson, Fluorescence probe partitioning between Lo/Ld phases in lipid membranes, Biochim. Biophys. Acta 1768 (2007) 2182–2194.
[41] L. Zhao, C.D. Kroenke, J. Song, D. Piwnica-Worms, J.J. Ackerman, J.J. Neil, Intracellular water-specific MR of microbead-adherent cells: the HeLa cell intracellular water exchange lifetime, NMR Biomed. 21 (2008) 159–164.
[42] J.F. Nagle, Area/lipid of bilayers from NMR, Biophys. J. 64 (1993) 1476–1481.
[43] N. Kučerka, S. Tristram-Nagle, J.F. Nagle, Structure of fully hydrated fluid phase lipid bilayers with monounsaturated chains, J. Membr. Biol. 208 (2006) 193–202.
[44] R. Zidovetzki, I. Levitan, Use of cyclodextrins to manipulate plasma membrane cholesterol content: evidence, misconceptions and control strategies, Biochim. Biophys. Acta 1768 (2007) 1311–1324.
[45] P. Reungpatthanaphong, C. Marbeuf-Gueye, L. Le Moyec, M. Salerno, A. Garnier-Suillerot, Decrease of P-glycoprotein activity in K562/ADR cells by MβCD and filipin and lack of effect induced by cholesterol oxidase indicate that this transporter is not located in rafts, J. Bioenerg. Biomembr. 36 (2004) 533–543.
[46] A.E. Cremesti, F.M. Goni, R. Kolesnick, Role of sphingomyelinase and ceramide in modulating rafts: do biophysical properties determine biologic outcome? FEBS Lett. 531 (2002) 47–53.
[47] V.G. Romanenko, Y. Fang, F. Byfield, A.J. Travis, C.A. Vandenberg, G.H. Rothblat, I. Levitan, Cholesterol sensitivity and lipid raft targeting of Kir2.1 channels, Biophys. J. 87 (2004) 3850–3861.
[48] I. Levitan, A.E. Christian, T.N. Tulenko, G.H. Rothblat, Membrane cholesterol content modulates activation of volume-regulated anion current (VRAC) in bovine endothelial cells, J. Gen. Physiol. 115 (2000) 405–416.
[49] Y. Okamoto, H. Ninomiya, S. Miwa, T. Masaki, Cholesterol oxidation switches the internalization pathway of endothelin receptor type A from caveolae to clathrin-coated pits in Chinese hamster ovary cells, J. Biol. Chem. 275 (2000) 6439–6446.
[50] H.M. Sobell, Actinomycin and DNA transcription, Proc. Natl. Acad. Sci. U. S. A. 82 (1985) 5328–5331.
[51] Y.H. Hsiang, R. Hertzberg, S. Hecht, L.F. Liu, Camptothecin induces protein-linked DNA breaks via mammalian DNA topoisomerase I, J. Biol. Chem. 260 (1985) 14873–14878.
[52] T. Tamaoki, H. Nomoto, I. Takahashi, Staurosporine, a potent inhibitor of phospholipid/Ca++ dependent protein kinase, Biochem. Biophys. Res. Commun. 135 (1986) 397–402.
[53] J.C. Mills, N.L. Stone, J. Erhardt, R.N. Pittman, Apoptotic membrane blebbing is regulated by myosin light chain phosphorylation, J. Cell Biol. 140 (1998) 627–636.

## Monitoring lipid order and maturation of endosomes by NR12S

In this chapter, a new application of a fluorescent membrane probe will be described. Previous experiments of cell staining using membrane fluorescent probes were accomplished at room temperature at short incubation time (minutes), while long term experiments with these probes and specifically with NR12S were never done.

Cell staining with NR12S for long incubation time at 37 °C showed that this probe is internalized and appears as a promising endocytosis marker that can monitor maturation of endosomes and changes of their lipid composition. The probe internalization is inhibited at 4 °C, suggesting that the process is energy-dependent. Our investigations showed that NR12S do not follow a particular endocytosis pathway, because neither chlorpromazine (inhibitor of clathrin-dependent endocytosis), nor methyl-ß-cyclodextrin (inhibitor of caveolin-dependent endocytosis) inhibited completely the internalization of NR12S. NR12S is internalized slower than transferrin which is already in the cytoplasm after 5 min at 37 °C, while these two markers colocalize after 30 min. Moreover, NR12S colocalizes with the marker of lysosomes above 1 h of incubation, with almost no colocalization with the ER-tracker. Remarkably, this long-term internalization is accompanied by a change of the color of our probe which is probably connected to the change of lipid composition. The phenomenon can be explained by the loss of lipid ordered phase in the endosomes, which is in line with the recently suggested decrease of cholesterol content and sphingomyelin hydrolysis during maturation of endosomes. This fundamental decrease of lipid order was observed by organelle fractionation and electron microscopy, but the novelty of our work was the finding of a simple in situ method to follow the change of lipid order in late endosomes and lysosomes.

Furthermore, the internalization of NR12S was compared to FM4-64, the most common fluorescent membrane probe for endocytosis studies. NR12S appears many-fold brighter and its internalization kinetics is slower. These options make it attractive both as a plasma membrane probe and as an endosomal tracker.

Briefly, the Nile red derivative probe NR12S could be described as a “smart” probe of endosomes. Due to its spectroscopic properties, it is able to sense lipid order in cytoplasmic compartments in addition to cell plasma membrane. By this way, a new application of NR12S was developed, in addition to sensing lipid order in cell plasma membrane and apoptosis detection.

The manuscript of an article on this work is presented below.

# Manuscript 3: Lipid order and maturation of endosomes studied by Nile Red-based membrane probe

Zeinab Darwich, Andrey S. Klymchenko,* Denis Dujardin and Yves Mély*

Laboratoire de Biophotonique et Pharmacologie, UMR 7213 CNRS, Université de Strasbourg, Faculté de Pharmacie, 74, Route du Rhin, 67401 ILLKIRCH Cedex, France

* Corresponding authors: tel: +33 368 85 42 55, +33 368 85 42 63; fax: +33 368 85 43 13; e-mail: andrey.klymchenko@unistra.fr; yves.mely@unistra.fr

**Abstract**

During maturation of endosomes, in addition to changes at the protein level and the decrease in pH, changes occur at the level of lipids. In the present work, we show that the loss of cholesterol and the hydrolysis of sphingomyelin resulting in a loss of lipid order in the membranes of late endosomes and lysosomes can be monitored using the environment-sensitive membrane probe NR12S. Cellular internalization studies of this probe in HeLa cells using fluorescence microscopy in presence of endocytosis markers and inhibitors show that this membrane probe can follow different energy-dependent endocytosis pathways and change its color in response to the loss of the lipid ordered phase in late endosomes and lysosomes, which takes place 2 h after its initial binding to cell plasma membranes. In comparison to the common endocytosis marker FM4-64, NR12S is many-fold brighter, its extracellular fluorescence can be switched off by sodium dithionite and it can monitor *in situ* changes in the lipid organization of the endosomes through fluorescence ratiometric microscopy.

**Introduction**

Cell plasma membranes allow the transport of material from the outside to the inside of the cells through endocytosis (Marsh and Helenius 2006), (Mercer, Schelhaas et al. 2010). Many events occur during the endocytosis process, starting by the formation of vesicles called early endosomes, which can be recycled to the cell plasma membrane (Huotari and Helenius 2011), (Steinman, Mellman et al. 1983), or maturate into late endosomes, and then transform into

lysosomes (Canton and Battaglia 2012). It is well-established that endosomes differ by their Rab protein content (Mercer, Schelhaas et al. 2010) and some of them exhibit a gradual change of their internal pH and redox potential (Lafourcade, Sobo et al. 2008). Lysosomes are enriched with lysosomal hydrolases and so have an acid pH with a perinuclear localization (Bucci, Thomsen et al. 2000). In contrast, much less is known about the lipid composition and its changes during these maturation processes.

This problem is of particularly interest since the lipid composition of the plasma membranes differs strongly from that of intracellular compartments (Mobius, van Donselaar et al. 2003). Differences particularly concern cholesterol, which is mainly localized in cell plasma membranes (Yeagle 1985) and is essential to maintain cell viability and normal cell functions. Moreover, cholesterol participates in many membrane-based processes such as vesicle sorting and receptor signaling (Gorin, Gabitova et al. 2012). Cholesterol is mainly synthesized in the endoplasmic reticulum (ER), but it is then delivered to other organelles and the cell plasma membrane, so that the cholesterol content in the ER is low (van Meer, Voelker et al. 2008). Previous reports showed that early endosomes have almost the same composition as the plasma membrane, while after maturation, late endosomes exhibit lower cholesterol content (Kobayashi, Beuchat et al. 2002) due to its extraction by NPC1 and NPC2 proteins (Huotari and Helenius 2011). Remarkably, mutant forms of these proteins cause Niemann-Pick disease, a lysosomal storage disorder in which cholesterol accumulates in late endosomes and endolysosomes (Karten, Peake et al. 2009). Cholesterol extraction from late endosomes is also associated with sphingomyelin (SM) hydrolysis into ceramide (Kolter and Sandhoff 2010). These two lipids are known to interact together in the plasma membrane to form the packed domains of liquid ordered phase, so-called rafts (Simons and Ikonen 1997), playing important biological functions, including cholesterol distribution and transport (Ridgway 2000). Therefore, disappearance of cholesterol and SM from the endosomes may drastically affect the lipid order of the endosomal membranes. Moreover, it was suggested that further conversion of endosomes into lysosomes results in an almost complete loss of cholesterol (Möbius, Van Donselaar et al. 2003).

However, it remains a challenge to monitor in situ the changes of the endosomal membranes during the maturation, because the well-established methods in this field are based on suborganellar fractionation (Kobayashi, Beuchat et al. 2002) or requires cellular fixation for

subsequent electron microscopy or immunofluorescence analysis. To overcome these limitations, a potential approach is to monitor endosomal membranes using membrane probes, as they could directly label plasma membranes and then internalize inside the cells through endocytosis. However, though typical membrane probes, such as FM4-64, can be used as endosomal markers (Bolte, Talbot et al. 2004) , (Hickey, Jacobson et al. 2002), they do not allow monitoring the lipid composition of the endosomes. To reach this goal, our objective was to use a recently developed membrane probe based on Nile Red, NR12S, which binds specifically cell plasma membranes and is highly sensitive to lipid composition (Kucherak, Oncul et al. 2010). Its fluorescence emission senses changes in the lipid order, with a shift toward shorter wavelengths when SM- and cholesterol-rich lipid ordered phase (Lo) is compared to a lipid disordered phase. Moreover, due to its zwitterionic group and long alkyl chain, this probe stains selectively the outer leaflet of cell plasma membranes with very slow flip-flop kinetics even at 37 °C. In the present work, internalization of NR12S probe into live cells was monitored by fluorescence microscopy. Our data show that NR12S can be used not only as an endocytosis marker but also to monitor changes in the lipid order of endosomal membranes. Indeed, late endosomes and lysosomes were found to be characterized by much lower lipid order, compared to plasma membranes, validating the recently proposed decrease in cholesterol content and SM hydrolysis in these compartments.

**Materials and methods**

All chemicals and solvents for synthesis were from Sigma-Aldrich.

**Cell lines, culture conditions and treatment.** HeLa cells were cultured in Dulbecco's modified Eagle medium (D-MEM, high glucose, Invitrogen) supplemented with 10% (v/v) fetal bovine serum (FBS, Lonza), 1% antibiotic solution (penicillin-streptomycin, Invitrogen) in a humidified incubator with 5% $CO_2$ /95% air atmosphere at 37°C.

**Endocytosis studies and NR12S uptake.** Alexa Fluor 488 conjugate of transferrin from human serum, Lysotracker Green DND-26, ER- Tracker Green (BODIPY FL glibenclamide) and FM4-64 probe were from Invitrogen. Chlorpromazine and methyl-ß-cyclodextrin were from Sigma-Aldrich. To follow NR12S uptake, HeLa cells were stained with 0.2 µM NR12S in Opti-MEM for 5, 15, 30 min, 2 h and 4 h at 37 °C, then were visualized under two-photon microscope with or without sodium dithionite. Cells were also incubated with the same concentration of NR12S in Opti-MEM at 4 °C for 2 h and 4 h. Inhibition of NR12S

internalization was performed by pre-incubation of cells for 30 min with chlorpromazine (10µg/mL), then NR12S was added in the presence of this inhibitor for 30 min at 37 °C. Also cells were pre-treated with methyl-β-cyclodextrin (5 mM) for 2 h and then stained with NR12S for 30 min at 37 °C.

For colocalization with transferrin, cells were stained with NR12S for 5 min and then transferrin (20 µg/mL) was added for 5, 30 and 60 min at 37 °C before the measurements. For colocalizations with Lysotracker or ER-tracker, cells were stained with each marker (50 nM for Lysotracker and 0.75 µM for ER-tracker) for 30 min at 37 °C and then with NR12S for 5 min. For 30 min incubation time with NR12S, cells were stained with NR12S together with each marker for 30 min. For longer incubation times, cells were stained with NR12S, then 30 min before observation with the microscope, Lysotracker or ER-tracker was added. To compare the uptake of NR12S to FM4-64, cells were incubated with 1 µM of either NR12S or FM4-64 for 5 min, 30 min and 60 min at 37 °C. After staining, cells were washed gently twice with HBSS (Hank's Buffered Salt Solution) before visualization on the microscope.

**Fluorescence microscopy**

**Two-photon microscopy:** Fluorescence microscopy experiments were performed by using a home-built two-photon laser scanning set-up based on an Olympus IX70 inverted microscope with an Olympus 60x 1.2NA water immersion objective (Clamme, Azoulay et al. 2003). Two-photon excitation was provided by a titanium-sapphire laser (Tsunami, Spectra Physics) and photons were detected with Avalanche Photodiodes (APD SPCM-AQR-14-FC, Perkin Elmer) connected to a counter/timer PCI board (PCI6602, National Instrument). Imaging was carried out using two fast galvo mirrors in the descanned fluorescence collection mode. Typical acquisition time was 5 s with an excitation power around 30 mW ($\lambda$ = 830 nm) at the laser output level. Images corresponding to the blue and red channels were recorded simultaneously using a dichroic mirror (Beamsplitter 585 DCXR), and two APDs. The images were processed with a home-made program under LabView that generates a ratiometric image. This program was used to calculate for each pixel the ratio of the integral intensity of the green region (below 585 nm) to the integral intensity of the red region (above 585 nm) and code it in a pseudo-color scale. The intensity is defined by the integral intensity recorded for both channels at a given pixel. To avoid artifacts, the Green/Red ratio at a given pixel was only calculated when the integral intensity of both regions exceeds a threshold value.

**Confocal microscopy:** Cells were observed using a confocal laser scanning microscope Leica SPE II. The microscope laser configurations generate different excitation wavelengths, among them, 488 and 561 nm were used for Alexa Fluor 488 and NR12S excitations, respectively. Images were acquired with a HXC PL APO 63x/1.40 OIL CS objective and processed with Fiji program.

**Results**

**NR12S internalization and sensitivity to lipid composition** HeLa cells were stained with the Nile Red derivative dye, NR12S for 5 min, 15 min, 30 min, 2 h and 4 h at 37° C. At short incubation times, the fluorescence of the probe was mainly located at the plasma membrane (Fig 1A, C, E). After longer incubation times (≥ 30 min), intracellular fluorescence of NR12S became clearly visible (Fig 1G, I). After 2 h of incubation, this internalization was accompanied by a change in the color (Fig 1G). This color change is related to the change of the ratio of the green to the red regions of NR12S emission spectrum, split close to the middle at 585 nm (Kucherak, Oncul et al. 2010), (Darwich, Klymchenko et al. 2012). Previous work with model vesicles and live cells suggests that this color change corresponds to a decrease in the fraction of the liquid ordered phase in the labeled intracellular compartments. We hypothesized that the internalized probe detects changes in the lipid composition of the endosomal compartments, related to a decrease in the cholesterol and/or sphingomyelin content. An important property of NR12S probe is its ability to be bleached by sodium dithionite ($Na_2S_2O_4$). As this salt is not efficiently internalized in cells, it could be used to bleach exclusively the fluorescence of NR12S in the outer leaflet of the plasma membrane, while preserving the fluorescence in the intracellular compartments (Fig 1B, D, F, H, J). Indeed, it can be seen that after addition of 20 mM sodium dithionite, the fluorescence of NR12S totally disappears at the plasma membrane, so that only fluorescent dots inside the cells could be observed, probably corresponding to endosomes stained with NR12S. The use of dithionite improved thus the visualization of the probe internalization and allowed us to confirm that the change in the emission color of the probe is related to the intracellular compartments.

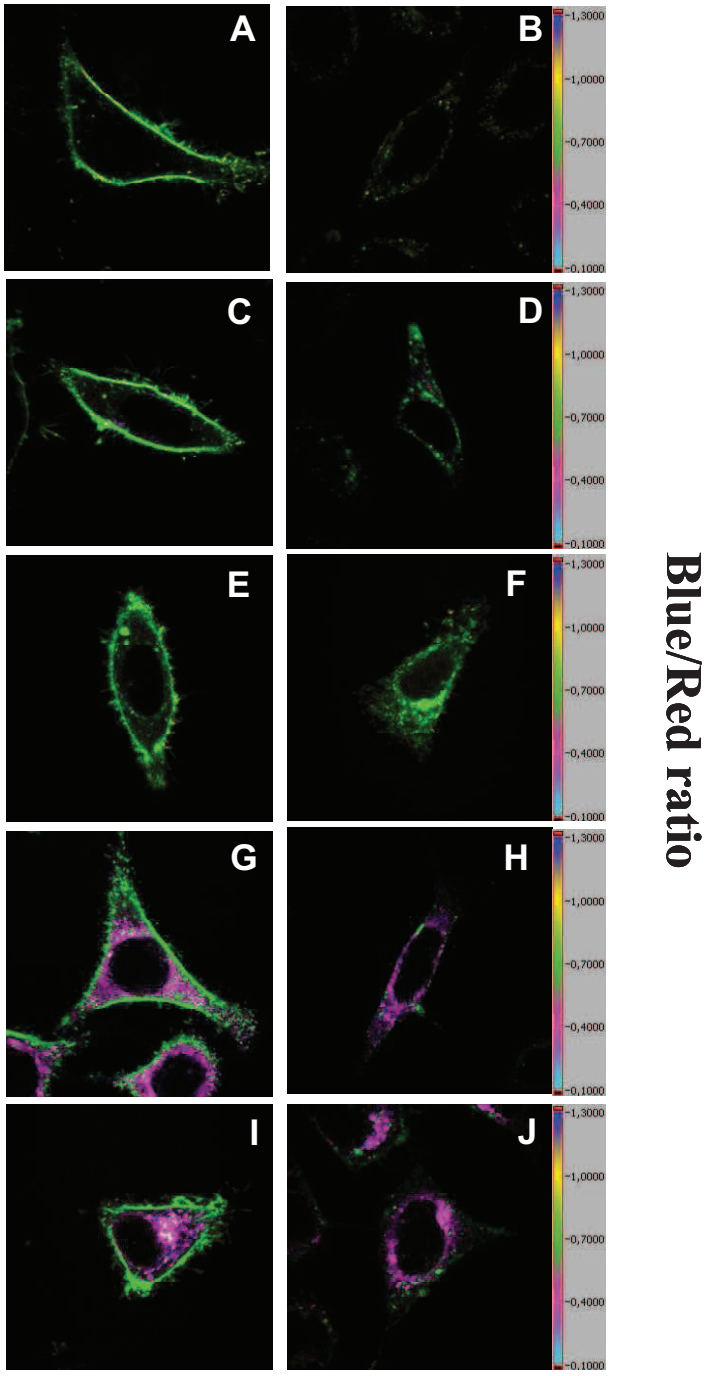


**Figure 1.** Fluorescence imaging of NR12S internalization using two-photon microscopy. Internalization of NR12S after 5 min (A, B), 15 min (C, D), 30 min (E, F), 2 h (G, H) and 4 h (I, J) at 37° C without (left panels) and with 20 mM of sodium dithionite (right panels). The pseudo-color scale corresponds to the ratio of Green/Red regions. The green color coding for a high ratio (0.7) and the pink coding for a low ratio (0.4) correspond to Lo and Ld phases, respectively (JACS 2010). NR12S concentration was 0.2 μM. Two-photon excitation (830 nm) was used. (Kucherak, Oncul et al. 2010).

To confirm that NR12S enters into cells through endocytosis, cells were incubated with NR12S at 4° C, in order to inhibit in large part, the active endocytosis-based transport of molecules through the plasma membrane (Bergen, Kwon et al. 2007), (Faklaris, Joshi et al. 2009). Our fluorescence images using two-photon microscopy show that NR12S remains at the plasma membrane even after 2 and 4 hours of incubation at 4 °C (Figure 2). This observation suggests that at 37 °C, NR12S does marginally diffuse through the cell plasma membrane. Therefore, NR12S is mainly internalized via an energy-dependent pathway at 37°C.

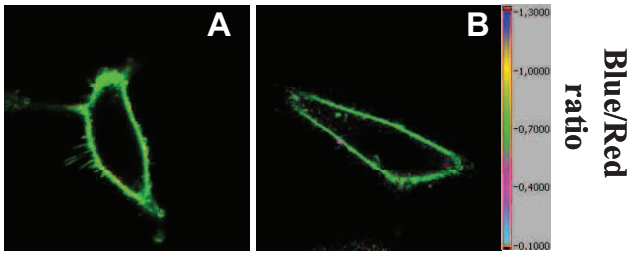


**Figure 2.** Fluorescence images of cells incubated with NR12S at 4 ° C after 2 hours (A), and 4 hours (B). NR12S concentration was 0.2 µM. Two-photon excitation (830 nm) was used.

We further applied different endocytosis inhibitors, i.e. chlorpromazine, and methyl-ß-cyclodextrin, in order to identify the pathway of the endocytotic uptake of NR12S (Figure 3). Chlorpromazine is an inhibitor of clathrin-mediated endocytosis (Hussain, Leong et al. 2010), (Parker, Chitcholtan et al. 2010), while methyl-ß-cyclodextrin extracts cholesterol and thus, mainly inhibits caveolin-associated endocytosis (Subtil, Gaidarov et al. 1999), (Rodal, Skretting et al. 1999). In our experiments, the probes were incubated with the cells for 30 min at 37 °C with and without the corresponding inhibitor. Fluorescence imaging showed that the accumulation of the internalized probe next to nucleus, probably in lysosomes and/or late endosomes (Fig 3A, arrow), disappears after chlorpromazine treatment (Fig 3B), so the internalization of NR12S is probably slowed down by chlorpromazine. Cells treated with methyl-ß-cyclodextrin showed also some internalization of NR12S, after 30 min of incubation (Fig 3C) but also less than in the case of non-treated cells, since patches of internalized probe were also absent. The visible effects of chlorpromazine and methyl-ß-cyclodextrin indicate that NR12S follows at least clathrin- and caveolin-dependent endocytosis. This result was

expected, since this probe binds rather homogeneously to the outer leaflet of the cell plasma membrane, and should thus be present in the different types of endosomes.

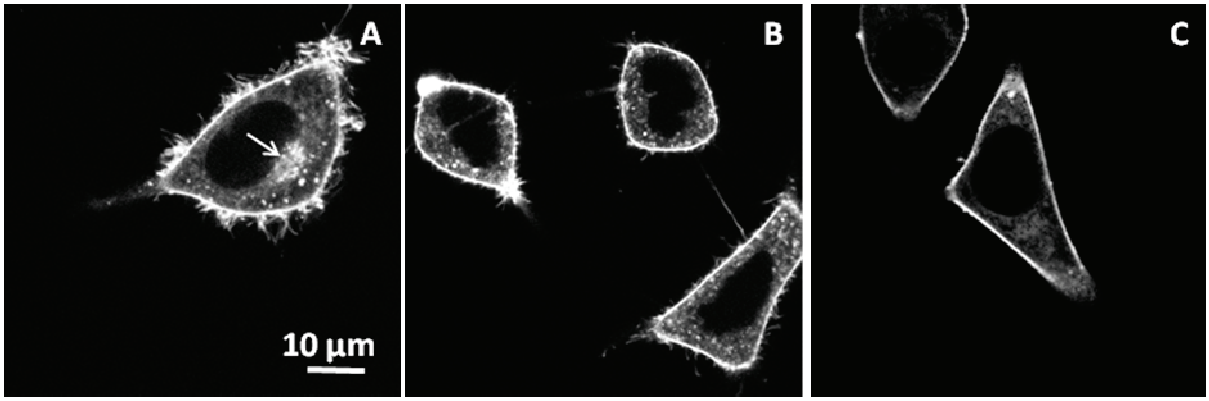


**Figure 3.** Inhibition of NR12S internalization. NR12S alone for 30 min in non-treated cells (A), in presence of Chlorpromazine 10 µg/mL for 30 min (B), or methyl-ß-cyclodextrin 5 mM for 2 h (C). NR12S concentration was 0.05 µM. Arrow shows a patch of internalized NR12S molecules in non-treated cells.

To further characterize the mechanism of NR12S entry in the cells, we analyzed the colocalization between our probe and known endosomal markers. Primarily, we used fluorescently labeled transferrin, which is a marker for clathrin-mediated endocytosis due to receptor-specific binding (Dickson, Hanover et al. 1983) (Ghosh, Gelman et al. 1994). The endocytosis process of NR12S was directly compared with that of transferrin by colocalization experiments in HeLa cells using confocal microscopy. To this end, NR12S and Alexa 488-labeled transferrin were added simultaneously to the cells and imaged after 5, 30 and 60 min incubation. The colocalization between NR12S and transferrin was not clearly seen after 5 min. This is probably related to the strong fluorescence of NR12S in cell plasma membranes, so that the fluorescence of early endosomes is barely detectable (Fig. 4D). Interestingly, a clear colocalization appeared after 30 min and 60 min (Fig. 4H and 4I). This difference with the early incubation time is probably connected with the differences in the staining contrast for these two probes. Indeed, Alexa 488-labeled transferrin internalizes as soon as it binds the receptor at the plasma membrane. In contrast, NR12S stains the whole lipid membrane, so that the newly formed vesicles represent a very small fraction of the probe fluorescence, and thus are less visible. However, after longer incubation time, the fraction of dye accumulated in the endosomes becomes comparable with that at the membrane and

becomes visible. Therefore, we could conclude that NR12S colocalizes well with transferrin, and is thus partly internalized through clathrin-dependent endocytosis, in line with our data using chlorpromazine.

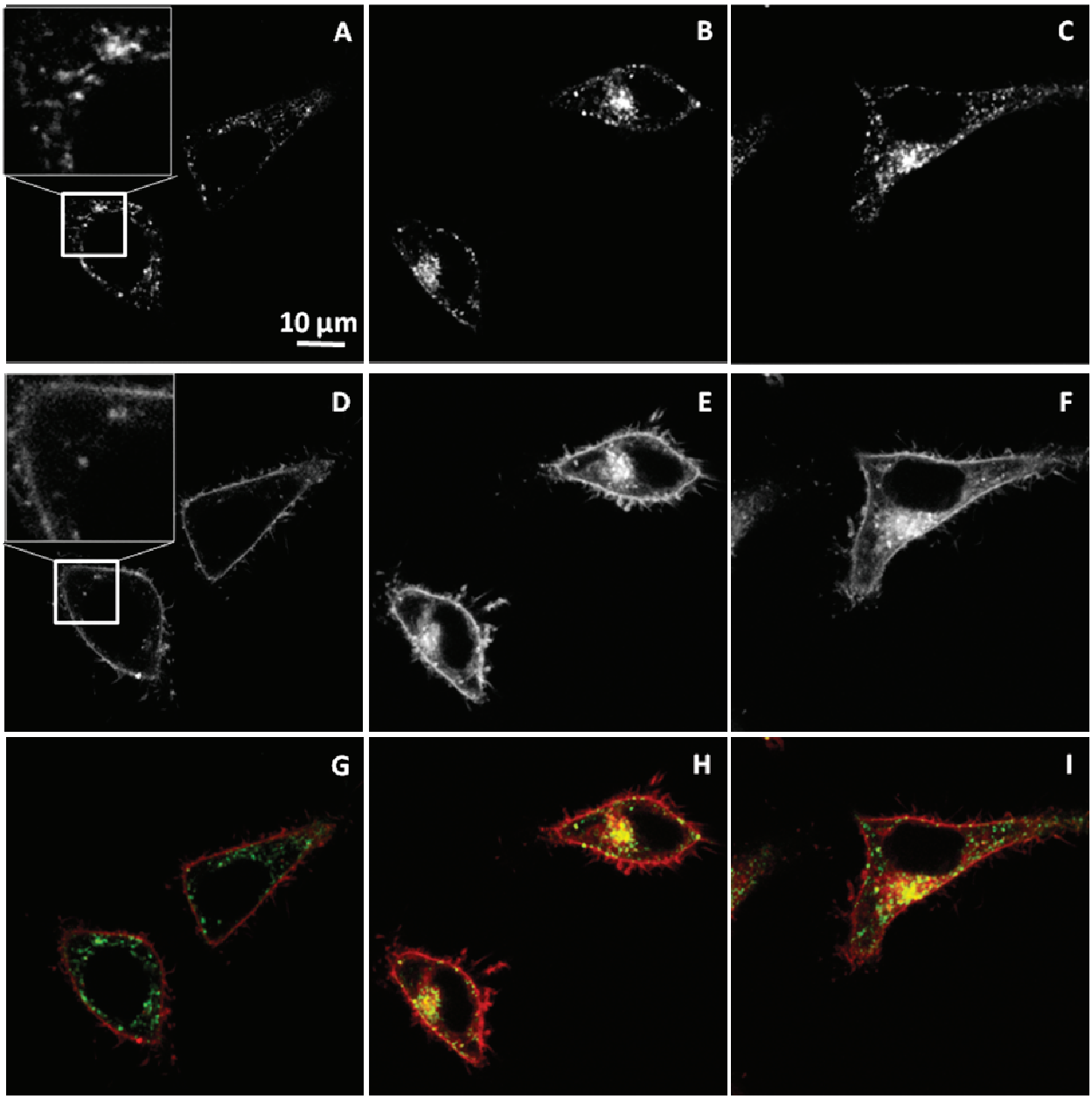


**Figure 4.** Colocalization of NR12S (0.05 µM) with transferrin (20 µg/mL) after 5 min (A, D, G), 30 min (B, E, H), or 60 min (C, F, I). Images corresponding to staining with Alexafluor-488 transferrin (upper panels), NR12S (middle panels) and their merge (bottom panels) are shown.

The fate of NR12S inside the cytoplasm was further monitored by colocalization experiments with lysotracker a marker of lysosomes. Fluorescence confocal images revealed that NR12S

does not colocalize with the lysosome tracker below 30 min of incubation (Fig. 5A, F and K), while their colocalization improves drastically for longer incubation times, so that after 2 h both probes are concentrated close to the nucleus (Fig. 5N and O), where the lysosomes are mainly localised. This observation shows that it takes about 2 h for the dye to go from the plasma membrane up to the lysosome. This time fits well with the described time frame of the endocytosis process, starting from formation of the endosomal vesicle up to its conversion into late endosomes and lysosomes (Möbius, Van Donselaar et al. 2003). Moreover, these results shed light on our two-color imaging data (Fig. 1), where NR12S probe showed changes in its emission ratio also after 2 h of incubation. We can now suggest that the probe evidenced changes in the lipid composition and order in the late endosomes and lysosomes. We could easily exclude an effect of pH, as in control experiments, the fluorescence of NR12S does not change in the pH range between 3.5 and 8.4. Thus, the NR12S probe data suggest that late endosomes and especially lysosomes present a lower fraction of Lo phase as compared to plasma membranes and early endosomes. This observation supports the hypothesis that endosomal compartments lose cholesterol and sphingomyelin during maturation (Möbius, Van Donselaar et al. 2003), (Karten, Peake et al. 2009) (Kolter and Sandhoff 2010).

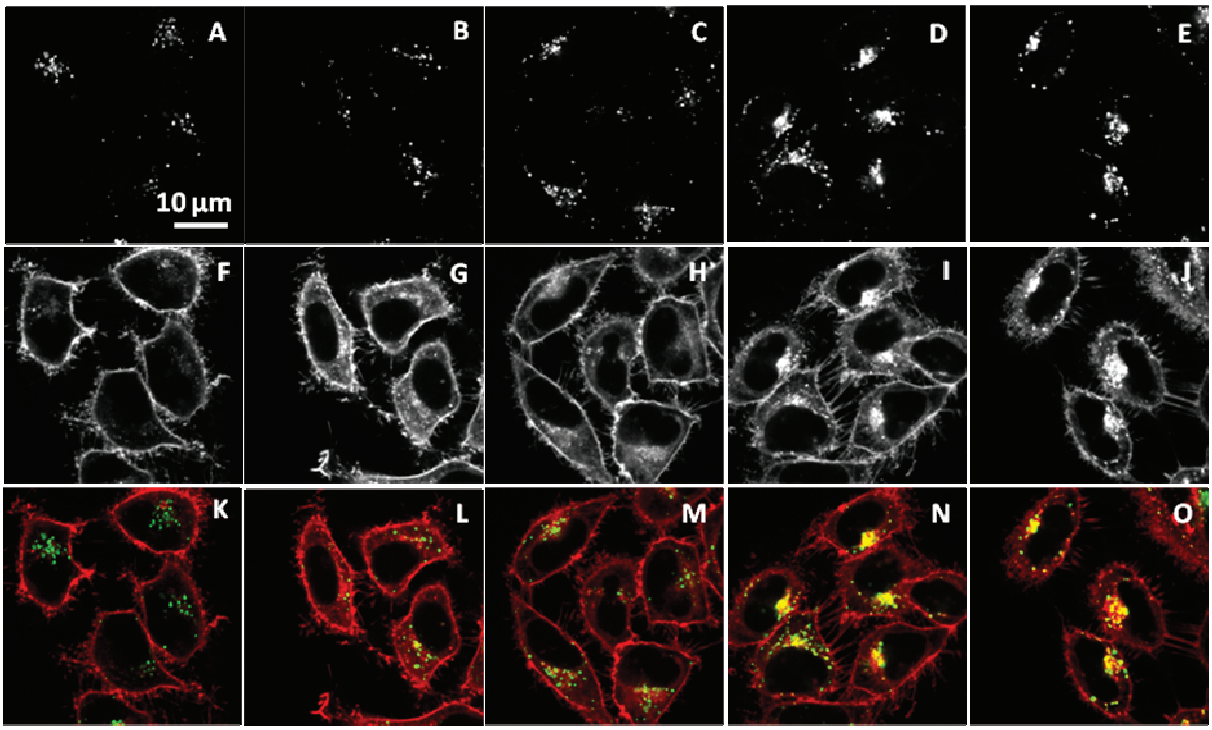

**Figure 5.** Colocalization of NR12S probe with lysotracker (50 nM) after 5 min (A, F and K), 30 min (B, G and L), 1 h (C, H and M), 2 h (D, I and N), and 4 h (E, J and O) of incubation with NR12S (0.05 μM). Images correspond to staining with Alexa488-lysotracker (upper panels), NR12S (middle panels) and their merge (bottom panels).

However, it cannot be excluded that after 2 h, some part of the internalized dye is localized in the ER, where the content of cholesterol and SM is also rather low (Möbius, Van Donselaar et al. 2003), thus explaining the observed decrease in the lipid order. To address this point, colocalization of NR12S with ER marker was further tested. After 5 min (Fig. 6A), the plasma membrane stained by the probe appears in red, while the ER appears separately as green cytoplasmic filaments. After 2h and 4h, NR12S fluorescence is mainly observed either at the membranes or inside the cells in form of dots, while the green staining, corresponding to ER appears in the form of dense filaments (Fig. 6B and 6C). Thus, after 2 and 4h of incubation, the major part of the probe likely remains in the late endosomes and lysosomes with no significant localization within the ER. This could be explained by the fact that NR12S probe stained selectively the outer leaflet of the plasma membrane with no flip-flop (Kucherak, Oncul et al. 2010). Therefore, it gets into the inner leaflet of the endosomes and remains there for all the endosomal lifetime, until it converts into lysosome and/or fuses with the other intracellular compartments. The obtained result also confirms that the changes in the lipid order observed by the probe are related to the endosomal and lysosomal compartments.

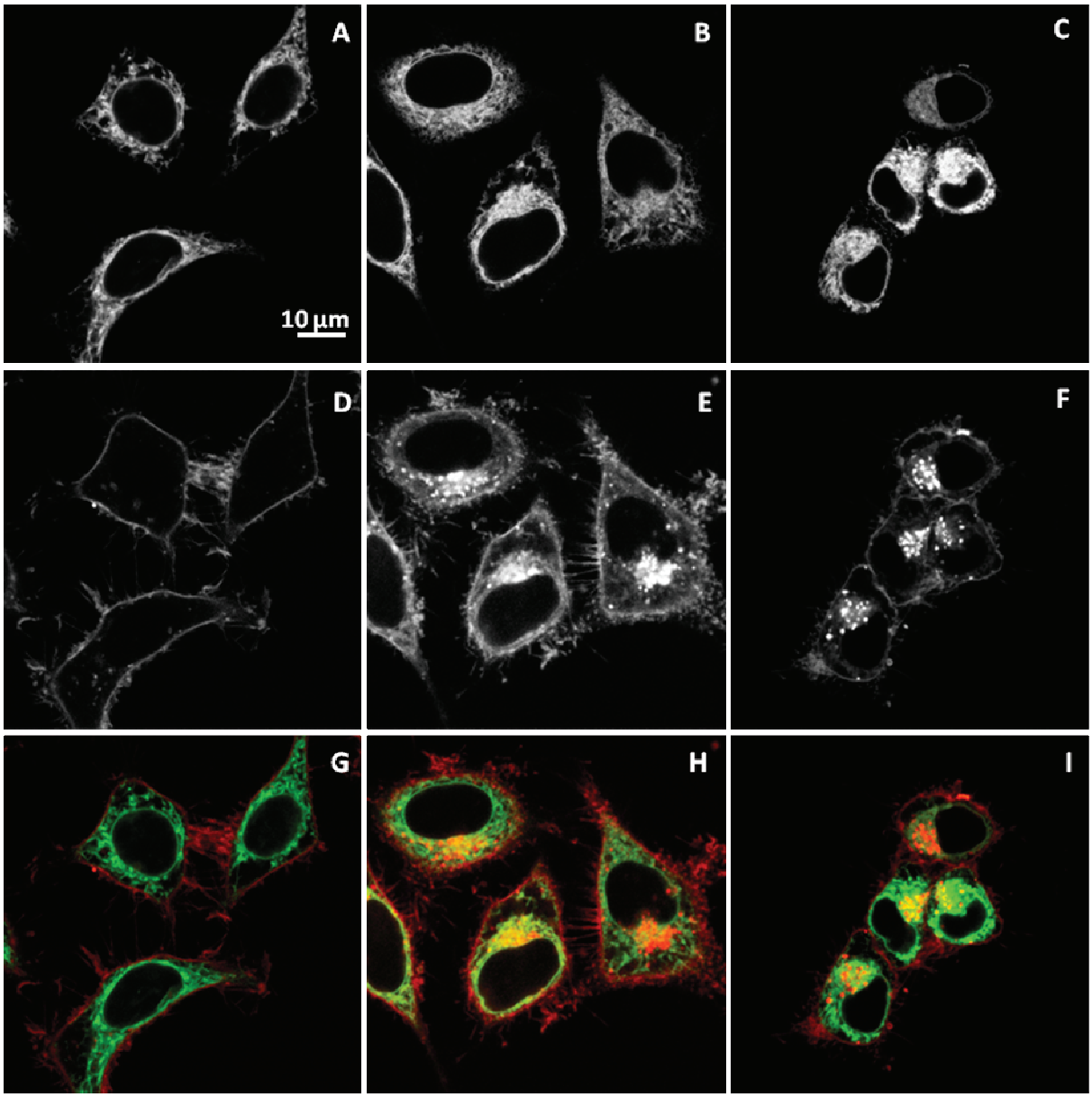


**Figure 6**. Colocalization of NR12S (0.05 µM) with ER-tracker (0.75 µM) after 5 min (A, D and G), 2 h (B, E and H), 4 h (C, F and I). Images correspond to staining with Alexa-488 ER-tracker (upper panels), NR12S (middle panels) and their merge (bottom panels).

As NR12S appears as a "smart" marker of endocytic compartments, which could report on the change in their lipid composition with time, we compared it with FM4-64, one of the most common fluorescent membrane probe used for endocytosis studies. Confocal fluorescence imaging shows that NR12S appears much brighter than FM4-64 (Fig. 7). Therefore, NR12S could be easily used at a concentration as low as 10 nM for fluorescence imaging (Darwich, Klymchenko et al. 2012), while the concentration needed for FM4-64 is 100-fold higher. The

second remarkable difference is that FM4-64 internalizes much faster than NR12S. Indeed, while a large fraction of FM4-64 is already internalized after 5 min, showing even some clusters in the perinuclear region (Fig. 7D, arrow), NR12S is mainly observed at the cell plasma membrane at the same time (Fig. 7A). For better comparison of the internalization of both probes, we compared the number of cells with probe clusters inside the cytoplasm (Fig 7D, arrow). FM4-64 was significantly more internalized after 5 min than NR12S, since 86% of cells show an accumulation of FM4-64 in form of patches in the perinuclear region (42 cells were analyzed for each probe) versus only 19% in the case of NR12S. At longer incubation times, FM4-64 shows almost exclusive intracellular fluorescence (Fig. 7E and F), while NR12S shows both plasma membrane and intracellular staining (Fig. 7B and C). This significant difference between the two membrane probes could be related to differences in their chemical structure. One reason could be the positive charge of FM4-64, which favors faster internalization of the dye compared to the neutral zwitterionic NR12S. Moreover, flip-flop kinetics of FM4-64 is not known, while it was shown that NR12S does not undergo considerable flip-flop for hours in model membranes (Kucherak, Oncul et al. 2010). Finally, we cannot exclude that these probes could redistribute differently at the membrane surface. The positive charge of FM4-64 may favor its binding to lipids and proteins involved in endocytosis, while the neutral NR12S probe redistributes more homogeneously within the plasma membrane. Comparison with FM4-64 shows that NR12S is much brighter and its internalization kinetics is slower. These features make it attractive both as plasma membrane probe and as an endosomal tracker. Moreover, NR12S presents a unique feature of detecting the changes in the lipid composition of the membrane, which allowed us to detect the loss of the lipid order in late endosomes and lysosomes.

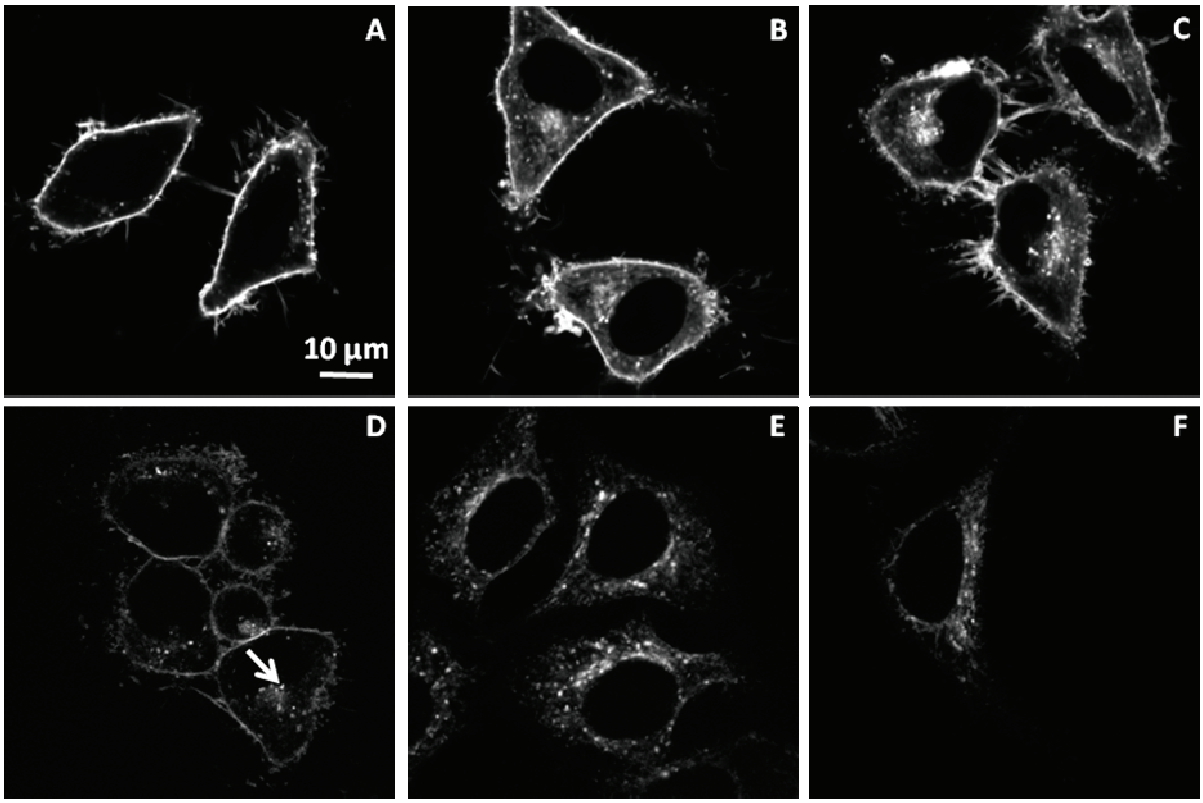


**Figure 7.** Fluorescence images of cell incubated with NR12S (A-C) and FM4-64 (D-F) for 5 min (A, D), 30 min (B, E), and 1 h (C, F) at 37°C. Arrow in Fig D shows the patch of FM4-64 already visible after 5 min in contrast to NR12S. Concentration of probes was 1 µM.

**Conclusions**

Internalization of the membrane probe NR12S, which is sensitive to lipid composition and does not undergo fast flip-flop, was studied in HeLa cells. The probe was found to follow non-specifically several energy-dependent endocytosis pathways and constitute thus, a general marker of endocytosis. Importantly, at long internalization times (≥2 h), the probe localized in late endosomes and lysosomes shows a dramatic change in its emission color, which could be assigned to a decrease in the lipid order of the endosomal membranes connected with cholesterol depletion and sphingomyelin hydrolysis. NR12S constitutes thus, an improved and powerful tool for endocytosis monitoring, because it is very simple to use, very bright, can work at concentrations as low as 10 nM, its extracellular fluorescence can be turned off, and it allows monitoring the change of lipid composition during endosome maturation.

Bergen, J. M., E. J. Kwon, et al. (2007). "Application of an Environmentally Sensitive Fluorophore for Rapid Analysis of the Binding and Internalization Efficiency of Gene Carriers." Bioconjugate **19**(1): 377-384.

Bolte, S., C. Talbot, et al. (2004). "FM-dyes as experimental probes for dissecting vesicle trafficking in living plant cells." Journal of Microscopy **214**(2): 159-173.

Bucci, C., P. Thomsen, et al. (2000). "Rab7: a key to lysosome biogenesis." Mol Biol Cell **11**(2): 467-480.

Canton, I. and G. Battaglia (2012). "Endocytosis at the nanoscale." Chemical Society Reviews **41**(7): 2718-2739.

Clamme, J. P., J. Azoulay, et al. (2003). "Monitoring of the Formation and Dissociation of Polyethylenimine/DNA Complexes by Two Photon Fluorescence Correlation Spectroscopy." Biophysical Journal **84**(3): 1960-1968.

Darwich, Z., A. S. Klymchenko, et al. (2012). "Detection of apoptosis through the lipid order of the outer plasma membrane leaflet." Biochim Biophys Acta.

Dickson, R. B., J. A. Hanover, et al. (1983). "Divergence of epidermal growth factor and transferrin during receptor-mediated endocytosis." Biochemistry **22**(24): 5667-5674.

Faklaris, O., V. Joshi, et al. (2009). "Photoluminescent Diamond Nanoparticles for Cell Labeling: Study of the Uptake Mechanism in Mammalian Cells." ACS Nano **3**(12): 3955-3962.

Ghosh, R. N., D. L. Gelman, et al. (1994). "Quantification of low density lipoprotein and transferrin endocytic sorting HEp2 cells using confocal microscopy." Journal of Cell Science **107**(8): 2177-2189.

Gorin, A., L. Gabitova, et al. (2012). "Regulation of cholesterol biosynthesis and cancer signaling." Curr Opin Pharmacol **21**: 21.

Hickey, P. C., D. J. Jacobson, et al. (2002). "Live-cell imaging of vegetative hyphal fusion in Neurospora crassa." Fungal Genetics and Biology **37**(1): 109-119.

Huotari, J. and A. Helenius (2011). "Endosome maturation." Embo J **30**(17): 3481-3500.

Hussain, K. M., K. L. J. Leong, et al. (2010). "The Essential Role of Clathrin-mediated Endocytosis in the Infectious Entry of Human Enterovirus 71." Journal of Biological Chemistry **286**(1): 309-321.

Karten, B., K. B. Peake, et al. (2009). "Mechanisms and consequences of impaired lipid trafficking in Niemann-Pick type C1-deficient mammalian cells." Biochim Biophys Acta **1791**(7): 659-670.

Kobayashi, T., M.-H. Beuchat, et al. (2002). "Separation and Characterization of Late Endosomal Membrane Domains." Journal of Biological Chemistry **277**(35): 32157-32164.

Kolter, T. and K. Sandhoff (2010). "Lysosomal degradation of membrane lipids." FEBS Lett **584**(9): 1700-1712.

Kucherak, O. A., S. Oncul, et al. (2010). "Switchable Nile Red-Based Probe for Cholesterol and Lipid Order at the Outer Leaflet of Biomembranes." J Am Chem Soc **132**(13): 4907-4916.

Lafourcade, C., K. Sobo, et al. (2008). "Regulation of the V-ATPase along the endocytic pathway occurs through reversible subunit association and membrane localization." PLoS One **3**(7).

Marsh, M. and A. Helenius (2006). "Virus entry: open sesame." Cell **124**(4): 729-740.

Mercer, J., M. Schelhaas, et al. (2010). "Virus Entry by Endocytosis." Annu Rev Biochem **79**(1): 803-833.

Mobius, W., E. van Donselaar, et al. (2003). "Recycling compartments and the internal vesicles of multivesicular bodies harbor most of the cholesterol found in the endocytic pathway." Traffic **4**(4): 222-231.

Möbius, W., E. Van Donselaar, et al. (2003). "Recycling Compartments and the Internal Vesicles of Multivesicular Bodies Harbor Most of the Cholesterol Found in the Endocytic Pathway." Traffic **4**(4): 222-231.

Parker, H., K. Chitcholtan, et al. (2010). "Uptake of Helicobacter pylori Outer Membrane Vesicles by Gastric Epithelial Cells." Infection and Immunity **78**(12): 5054-5061.

Ridgway, N. D. (2000). "Interactions between metabolism and intracellular distribution of cholesterol and sphingomyelin." Biochim Biophys Acta **12**: 2-3.

Rodal, S. K., G. Skretting, et al. (1999). "Extraction of Cholesterol with Methyl-Î²-Cyclodextrin Perturbs Formation of Clathrin-coated Endocytic Vesicles." Molecular Biology of the Cell **10**(4): 961-974.

Simons, K. and E. Ikonen (1997). "Functional rafts in cell membranes." Nature **387**(6633): 569-572.

Steinman, R. M., I. S. Mellman, et al. (1983). "Endocytosis and the recycling of plasma membrane." J Cell Biol **96**(1): 1-27.

Subtil, A., I. Gaidarov, et al. (1999). "Acute cholesterol depletion inhibits clathrin-coated pit budding." Proceedings of the National Academy of Sciences **96**(12): 6775-6780.

van Meer, G., D. R. Voelker, et al. (2008). "Membrane lipids: where they are and how they behave." Nat Rev Mol Cell Biol **9**(2): 112-124.

Yeagle, P. L. (1985). "Cholesterol and the cell membrane." Biochim Biophys Acta **822**(3-4): 267-287.

# *General Conclusions and Perspectives*

The aim of this work was to characterize new fluorescent membrane probes to monitor changes in lipid composition, lipid order and apoptosis. In particular, we were interested in new environment-sensitive molecules belonging to two families of probes: 3-hydroxyflavones and Nile red. This investigation was aimed to characterize new ratiometric membrane probes that overcome some of the drawbacks of the existing ones.

Firstly, a new series of recently designed 3-HF probes was studied. The blue-shifted absorption of these probes allows them to be used with a large range of conventional probes. Moreover these molecules are not phototoxic when applied in cells. A new generation of vertical flavone derivatives of F2N12S was synthesized in the laboratory. One of the new molecules, F66NS was found to be better than F2N12S in term of brightness while the second one, F46NS was better in term of sensibility to the environment.

Secondly, a new Nile red derivative probe, NR12S was described. In contrast to Nile Red, this environment-sensitive probe binds specifically to the plasma membrane. NR12S stays in the outer leaflet of the lipid bilayer and shows a very slow flip-flop to the inner leaflet. Its red-shifted absorption and emission compared to 3HC probes allows working at much lower concentrations, due to lower effect of auto-fluorescence. However, the probe shows some phototoxicity at high concentration, but this can be avoided by using the probe at low concentration. Similarly to 3-HF probes, NR12S shows color response to lipid order in lipid membranes, but in contrast to them it is not sensitive to the surface charge.

Both families of probes were examined first in model systems, such as large unilamellar vesicles for fluorescence spectroscopy and giant unilamellar vesicles for fluorescence microscopy. Then cell plasma membranes were studied.

The two series of probes exhibit several common features particularly interesting for our studies. All characterized probes showed to be:

1- Ratiometric, using the N*/T* ratio and the Green/Red ratio for 3-HF derivatives and NR12S, respectively.

2- Easy to use, allowing fast staining: for all our probes, only a few minutes are enough for a sufficient staining of membranes.

3- Sensitive to the lipid order, since the transition from Lo to Ld phase induces an increase of the N*/T* ratio of 3-HF probes and a decrease of the Green/Red ratio of NR12S. This change in lipid order is detected in biological membranes after extraction of cholesterol, oxidation of cholesterol or hydrolysis of sphingomyelin.

4- Sensitive to apoptosis induction: all studied probes show the same response to apoptosis as after loss of Lo phase and can thus be used as an alternative to the annexin V assay.

Another new application of the membrane fluorescent probe NR12S is monitoring the change of lipid (cholesterol) composition during endocytosis. Indeed, long term experiments on living cells with NR12S at 37°C revealed a change of the color of NR12S in the intracellular compartments. Using endocytosis markers and inhibitors, we showed that our probe was internalized via an energy-dependent, non-specific endocytosis. Thus, the observed change of color reveals a change of lipid composition, likely related to the loss of cholesterol and sphingomyelin hydrolysis occurring during endosome maturation. The novelty of our approach in comparison to other methods (suborganellar fractionation and electron microscopy) is its capacity to monitor the changes in lipid composition (cholesterol and sphingomyelin) directly in living cells. Moreover, comparison of NR12S to another fluorescent membrane probe (FM4-64) used to monitor endocytosis revealed that our probe is much brighter in addition to its ability to sense the lipid membrane properties.

In conclusion, the new developed fluorophores are attractive tools to monitor changes in lipid membranes. These probes are thus potential candidates for a variety of applications related to changes in lipid composition (a) in plasma membranes in the case of short term experiments and (b) during endocytosis for long term experiments with NR12S.

To further extend this work in the future, many perspectives and applications could be proposed. First, several points should be addressed to extend the use of our probes. For instance, our probes could not be used in the presence of serum, probably due to the fact that our probes are retained by the proteins of the serum. This problem may be solved by optimizing the staining and finding a more appropriate protocol. Moreover, efforts need to be done to improve the photostability and phototoxicity of the 3HF and Nile Red probes.

Recently, to observe selective staining of the Lo phase by NR12S, a quencher was synthesized in the laboratory. This quencher based on the black hole quencher 2 (BHQ-2) presents the same zwitterionic group as NR12S but a more steric alkyl chain. Due to its bulky alkyl chain, this inhibitor is thought to quench NR12S in the Ld phase, but not in the Lo phase. Preliminary studies with lipid membrane models (LUVs and GUVs) report promising data on quenching only one phase.

With the aim to visualize lipid rafts in the cell plasma membrane, colocalization of NR12S with cholera toxin was performed. Preliminary results showed that NR12S stains homogeneously the membrane whereas cholera toxin is restricted to membrane domains and is absent in retraction fibers. So, further work is needed to allow direct monitoring of lipid rafts in cell plasma membranes. To validate the raft hypothesis with the help of our probe, FRET experiments could be envisioned using a blue emitting labeled cholera toxin as the donor and NR12S as the acceptor.

In addition to these fundamental applications, the presented probes may also be useful in biomedical applications for monitoring the membrane changes related to several diseases (Maxfield and Tabas 2005). They could also be used to further monitor the role of lipid rafts in prion disease (Taylor and Hooper 2006), Alzheimer's disease (Cordy 2006) and prostate cancer (Freeman et al. 2005).

# *References*

Aggeler, J. and Z. Werb (1982). "Initial events during phagocytosis by macrophages viewed from outside and inside the cell: membrane-particle interactions and clathrin." J Cell Biol **94**(3): 613-623.

Alakoskela, J.-M. I. and P. K. J. Kinnunen (201). "Probing Phospholipid Main Phase Transition by Fluorescence Spectroscopy and a Surface Redox Reaction." The Journal of Physical Chemistry B **105**(45): 11294-11301.

Alnemri, E. S., D. J. Livingston, et al. (1996). "Human ICE/CED-3 protease nomenclature." Cell **87**(2): 171.

Ameisen, J. C. and A. Capron (1991). "Cell dysfunction and depletion in AIDS: the programmed cell death hypothesis." Immunol Today **12**(4): 102-105.

Anderson, H. A., Y. Chen, et al. (1996). "Bound simian virus 40 translocates to caveolin-enriched membrane domains, and its entry is inhibited by drugs that selectively disrupt caveolae." Mol Biol Cell **7**(11): 1825-1834.

Anderson, R. G. (1998). "The caveolae membrane system." Annu Rev Biochem **67**: 199-225.

Aridor, M. and L. A. Hannan (2000). "Traffic jam: a compendium of human diseases that affect intracellular transport processes." Traffic **1**(11): 836-851.

Aridor, M. and L. A. Hannan (2002). "Traffic jams II: an update of diseases of intracellular transport." Traffic **3**(11): 781-790.

Bagatolli, L. A. (2006). "To see or not to see: Lateral organization of biological membranes and fluorescence microscopy." Biochimica et Biophysica Acta (BBA) - Biomembranes **1758**(10): 1541-1556.

Bagatolli, L. A., J. H. Ipsen, et al. (2010). "An outlook on organization of lipids in membranes: Searching for a realistic connection with the organization of biological membranes." Progress in Lipid Research **49**(4): 378-389.

Bailey, R. W., T. Nguyen, et al. (2009). "Sequence of Physical Changes to the Cell Membrane During Glucocorticoid-Induced Apoptosis in S49 Lymphoma Cells." Biophys J **96**(7): 2709-2718.

Balasubramanian, K., E. M. Bevers, et al. (2001). "Binding of annexin V to membrane products of lipid peroxidation." Biochemistry **40**(30): 8672-8676.

Bayer, N., D. Schober, et al. (2001). "Inhibition of clathrin-dependent endocytosis has multiple effects on human rhinovirus serotype 2 cell entry." J Biol Chem **276**(6): 3952-3962.

Benmerah, A., M. Bayrou, et al. (1999). "Inhibition of clathrin-coated pit assembly by an Eps15 mutant." J Cell Sci **112 ( Pt 9)**: 1303-1311.

Betz, W. J., F. Mao, et al. (1996). "Imaging exocytosis and endocytosis." Current Opinion in Neurobiology **6**(3): 365-371.

Blankenberg, F. G. and J. F. Norfray (2011). "Multimodality molecular imaging of apoptosis in oncology." AJR Am J Roentgenol **197**(2): 308-317.

Bolte, S., C. Talbot, et al. (2004). "FM-dyes as experimental probes for dissecting vesicle trafficking in living plant cells." Journal of Microscopy **214**(2): 159-173.

Bondar, O. P. and E. S. Rowe (1999). "Preferential interactions of fluorescent probe Prodan with cholesterol." Biophys J **76**(2): 956-962.

Bose, S., I. Tuunainen, et al. (2004). "Binding of cationic liposomes to apoptotic cells." Anal Biochem **331**(2): 385-394.

Bossy-Wetzel, E. and D. R. Green (2000). "Detection of apoptosis by annexin V labeling." Methods Enzymol **322**: 15-18.

Brauers, E., A. Dreier, et al. (2010). "Differential effects of myopathy-associated caveolin-3 mutants on growth factor signaling." Am J Pathol **177**(1): 261-270.

Bretscher, M. (1984). "Endocytosis: relation to capping and cell locomotion." Science **224**(4650): 681-686.

Brodsky, F. M., C. Y. Chen, et al. (2001). "Biological basket weaving: formation and function of clathrin-coated vesicles." Annu Rev Cell Dev Biol **17**: 517-568.

Brown, D. A. and J. K. Rose (1992). "Sorting of GPI-anchored proteins to glycolipid-enriched membrane subdomains during transport to the apical cell surface." Cell **68**(3): 533-544.

Bursch, W., F. Oberhammer, et al. (1992). "Cell death by apoptosis and its protective role against disease." Trends Pharmacol Sci **13**(6): 245-251.

Callera, G. E., A. C. Montezano, et al. (2007). "Vascular signaling through cholesterol-rich domains: implications in hypertension." Curr Opin Nephrol Hypertens **16**(2): 90-104.

Canton, I. and G. Battaglia (2012). "Endocytosis at the nanoscale." Chemical Society Reviews **41**(7): 2718-2739.

Catalan, J., P. Perez, et al. (1991). "Analysis of the solvent effect on the photophysics properties of 6-propionyl-2-(dimethylamino)naphthalene (PRODAN)." J Fluoresc **1**(4): 215-223.

Cataldo, A. M., C. M. Peterhoff, et al. (2000). "Endocytic pathway abnormalities precede amyloid beta deposition in sporadic Alzheimer's disease and Down syndrome: differential effects of APOE genotype and presenilin mutations." Am J Pathol **157**(1): 277-286.

Cavalli, V., M. Corti, et al. (2001). "Endocytosis and signaling cascades: a close encounter." FEBS Lett **498**(2-3): 190-196.

Cerbon, J. and V. Calderon (1991). "Changes of the compositional asymmetry of phospholipids associated to the increment in the membrane surface potential." Biochim Biophys Acta **1067**(2): 139-144.

Chan, S. L. and M. P. Mattson (1999). "Caspase and calpain substrates: roles in synaptic plasticity and cell death." J Neurosci Res **58**(1): 167-190.

Chapman, D. (1975). "Phase transitions and fluidity characteristics of lipids and cell membranes." Quarterly Reviews of Biophysics **8**(02): 185-235.

Chattopadhyay, A. (1990). "Chemistry and biology of N-(7-nitrobenz-2-oxa-1,3-diazol-4-yl)-labeled lipids: fluorescent probes of biological and model membranes." Chem Phys Lipids **53**(1): 1-15.

Cheng, Y.-M., S.-C. Pu, et al. (2005). "Spectroscopy and Femtosecond Dynamics of 7-N,N-Diethylamino-3-hydroxyflavone. The Correlation of Dipole Moments among Various States To Rationalize the Excited-State Proton Transfer Reaction." The Journal of Physical Chemistry A **109**(51): 11696-11706.

Cheng, Z. J., R. D. Singh, et al. (2006). "Membrane microdomains, caveolae, and caveolar endocytosis of sphingolipids." Mol Membr Biol **23**(1): 101-110.

Chimini, G. and P. Chavrier (2000). "Function of Rho family proteins in actin dynamics during phagocytosis and engulfment." Nat Cell Biol **2**(10): E191-196.

Chou, P.-T., M. L. Martinez, et al. (1993). "The observation of solvent-dependent proton-transfer / charge-transfer lasers from 4' -diethylamino-3-hydroxyflavone." Chemical Physics Letters **204**(5–6): 395-399.

Chou, P.-T., S.-C. Pu, et al. (2005). "Femtosecond Dynamics on Excited-State Proton/ Charge-Transfer Reaction in 4‘-N,N-Diethylamino-3-hydroxyflavone. The Role of Dipolar Vectors in Constructing a Rational Mechanism." The Journal of Physical Chemistry A **109**(17): 3777-3787.

Clague, M. J. (1998). "Molecular aspects of the endocytic pathway." Biochem J **336 ( Pt 2)**: 271-282.

Cohen, G. M. (1997). "Caspases: the executioners of apoptosis." Biochem J **326 ( Pt 1)**: 1-16.

Connor, J. and A. J. Schroit (1988). "Transbilayer movement of phosphatidylserine in erythrocytes: inhibition of transport and preferential labeling of a 31,000-dalton protein by sulfhydryl reactive reagents." Biochemistry **27**(3): 848-851.

Cordy, J. M., N. M. Hooper, et al. (2006). "The involvement of lipid rafts in Alzheimer's disease." Mol Membr Biol **23**(1): 111-122.

Curtin, J. F. and T. G. Cotter (2003). "Apoptosis: Historical perspectives." Essays Biochem **39**: 1-10.

Damjanovich, S., G. Vereb, et al. (1995). "Structural hierarchy in the clustering of HLA class I molecules in the plasma membrane of human lymphoblastoid cells." Proceedings of the National Academy of Sciences **92**(4): 1122-1126.

Damke, H. (1996). "Dynamin and receptor-mediated endocytosis." FEBS Lett **389**(1): 48-51.

Danielli, J. F. and H. Davson (1935). "A contribution to the theory of permeability of thin films." Journal of Cellular and Comparative Physiology **5**(4): 495-508.

Danielsen, E. M. and B. van Deurs (1995). "A transferrin-like GPI-linked iron-binding protein in detergent-insoluble noncaveolar microdomains at the apical surface of fetal intestinal epithelial cells." J Cell Biol **131**(4): 939-950.

Demchenko, A. P., Y. Mely, et al. (2009). "Monitoring biophysical properties of lipid membranes by environment-sensitive fluorescent probes." Biophys J **96**(9): 3461-3470.

Diaz, G., M. Melis, et al. (2008). "Hydrophobic characterization of intracellular lipids in situ by Nile Red red/yellow emission ratio." Micron **39**(7): 819-824.

Dietrich, C., B. Yang, et al. (2002). "Relationship of Lipid Rafts to Transient Confinement Zones Detected by Single Particle Tracking." Biophys J **82**(1): 274-284.

Doherty, G. J. and H. T. McMahon (2008). "Mediation, modulation, and consequences of membrane-cytoskeleton interactions." Annu Rev Biophys **37**: 65-95.

Doherty, G. J. and H. T. McMahon (2009). "Mechanisms of endocytosis." Annu Rev Biochem **78**: 857-902.

Duportail, G., A. Klymchenko, et al. (2001). "Neutral fluorescence probe with strong ratiometric response to surface charge of phospholipid membranes." FEBS Lett **508**(2): 196-200.

Duportail, G., A. Klymchenko, et al. (2002). "On the Coupling Between Surface Charge and Hydration in Biomembranes: Experiments with 3-Hydroxyflavone Probes." J Fluoresc **12**(2): 181-185.

Dupree, P., R. G. Parton, et al. (1993). "Caveolae and sorting in the trans-Golgi network of epithelial cells." EMBO J **12**(4): 1597-1605.

Duvall, E., A. H. Wyllie, et al. (1985). "Macrophage recognition of cells undergoing programmed cell death (apoptosis)." Immunology **56**(2): 351-358.

Edidin, M., M. C. Zúñiga, et al. (1994). "Truncation mutants define and locate cytoplasmic barriers to lateral mobility of membrane glycoproteins." Proceedings of the National Academy of Sciences **91**(8): 3378-3382.

Eggeling, C., C. Ringemann, et al. (2009). "Direct observation of the nanoscale dynamics of membrane lipids in a living cell." Nature **457**(7233): 1159-1162.

Ehrlich, M., W. Boll, et al. (2004). "Endocytosis by Random Initiation and Stabilization of Clathrin-Coated Pits." Cell **118**(5): 591-605.

Elmore, S. (2007). "Apoptosis: a review of programmed cell death." Toxicol Pathol **35**(4): 495-516.

Erickson, G. F. (1997). "Defining apoptosis: players and systems." J Soc Gynecol Investig **4**(5): 219-228.

Ewers, H. and A. Helenius (2011). "Lipid-mediated endocytosis." Cold Spring Harb Perspect Biol **3**(8): a004721.

Fadok, V. A., D. J. Laszlo, et al. (1993). "Particle digestibility is required for induction of the phosphatidylserine recognition mechanism used by murine macrophages to phagocytose apoptotic cells." J Immunol **151**(8): 4274-4285.

Fadok, V. A., J. S. Savill, et al. (1992). "Different populations of macrophages use either the vitronectin receptor or the phosphatidylserine receptor to recognize and remove apoptotic cells." J Immunol **149**(12): 4029-4035.

Fadok, V. A., D. R. Voelker, et al. (1992). "Exposure of phosphatidylserine on the surface of apoptotic lymphocytes triggers specific recognition and removal by macrophages." J Immunol **148**(7): 2207-2216.

Feigenson, G. W. (2006). "Phase behavior of lipid mixtures." Nat Chem Biol **2**(11): 560-563.

Feigenson, G. W. (2007). "Phase boundaries and biological membranes." Annu Rev Biophys Biomol Struct **36**: 63-77.

Feigenson, G. W. and J. T. Buboltz (2001). "Ternary Phase Diagram of Dipalmitoyl-PC/Dilauroyl-PC/Cholesterol: Nanoscopic Domain Formation Driven by Cholesterol." Biophys J **80**(6): 2775-2788.

Feng, Y., B. Press, et al. (1995). "Rab 7: an important regulator of late endocytic membrane traffic." J Cell Biol **131**(6 Pt 1): 1435-1452.

Fesus, L. (1993). "Biochemical events in naturally occurring forms of cell death." FEBS Lett **328**(1-2): 1-5.

Fluhler, E., V. G. Burnham, et al. (1985). "Spectra, membrane binding, and potentiometric responses of new charge shift probes." Biochemistry **24**(21): 5749-5755.

Forgac, M. (1992). "Structure, function and regulation of the coated vesicle V-ATPase." J Exp Biol **172**: 155-169.

Fortin, D. L., M. D. Troyer, et al. (2004). "Lipid rafts mediate the synaptic localization of alpha-synuclein." J Neurosci **24**(30): 6715-6723.

Fra, A. M., E. Williamson, et al. (1995). "De novo formation of caveolae in lymphocytes by expression of VIP21-caveolin." Proc Natl Acad Sci U S A **92**(19): 8655-8659.

Freeman, M. R., B. Cinar, et al. (2005). "Membrane rafts as potential sites of nongenomic hormonal signaling in prostate cancer." Trends Endocrinol Metab **16**(6): 273-279.

Fridriksson, E. K., P. A. Shipkova, et al. (1999). "Quantitative Analysis of Phospholipids in Functionally Important Membrane Domains from RBL-2H3 Mast Cells Using Tandem High-Resolution Mass Spectrometry†." Biochemistry **38**(25): 8056-8063.

Fuhrmann, H., G. Dobeleit, et al. (2002). "Cholesterol Oxidase and Resistance of Rhodococcus equi to Peroxidative Stress in vitro in the Presence of Cholesterol." Journal of Veterinary Medicine, Series B **49**(6): 310-311.

Gao, F., E. Mei, et al. (2006). "Probing lipid vesicles by bimolecular association and dissociation trajectories of single molecules." J Am Chem Soc **128**(14): 4814-4822.

Geuze, H. J., W. Stoorvogel, et al. (1988). "Sorting of mannose 6-phosphate receptors and lysosomal membrane proteins in endocytic vesicles." J Cell Biol **107**(6 Pt 2): 2491-2501.

Ghoshroy, K. B., W. Zhu, et al. (1997). "Investigation of Membrane Disruption in the Reaction Catalyzed by Cholesterol Oxidase†." Biochemistry **36**(20): 6133-6140.

Goncalves, M. S. (2009). "Fluorescent labeling of biomolecules with organic probes." Chem Rev **109**(1): 190-212.

Gorter, E. and F. Grendel (1925). "On Bimolecular Layers of Lipoids on the Chromocytes of the Blood." J Exp Med **41**(4): 439-443.

Greenspan, P. and S. D. Fowler (1985). "Spectrofluorometric studies of the lipid probe, nile red." J Lipid Res **26**(7): 781-789.

Gronberg, L. and J. P. Slotte (1990). "Cholesterol oxidase catalyzed oxidation of cholesterol in mixed lipid monolayers: effects of surface pressure and phospholipid composition on catalytic activity." Biochemistry **29**(13): 3173-3178.

Gross, E., R. S. Bedlack, et al. (1994). "Dual-wavelength ratiometric fluorescence measurement of the membrane dipole potential." Biophys J **67**(1): 208-216.

Groux, H., D. Monte, et al. (1991). "[Activation of CD4+ T-lymphocytes in asymptomatic HIV infected patients induce the program action of lymphocyte death by apoptosis]." C R Acad Sci III **312**(12): 599-606.

Gruenberg, J. (2001). "The endocytic pathway: a mosaic of domains." Nat Rev Mol Cell Biol **2**(10): 721-730.

Hammes, A., T. K. Andreassen, et al. (2005). "Role of endocytosis in cellular uptake of sex steroids." Cell **122**(5): 751-762.

Hammond, A. T., F. A. Heberle, et al. (2005). "Crosslinking a lipid raft component triggers liquid ordered-liquid disordered phase separation in model plasma membranes." Proc Natl Acad Sci U S A **102**(18): 6320-6325.

Hancock, J. F. (2006). "Lipid rafts: contentious only from simplistic standpoints." Nat Rev Mol Cell Biol **7**(6): 456-462.

Hannun, Y. A. (1996). "Functions of ceramide in coordinating cellular responses to stress." Science **274**(5294): 1855-1859.

Hanshaw, R. G., C. Lakshmi, et al. (2005). "Fluorescent detection of apoptotic cells by using zinc coordination complexes with a selective affinity for membrane surfaces enriched with phosphatidylserine." Chembiochem **6**(12): 2214-2220.

Hanshaw, R. G. and B. D. Smith (2005). "New reagents for phosphatidylserine recognition and detection of apoptosis." Bioorganic & Medicinal Chemistry **13**(17): 5035-5042.
Hao, M., S. X. Lin, et al. (2002). "Vesicular and non-vesicular sterol transport in living cells. The endocytic recycling compartment is a major sterol storage organelle." J Biol Chem **277**(1): 609-617.
Henley, J. R., E. W. Krueger, et al. (1998). "Dynamin-mediated internalization of caveolae." J Cell Biol **141**(1): 85-99.
Heyder, P., U. S. Gaipl, et al. (2003). "Early detection of apoptosis by staining of acid-treated apoptotic cells with FITC-labeled lectin from Narcissus pseudonarcissus." Cytometry A **55**(2): 86-93.
Hickey, P. C., D. J. Jacobson, et al. (2002). "Live-cell imaging of vegetative hyphal fusion in Neurospora crassa." Fungal Genetics and Biology **37**(1): 109-119.
Higgins, C. F. (1994). "Flip-flop: the transmembrane translocation of lipids." Cell **79**(3): 393-395.
Hinshaw, J. E. (2000). "Dynamin and its role in membrane fission." Annu Rev Cell Dev Biol **16**: 483-519.
Hirata, H., A. Takahashi, et al. (1998). "Caspases are activated in a branched protease cascade and control distinct downstream processes in Fas-induced apoptosis." J Exp Med **187**(4): 587-600.
Ho, C., S. J. Slater, et al. (1995). "Hydration and Order in Lipid Bilayers." Biochemistry **34**(18): 6188-6195.
Hoeller, D., S. Volarevic, et al. (2005). "Compartmentalization of growth factor receptor signalling." Curr Opin Cell Biol **17**(2): 107-111.
Holl, M. M. B. (2008). Cell Plasma Membranes and Phase Transitions

Phase Transitions in Cell Biology. G. H. Pollack and W.-C. Chin, Springer Netherlands**:** 171-181.
Hopkins, C. R. (1983). "Intracellular routing of transferrin and transferrin receptors in epidermoid carcinoma A431 cells." Cell **35**(1): 321-330.
Hornick, C. A., D. Y. Hui, et al. (1997). "A role for retrosomes in intracellular cholesterol transport from endosomes to the plasma membrane." Am J Physiol **273**(3 Pt 1): C1075-1081.
Igarashi, K., K. Asai, et al. (1995). "Specific binding of a synthetic peptide derived from an antibody complementarity determining region to phosphatidylserine." J Biochem **117**(2): 452-457.
Ikonen, E. (2001). "Roles of lipid rafts in membrane transport." Curr Opin Cell Biol **13**(4): 470-477.
Ikonen, E. and M. Holtta-Vuori (2004). "Cellular pathology of Niemann-Pick type C disease." Semin Cell Dev Biol **15**(4): 445-454.
Ira and G. Krishnamoorthy (1998). "Probing the dynamics of planar supported membranes by Nile red fluorescence lifetime distribution." Biochimica et Biophysica Acta (BBA) - Biomembranes **1414**(1–2): 255-259.
Jacobson, K. and C. Dietrich (1999). "Looking at lipid rafts?" Trends Cell Biol **9**(3): 87-91.
Jin, L., A. C. Millard, et al. (2006). "Characterization and Application of a New Optical Probe for Membrane Lipid Domains." Biophys J **90**(7): 2563-2575.
Johannes, L. and C. Lamaze (2002). "Clathrin-dependent or not: is it still the question?" Traffic **3**(7): 443-451.
Jose, J. and K. Burgess (2006). "Syntheses and Properties of Water-Soluble Nile Red Derivatives." J Org Chem **71**(20): 7835-7839.
Jurkiewicz, P., J. Sýkora, et al. (2005). "Solvent Relaxation in Phospholipid Bilayers: Principles and Recent Applications." J Fluoresc **15**(6): 883-894.
Jury, E. C., P. S. Kabouridis, et al. (2004). "Altered lipid raft-associated signaling and ganglioside expression in T lymphocytes from patients with systemic lupus erythematosus." J Clin Invest **113**(8): 1176-1187.
Jutras, I. and M. Desjardins (2005). "Phagocytosis: at the crossroads of innate and adaptive immunity." Annu Rev Cell Dev Biol **21**: 511-527.
Kaur, Y. and P. M. Horowitz (2004). "Prodan fluorescence mimics the GroEL folding cycle." Protein J **23**(7): 475-481.

Kayalar, C., T. Ord, et al. (1996). "Cleavage of actin by interleukin 1 beta-converting enzyme to reverse DNase I inhibition." Proc Natl Acad Sci U S A **93**(5): 2234-2238.

Kenworthy, A. K. (2008). "Have we become overly reliant on lipid rafts?" EMBO Rep **9**(6): 531-535.

Kirchhausen, T. (2000). "Clathrin." Annu Rev Biochem **69**: 699-727.

Kirkham, M. and R. G. Parton (2005). "Clathrin-independent endocytosis: new insights into caveolae and non-caveolar lipid raft carriers." Biochim Biophys Acta **1746**(3): 349-363.

Klein, U., G. Gimpl, et al. (1995). "Alteration of the Myometrial Plasma Membrane Cholesterol Content with .beta.-Cyclodextrin Modulates the Binding Affinity of the Oxytocin Receptor." Biochemistry **34**(42): 13784-13793.

Klinkner, A. M., P. J. Bugelski, et al. (1997). "A novel technique for mapping the lipid composition of atherosclerotic fatty streaks by en face fluorescence microscopy." J Histochem Cytochem **45**(5): 743-753.

Klymchenko, A. S., G. Duportail, et al. (2003). "Ultrasensitive two-color fluorescence probes for dipole potential in phospholipid membranes." Proc Natl Acad Sci U S A **100**(20): 11219-11224.

Klymchenko, A. S., S. Furukawa, et al. (2007). "Supramolecular Hydrophobic−Hydrophilic Nanopatterns at Electrified Interfaces." Nano Lett **7**(3): 791-795.

Klymchenko, A. S., Y. Mely, et al. (2004). "Simultaneous probing of hydration and polarity of lipid bilayers with 3-hydroxyflavone fluorescent dyes." Biochim Biophys Acta **1665**(1-2): 6-19.

Klymchenko, A. S., S. Oncul, et al. (2009). "Visualization of lipid domains in giant unilamellar vesicles using an environment-sensitive membrane probe based on 3-hydroxyflavone." Biochim Biophys Acta **1788**(2): 495-499.

Koopman, G., C. P. Reutelingsperger, et al. (1994). "Annexin V for flow cytometric detection of phosphatidylserine expression on B cells undergoing apoptosis." Blood **84**(5): 1415-1420.

Kornfeld, S. and I. Mellman (1989). "The biogenesis of lysosomes." Annu Rev Cell Biol **5**: 483-525.

Kraayenhof, R., G. J. Sterk, et al. (1993). "Probing biomembrane interfacial potential and pH profiles with a new type of float-like fluorophores positioned at varying distance from the membrane surface." Biochemistry **32**(38): 10057-10066.

Krasnowska, E. K., E. Gratton, et al. (1998). "Prodan as a membrane surface fluorescence probe: partitioning between water and phospholipid phases." Biophys J **74**(4): 1984-1993.

Krauss, M. and V. Haucke (2012). "Shaping membranes for endocytosis." Rev Physiol Biochem Pharmacol **161**: 45-66.

Kreit, J., G. Lefebvre, et al. (1992). "A colorimetric assay for measuring cell-free and cell-bound cholesterol oxidase." Lipids **27**(6): 458-465.

Kreit, J. and N. S. Sampson (2009). "Cholesterol oxidase: physiological functions." FEBS J **276**(23): 6844-6856.

Kressel, M. and P. Groscurth (1994). "Distinction of apoptotic and necrotic cell death by in situ labelling of fragmented DNA." Cell Tissue Res **278**(3): 549-556.

Krishna, M. M. G. (1999). "Excited-State Kinetics of the Hydrophobic Probe Nile Red in Membranes and Micelles." The Journal of Physical Chemistry A **103**(19): 3589-3595.

Krishnan, S., M. P. Nambiar, et al. (2004). "Alterations in lipid raft composition and dynamics contribute to abnormal T cell responses in systemic lupus erythematosus." J Immunol **172**(12): 7821-7831.

Kruidering, M. and G. I. Evan (2000). "Caspase-8 in apoptosis: the beginning of "the end"?" IUBMB Life **50**(2): 85-90.

Kucherak, O. A., S. Oncul, et al. (2010). "Switchable Nile Red-Based Probe for Cholesterol and Lipid Order at the Outer Leaflet of Biomembranes." J Am Chem Soc **132**(13): 4907-4916.

Kuhry, J.-G., P. Fonteneau, et al. (1983). "TMA-DPH: A suitable fluorescence polarization probe for specific plasma membrane fluidity studies in intact living cells." Cell Biochemistry and Biophysics **5**(2): 129-140.

Kuhry, J. G., G. Duportail, et al. (1985). "Plasma membrane fluidity measurements on whole living cells by fluorescence anisotropy of trimethylammoniumdiphenylhexatriene." Biochim Biophys Acta **845**(1): 60-67.

Kundu, A., R. T. Avalos, et al. (1996). "Transmembrane domain of influenza virus neuraminidase, a type II protein, possesses an apical sorting signal in polarized MDCK cells." J Virol **70**(9): 6508-6515.

Kurzchalia, T. V. and R. G. Parton (1999). "Membrane microdomains and caveolae." Curr Opin Cell Biol **11**(4): 424-431.

Kusumi, A., Y. Sako, et al. (1993). "Confined lateral diffusion of membrane receptors as studied by single particle tracking (nanovid microscopy). Effects of calcium-induced differentiation in cultured epithelial cells." Biophys J **65**(5): 2021-2040.

Laakko, T., L. King, et al. (2002). "Versatility of merocyanine 540 for the flow cytometric detection of apoptosis in human and murine cells." J Immunol Methods **261**(1–2): 129-139.

Lagerholm, B. C., G. E. Weinreb, et al. (2004). "Detecting microdomains in intact cell membranes." Annual Review of Physical Chemistry **56**(1): 309-336.

Lakowicz, J. R. (2006). Principles of Fluorescence Spectroscopy New York, Springer.

Lange, Y. and B. V. Ramos (1983). "Analysis of the distribution of cholesterol in the intact cell." Journal of Biological Chemistry **258**(24): 15130-15134.

Lange, Y., J. Ye, et al. (1998). "Circulation of cholesterol between lysosomes and the plasma membrane." J Biol Chem **273**(30): 18915-18922.

Langmuir, I. (1917). "The constitution and fundamental properties of solids and liquids. II. Liquids.1 " J Am Chem Soc **39**(9): 1848-1906.

Leist, M. and M. Jaattela (2001). "Four deaths and a funeral: from caspases to alternative mechanisms." Nat Rev Mol Cell Biol **2**(8): 589-598.

Lenne, P.-F., L. Wawrezinieck, et al. (2006). "Dynamic molecular confinement in the plasma membrane by microdomains and the cytoskeleton meshwork." EMBO J **25**(14): 3245-3256.

Lentz, B. R. (1993). "Use of fluorescent probes to monitor molecular order and motions within liposome bilayers." Chem Phys Lipids **64**(1–3): 99-116.

Lindner, R. and H. Y. Naim (2009). "Domains in biological membranes." Exp Cell Res **315**(17): 2871-2878.

Lingwood, D. and K. Simons (2010). "Lipid Rafts As a Membrane-Organizing Principle." Science **327**(5961): 46-50.

Lisanti, M. P. and E. Rodriguez-Boulan (1990). "Glycophospholipid membrane anchoring provides clues to the mechanism of protein sorting in polarized epithelial cells." Trends in Biochemical Sciences **15**(3): 113-118.

Liscum, L. and N. J. Munn (1999). "Intracellular cholesterol transport." Biochim Biophys Acta **1438**(1): 19-37.

Liu, X., C. N. Kim, et al. (1996). "Induction of apoptotic program in cell-free extracts: requirement for dATP and cytochrome c." Cell **86**(1): 147-157.

Lombardi, D., T. Soldati, et al. (1993). "Rab9 functions in transport between late endosomes and the trans Golgi network." EMBO J **12**(2): 677-682.

Lommerse, P. H. M., H. P. Spaink, et al. (2004). "In vivo plasma membrane organization: results of biophysical approaches." Biochimica et Biophysica Acta (BBA) - Biomembranes **1664**(2): 119-131.

London, E. and D. A. Brown (2000). "Insolubility of lipids in Triton X-100: physical origin and relationship to sphingolipid/cholesterol membrane domains (rafts)." Biochimica et Biophysica Acta (BBA) - Biomembranes **1508**(1–2): 182-195.

Lu, Z., S. J. Lord, et al. (2006). "Long-wavelength analogue of PRODAN: synthesis and properties of Anthradan, a fluorophore with a 2,6-donor-acceptor anthracene structure." J Org Chem **71**(26): 9651-9657.

Luo, C., K. Wang, et al. (2008). "The functional roles of lipid rafts in T cell activation, immune diseases and HIV infection and prevention." Cell Mol Immunol **5**(1): 1-7.

Luzio, J. P., M. D. Parkinson, et al. (2009). "The delivery of endocytosed cargo to lysosomes." Biochem Soc Trans **37**(Pt 5): 1019-1021.

Luzio, J. P., P. R. Pryor, et al. (2007). "Lysosomes: fusion and function." Nat Rev Mol Cell Biol **8**(8): 622-632.

M'Baye, G., Y. Mély, et al. (2008). "Liquid Ordered and Gel Phases of Lipid Bilayers: Fluorescent Probes Reveal Close Fluidity but Different Hydration." Biophys J **95**(3): 1217-1225.
Maniak, M. (2001). "Fluid-phase uptake and transit in axenic Dictyostelium cells." Biochim Biophys Acta **1525**(3): 197-204.
Marks, D., H. Zhang, et al. (1997). "Solvent dependence of (sub)picosecond proton transfer in photo-excited [2,2′-bipyridyl]-3,3′-diol." Chemical Physics Letters **275**(3–4): 370-376.
Marsh, M. and A. Helenius (2006). "Virus entry: open sesame." Cell **124**(4): 729-740.
Marsh, M. and H. T. McMahon (1999). "The structural era of endocytosis." Science **285**(5425): 215-220.
Massey, J. B. (1998). "Effect of cholesteryl hemisuccinate on the interfacial properties of phosphatidylcholine bilayers." Biochim Biophys Acta **1415**(1): 193-204.
Matter, K. and I. Mellman (1994). "Mechamisms of cell polarity: sorting and transport in epithelial cells." Curr Opin Cell Biol **6**(4): 545-554.
Maxfield, F. R. and T. E. McGraw (2004). "Endocytic recycling." Nat Rev Mol Cell Biol **5**(2): 121-132.
Maxfield, F. R. and I. Tabas (2005). "Role of cholesterol and lipid organization in disease." Nature **438**(7068): 612-621.
McCarthy, M. J., L. L. Rubin, et al. (1997). "Involvement of caspases in sympathetic neuron apoptosis." J Cell Sci **110 ( Pt 18)**: 2165-2173.
McMorrow, D. and M. Kasha (1984). "Intramolecular excited-state proton transfer in 3-hydroxyflavone. Hydrogen-bonding solvent perturbations." The Journal of Physical Chemistry **88**(11): 2235-2243.
Meer, G. V. (1989). "Lipid Traffic in Animal Cells." Annu Rev Cell Biol **5**(1): 247-275.
Meers, P. and T. Mealy (1993). "Calcium-dependent annexin V binding to phospholipids: stoichiometry, specificity, and the role of negative charge." Biochemistry **32**(43): 11711-11721.
Meier, P., A. Finch, et al. (2000). "Apoptosis in development." Nature **407**(6805): 796-801.
Mellman, I. (1996). "Endocytosis and molecular sorting." Annu Rev Cell Dev Biol **12**: 575-625.
Mercer, J., M. Schelhaas, et al. (2010). "Virus Entry by Endocytosis." Annu Rev Biochem **79**(1): 803-833.
Michel, V. and M. Bakovic (2007). "Lipid rafts in health and disease." Biol Cell **99**(3): 129-140.
Mishra, A., R. K. Behera, et al. (2000). "Cyanines during the 1990s: A Review." Chem Rev **100**(6): 1973-2012.
Miskovsky, P. (2002). Current Drug Targets.
Miyazawa, A., H. Inoue, et al. (1992). "Monoclonal antibody analysis of phosphatidylserine and protein kinase C localizations in developing rat cerebellum." J Neurochem **59**(4): 1547-1554.
Mobius, W., E. van Donselaar, et al. (2003). "Recycling compartments and the internal vesicles of multivesicular bodies harbor most of the cholesterol found in the endocytic pathway." Traffic **4**(4): 222-231.
Moreno-Ruiz, E., M. Galán-Díez, et al. (2009). "Candida albicans internalization by host cells is mediated by a clathrin-dependent mechanism." Cellular Microbiology **11**(8): 1179-1189.
Moreno, F., M. Cortijo, et al. (1999). "The fluorescent probe prodan characterizes the warfarin binding site on human serum albumin." Photochem Photobiol **69**(1): 8-15.
Morris, R. G., A. D. Hargreaves, et al. (1984). "Hormone-induced cell death. 2. Surface changes in thymocytes undergoing apoptosis." Am J Pathol **115**(3): 426-436.
Mouritsen, O. G. (2011). "Lipidology and lipidomics--quo vadis? A new era for the physical chemistry of lipids." Physical Chemistry Chemical Physics **13**(43): 19195-19205.
Mukherjee, S. and F. R. Maxfield (2004). "Membrane domains." Annu Rev Cell Dev Biol **20**(1): 839-866.
Munro, S. (2003). "Lipid rafts: elusive or illusive?" Cell **115**(4): 377-388.
Nagata, S. (1997). "Apoptosis by death factor." Cell **88**(3): 355-365.
Neufeld, E. B., A. M. Cooney, et al. (1996). "Intracellular Trafficking of Cholesterol Monitored with a Cyclodextrin." Journal of Biological Chemistry **271**(35): 21604-21613.

Newman, S. L., J. E. Henson, et al. (1982). "Phagocytosis of senescent neutrophils by human monocyte-derived macrophages and rabbit inflammatory macrophages." J Exp Med **156**(2): 430-442.

Nonis, D., M. H. Schmidt, et al. (2008). "Ataxin-2 associates with the endocytosis complex and affects EGF receptor trafficking." Cell Signal **20**(10): 1725-1739.

Obaid, A. L., L. M. Loew, et al. (2004). "Novel naphthylstyryl-pyridium potentiometric dyes offer advantages for neural network analysis." J Neurosci Methods **134**(2): 179-190.

Oncul, S., A. S. Klymchenko, et al. (2010). "Liquid ordered phase in cell membranes evidenced by a hydration-sensitive probe: effects of cholesterol depletion and apoptosis." Biochim Biophys Acta **1798**(7): 1436-1443.

Orlandi, P. A. and P. H. Fishman (1998). "Filipin-dependent inhibition of cholera toxin: evidence for toxin internalization and activation through caveolae-like domains." J Cell Biol **141**(4): 905-915.

Ormson, S. M., R. G. Brown, et al. (1994). "Switching between charge- and proton-transfer emission in the excited state of a substituted 3-hydroxyflavone." Journal of Photochemistry and Photobiology A: Chemistry **81**(2): 65-72.

Otsuki, Y., Z. Li, et al. (2003). "Apoptotic detection methods--from morphology to gene." Prog Histochem Cytochem **38**(3): 275-339.

Owen, D. M., M. A. A. Neil, et al. (2007). "Optical techniques for imaging membrane lipid microdomains in living cells." Seminars in Cell & Developmental Biology **18**(5): 591-598.

Packard, B. Z., A. Komoriya, et al. (2001). "Caspase 8 activity in membrane blebs after anti-Fas ligation." J Immunol **167**(9): 5061-5066.

Palade, G. E. (1953). "An electron microscope study of the mitochondrial structure." J Histochem Cytochem **1**(4): 188-211.

Parasassi, T., G. De Stasio, et al. (1990). "Phase fluctuation in phospholipid membranes revealed by Laurdan fluorescence." Biophys J **57**(6): 1179-1186.

Parasassi, T., G. De Stasio, et al. (1991). "Quantitation of lipid phases in phospholipid vesicles by the generalized polarization of Laurdan fluorescence." Biophys J **60**(1): 179-189.

Parasassi, T., M. Di Stefano, et al. (1994). "Cholesterol modifies water concentration and dynamics in phospholipid bilayers: a fluorescence study using Laurdan probe." Biophys J **66**(3 Pt 1): 763-768.

Parton, R. G., M. Hanzal-Bayer, et al. (2006). "Biogenesis of caveolae: a structural model for caveolin-induced domain formation." J Cell Sci **119**(Pt 5): 787-796.

Parton, R. G. and K. Simons (2007). "The multiple faces of caveolae." Nat Rev Mol Cell Biol **8**(3): 185-194.

Patra, S. K., A. Alonso, et al. (1999). "Liposomes Containing Sphingomyelin and Cholesterol: Detergent Solubilisation and Infrared Spectroscopic Studies." Journal of Liposome Research **9**(2): 247-260.

Pike, L. J. (2003). "Lipid rafts." J Lipid Res **44**(4): 655-667.

Pike, L. J. (2006). "Rafts defined: a report on the Keystone Symposium on Lipid Rafts and Cell Function." J Lipid Res **47**(7): 1597-1598.

Piper, R. C. and J. P. Luzio (2001). "Late endosomes: sorting and partitioning in multivesicular bodies." Traffic **2**(9): 612-621.

Pivovarenko, V., O. Vadzyuk, et al. (2006). "Fluorometric Detection of Adenosine Triphosphate with 3-Hydroxy-4′-(dimethylamino)flavone in Aqueous Solutions." J Fluoresc **16**(1): 9-15.

Praefcke, G. J. and H. T. McMahon (2004). "The dynamin superfamily: universal membrane tubulation and fission molecules?" Nat Rev Mol Cell Biol **5**(2): 133-147.

Pralle, A., P. Keller, et al. (2000). "Sphingolipid-Cholesterol Rafts Diffuse as Small Entities in the Plasma Membrane of Mammalian Cells." J. Cell Biol. **148**(5): 997-1008.

Radeva, G. and F. J. Sharom (2004). "Isolation and characterization of lipid rafts with different properties from RBL-2H3 (rat basophilic leukaemia) cells." Biochem J **380**(Pt 1): 219-230.

Reed, J. C. (2000). "Mechanisms of apoptosis." Am J Pathol **157**(5): 1415-1430.

Reichardt, C. (1994). "Solvatochromic Dyes as Solvent Polarity Indicators." Chem Rev **94**(8): 2319-2358.

Ren, Y. and J. Savill (1998). "Apoptosis: the importance of being eaten." Cell Death Differ **5**(7): 563-568.

Rothberg, K. G., J. E. Heuser, et al. (1992). "Caveolin, a protein component of caveolae membrane coats." Cell **68**(4): 673-682.

Rothberg, K. G., Y. S. Ying, et al. (1990). "Cholesterol controls the clustering of the glycophospholipid-anchored membrane receptor for 5-methyltetrahydrofolate." J Cell Biol **111**(6): 2931-2938.

Sackett, D. L., J. R. Knutson, et al. (1990). "Hydrophobic surfaces of tubulin probed by time-resolved and steady-state fluorescence of nile red." J Biol Chem **265**(25): 14899-14906.

Salvesen, G. S. and V. M. Dixit (1997). "Caspases: intracellular signaling by proteolysis." Cell **91**(4): 443-446.

Saslowsky, D. E., J. Lawrence, et al. (2002). "Placental Alkaline Phosphatase Is Efficiently Targeted to Rafts in Supported Lipid Bilayers." Journal of Biological Chemistry **277**(30): 26966-26970.

Scheiffele, P., A. Rietveld, et al. (1999). "Influenza Viruses Select Ordered Lipid Domains during Budding from the Plasma Membrane." Journal of Biological Chemistry **274**(4): 2038-2044.

Schmid, S. L. (1997). "Clathrin-coated vesicle formation and protein sorting: an integrated process." Annu Rev Biochem **66**: 511-548.

Schmidt, K., M. Schrader, et al. (2001). "Regulated Apical Secretion of Zymogens in Rat Pancreas." Journal of Biological Chemistry **276**(17): 14315-14323.

Schnitzer, J. E., P. Oh, et al. (1994). "Filipin-sensitive caveolae-mediated transport in endothelium: reduced transcytosis, scavenger endocytosis, and capillary permeability of select macromolecules." J Cell Biol **127**(5): 1217-1232.

Schroeder, R., E. London, et al. (1994). "Interactions between saturated acyl chains confer detergent resistance on lipids and glycosylphosphatidylinositol (GPI)-anchored proteins: GPI-anchored proteins in liposomes and cells show similar behavior." Proceedings of the National Academy of Sciences **91**(25): 12130-12134.

Sengupta, P. K. and M. Kasha (1979). "Excited state proton-transfer spectroscopy of 3-hytdroxyflavone and quercetin." Chemical Physics Letters **68**(2–3): 382-385.

Shaner, N. C., G. H. Patterson, et al. (2007). "Advances in fluorescent protein technology." J Cell Sci **120**(Pt 24): 4247-4260.

Sharma, P., R. Varma, et al. (2004). "Nanoscale Organization of Multiple GPI-Anchored Proteins in Living Cell Membranes." Cell **116**(4): 577-589.

Shaw, A. S. (2006). "Lipid rafts: now you see them, now you don't." Nat Immunol **7**(11): 1139-1142.

Shynkar, V. V., A. S. Klymchenko, et al. (2005). "Two-color fluorescent probes for imaging the dipole potential of cell plasma membranes." Biochim Biophys Acta **1712**(2): 128-136.

Shynkar, V. V., A. S. Klymchenko, et al. (2007). "Fluorescent biomembrane probe for ratiometric detection of apoptosis." J Am Chem Soc **129**(7): 2187-2193.

Shynkar, V. V., A. S. Klymchenko, et al. (2004). "Dynamics of Intermolecular Hydrogen Bonds in the Excited States of 4‘-Dialkylamino-3-hydroxyflavones. On the Pathway to an Ideal Fluorescent Hydrogen Bonding Sensor." The Journal of Physical Chemistry A **108**(40): 8151-8159.

Sigismund, S., E. Argenzio, et al. (2008). "Clathrin-mediated internalization is essential for sustained EGFR signaling but dispensable for degradation." Dev Cell **15**(2): 209-219.

Silverstein, S. C. (1977). "Endocytic uptake of particles by mononuclear phagocytes and the penetration of obligate intracellular parasites." Am J Trop Med Hyg **26**(6 Pt 2): 161-169.

Simons, K. and M. J. Gerl (2010). "Revitalizing membrane rafts: new tools and insights." Nat Rev Mol Cell Biol **11**(10): 688-699.

Simons, K. and E. Ikonen (1997). "Functional rafts in cell membranes." Nature **387**(6633): 569-572.

Simons, K. and D. Toomre (2000). "Lipid rafts and signal transduction." Nat Rev Mol Cell Biol **1**(1): 31-39.

Simons, K. and G. Van Meer (1988). "Lipid sorting in epithelial cells." Biochemistry **27**(17): 6197-6202.

Simons, K. and M. Zerial (1993). "Rab proteins and the road maps for intracellular transport." Neuron **11**(5): 789-799.
Simson, R., E. D. Sheets, et al. (1995). "Detection of temporary lateral confinement of membrane proteins using single-particle tracking analysis." Biophys J **69**(3): 989-993.
Singer, S. J. and G. L. Nicolson (1972). "The fluid mosaic model of the structure of cell membranes." Science **175**(4023): 720-731.
Slavik, J. (1982). "Anilinonaphthalene sulfonate as a probe of membrane composition and function." Biochim Biophys Acta **694**(1): 1-25.
Somsel Rodman, J. and A. Wandinger-Ness (2000). "Rab GTPases coordinate endocytosis." J Cell Sci **113 Pt 2**: 183-192.
Steinman, R. M., I. S. Mellman, et al. (1983). "Endocytosis and the recycling of plasma membrane." J Cell Biol **96**(1): 1-27.
Stekhoven, F. M., J. Tijmes, et al. (1994). "Monoclonal antibody to phosphatidylserine inhibits Na+/K(+)-ATPase activity." Biochim Biophys Acta **1194**(1): 155-165.
Swanson, J. A. and C. Watts (1995). "Macropinocytosis." Trends Cell Biol **5**(11): 424-428.
Swetha, M. G., V. Sriram, et al. (2011). "Lysosomal Membrane Protein Composition, Acidic pH and Sterol Content are Regulated via a Light-Dependent Pathway in Metazoan Cells." Traffic **12**(8): 1037-1055.
Sýkora, J., P. Kapusta, et al. (2002). "On What Time Scale Does Solvent Relaxation in Phospholipid Bilayers Happen?" Langmuir **18**(3): 571-574.
Tanaka, M., H. Ito, et al. (1994). "Hypoxia induces apoptosis with enhanced expression of Fas antigen messenger RNA in cultured neonatal rat cardiomyocytes." Circ Res **75**(3): 426-433.
Taniguchi, Y., T. Ohba, et al. (2006). "Rapid phase change of lipid microdomains in giant vesicles induced by conversion of sphingomyelin to ceramide." Biochim Biophys Acta **1758**(2): 145-153.
Thornberry, N. A. and Y. Lazebnik (1998). "Caspases: enemies within." Science **281**(5381): 1312-1316.
Tooze, J. and M. Hollinshead (1991). "Tubular early endosomal networks in AtT20 and other cells." J Cell Biol **115**(3): 635-653.
Tooze, S. A. (1998). "Biogenesis of secretory granules in the trans-Golgi network of neuroendocrine and endocrine cells." Biochimica et Biophysica Acta (BBA) - Molecular Cell Research **1404**(1–2): 231-244.
Torgersen, M. L., G. Skretting, et al. (2001). "Internalization of cholera toxin by different endocytic mechanisms." J Cell Sci **114**(Pt 20): 3737-3747.
Uchida, K., K. Emoto, et al. (1998). "Induction of apoptosis by phosphatidylserine." J Biochem **123**(6): 1073-1078.
Van Cruchten, S. and W. Van Den Broeck (2002). "Morphological and biochemical aspects of apoptosis, oncosis and necrosis." Anat Histol Embryol **31**(4): 214-223.
van Engeland, M., L. J. Nieland, et al. (1998). "Annexin V-affinity assay: a review on an apoptosis detection system based on phosphatidylserine exposure." Cytometry **31**(1): 1-9.
van Meer, G. and K. Simons (1988). "Lipid polarity and sorting in epithelial cells." J Cell Biochem **36**(1): 51-58.
van Meer, G., D. R. Voelker, et al. (2008). "Membrane lipids: where they are and how they behave." Nat Rev Mol Cell Biol **9**(2): 112-124.
Varma, R. and S. Mayor (1998). "GPI-anchored proteins are organized in submicron domains at the cell surface." Nature **394**(6695): 798-801.
Vaux, D. L., S. Cory, et al. (1988). "Bcl-2 gene promotes haemopoietic cell survival and cooperates with c-myc to immortalize pre-B cells." Nature **335**(6189): 440-442.
Veatch, S. L. and S. L. Keller (2005). "Miscibility Phase Diagrams of Giant Vesicles Containing Sphingomyelin." Phys Rev Lett **94**(14): 148101.
Vereb, G., J. Matkó, et al. (2000). "Cholesterol-dependent clustering of IL-2Rα and its colocalization with HLA and CD48 on T lymphoma cells suggest their functional association with lipid rafts." Proceedings of the National Academy of Sciences **97**(11): 6013-6018.

Vereb, G., J. Szollosi, et al. (2003). "Dynamic, yet structured: The cell membrane three decades after the Singer-Nicolson model." Proc Natl Acad Sci U S A **100**(14): 8053-8058.

Vermes, I., C. Haanen, et al. (1995). "A novel assay for apoptosis. Flow cytometric detection of phosphatidylserine expression on early apoptotic cells using fluorescein labelled Annexin V." J Immunol Methods **184**(1): 39-51.

Vida, T. and B. Gerhardt (1999). "A cell-free assay allows reconstitution of Vps33p-dependent transport to the yeast vacuole/lysosome." J Cell Biol **146**(1): 85-98.

Vrielink, A., L. F. Lloyd, et al. (1991). "Crystal structure of cholesterol oxidase from Brevibacterium sterolicum refined at 1.8 A resolution." J Mol Biol **219**(3): 533-554.

Waheed, A. A. and E. O. Freed (2009). "Lipids and membrane microdomains in HIV-1 replication." Virus Research **143**(2): 162-176.

Wallach, D., E. E. Varfolomeev, et al. (1999). "Tumor necrosis factor receptor and Fas signaling mechanisms." Annu Rev Immunol **17**: 331-367.

Wang, L. H., K. G. Rothberg, et al. (1993). "Mis-assembly of clathrin lattices on endosomes reveals a regulatory switch for coated pit formation." J Cell Biol **123**(5): 1107-1117.

Wang, N., D. L. Silver, et al. (2000). "Specific Binding of ApoA-I, Enhanced Cholesterol Efflux, and Altered Plasma Membrane Morphology in Cells Expressing ABC1." Journal of Biological Chemistry **275**(42): 33053-33058.

Watanabe, M., M. Hitomi, et al. (2002). "The pros and cons of apoptosis assays for use in the study of cells, tissues, and organs." Microsc Microanal **8**(5): 375-391.

Weber, G. and F. J. Farris (1979). "Synthesis and spectral properties of a hydrophobic fluorescent probe: 6-propionyl-2-(dimethylamino)naphthalene." Biochemistry **18**(14): 3075-3078.

West, M. A., M. S. Bretscher, et al. (1989). "Distinct endocytotic pathways in epidermal growth factor-stimulated human carcinoma A431 cells." J Cell Biol **109**(6 Pt 1): 2731-2739.

White, M. K. and C. Cinti (2004). "A morphologic approach to detect apoptosis based on electron microscopy." Methods Mol Biol **285**: 105-111.

Williamson, P., A. Kulick, et al. (1992). "Ca2+ induces transbilayer redistribution of all major phospholipids in human erythrocytes." Biochemistry **31**(27): 6355-6360.

Williamson, P. and R. A. Schlegel (1994). "Back and forth." Mol Membr Biol **11**(4): 199-216.

Willingham, M. C. and I. Pastan (1984). "Endocytosis and exocytosis: current concepts of vesicle traffic in animal cells." Int Rev Cytol **92**: 51-92.

Woolfe, G. J. and P. J. Thistlethwaite (1981). "Direct observation of excited state intramolecular proton transfer kinetics in 3-hydroxyflavone." J Am Chem Soc **103**(23): 6916-6923.

Wyllie, A. H. (1980). "Glucocorticoid-induced thymocyte apoptosis is associated with endogenous endonuclease activation." Nature **284**(5756): 555-556.

Yamashiro, D. J. and F. R. Maxfield (1984). "Acidification of endocytic compartments and the intracellular pathways of ligands and receptors." J Cell Biochem **26**(4): 231-246.

Yarar, D., C. M. Waterman-Storer, et al. (2005). "A dynamic actin cytoskeleton functions at multiple stages of clathrin-mediated endocytosis." Mol Biol Cell **16**(2): 964-975.

Yoshimori, T., P. Keller, et al. (1996). "Different biosynthetic transport routes to the plasma membrane in BHK and CHO cells." J Cell Biol **133**(2): 247-256.

Zamzami, N., C. El Hamel, et al. (2000). "Bid acts on the permeability transition pore complex to induce apoptosis." Oncogene **19**(54): 6342-6350.

Zhong, D., A. Douhal, et al. (2000). "Femtosecond studies of protein–ligand hydrophobic binding and dynamics: Human serum albumin." Proceedings of the National Academy of Sciences **97**(26): 14056-14061.

Zidovetzki, R. and I. Levitan (2007). "Use of cyclodextrins to manipulate plasma membrane cholesterol content: Evidence, misconceptions and control strategies." Biochimica et Biophysica Acta (BBA) - Biomembranes **1768**(6): 1311-1324.

Ziello, J. E., Y. Huang, et al. (2010). "Cellular endocytosis and gene delivery." Mol Med **16**(5-6): 222-229.

Zwaal, R. F. and A. J. Schroit (1997). "Pathophysiologic implications of membrane phospholipid asymmetry in blood cells." Blood **89**(4): 1121-1132.

Zweifach, A. (2000). "FM1-43 reports plasma membrane phospholipid scrambling in T-lymphocytes." Biochem J **349**(Pt 1): 255-260.

# *Appendix:*

# *Publication 3*

In addition to my dissertation work, I had the opportunity to collaborate on another project that is presented in paper shortly introduced below:

## A FRET-based probe with a chemically deactivatable quencher

A new concept of a chemically deactivatable quencher is proposed for a FRET-based probe that turns-on its fluorescence by either an enzymatic cleavage or a chemical reagent (sodium dithionite). A caspase-3 activity-sensitive probe containing a peptide which was used to link a fluorescent dye NR12S and a ‘‘chemically deactivatable quencher’’ was developed. The synthesized probe was shown to turn-on its fluorescence in response to both recombinant and endogenous caspase-3 stimuli produced by apoptosis, whereas it can be turned-on independently by dithionite deactivation of the quencher. The advantages of this novel strategy over traditional ‘‘turn-on’’ probes include control for internalization and localization of the probe in living cells in response to specific stimulus so it is ideal for assaying different biological stimuli. This work opens the way for the development of a new generation of enzymatic probes containing an internal control.

ChemComm

View Online / Journal Homepage / Table of Contents for this issue
Dynamic Article Links

Cite this: *Chem. Commun.*, 2012, **48**, 3224–3226

www.rsc.org/chemcomm

COMMUNICATION

# A FRET-based probe with a chemically deactivatable quencher†

**Geoffray Leriche,[a] Ghyslain Budin,[a] Zeinab Darwich,[b] Denis Weltin,[c] Yves Mély,[b] Andrey S. Klymchenko[b] and Alain Wagner*[a]**

***Received 2nd December 2011, Accepted 27th January 2012***
**DOI: 10.1039/c2cc17542h**



**A new concept of a chemically deactivatable quencher is proposed for a FRET-based probe that turns-on its fluorescence by either an enzymatic cleavage or a chemical reagent (sodium dithionite). This concept allowed us to quantify the caspase-3 cleavage activity in solution and to reveal unreacted probes in cell experiments.**

Fluorescence is widely used to study biological processes in living cells. Recently, turn-on probes have been developed to measure cell enzymatic activity, pH alterations and to detect singlet oxygen, nitric oxide and highly reactive oxygen species (hROS).[1]

Common turn-on probes are designed by linking a fluorescent dye and a quencher together *via* a biologically labile covalent bond. The most frequently used quencher moieties are non-emitting dyes, which act as FRET acceptors for the covalently bound fluorescent dye. The fluorescence is often turned-on by the enzymatic cleavage of the linker, resulting in separation of the fluorescent dye from the quencher (Scheme 1A). This strategy was used to image different enzymes activities such as cathepsins, caspases and MMPs.[2] Recently, this approach was also used to image free thiols in cells by the cleavage of either a disulfide bridge[3] or a vinyl sulfide group.[4]

Currently used turn-on fluorescent probes are not detectable until activation leading to a high signal-to-noise ratio, which is advantageous for live cell imaging. However, in the case where there is no or weak signal, it is impossible to assess whether this is due to weak biological activity, insufficient probe concentration or inappropriate cellular localization of the probe. Having the ability to detect the substrate entering within the cells would have far reaching applications in biology.

The strategy developed here relies on the design of a probe whose fluorescence can be turned-on either by a biological stimulus or by a chemical reagent. The probe contains a central biosensitive bond that links a fluorescent dye and a chemically deactivatable quencher. When the labile bond is cleaved, the fluorescence is turned-on enabling the biological stimulus to be detected (Scheme 1A). Then, a chemical reagent capable of deactivating the quencher can be used to turn-on fluorescence of the unreacted probe (Scheme 1B), allowing estimation of biological cleavage. This is particularly important for intracellular studies where the probe localisation and concentration are difficult to predict.

We selected an azo-based molecule as a suitable quencher[5] and dithionite as a chemical reagent of relatively low toxicity.[6] The azo-groups are known to react readily and under mild reduction conditions with dithionite[7] leading to N=N bond cleavage. Consequently, when the azo-quencher is linked to a fluorescent dye, dithionite can deactivate the quencher and turn-on the fluorescence.

Dabcyl (4-(4′-dimethylamino-phenylazo)benzoic acid) is a common azo-based quencher widely used in a variety of biomolecular applications and nucleic acid probes.[8] To the best of our knowledge no information on Dabcyl reduction with dithionite has been published. The **Dabcyl** dye was then incubated with a 1 mM sodium dithionite solution in phosphate buffer (pH 7.4, 100 mM) and the azo bond cleavage was monitored using UV spectrophotometry at 460 nm. The half-life of **Dabcyl** was longer than 13 minutes (Fig. S1, ESI†) and could not be transposed to live cells. To overcome this low reactivity, we used a highly reactive (4-hydroxy-2-methoxy-phenylazo) benzoic acid **CDQ** (Fig. 1) as a suitable chemically deactivatable quencher candidate.[9] This molecule has a UV profile similar to **Dabcyl**, but undergoes a faster cleavage. With a 1 mM sodium dithionite solution, this compound exhibited a half-life of less than 1 second and total cleavage was achieved in less than 15 seconds (Fig. S1 and S2, ESI†).

Considering these results, we linked the chemically deactivatable quencher (CDQ) to a fluorescent dye. Its absorption spectrum overlaps with the emission of the 7-diethylaminocoumarin-3-carboxylic acid (DEAC), which has a 470-nm emission maximum (Fig. S3, ESI†). The corresponding chemically deactivatable probe **2** (Fig. 1) was synthesized in five steps with an overall yield of 19% (see ESI†).

Quencher deactivation kinetics was investigated by adding dithionite (1 mM) to the FRET-based probe **2**. A rapid 17-fold increase of fluorescence intensity was observed following cleavage of **2**, with a short half life of ~10 seconds (Fig. 2A and B). We verified the photostability of the fluorescent dye **1** and its stability towards dithionite (Fig. 2A). The deactivation of **2** in the presence of dithionite was complete, as it can be seen from the disappearance of its absorption peak at 490 nm (Fig. S4, ESI†). Since **2** showed very good quencher deactivation properties, we used this couple of CDQ/DEAC groups in the design of a fluorometric dual turn-on caspase-3 sensitive probe.[10]

We synthesized a dual probe: CDQ-DEVD-G-DEAC **3**. This probe consists of three parts: an L-amino acid effector caspase-3 recognition sequence (DEVD)[11] that is flanked by

[a] *Laboratory of Functional Chemo-Systems UMR 7199, 74 Route du Rhin, 67401, Illkirch, France. E-mail: wagner@bioorga.u-strasbg.fr; Fax: +33 368854306*
[b] *Laboratoire de Pharmacologie et Physicochimie, UMR 7213 CNRS, 74 Route du Rhin, 67401, Illkirch, France*
[c] *PhytoDia SAS, Boulevard Sébastien Brant, 67412 Illkirch, France*
† Electronic supplementary information (ESI) available. See DOI: 10.1039/c2cc17542h

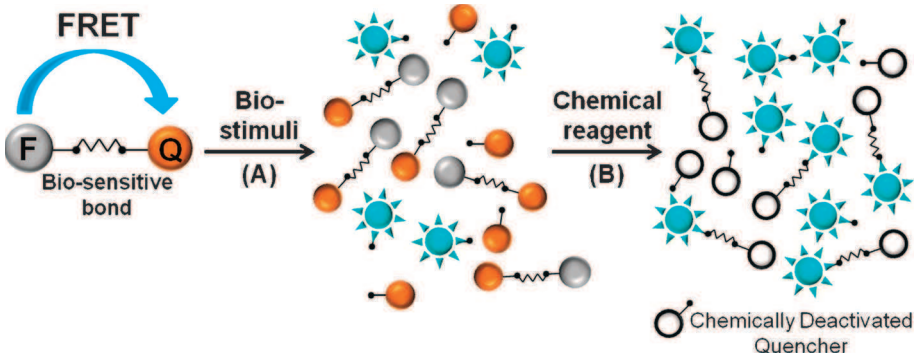


**Scheme 1** Principle of FRET-based probe with a chemically deactivatable quencher. (A) In the presence of biological stimuli, the labile bond is cleaved and the fluorescence is turned-on enabling the biological stimuli to be detected. (B) The introduction of a chemically deactivatable quencher allows us to reveal the presence of an inactivated probe by treatment with a chemical reagent.

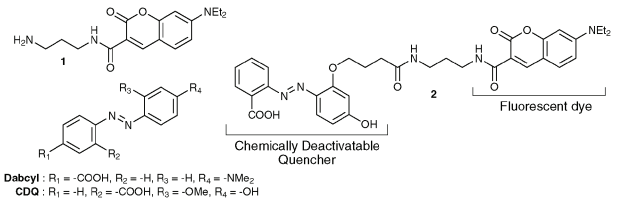


**Fig. 1** Structures of cleavable quenchers (**Dabcyl** and **CDQ**), modified DEAC **1**, and probe **2**.

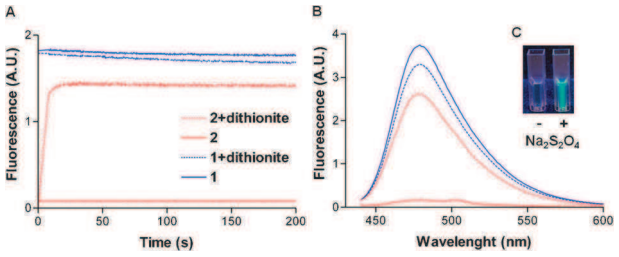


**Fig. 2** Quencher deactivation analysis in FRET-based probe. (A) Deactivation kinetics of **1** (dashed blue line) and **2** (dashed red line) with 1 mM of sodium dithionite. Photo-stability of **1** (solid blue line) and **2** (solid red line). Excitation and emission wavelengths were 430 and 476 nm, respectively. (B) Emission fluorescence spectra of compounds **1** (blue lines) and **2** (red lines) before (solid lines) and after deactivation with 1 mM of dithionite solution (dashed lines). All data were recorded with a probe concentration of 2 μM in phosphate buffer (pH 7.4, 100 mM). (C) Cuvettes under a UV-lamp containing **2** (20 μM) without and with dithionite (1 mM).

the chemically deactivatable quencher (CDQ) and the fluorescent dye (DEAC). Probe **3** was synthesized in 12 steps using Fmoc chemistry in solution (see ESI†). After the quencher moiety of **3** was deactivated by dithionite, the fluorescence signal was increased by 22-fold (Fig. S5, ESI†). Thus, the quenching efficacy and therefore the turn-on property of probe **3** was as good as those of probe **2**, despite the longer peptide linker length in the former.

*In vitro* enzyme kinetic studies were performed using human recombinant caspase-3 enzyme, probe **3**, and the commercially available turn-on fluorescent substrate Ac-DEVD-AMC **4**, used as control (AMC = 7-amino-4-methylcoumarin). Both probes were incubated with caspase-3 at 25 °C in buffer and showed comparable fluorescence enhancement kinetics (Fig. 3A and Fig. S6, ESI†). This result indicates that the CDQ/DEAC pair does not perturb the enzymatic activity of caspase-3. After 300 minutes, when saturation curves were

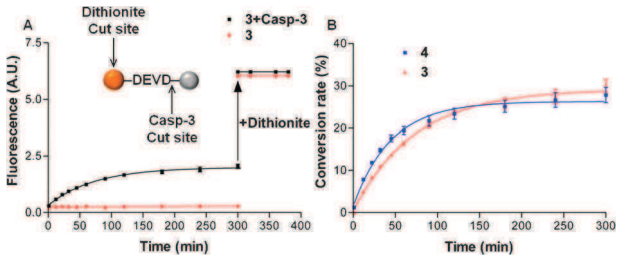


**Fig. 3** Response to caspase-3 cleavage and dithionite quencher deactivation. (A) Cleavage kinetics of **3** at 2 μM by human recombinant caspase-3 at 25 or 0 ng $mL^{-1}$ (black and red lines, respectively). The arrow indicates the addition of dithionite (1 mM for 1 min) to cleave probe excess. (B) Conversion rates for **3** and **4** calculated from dithionite cleavage or AMC standard, respectively.

observed, dithionite (1 mM, 1 min) was added to the reaction mixture with **3**. A 3.1-fold fluorescence increase was observed, indicating that some unreacted probe was still present. This incomplete conversion might be imputed to enzyme inhibition by the reaction product. The chemical deactivation of the quencher enables us to calculate the total concentration and the conversion rate of the fluorescent substrate (Fig. 3B). After 300 minutes, 30% of **3** had been enzymatically cleaved by the recombinant caspase-3. To estimate the amount of uncleaved probe **4**, the fluorescence intensity was compared to the free fluorescent dye, AMC, at the same concentration (2 μM). A 3.5-fold difference was recorded, which is similar to the signal observed for probe **3** (Fig. S6, ESI†). Thus, the chemically deactivatable quencher allows direct estimation of the probe conversion rate.

In the control experiment, a competitive inhibition study of caspase-3 was performed using a commercially available inhibitor, Ac-DEVD-CHO **5** (Fig. S7, ESI†). As expected, an increase in the inhibitor concentration slowed down the enzymatic cleavage.

The chemical activation of **3** was then studied in tissue culture. HeLa cells were incubated for 1 hour with **3**. After washing out probe excess, cells were incubated with dithionite. In the control experiment, cells were treated with HEPES buffer, instead of dithionite (Fig. 4A). The quencher deactivation was monitored using live-cell imaging (Fig. 4). Fluorescence could be clearly seen in dithionite treated cells after 15 minutes and the intensity continued to increase for 45 minutes. After 45 minutes, a maximum intensity was reached indicating that all the probes were chemically turned-on. It confirms that dithionite can abolish the

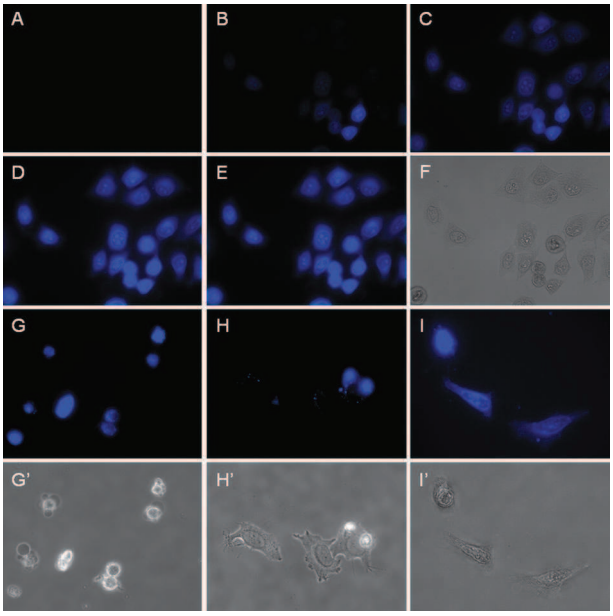


**Fig. 4** Fluorescence and brightfield microscopy images of HeLa cells treated with **3** (40 μM, 1 h). (A–F) Quencher deactivation kinetics with dithionite (10 mM) at different time points: 15 (B), 30 (C), 45 (D), 60 min (E). In the control experiment (A), the cells were incubated with HEPES buffer. (F) Brightfield image of cells after 60 min of dithionite treatment. (G–H′) Response of **3** to apoptotic cells (pre-treated with Actinomycin D (0.5 μg $mL^{-1}$, 18 h)). (I and I′) Quencher deactivation with dithionite (10 mM, 45 min) in apoptotic cells. The images were acquired with the same camera settings, but with a different fluorescence scale ranging from 2700 to 7360 (G–H) and from 7880 to 36 010 (all others). The image size was 219 × 163 μm (A–H′) and 146 × 109 μm (I and I′).

FRET-quenching in **3** in healthy cells. Compared to an *in vitro* experiment, *in vivo* dithionite-mediated quencher deactivation is much slower due to the low dithionite membrane permeability. It should be noted that the cells treated with dithionite showed slightly different morphology, which could be connected with cell shrinkage (Fig. S8, ESI†). However, after dithionite treatment the morphology remained unchanged for the experiment timescale. According to luciferase ATP assay, the dithionite cytotoxicity was low, even at a 10 mM concentration (Fig. S9, ESI†). Numerous reports showed that dithionite can be used as a reductive agent in cell culture, without strong cytotoxicity effects at the millimolar range.[12]

Then we assessed cell internalization of probe **3** as a function of incubation time. Cells were treated with 40 μM of **3** for different times (15, 30, 60 and 120 min), washed and incubated with 10 mM of dithionite for 45 min (Fig. S8, ESI†). Results showed an increase in the probe internalization during the first hour of incubation, and then reached a plateau. This allowed us to determine the optimal incubation time of the cells with the probe, which would not be possible for classical turn-on probes.

The biological activation of **3** in live HeLa cells was then tested. Apoptosis was induced to activate caspase-3, which can cleave the DEVD peptide linker in **3**. Cells were incubated with Actinomycin D for 18 hours and then with **3** for 1 hour. Cells undergoing apoptosis were recognized by their rounded morphology and bright blue fluorescence, indicating that **3** had been cleaved in these cells. In addition, we observed different levels of fluorescence intensity for the Actinomycin-D-treated cells, which is most likely due to the cells being in different stages of apoptosis (Fig. 4G and G′). In contrast, cells with a healthy morphology had only very low levels of fluorescence (Fig. 4H and H′), in line with data on non-treated HeLa cells (Fig. 4A). The quencher was further deactivated in the cells by 10 mM dithionite treatment for 45 minutes. A strong increase in fluorescence was observed in both apoptotic and healthy cells (Fig. 4I and I′), indicating the presence of uncleaved probe **3** in the both cell populations and confirms the presence of the probe in non-fluorescent healthy cells. Thus, we have shown that the fluorescence of probe **3** is only turned-on in apoptotic cells, and the "chemically deactivatable quencher" confirms the presence of the probe in all cells.

In conclusion, we have developed a caspase-3 activity-sensitive probe containing a DEVD peptide which was used to link a fluorescent dye and a "chemically deactivatable quencher". The synthesized probe was shown to turn-on its fluorescence in response to both recombinant and endogenous caspase-3 stimuli, whereas it can be turned-on independently by dithionite deactivation of the quencher. The advantages of this novel strategy over traditional "turn-on" probes include control for internalization and localization of the probe in living cells, irrespective of whether they contain the biological stimulus or not. The "chemically deactivatable quencher" concept can be applied to all "turn-on probes" with a fluorescent dye-linker-quencher structure for assaying different biological stimuli. These results pave the way for the development of a new generation of enzymatic probes containing an internal control.

We thank D. Dujardin and R. Vauchelles from PIQ imaging platform for help with fluorescence imaging.

## Notes and references

1 H. Kobayashi, M. Ogawa, R. Alford, P. L. Choyke and Y. Urano, *Chem. Rev.*, 2010, **110**, 2620–2640.
2 (*a*) R. Weissleder, C. H. Tung, U. Mahmood and A. Bogdanov, *Nat. Biotechnol.*, 1999, **17**, 375–378; (*b*) C. Bremer, C.-H. Tung and R. Weissleder, *Nat. Med.*, 2001, **7**, 743–748; (*c*) C.-H. Tung, *Pept. Sci.*, 2004, **76**, 391–403.
3 (*a*) J. Razkin, V. Josserand, D. Boturyn, Z.-H. Jin, P. Dumy, M. Favrot, J.-L. Coll and I. Texier, *ChemMedChem*, 2006, **1**, 1069–1072; (*b*) W. Gao, R. Langer and O. C. Farokhzad, *Angew. Chem., Int. Ed.*, 2010, **49**, 6567–6571.
4 H.-Y. Shiu, H.-C. Chong, Y.-C. Leung, M.-K. Wong and C.-M. Che, *Chem.–Eur. J.*, 2010, **16**, 3308–3313.
5 K. E. Sapsford, L. Berti and I. L. Medintz, *Angew. Chem., Int. Ed.*, 2006, **45**, 4562–4589.
6 (*a*) J. M. Bergen, E. J. Kwon, T. W. Shen and S. H. Pun, *Bioconjugate Chem.*, 2008, **19**, 377–384; (*b*) O. A. Kucherak, S. Oncul, Z. Darwich, D. A. Yushchenko, Y. Arntz, P. Didier, Y. Mély and A. S. Klymchenko, *J. Am. Chem. Soc.*, 2010, **132**, 4907–4916.
7 (*a*) T. L. Schlick, Z. Ding, E. W. Kovacs and M. B. Francis, *J. Am. Chem. Soc.*, 2005, **127**, 3718–3723; (*b*) G. Budin, M. Moune-Dimala, G. Leriche, J.-M. Saliou, J. Papillon, S. Sanglier-Cianférani, A. Van Dorsselaer, V. Lamour, L. Brino and A. Wagner, *ChemBioChem*, 2010, **11**, 2359–2361.
8 (*a*) S. Tyagi, S. a. Marras and F. R. Kramer, *Nat. Biotechnol.*, 2000, **18**, 1191–1196; (*b*) S. Bernacchi and Y. Mély, *Nucleic Acids Res.*, 2001, **29**, E62.
9 G. Leriche, G. Budin, L. Brino and A. Wagner, *Eur. J. Org. Chem.*, 2010, **2010**, 4360–4364.
10 M. Hu, L. Li, H. Wu, Y. Su, P.-Y. Yang, M. Uttamchandani, Q.-H. Xu and S. Q. Yao, *J. Am. Chem. Soc.*, 2011, **133**, 12009–12020.
11 R. V. Talanian, C. Quinlan, S. Trautz, M. C. Hackett, J. A. Mankovich, D. Banach, T. Ghayur, K. D. Brady and W. W. Wong, *J. Biol. Chem.*, 1997, **272**, 9677–9682.
12 (*a*) J. C. McIntyre and R. G. Sleight, *Biochemistry*, 1991, **30**, 11819–11827; (*b*) L. Dafik, V. Kalsani, A. K. L. Leung and K. Kumar, *J. Am. Chem. Soc.*, 2009, **131**, 12091–12093.

 

# Publications

**Articles in peer-reviewed journals:**

1. **Darwich, Z.,** Klymchenko, A., Kucherak, O.A., Richert, L., Mély, Y. Detection of apoptosis through the lipid order of the outer plasma membrane leaflet. *Biochimica et Biophysica Acta Biomembranes* **2012,** 1818, 3048-3054;
2. **Darwich, Z.,** Kucherak, O.A., Richert, L., Klymchenko, A., Mély, Y. Rational design of membrane probes for apoptosis based on 3-hydroxyflavone. *Methods Appl. Fluoresc.* **2013**;
3. **Darwich, Z.,** Kucherak, O.A., Richert, L., DuJardin, D., Klymchenko, A., Mély, Y. Lipid order and maturation of endosomes studied by Nile Red-based membrane probe (in preparation);
4. Perino, A., Morin-Picardat, E., **Darwich, Z.,** Weltin, D., Mély, Y., Remy, J.S., Klymchenko, A., Wagner, A. Photopolymerized micelles of diacetylene amphiphile: properties and interactions with cells (in revision *Chem. Comm*);
5. Leriche, G., Budin, G., **Darwich, Z.,** Weltin, D., Mély, Y., Klymchenko, A.S., Wagner, A. A FRET-based probe with a chemically deactivable quencher. *Chem. Commun.* **2012,** 48, 3224–3226 ;
6. Kucherak, O.A., Oncul, S., **Darwich, Z.,** Yushchenko, D.A., Arntz, Y., Didier, P., Mély, Y., Klymchenko, A. Switchable Nile Red-based probe for cholesterol and lipid order at the outer leaflet of biomembranes. *J.Am.Chem.Soc.* **2010,** 132, 4907-4916.

**Chapters :**

**Darwich, Z.**, Klymchenko, S., Mély, Y. **Monitoring membrane properties and apoptosis using membrane probes of the 3-hydroxyflavone family** in *Fluorescence Spectroscopy and Microscopy: Methods and Protocols.*

**Results were presented at the following congresses:**

1. **Zeinab Darwich**, Oleksander A. Kucherak, Youri Arntz, Pascal Didier, Andrey S. Klymchenko, Yves Mély. **Switchable Nile-Red based probe for quantification of cholesterol-rich liquid ordered phase in cell membranes**. Groupe d'Etudes des Membranes-GEM XV- Paris, France, April 2012 (Oral Communication);

2. **Zeinab Darwich**, Oleksander A. Kucherak, Youri Arntz, Pascal Didier, Andrey S. Klymchenko, Yves Mély. **Studies of apoptosis and lipid order of cell membranes using new fluorescent probes.** 12$^{th}$ International Conference on Methods and Applications of Fluorescence: Spectroscopy, Imaging and Probes MAF12- Strasbourg, France, September 2011 (Poster);

3. **Zeinab Darwich**, Oleksander A. Kucherak, Youri Arntz, Pascal Didier, Andrey S. Klymchenko, Yves Mély. **Studies of apoptosis and lipid order of cell membranes using new fluorescent probes.** Journée Campus Illkirch- JCI- Illkirch 2010 (Poster).

# Sondes fluorescentes membranaires ratiométriques pour l'étude des changements d'ordre lipidique lors de l'apoptose et de l'endocytose

Les membranes plasmiques des cellules eucaryotes constituent une barrière sélective permettant une protection du milieu intracellulaire. La membrane plasmique est essentiellement constituée d'une bicouche de lipides incorporant de nombreuses protéines. Les lipides constitutifs de cette bicouche sont des phospholipides tels que phosphatidylcholine (PC), phosphatidyléthanolamine (PE), phosphatidylsérine (PS), des sphingolipides tels que la sphingomyéline (SM) et des stérols tel le cholestérol. Parmi les propriétés membranaires, l'une des plus remarquables, qui retiendra notre attention, est l'asymétrie membranaire, avec PC et SM essentiellement présents dans le feuillet externe et PE et PS dans le feuillet interne.

Durant la dernière décennie, l'étude des domaines lipidiques fût l'une des préoccupations majeures des "membranologues". L'hypothèse actuellement la plus communément admise est la coexistence, notamment dans le feuillet externe de la membrane, de domaines lipidiques différents, d'une part ceux riches en SM et cholestérol, présentant une phase dite liquide ordonnée (Lo) et d'autre part ceux riches en lipides insaturés en phase liquide désordonnée (Ld). La coexistence de tels domaines résulte d'une séparation de phase classique au niveau membranaire entre la phase ordonnée Lo et la phase désordonnée Ld. Outre leur différence d'ordre membranaire, ces deux phases diffèrent également par d'autres propriétés physiques telles l'hydratation et la polarité. Il en résulte notamment une distribution différente des protéines membranaires entre ces deux phases. Plusieurs approches biophysiques et biologiques confirment cette hypothèse mais toujours de manière indirecte (études par spectroscopie, isolement de fractions membranaires résistantes aux détergents,..). En effet, les limites de résolution tant spatiale que temporelle de différentes microscopies ne permettent pas la visualisation de tels domaines lipidiques transitoires (de durée de vie ~ 10 ms), dont les tailles sont probablement inférieures à 100 nm.

Afin de visualiser ces domaines lipidiques et de caractériser leurs propriétés biophysiques notamment au niveau des membranes cellulaires, différentes sondes fluorescentes membranaires ont été développées. Mon travail de thèse a été focalisé sur deux familles de sondes fluorescentes membranaires synthétisées au laboratoire. Ces sondes présentant un groupe zwitterionique et une longue chaîne alkyle imitant les lipides, se lient spécifiquement et à haute affinité au feuillet lipidique externe de la membrane plasmique cellulaire. Le but de mon travail a été de caractériser ces sondes sur des modèles lipidiques (liposomes) puis sur des cellules eucaryotes vivantes. Au niveau de leurs applications, je me suis intéressée à l'étude des changements d'ordre lipidique membranaire survenant lors de l'apoptose et de l'endocytose.

**Sondes 3-Hydroxyflavones.** La première série de sondes appartient à la famille des 3-hydroxyflavones, Ces molécules sont caractérisées par une émission duale due à une réaction de transfert de proton à l'état excité (ESIPT) induisant une tautomérisation entre 2 formes excitées : une forme dite normale (N*) et sa forme tautomère (T*), ce qui permet de caractériser leur environnement par le rapport d'intensité des deux bandes d'émission (N*/T*).

La première sonde de cette famille que nous avons étudié, F2N12S, montre un important solvatochromisme ainsi qu'une bonne sensibilité à la composition lipidique membranaire. Nous avons observé que le rapport N*/T* de cette sonde s'accroît après extraction du cholestérol, de manière similaire à ce qui avait été observé après induction d'apoptose. A l'aide de modèles de membranes lipidiques (vésicules unilamellaires de grande taille, LUVs,

et géantes, GUVs), nous avons montré que la sonde présente une excellente sensibilité à la phase lipidique et qu'elle permet de visualiser de manière différentielle les phases Lo et Ld, suggérant que la réponse de la sonde lors de l'apoptose est en partie liée au changement de composition lipidique consécutive à la perte d'asymétrie membranaire.

Par la suite, nous avons comparé la réponse de F2N12S à celle de trois nouvelles sondes F46NS, F66NS et F86NS (Figure 1), présentant un groupe zwitterionique du côté opposé à la chaîne alkyl, ce qui leur confère une insertion verticale dans la membrane. Ces nouvelles sondes présentent des propriétés spectroscopiques améliorées par rapport à F2N12S (Figure 2), sauf pour F86NS. Ainsi, F66NS est plus brillante que F2N12S du fait de sa meilleure insertion dans la bicouche lipidique sans doute due à sa longue chaîne alkyl, alors que F46NS montre une meilleure sensibilité à la composition lipidique.

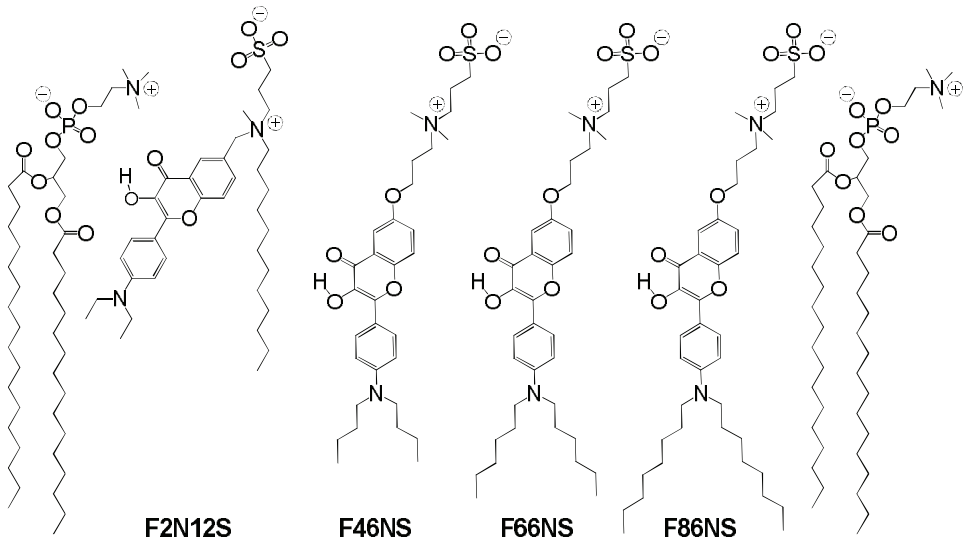


**Figure 1 :** Structure de F2N12S et ses sondes dérivées (F46NS, F66NS et F86NS).

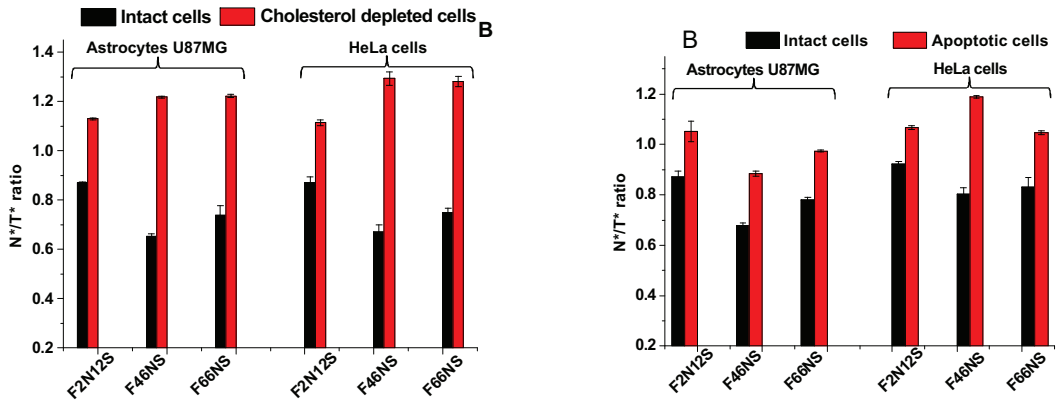


**Figure 2 :** Intensités intégrées des sondes F2N12S, F46NS et F66NS. Rapport N*/T* des différentes sondes dans des cellules U87MG et HeLa saines ou appauvries en cholestérol (A) ou apoptotiques (B).

La réponse des ces sondes a été également suivie par imagerie ratiométrique de fluorescence (Figure 3) et par cytométrie de flux (Figure 4). Ainsi, les cellules traitées à la méthyl-ß-cyclodextrine et celles rendues apoptotiques présentent un rapport N*/T* inférieur à celui des cellules intactes (Figure 2). Les images confirment également une meilleure intensité de fluorescence pour F66NS comparée à F2N12S et F46NS.

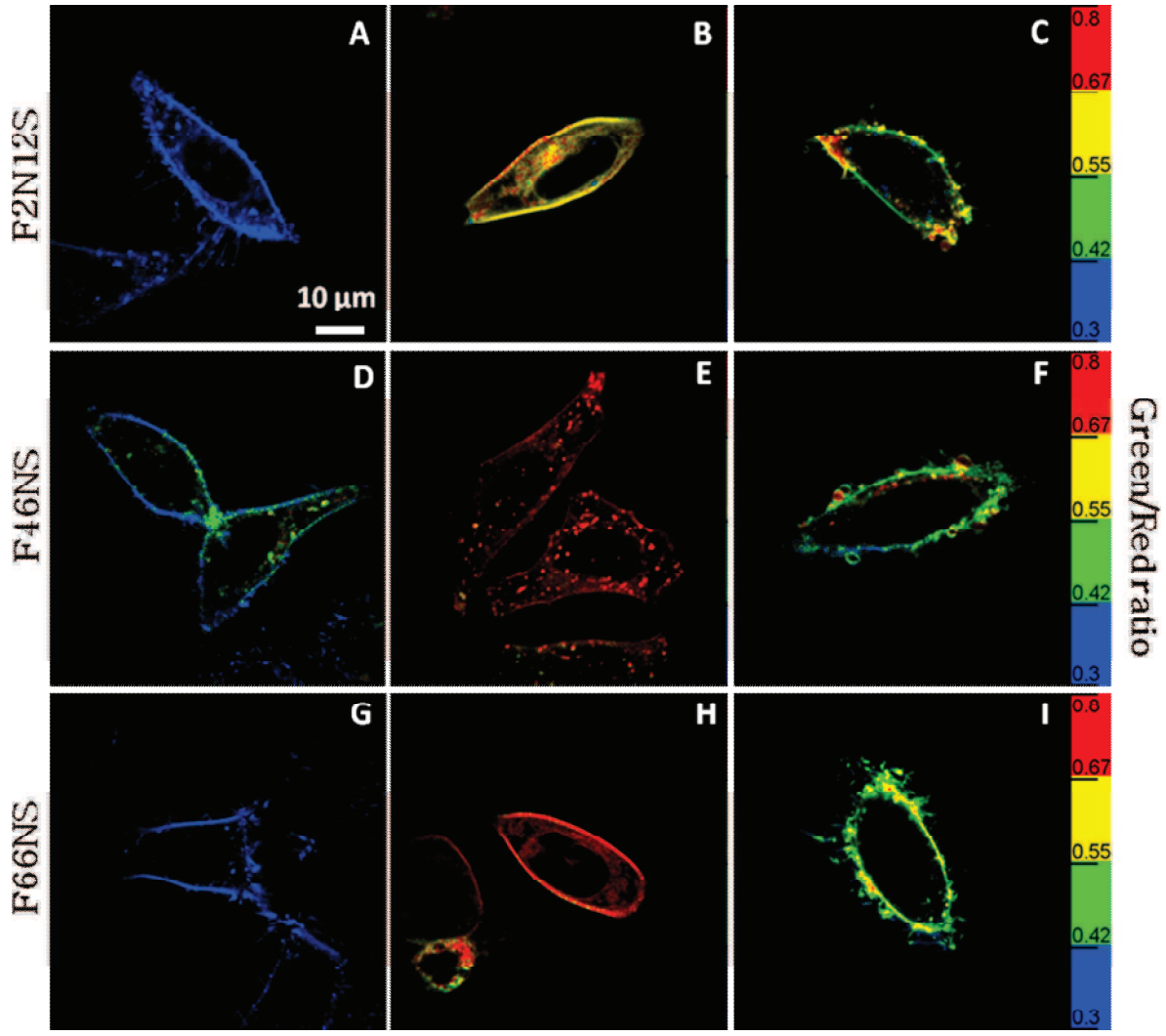


**Figure 3 :** Application de nouvelles sondes 3-HF en imagerie ratiométrique avec des cellules intactes (A, D, G), des cellules appauvries en cholestérol (B, E, H) et des cellules en apoptose (C, F, I).

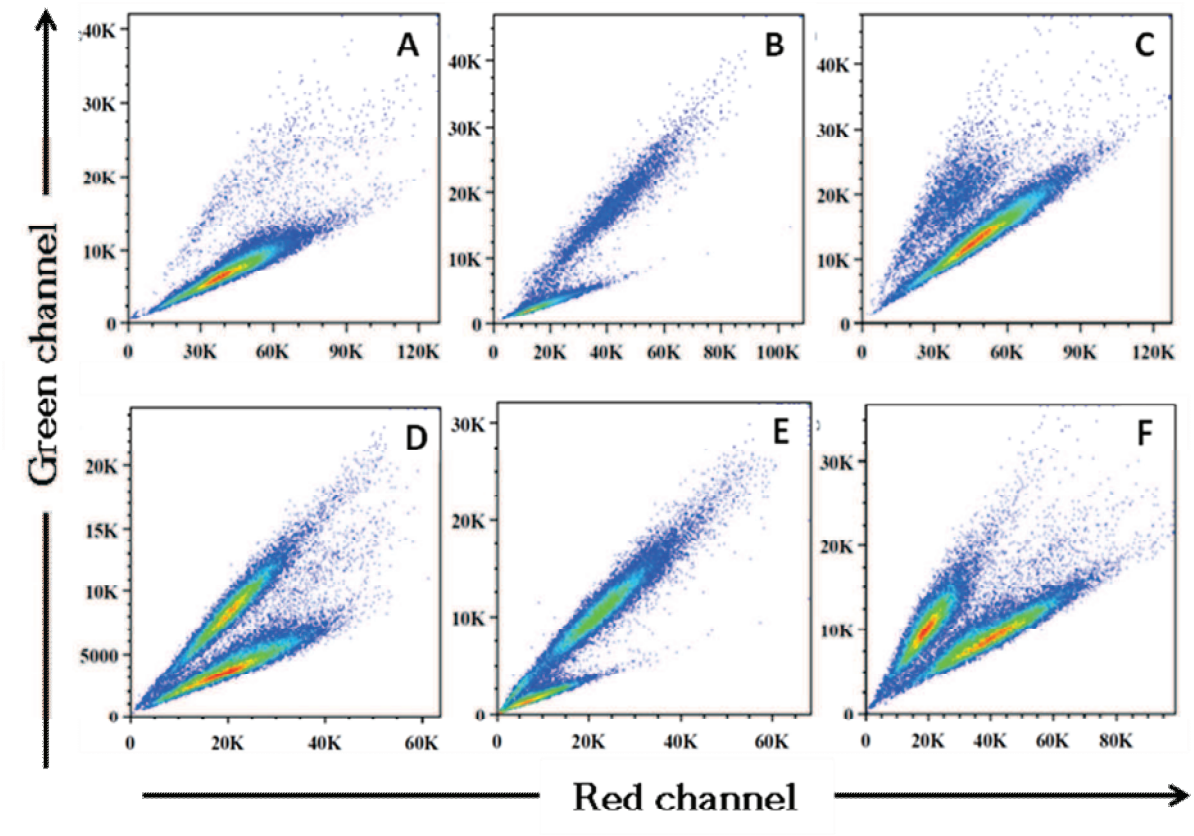


**Figure 4 :** Application de nouvelles sondes 3-HF pour la cytométrie de flux. Cellules intactes (A-C) et cellules apoptotiques (D-F) marquées avec F2N12S (A, D), F46NS (B, E) et F66NS (C, F). Pour chaque sonde (0.1µM), l'intensité de fluorescence du canal rouge (axe des abscisses) et du canal vert (axe des ordonnées) est représentée.

**Sonde dérivée du Rouge Nil, NR12S,** Le Rouge Nil présente de bonnes propriétés spectrales pour les applications biologiques, mais ne permet pas de marquage spécifique des biomembranes. En utilisant la même stratégie que pour F2N12S, nous avons développé un dérivé de cette sonde capable de marquer spécifiquement la membrane plasmique, en y greffant un groupe zwitterionique et une longue chaîne alkyle. Cette sonde présente une émission dans le rouge, adaptée aux applications biologiques, ainsi qu'une large bande d'émission, permettant une mesure ratiométrique à partir des deux bords du spectre.

Des études menées sur des LUVs, en utilisant le dithionite comme réducteur pour inhiber spécifiquement la fluorescence de NR12S sur le feuillet membranaire externe montrent que cette sonde marque spécifiquement ce feuillet externe et présente un flip-flop très lent entre les deux feuillets. Le marquage de GUVs de phases lipidiques différentes (Lo, Ld, ou Lo + Ld) a permis de montrer en outre un excellent contraste du rapport d'intensité.

Les études spectroscopiques menées avec des cellules ont montré que NR12S est capable de détecter le changement de composition lipidique après extraction du cholestérol, après traitement par la sphingomyélinase ou la cholestérol oxidase ainsi qu'après induction de l'apoptose par différents agents. Ces différents traitements induisent tous un effet identique sur le spectre d'émission de NR12S, avec un déplacement de la bande d'émission vers le rouge comparable au déplacement observé lors du passage d'une phase Ld vers une phase Lo sur des liposomes.

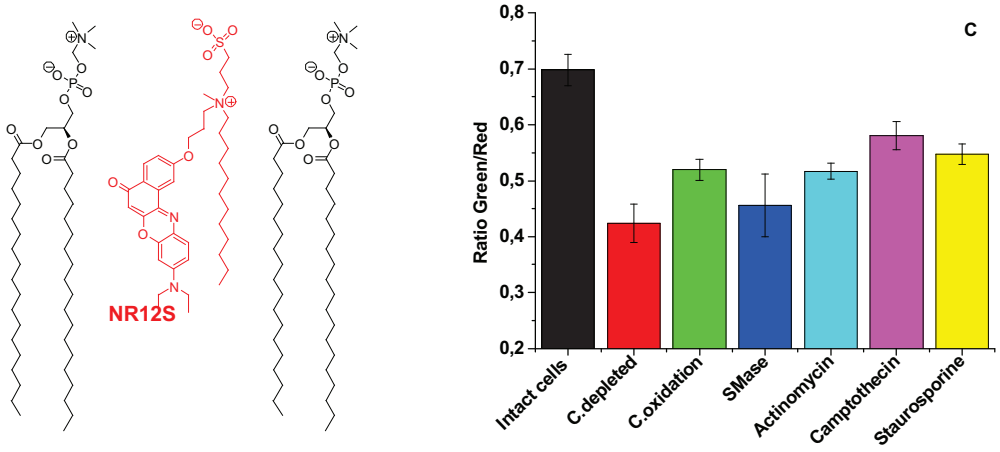


**Figure 5 :** Structure de la sonde NR12S (gauche). Ratio vert/rouge de NR12S en fonction de différents traitements (droite).

Des expériences de microscopie de fluorescence ont également été réalisées sur des cellules marquées avec NR12S. Les images ratiométriques montrent des rapports différents entre cellules intactes d'une part et cellules traitées au méthyl-ß-cyclodextrine et cellules apoptotiques d'autre part. On observe pour ces dernières, une diminution du rapport vert/rouge, cohérente avec les résultats de spectroscopie de fluorescence.

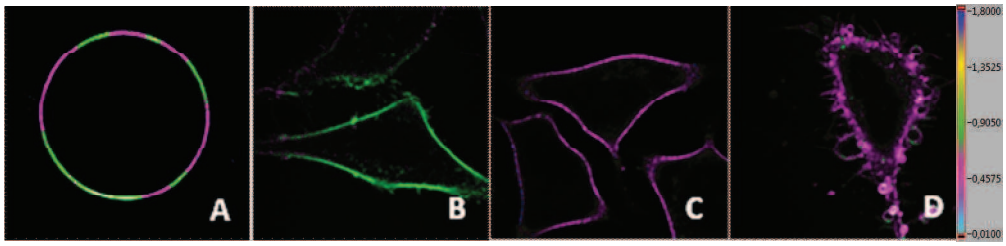


**Figure 6 :** Application de la sonde NR12S en imagerie ratiométique avec des vésicules géantes (A), des cellules vivantes (B), des cellules appauvries en cholestérol (C) et des cellules en apoptose.

NR12S ayant démontré sa capacité à détecter l'apoptose par spectroscopie et microscopie de fluorescence, cette sonde a été utilisée pour valider également cette application par cytométrie de flux. Le protocole utilisant l'annexine V couplée à la fluorescéine est actuellement le plus utilisé pour différencier les cellules intactes des cellules apoptotiques, en mettant à profit la liaison de l'Annexine V aux phospholipides PS exposés sur le feuillet externe des membranes plasmiques des cellules apoptotiques. Les mesures en cytométrie de flux effectuées avec NR12S, par détection de sa fluorescence simultanément dans 2 canaux (bords vert et rouge du spectre) ont mis en évidence une bonne séparation des populations de cellules saines et apoptotiques. L'application de NR12S pour la cytométrie de flux présente des avantages par rapport au test à l'annexine V, de part sa simplicité d'application ainsi que par l'absence d'artefacts liés au traitement des cellules (trypsinisation dans le cas des cellules adhérentes) lors de la préparation des échantillons.

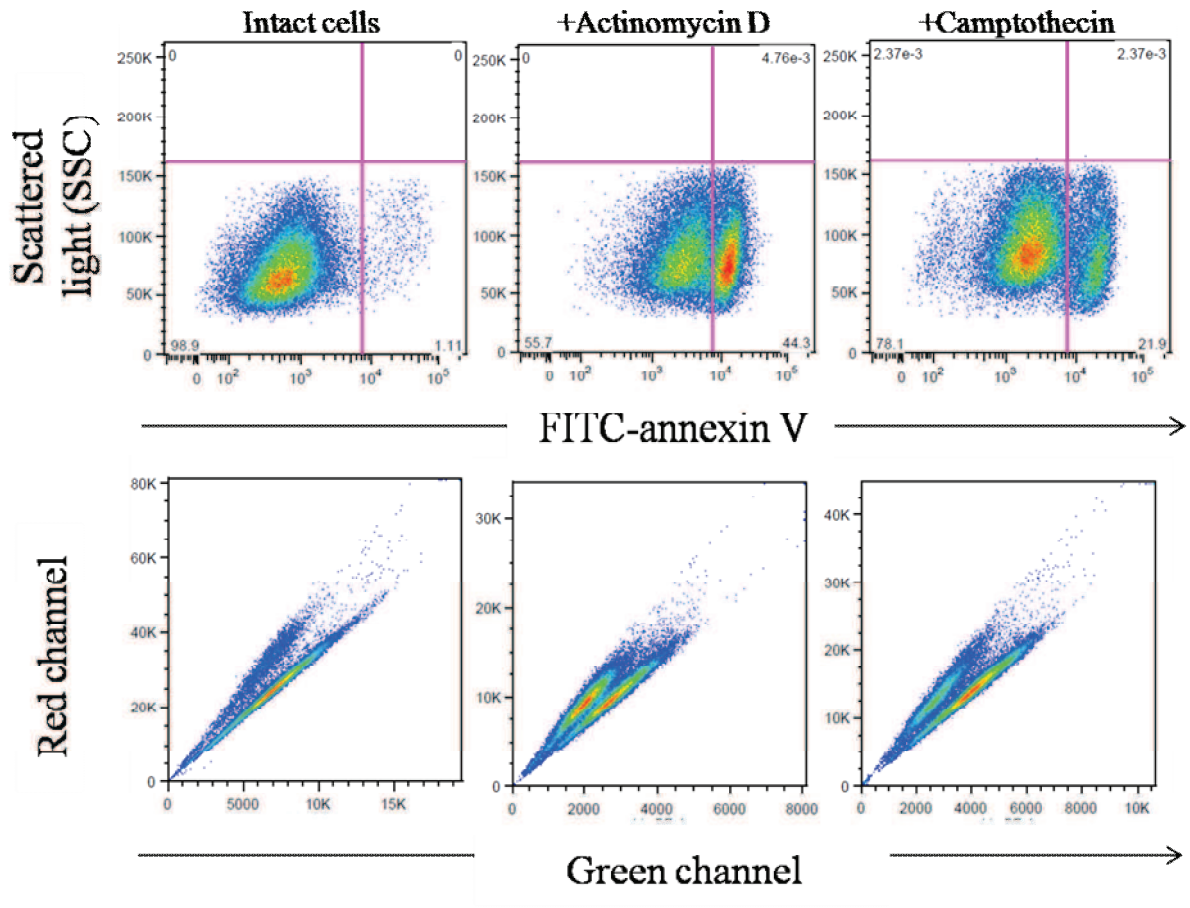


**Figure 7 :** Application de la sonde NR12S en cytométrie de flux.

Ces résultats indiquent donc que NR12S est une sonde fluorescente sensible à l'ordre lipidique, permettant de détecter l'apoptose, par la réduction de l'ordre lipidique du feuillet externe de la membrane plasmique.

Par ailleurs, nous avons mis en évidence que pour des temps d'incubation plus longs à 37 °C, NR12S est internalisé dans le cytoplasme, ce qui se traduit par une augmentation progressive de la fluorescence cytoplasmique de la sonde, aboutissant à une accumulation de celle-ci près du noyau, avec un changement de couleur. Ceci nous a conduit à disséquer la voie d'internalisation de cette sonde. Les études menées à 4 °C montrent une forte diminution de l'internalisation de NR12S dans le cytoplasme. Des études complémentaires de colocalisation avec des marqueurs comme la transferrine, la cholera-toxine, le Lysotracker ou l'ER-tracker suggèrent que l'internalisation de NR12S suit la voie classique de l'endocytose. Le changement de couleur observé est probablement lié au changement de composition lipidique de la membrane des endosomes, suite à la diminution de la quantité de cholestérol. De ce fait cette sonde apparait être un bon outil pour suivre la maturation des endosomes.

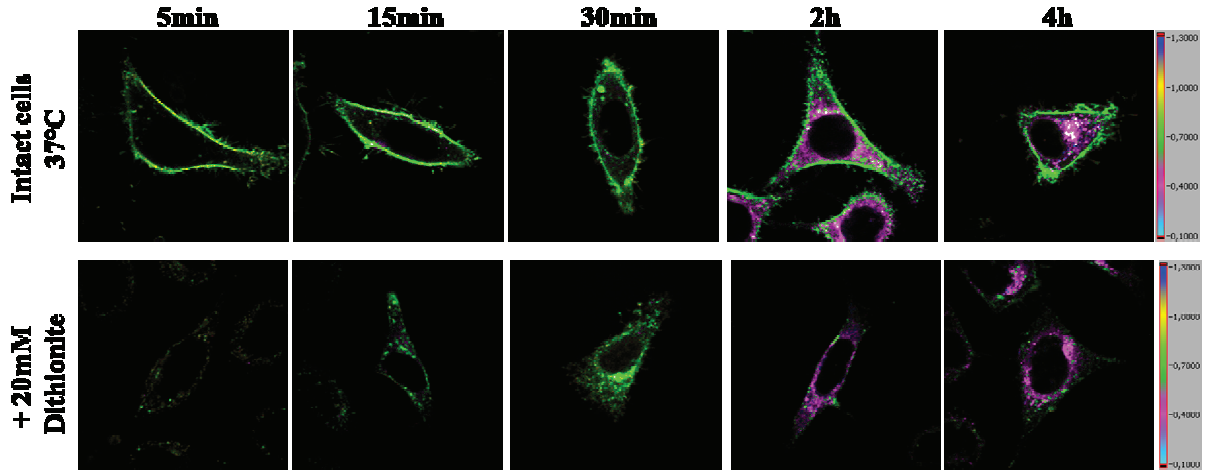


**Figure 8 :** Internalisation de la sonde NR12S accompagnée du changement de couleur.

Enfin, nous avons entrepris de développer un inhibiteur capable d'éteindre la fluorescence de NR12S dans la phase désordonnée Ld, ce qui devrait permettre d'observer sélectivement la fluorescence de NR12S dans la phase ordonnée Lo. Cet inhibiteur à base d'une molécule commerciale le Black hole quencher 2 présente un groupement zwittérionique similaire à NR12S mais une chaîne alkyle plus encombrée, afin d'exclure cet inhibiteur des phases ordonnées. Des études préliminaires par microscopie sur des GUVs et par spectroscopie de fluorescence sur des LUVs ont permis de mettre en évidence que cet inhibiteur induit une diminution de fluorescence accompagnée d'un déplacement du spectre vers le bleu de NR12S, confirmant la disparition de la fluorescence dans la phase désordonnée et sa persistance dans la phase ordonnée. L'efficacité de cet inhibiteur de fluorescence reste cependant à confirmer au niveau cellulaire, afin de pouvoir distinguer les différents domaines lipidiques.

En résumé, les sondes fluorescentes membranaires conçues au laboratoire, que nous avons caractérisées sur des modèles lipidiques et des cellules, s'avèrent d'excellents outils comme sondes sensibles à l'environnement, pour des applications en recherche fondamentale et appliquée. Ces sondes fluorescentes présentent l'avantage de leur simplicité d'utilisation ainsi qu'une absence de phototoxicité reliées aux faibles concentrations (~ 10 nM) requises pour suivre les phénomènes étudiés.

**Zeinab DARWICH**

# SONDES FLUORESCENTES MEMBRANAIRES RATIOMETRIQUES POUR L'ETUDE DES CHANGEMENTS D'ORDRE LIPIDIQUE LORS DE L'APOPTOSE ET DE L'ENDOCYTOSE

Les techniques de fluorescence sont très puissantes pour l'étude des processus biologiques. Les applications de ces techniques requièrent une amélioration constante des sondes fluorescentes, avec un intérêt particulier pour les sondes sensibles à l'environnement. Le but de ce travail était de caractériser et d'appliquer de nouvelles sondes fluorescentes pour l'étude des biomembranes. A cet effet, deux familles de sondes ont été pris en compte. La première famille (F2N12S, F46NS et F66NS) est basée sur le fluorophore 3-hydroxyflavone, qui est caractérisé par une émission duale due à une réaction de transfert de proton à l'état excité. Ces sondes permettent la caractérisation des propriétés de leur environnement par le rapport d'intensité de leurs deux bandes (N*/T*). La seconde famille est basée sur le fluorophore hautement solvatochromique Rouge Nil (NR12S), présentant une seule bande d'émission permettant une mesure ratiométrique à partir des deux bords du spectre. Les propriétés de ces sondes ont été caractérisées dans des modèles lipidiques, puis dans ses membranes plasmiques de cellules eucaryotes vivantes en utilisant diverses techniques de fluorescence (la spectroscopie de fluorescence, la microscopie et la cytométrie de flux). Par la suite, ces sondes ont été utilisées pour l'étude de l'ordre lipidique membranaire en réponse à divers stimuli. Ces sondes sont capables de mettre en évidence et suivre les changements de la membrane plasmique de la cellule au cours de l'apoptose. En outre, nous avons mis au point une nouvelle application de la sonde NR12S, qui est le suivi de l'ordre lipidique des compartiments endocytaires au cours de la maturation des endosomes. Par conséquent, les sondes fluorescentes membranaires décrites apparaissent comme de bons outils pour caractériser les propriétés physico-chimiques de la membrane et la relation entre la phase lipidique et les phénomènes physiologiques comme l'apoptose et l'endocytose.

Fluorescence techniques are powerful tools for studying biological processes. Therefore, the need for improved fluorescent probes used with these techniques continuously increases. The task of the present work was to characterize and to apply new fluorescent probes for biomembrane studies. For this purpose, two families of environment-sensitive probes have been considered. The first family is based on the 3-hydroxyflavone fluorophore (F2N12S, F46NS and F66NS). These dyes undergo an excited state intramolecular proton transfer reaction leading to their dual emission, highly sensitive to the environment. These probes allow the characterization of their environment properties through the ratio of intensities of their two bands (N*/T*) and present improved properties compared to F2N12S. The second family is based on the highly solvatochromic Nile Red fluorophore, exhibiting one emission band allowing a ratiometric measurement between its blue- and red-parts. We focused on one representative probe NR12S, which is a close structural analogue of F2N12S. The probe properties were characterized in lipid models, and in plasma membranes of living cells using a variety of fluorescence techniques (fluorescence spectroscopy, microscopy and flow cytometry). NR12S was then applied to study the lipid order in cell plasma membranes and its changes in response to several stimuli. Interestingly, this probes can evidence and monitor changes in the cell plasma membrane during apoptosis. Moreover, one novel application of the fluorescent membrane probe NR12S was the monitoring of lipid order in endocytic compartments during the maturation of endosomes. Thus, the described fluorescent membrane probes appear as powerful tools to determine the physico-chemical properties of the membrane and the relationship between lipid phase and physiological phenomena, such as apoptosis and endocytosis.

**Zeinab DARWICH**

# SONDES FLUORESCENTES MEMBRANAIRES RATIOMETRIQUES POUR L'ETUDE DES CHANGEMENTS D'ORDRE LIPIDIQUE LORS DE L'APOPTOSE ET DE L'ENDOCYTOSE

Les techniques de fluorescence sont très puissantes pour l'étude des processus biologiques. Les applications de ces techniques requièrent une amélioration constante des sondes fluorescentes, avec un intérêt particulier pour les sondes sensibles à l'environnement. Le but de ce travail était de caractériser et d'appliquer de nouvelles sondes fluorescentes pour l'étude des biomembranes. A cet effet, deux familles de sondes ont été pris en compte. La première famille (F2N12S, F46NS et F66NS) est basée sur le fluorophore 3-hydroxyflavone, qui est caractérisé par une émission duale due à une réaction de transfert de proton à l'état excité. Ces sondes permettent la caractérisation des propriétés de leur environnement par le rapport d'intensité de leurs deux bandes (N*/T*). La seconde famille est basée sur le fluorophore hautement solvatochromique Rouge Nil (NR12S), présentant une seule bande d'émission permettant une mesure ratiométrique à partir des deux bords du spectre. Les propriétés de ces sondes ont été caractérisées dans des modèles lipidiques, puis dans ses membranes plasmiques de cellules eucaryotes vivantes en utilisant diverses techniques de fluorescence (la spectroscopie de fluorescence, la microscopie et la cytométrie de flux). Par la suite, ces sondes ont été utilisées pour l'étude de l'ordre lipidique membranaire en réponse à divers stimuli. Ces sondes sont capables de mettre en évidence et suivre les changements de la membrane plasmique de la cellule au cours de l'apoptose. En outre, nous avons mis au point une nouvelle application de la sonde NR12S, qui est le suivi de l'ordre lipidique des compartiments endocytaires au cours de la maturation des endosomes. Par conséquent, les sondes fluorescentes membranaires décrites apparaissent comme de bons outils pour caractériser les propriétés physico-chimiques de la membrane et la relation entre la phase lipidique et les phénomènes physiologiques comme l'apoptose et l'endocytose.

Fluorescence techniques are powerful tools for studying biological processes. Therefore, the need for improved fluorescent probes used with these techniques continuously increases. The task of the present work was to characterize and to apply new fluorescent probes for biomembrane studies. For this purpose, two families of environment-sensitive probes have been considered. The first family is based on the 3-hydroxyflavone fluorophore (F2N12S, F46NS and F66NS). These dyes undergo an excited state intramolecular proton transfer reaction leading to their dual emission, highly sensitive to the environment. These probes allow the characterization of their environment properties through the ratio of intensities of their two bands (N*/T*) and present improved properties compared to F2N12S. The second family is based on the highly solvatochromic Nile Red fluorophore, exhibiting one emission band allowing a ratiometric measurement between its blue- and red-parts. We focused on one representative probe NR12S, which is a close structural analogue of F2N12S. The probe properties were characterized in lipid models, and in plasma membranes of living cells using a variety of fluorescence techniques (fluorescence spectroscopy, microscopy and flow cytometry). NR12S was then applied to study the lipid order in cell plasma membranes and its changes in response to several stimuli. Interestingly, this probes can evidence and monitor changes in the cell plasma membrane during apoptosis. Moreover, one novel application of the fluorescent membrane probe NR12S was the monitoring of lipid order in endocytic compartments during the maturation of endosomes. Thus, the described fluorescent membrane probes appear as powerful tools to determine the physico-chemical properties of the membrane and the relationship between lipid phase and physiological phenomena, such as apoptosis and endocytosis.